

Master Thesis
15th of July 2021



Development of a non-equilibrium beach in a low-energy lake environment

Using the Noordstrand of the Marker Wadden as a case study

Fleur Willemijn Wellen

Committee: Prof. dr. ir. S.G.J. Aarninkhof
Ir. A.M. Ton
Ir. T. Vijverberg
Ir. R. Van Santen
Dr. ir. M. Zijlema

Disclaimer

This report is part of the Master's degree of the Faculty of Civil Engineering and Geosciences. It has been prepared with great care under the guidance of staff of Delft, University of Technology. However, the reader should realise that this report has been prepared for educational purposes and is judged on educational criteria. As a result, this report should not be considered as a professional consultancy report. Delft, University of Technology, cannot accept liability for all content of this report.

Development of a non-equilibrium beach in a low-energy lake environment

Using the Noordstrand of the Marker Wadden as a case study

MSc. Thesis

by

Fleur Willemijn Wellen

In partial fulfilment of the requirements for the degree of

Master of Science

in Hydraulic Engineering,

at Delft University of Technology,

to be defended publicly on the 15th of July 2021

Faculty of Civil Engineering and Geosciences,
at Delft University of Technology

July 4, 2021

Thesis Committee	Prof. dr. ir.	S.G.J. Aarninkhof	Delft University of Technology
	Ir.	A.M. Ton	Delft University of Technology
	Ir.	T. Vijverberg	Royal Boskalis Westminster N.V.
	Ir.	R. Van Santen	Arcadis Nederland B.V.
	Dr. ir.	M. Zijlema	Delft University of Technology



Preface

This thesis is the final part of the master programme Hydraulic Engineering at Delft University of Technology and thus marks the end of my time as a civil engineering student in Delft.

For my thesis I was looking for a project in which data analysis, modelling and fieldwork were combined. The combination of theory and practical skills have sparked my interest ever since I was part of the NIOZ research crew aboard the RV Pelagia and I followed the course Fieldwork in Hydraulic Engineering (every student should follow this course to experience what it is like to be a true engineer!). The proposed research of the Noordstrand included all three and I was lucky to be involved in this project for approximately 9 months. This research would not have been possible without everyone's support, for which I am very grateful.

First I would like to thank my graduation committee: Stefan Aarninkhof for being the chair and always making time for our discussions, Marcel Zijlema for his help regarding the computational modelling part of this thesis and sparking my interest in CFD modelling in the first place, Robbin van Santen and Thomas Vijverberg for their time and expertise, guiding me in the good direction and contributing to the different aspects of this research making it relevant for the Marker Wadden project. Last but not least I would like to thank my daily supervisor Anne Ton, not only for introducing me into the wonderful world of low-energy systems, but also for her support and feedback during the entire process. Thanks for pushing me to start the data analysis (Python is no longer scary), helping me to organise our field trips to the Marker Wadden (the organisation was more elaborated than I initially thought) and (re)reading my thesis (enabling me to challenge myself). I want to thank Sander van Nederveen for his support regarding the IDM part of my research. Last I would like to thank Karel Karsen for his support and making studying at the faculty available to me when I needed it the most.

This research would not have been possible without the help of the Boskalis Marker Wadden crew: always eager to help. Worth special mentioning is the help of Simon van Riet, providing me with essential Marker Wadden data, photos and introducing me to the right people if I needed to arrange field campaigns to the islands. I am grateful to Natuurmonumenten for arranging the monthly transit to the Marker Wadden aboard the Marker Wadden II or the impressive Abel Tasman and the transportation on the Marker Wadden itself (either in the form of a private tour of one of the island wards or lending us the 4WD). Thanks to Arjen from Rijkswaterstaat for making me part of the monitoring campaign by showing me how the different instruments work and letting me clean the FL66 equipment with a scrubber.

Last I want to thank my family and friends. My parents and sister for their unconditional support and their interest in my research. I want to thank Daniël for his wise words and voice messages when I needed them the most; Kasper for taking me on daily bike rides after introducing me to my new hobby: cycling and triathlons; and all the other boys from HCI8+ Royaal. I want to thank my master friends for being able to discuss my master thesis and other non-study related matter with them, especially Madelief. Our weekly coffee breaks were a moment to look forward to at the start of each week when working from home. I want to thank Mindy, Judith, Nora, Tom, Thijs, Stud20, vvv'tjes and my other friends for their help during my thesis and the adventures we experienced together in the past years. I am grateful for my roommates which were almost like family to me during the past year. Thank you Aert and Lila for planning your thesis deadlines in the same weeks as mine and the numerous coffee breaks we enjoyed together. Thank you Lila, Sjon and Martin for joining me to the Marker Wadden and help me with my measurements. Thank you Lila, Flip, Sjon, Aert, Poes, Martin, Baps and Kurk for always being there for me.

Enjoy reading my thesis!

Fleur Wellen
Delft, June 2021

Abstract

The Houtribdijk was constructed in 1976 to separate the IJsselmeer and Markermeer, the latter would be reclaimed ('inpoldering') to create agricultural land: the Markerwaard. Due to changing political and environmental perspectives this never happened and the Markermeer remains an enclosed lake environment. Due to the lost connection with the IJsselmeer different environmental problems occurred in the Markermeer: nutrient availability decreased, turbidity increased as silt was retained and consequently the biodiversity of the area shrunk. The Markermeer was to be a habitat for different flora and fauna, but could no longer accommodate this function and thus something had to be done. The chosen solution of more shallow and natural areas inside the lake created a reciprocity: turbidity would decrease and removed silt could be used as building material for new land. This formed the concept of the Marker Wadden, an artificial archipelago built using locally available clay and fine sediment, predominantly protected by 'soft' edges ('zachte randen'). As the design and approach are very innovative and not much applied yet, this led to the foundation of Kennis- en Innovatieprogramma Marker Wadden (KIMA) and learning, monitoring of effects and innovation became part of the Marker Wadden project.

In this research we focus on the situation of the Noordstrand. This beach, protecting the northern part of the Marker Wadden, is the only beach with a non-equilibrium shoreline orientation with respect to the dominant wind and wave direction. Our limited understanding of this kind of systems became visible in real life when severe erosion of the Noordstrand was observed. The beach could no longer fulfil its recreational function as the width of the beachface decreased drastically. Furthermore, the dunes were subject to erosion and cliff formation was observed. The amount of erosion was substantial, underlining the need for a nourishment only a couple of years after construction was finished, whereas the first nourishment was planned 10 years after final commissioning. The understanding of how hydro- and morphodynamic processes at this beach interact and influence beach development are the missing keys to a better understanding of these kinds of sandy protections. Ultimately this could improve the maintenance strategy of existing sandy protections and the correct system framework for the design of new beaches in low-energy environments. As a result the main research questions are: *Which processes steer the morphological development of high-angle beaches with non-equilibrium orientation in low-energy lake environments? How do they influence morphology? Can our understanding be used for future maintenance (if needed) and construction of this kind of beaches?*; we attempt to find answers using available datasets and numerical models.

Some hints as to which processes can influence beach development in low-energy systems are found in literature and were later recognised in our Noordstrand system: the main forcing in the system is the wind, creating wind-driven currents and waves; due to limited refraction high-angle waves can cause enlarged longshore transport rates; the evolution of the beach mainly depends on storm events, during these events the combination of high water levels and high waves can cause severe erosion; and little recovery is expected as low-energy events do not have enough energy to reshape the beach. A severe gap in our knowledge of the development of *non-equilibrium oriented beaches in low-energy systems* is acknowledged.

To expand our knowledge we investigate available hydrodynamic and morphodynamic datasets of the Noordstrand. Using measurements obtained offshore we find that predominantly winds from the southwestern region cause a set-up of water level against the Houtribdijk. Winds from the opposite direction, northeast, cause a water level set-down at the Houtribdijk and the Noordstrand. Even milder wind conditions can cause water level fluctuations corresponding to changes in current magnitude and direction measured offshore of the Noordstrand. Additionally, the offshore measurements provide us with information regarding wave height, wave period and the current profile over depth. Using a peak-over-threshold method to identify the high-energy events we are able to further investigate the hydrodynamic processes during moments of high energy. The frequency and resolution of the morphodynamic measurements only allow us to come to conclusions regarding the general development of the beach and should be considered with care. These periodically obtained bathymetry, topography and elevation data near the waterline show a general regression of the shoreline, most erosion occurring in the southwestern part of the beach. Only some sedimentation lakeward from the submerged platform and near the soft edge is observed. Transect analysis shows that the location of most severe erosion and the location of maximum measured water level in the beach profile coincide: this could explain the observed cliff formation at the Noordstrand.

To be able to link the hydrodynamic and morphodynamic findings we adapt an existing Delft3D model to the Marker Wadden model, focusing on establishing a link between offshore measurements and nearshore processes to understand beach development. Using idealised wind schematization runs we are able to observe the general response of the Markermeer lake system and how this influences the nearshore hydrodynamics. Winds from southwestern to northern direction (225°, 245°, 290° and 335°) result in a flow parallel to the shoreline but opposite to the wind direction offshore (going in southwestern direction), closer to the beach the flow is in the opposite direction (going towards the northeast). This is the result of a rotation cell formed by the hard edge blocking part of the offshore flow. As a consequence the longshore current accelerates along the southwestern part of the Noordstrand, increasing its transport capacity. In case of northeastern wind directions (20° and 65°) flow directions are reversed, still an opposite flow direction between off- and nearshore is observed. In all cases the Markermeer bottom depth contour seems to enclose the region of the oppositely directed flow. Comparing *flow only* and the coupled *flow & waves* model runs we notice how waves enlarge the longshore current and push the region with enlarged flow velocities more towards the waterline. Additional sensitivity runs are used to validate model results (2DH versus 3D and the influence of the drying and flooding threshold depth) and explore the influence of external factors on the nearshore flow (for instance: the hard edge, the submerged platform and the sand extraction pit).

Combining literature, our hydrodynamic and morphodynamic data analysis and the D3D Marker Wadden model outcomes we are able to create a conceptual system description: the hypothesised explanation of the development of the Noordstrand. In the governing scenario (winds coming from the southwestern to northwestern segment), based on wind occurrence and link to high-energy events, we observe higher wave heights and a water level set-up against the Houtribdijk. Nearshore, influenced by the location and geometry of both the entire archipelago and Noordstrand, the flow is towards the northeast. This accelerating longshore current is formed by the rotation cell arising due to the presence of the breakwater in the southwest, blocking the offshore current. High-angle waves further accelerate this current in the surfzone. Waves stir the sediment near the shoreline and the longshore currents transports the eroded sediment from the transect. Due to the observed acceleration of this current along the southwestern part of the beach, positive gradients in transport capacity arise, causing erosion. Near the inner bend of the soft edge the longshore current slightly decelerates before it leaves our system, resulting in a local decrease in transport capacity and thus sedimentation. This entire process is intensified during high-energy events, leading to increased stirring by enlarged waves and increased transport rates due to a growth in longshore current magnitude. Significant changes in beach profile and shoreline are expected during high-energy events, but the gradual erosion during milder conditions has a powerful effect on the overall beach development too as these have a much higher occurrence. As most eroded sediment leaves our system and is 'lost', we believe the beach is structurally eroding. This means an equilibrium shoreline orientation is not formed in this case and periodical nourishments are needed. We have observed the cross-shore profile is still developing with the submerged platform width growing lakeward. The development of the Noordstrand, analysed using data obtained during our monthly field trips, after the most recent nourishment (December 2020), can be partly explained by linking measured wind conditions to our conceptual system description. On the other hand this analysis also highlights the complex interaction of different processes involved in the Noordstrand development as not all features can be explained.

Additional field measurements to validate nearshore model results are needed to verify if our conceptual system description is correct. Furthermore, our hypothesised explanation is based on one governing scenario identified by analysing only a short period of time (≈ 20 months). Supplementary recommendations regarding the Noordstrand are presented in this report. For non-equilibrium oriented beaches in low-energy systems in general, we have learnt that these beaches are profoundly different from beaches in a high-energy environments and deviate from sandy protections with an equilibrium shoreline orientation. The effects of different hydrodynamic processes should be included in system design and its link to the bigger system (e.g. the Markermeer) has to be understood to prevent unexpected development of the beach. Moreover, we can conclude the different processes are very system- and site-specific, man-made ingenuities might have negative secondary effects on flow and beach development. This combined leads to the main recommendation: we need to *change our way of thinking and designing* in this kind of systems. Instead of designing a beach solemnly based on the wave climate, we need to consider the entire system. We need to consider all hydrodynamic processes such as water level set-up (or -down), lake circulation currents and its nearshore components. To conclude we have observed that the term *low-energy* does not mean nothing exciting happens in our system especially when taking into consideration that we are only beginning to understand the different aspects of this and other low-energy systems and there is much more to learn.

Table of Contents

Preface	iii
Abstract	v
List of Abbreviations	xii
List of Symbols	xiv
List of Terms	xvi
I Preparation - Getting Started	1
1 Introduction	2
1.1 Historical Background	2
1.2 Study Site - Marker Wadden	3
1.3 Reading Guide	4
2 Research Proposal	5
2.1 Problem Analysis	5
2.2 Research Questions	8
2.3 Methodology	9
2.4 Research Scope	10
II System Analysis - An Overview	12
3 Literature Review	13
3.1 Lake Environment	13
3.2 Hydrodynamic Processes	15
3.3 Morphodynamic Processes	17
3.4 Conclusion	19
3.5 Link Problem Statement	19
4 System Understanding	20
4.1 Available Literature	20
4.2 Design Marker Wadden	21
4.3 New Research	22
4.4 Time Line	23
4.5 Conclusion	24
III Data Analysis - Getting a Feeling	26
5 Methodology - Data Processing	27
5.1 Considered Period of Time	27
5.2 Hydrodynamics	28
5.3 Morphodynamics	30
6 Hydrodynamics	32
6.1 General Data Analysis	32
6.2 High-Energy Events	38

6.3	Conclusions	46
7	Morphodynamics	47
7.1	General Erosion	48
7.2	Analysis High-Energy Period	49
7.3	Conclusions	54
7.4	Exploratory Morphodynamic Analysis - Fieldwork Data	55
IV	Modelling - Filling the Gaps	57
8	D3D Model Marker Wadden	58
8.1	Delft3D	58
8.2	Marker Wadden Model	59
8.3	Calibration and Validation	65
8.4	Scenarios	67
9	D3D Model Results	70
9.1	Idealised Wind Schematization Runs	70
9.2	Comparing Flow & Waves to Only Flow	82
9.3	Sensitivity and Exploratory Model Runs	83
9.4	Conclusions	87
V	Conclusions - Creating the Total Picture	88
10	Discussion	89
10.1	Getting the Total Picture	89
10.2	Development Noordstrand	94
10.3	Monitoring and Maintenance	106
10.4	Critical Remarks	108
10.5	Exploratory Research	110
10.6	Building with Nature - a System Engineering Approach	113
11	Conclusion & Recommendations	114
11.1	Conclusion	114
11.2	Recommendations	118
	Bibliography	121
VI	Appendices	124
A	Measuring Instruments and Available Data	125
A.1	FL 66 - Measuring Instruments	125
A.2	GPS - Measuring Instruments	126
B	Data Analysis: Hydrodynamics	128
B.1	Data-processing	128
B.2	General	128
B.3	High-Energy Events - General	131
B.4	High-Energy Events - Individual Events	134
B.5	Additional Peak-over-Threshold Methods	156
C	Data Analysis: Morphodynamics	158
C.1	Data-processing	158
C.2	General	159

C.3	Transects 2019 Q3 - 2020 Q1	161
D	D3D Model Set-up	170
D.1	Introduction Delft3D	170
D.2	Domain, Grid and Bathymetry	172
D.3	Calibration	173
E	D3D Model Results	179
E.1	Idealised Wind Schematization Runs	179
E.2	Comparing Flow & Waves to Only Flow	190
E.3	Sensitivity and Exploratory Runs	195
F	Exploratory Research - D3D Morphology	199
F.1	Set-up Marker Wadden Morphological Model	199
F.2	Results	200
G	GPS Plan	205
G.1	Measurements	205
G.2	Planning	206
G.3	Data Management	206
H	Overview Fieldwork	207
H.1	Fieldwork December 2020	207
H.2	Fieldwork January 2021	208
H.3	Fieldwork March 2021	208
H.4	Fieldwork April 2021	209
I	Integral Design and Management	210
I.1	Analysing Key Points	210
I.2	This Research - a System Engineering Approach	212

List of Abbreviations

Abbreviation	Description
2DH	Depth-averaged
2DH SWE	Depth-integrated shallow water equations
ADCP	Acoustic Doppler Current Profiler
ADI	Alternating Direction Implicit
ADV	Vector Acoustic Doppler Velocimeter
ALTI	Altimeter
AQD	Aquadopp HR
Bft	Beaufort
BwN	Building With Nature
D3D	Delft3D
DMS	Data Management System
FH	Hourly average wind speed (m/s)
FL66	Offshore measuring station near Noordstrand
FL67	Offshore measuring station near Houtribdijk
FM	Flexible Mesh
GNSS	Global Navigation Satellite System
HE	High-Energy
HRD	Houtribdijk
HT	High Tide
KIMA	Kennis- en Innovatieprogramma Marker Wadden
KNMI	Koninklijk Nederlands Meteorologisch Instituut
LakeSIDE	Lake Shore Interconnecting Defence and Environment
LT	Low Tide
NaN	Not a Number
NAP	Normaal Amsterdams Peil
NS	Noordstrand
PoT	Peak-over-Threshold
STB	Stepgauge (Stappenbaak)
WL	Water level
WL_fluc	Water level fluctuation (10 day average removed)

List of Symbols

Symbol	Unit	Description
α	-	Initial wave growth term
β	-	Exponential wave growth term
$\frac{H}{L}$	-	Steepness relation
$\frac{h}{L}$	-	Water depth to wave length ratio
μ	-	Mean
ρ_{air}	kg/m^3	Density of air
ρ_0	kg/m^3	Reference density of water
$\tau_{b,x}$	N/m^2	Bottom shear stress in x direction
$\tau_{b,y}$	N/m^2	Bottom shear stress in y direction
$\tau_{w,x}$	N/m^2	Wind shear stress in x direction
$\tau_{w,y}$	N/m^2	Wind shear stress in y direction
ζ	m	Water level
σ^2	-	Variance
BED	-	Current-related bedload transport factor
$BEDW$	-	Wave-related bedload sediment transport factor
C	$m^{1/2}/s$	Chézy coefficient
C_d	-	Wind drag coefficient
C_f	-	Friction coefficient
D_{50}	μm	Median sediment diameter
DPS	m	Bottom depth
E		Sum of squared residuals
E	J/m^2	Wave energy
f	$1/s$	Coriolis parameter
g	m/s^2	Gravitational acceleration
h	m	Water depth
H	m	Wave height
H_{m0}	m	Significant wave height
H_b	m	Breaker height
H_S	m	Significant wave height
k_s	m	Nikuradse roughness height
L	m	Wave length
m_2	-	(dimensional) Coefficient
p_{atm}	N/m^2	Atmospheric pressure
s	-	Wave steepness
S	$m^3/s/m$	Transport
S_{in}	m/s^2	Source term (wind)
S_{total}	$m^3/s/m$	Total transport
S_y	$m^3/m/s$	Longshore sediment transport (per unit width)
SUS	-	Current-related suspended sediment transport factor
$SUSW$	-	Wave-related suspended sediment transport factor
t	s	Time
u	m/s	Flow velocity in x direction
u_*	m/s	Friction velocity
U_{10}	m/s	Averaged wind speed at 10 meter above surface
v	m/s	Flow velocity in y direction
V	m/s	Longshore current velocity at some level above the bed
ν_h	m^2/s	Horizontal viscosity
$S_{bedloadcurrent}$	$m^3/s/m$	Bedload transport due to currents
$S_{bedloadwaves}$	$m^3/s/m$	Bedload transport due to waves
$S_{suspendedwaves}$	$m^3/s/m$	Suspended transport due to waves

List of Terms

This list of terms is created solely for this thesis. The definitions and explanations are linked to the processes discussed in this research and some terms cannot be extended to other general systems, but are site-specific.

Term	Definition / Explanation
General:	<i>See also figure 1</i>
FL66	Offshore measuring station near Noordstrand
FL67	Offshore measuring station near Houtribdijk
Offshore	Lakeward of the Markermeer bottom contour (-4 meter NAP)
Nearshore	Area between waterline and Markermeer bottom contour (-4 meter NAP)
Sandy protections	Protection of hinterland by sand in the form of a beach system
Soft edge	Northeastern edge of the main part of the Noordstrand (see figure 1)
Hard edge	Breakwater in the southwest of the Noordstrand (see figure 1)
(Submerged) Platform	Offshore platform linked to Hallermeier's depth of closure (related to the wave base)
Noordstrand System	Considered part of the Noordstrand, from the hard edge to the soft edge (see figure 1)
Term	Definition / Explanation
Currents:	<i>See also figure 1</i>
Rotation cell	Due to partial blockage of the offshore wind-induced flow by the hard edge, a rotation cell which links offshore and nearshore wind-induced flow is formed
Jet-like current	Formed by the convergence of the northeastern going longshore current from the Noordstrand and a southwestern going current arriving from the northern edge of the beach (nearshore component of the general lake circulation pattern)
(General) Lake circulation pattern(s)/current(s)	Wind-induced currents formed indirectly in the Markermeer due to water level set-up or -down against the Houtribdijk; can be influenced by geometry of the Markermeer
Offshore current	Offshore current near the Noordstrand part of general wind-induced lake circulation
Nearshore current	Longshore current, flowing parallel to the shoreline in the nearshore
Term	Definition / Explanation
Nearshore current formed by:	<i>See also figure 1</i>
Wind-driven current	Current in top of the water column directly influenced by the wind shear stress and in the same direction as the wind forcing
Wave-driven current	Wave-induced longshore current, formed by obliquely incident waves breaking in the breakerzone (change in radiation stress balanced by bed shear stress)
Wind-induced current	Indirect result of the general lake circulation formed by the set-up against the Houtribdijk and influenced by local geometry

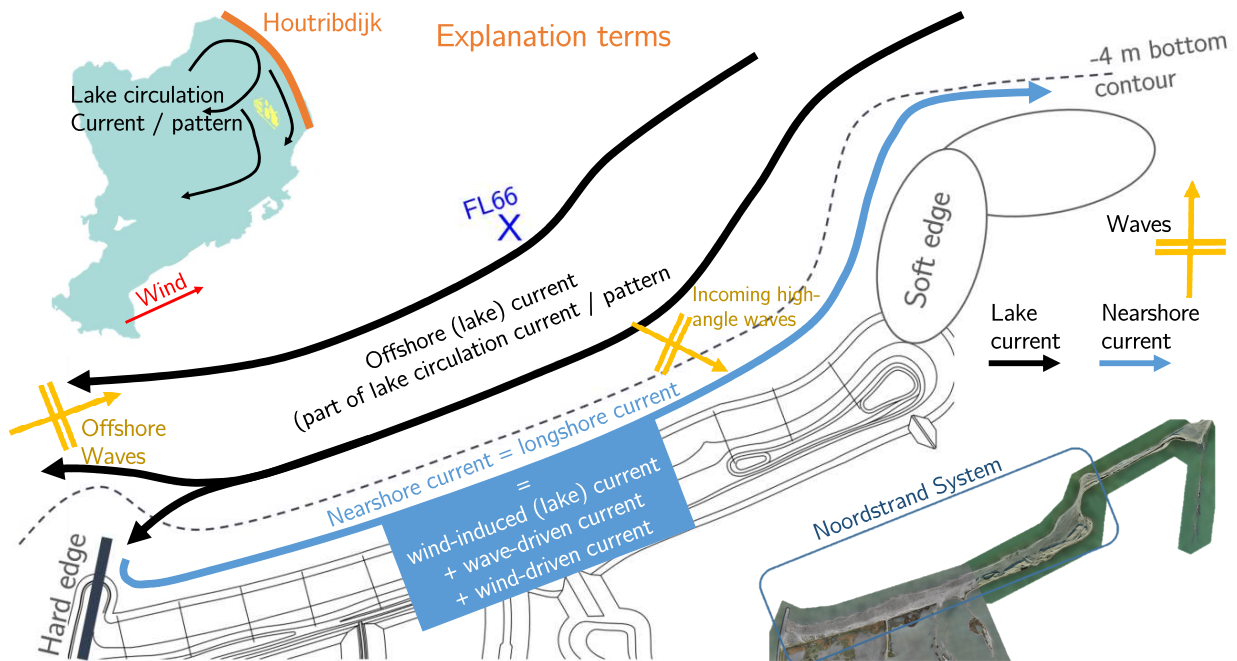


Figure 1: Explanation different terms used in our Noordstrand data analyses and system description. The lower right shows the considered area for our *Noordstrand system* (see also figure 2.3). The colours of the different processes and their description match. Note: we have used the current pattern and wave direction from scenario 3: set-up - general. The offshore and nearshore current patterns and wave information are different in every scenario.



Preparation - Getting Started

1

Introduction

Climate change has a significant effect on the low-lying Netherlands. The coming decades we have to deal with these effects which include more extreme weather events and an average sea-level rise of more than 0.20 meters in 100 years (Rijksoverheid, 2020). On the other hand, building new and maintaining current flood defences such as dikes and dams is expensive (Rijksoverheid, 2020). Be that as it may, the battle of the Netherlands with the water, both sea and riverine water, is not new. Whereas before early Roman times inhabitants mostly avoided living on the flood prone low-lying areas, this changed as civilisation grew and the need for fertile land expanded. Inhabiting lower laying areas meant the invention of early coastal and water management strategies (e.g. the construction of dikes and reclamation of fertile lands) (Borger and Ligtenag, 1998). Ongoing changes of the natural system meant continuous adaptation of the measures, until at some point the strengthening or heightening of, for instance, a dike is no longer enough. In that case more extreme and innovative measures have to be taken, of which the construction of the Afsluitdijk is a clear example.

In the next section, section 1.1, we provide some historical background which is needed to better understand the current situation and problems in the Marker Wadden, as these issues arose after the construction of the Afsluitdijk and later the Houtribdijk. Before elaborating the different problems even further a small introduction of the Marker Wadden is given in section 1.2, in which we also zoom-in on the Noordstrand. The last part, section 1.3, provides the reading guide for this thesis.

1.1 Historical Background

Whereas the Deltawerken of the Netherlands, for instance the Maeslantkering or Oorsterscheldekering, are rather well known, people tend to forget the first massive and innovative flood defence was already finished in 1932: The Afsluitdijk. This dam ('dijk' in Dutch, but it is more a dam than a dike) created the IJsselmeer by separating the former Zuiderzee from the North Sea, to protect the municipalities surrounding the Zuiderzee from floods. Another benefit of the creation of the Afsluitdijk, was the possibility to divide the IJsselmeer in separate compartments, which could be reclaimed and used as agricultural land. One of these plans included the reclamation of the Markerwaard. For this purpose the Houtribdijk was constructed and finished in 1976. However, over time, the main regard towards the reclamation of the Markerwaard by 'inpoldering' had changed. The reclamation remained part of ongoing political debates, until in 2002 it was finally decided not to recover the land. Leaving the lake on the southwestern side of the IJsselmeer the Markermeer.

Nonetheless, the open connection of the Markermeer and IJsselmeer had already vanished in 1976 after the creation of the Houtribdijk. Due to this lost connection with the IJsselmeer different environmental problems occurred in the Markermeer (section 2.1). With the attitude towards nature and ecology of the Dutch civilisation changing, becoming more aware and more concerned about mainly climate change and water pollution (Eurobarometer, 2008), and the classification of the Markermeer as a Natura 2000 project (Programmadirectie Natura 2000, 2009), meant these problems could no longer be overlooked.

In the past years different solutions for the problems of the Markermeer were investigated. In the end the involved parties agreed on the construction of an *artificial archipelago*: the Marker Wadden.

1.2 Study Site - Marker Wadden

The artificial islands of the Marker Wadden are located at the western side of the Markermeer, close to the Houtribdijk (left, figure 1.1). The location of the Marker Wadden inside the Markermeer make it a lake environment. The only 'hard' edge of the Markerwadden can be found on the north-western side, all the other borders provide soft edges, made of silt and sand (right, figure 1.1). The edges protect the hinterland, creating room for shallow waters and natural marshland. This provides a dynamic habitat, created to attract all kinds of birds, fish and insects (Posthoorn et al., 2019). Only the largest island is accessible for the public and accommodates a watch tower, harbour, recreational beach and several footpaths.

1.2.1 Noordstrand

The Noordstrand is located on the northern side of the Marker Wadden (in blue box right image, figure 1.1). The western part of the beach is connected to the 'hard' edge, whereas the eastern side is connected to a soft edge, which protrudes into the Markermeer to the west. Some facts are summarised to give the reader a small impression of the Noordstrand (table 1.1).

Table 1.1: Some facts of the Noordstrand at the Marker Wadden

Description	Value	Source
Length beach	≈ 1400 meter	Van Santen (2016)
Sediment diameter	≈ 350 μm	Van Santen (2016)
Initially designed beach width	30 m	Van Santen (2016)
Average depth Marker Wadden	≈ 4 m	Ton (2020)
Mean H_{m0}	0.26 m	Ton et al. (2020)
95-percentile H_{m0}	0.53 m	Ton et al. (2020)



Figure 1.1: Left: Overview of the central part of the Netherlands (adapted from Google Maps). The IJsselmeer and Markermeer are separated by the Houtribdijk, visible as the yellow line connecting Lelystad and Enkhuizen (N307). The Marker Wadden are in the north-eastern part of the Markermeer. The blue box shows the location of the Marker Wadden. Right: Zoom-in of the blue box, the final design of the Marker Wadden (adapted from Posthoorn et al. (2019)). The archipelago consisting of 5 different islands is clearly visible. The focus of this thesis is on the Noordstrand (blue box in top of figure).

1.3 Reading Guide

This report is split into five main parts focusing on the different elements of this research. This reading guide discusses the content of each part shortly.

Preparation - Getting Started

The first part contains the general introduction in chapter 1. This gives a short historical background of the creation of the Markermeer and introduces the Marker Wadden archipelago to the reader. Chapter 2 describes the research proposal, containing the problem analysis, the research questions, approach and research scope.

System Analysis - An Overview

An overview of the available literature concerning research regarding this kind of environments is presented in the second part. This starts with a general literature review in chapter 3. The findings are combined to form our current system understanding in chapter 4 and makes identification of the 'knowledge gaps' of our system possible.

Data Analysis - Getting a Feeling

To minimise the gaps in our knowledge we start by analysing available data. The methodology of this data analysis is given in chapter 5 focusing on the hydrodynamic and morphodynamic data. The outcomes of the hydrodynamic data analysis are described and analysed in chapter 6. Chapter 7 contains the results and analysis of the morphodynamic data.

Modelling - Filling the Gaps

The hydrodynamic and morphodynamic data analysis provide some hints regarding the processes influencing the development of the Noordstrand. Nevertheless the link between offshore and nearshore processes is missing. We use a Delft3D model to fill the missing gaps. The set-up of this model is presented in chapter 8. The results and analysis of the Delft3D model are given in chapter 9.

Conclusions - Creating the Total Picture

The results and conclusions of the last two parts are combined to create a conceptual system description of the Noordstrand. This is discussed together with the critical remarks concerning this research in chapter 10. The main conclusion, including the answers to the research questions, is given in chapter 11. This chapter also contains the final recommendations for the Noordstrand and future research.

Appendices

The appendices in the back of this report contain additional information on the data available (appendix A) and data analyses (appendix B and appendix C). More information on the set-up of the Delft3D Marker Wadden model can be found in appendix D. Appendix E gives additional information regarding the results of the D3D model runs. Some additional exploratory research is summarised in appendix F. Appendix I includes a short analysis on the System Engineering approach towards this project and Building with Nature projects in general. Part of this research included field trips to the Marker Wadden. The research plan for these trips can be found in appendix G. A summary of each field trip is given in appendix H.

2

Research Proposal

An introduction in the form of some historical context and a brief overview of the Marker Wadden was presented in the previous chapter. This chapter focuses on the outline of this thesis. First, the analysis of the problems, as already introduced in section 1.1, is broadened in section 2.1. In this analysis focus lies on the problems at the Noordstrand of the Marker Wadden, however the broader perspective of the problems is recognised and further elaborated. From the problem analysis the main research question follows in section 2.2, divided into smaller subquestions. These can be used as a guideline throughout the project. The research approach (methodology) is discussed in section 2.3. To define clear boundaries for our research the scope is presented in section 2.4. This section also includes a note on the data available.

2.1 Problem Analysis

The problem analysis is split into two parts: first the system of the Noordstrand of the Marker Wadden is discussed. This analysis continues to build on the discussion presented in the previous chapter. After this analysis the more general system is considered: how do sandy protections behave and develop in this kind of systems (systems somewhat similar to the Marker Wadden)? It is important to consider the broader perspective and investigate how this research can add value to other projects including sandy protections, especially at locations where the use of sandy protections is novel.

2.1.1 Noordstrand of the Marker Wadden

As discussed in section 1.1 the separation of the IJsselmeer and Markermeer by the Houtribdijk caused environmental problems. The nutrient availability in the lake was affected and the turbidity of the water increased as the silt was retained inside the Markermeer (Van Riel et al., 2019). The decrease of nutrients and the effects of climate change negatively influenced the biodiversity of the area as the number of birds and fish shrunk (Noordhuis, 2014). The Markermeer, in 2009 assigned a Natura 2000 project, was to be a habitat for different flora and fauna, but could no longer accommodate this. Different solutions were thought of including the creation of more shallow and natural areas inside the lake and measures to reduce the overall turbidity of the water (Noordhuis, 2014; Van Riel et al., 2019).

This idea created a reciprocity: removed silt could be used as building material for new land, creating gradual land to water transitions beneficial for nutrient availability and thus wildlife. This formed the initial concept of the Marker Wadden: creating an artificial archipelago, consisting of five islands, using locally available clay and fine sediment (Posthoorn et al., 2019). The construction of the Marker Wadden would greatly increase the biodiversity of the systems, as it was designed to accommodate various bird and fish species. Instead of well-known 'hard' edges as a rock-armoured or asphalt dike, the Marker Wadden would be predominantly protected by 'soft' edges (Dutch: 'zachte randen'). This was also translated to the program of requirements of the first phase (the construction of five islands forming the archipelago) of the Marker Wadden project. Main requirement no. 1 indicates: 'The capturing and fixing of silt' and one of the secondary requirements state: 'The Marker Wadden are a nature development project. Therefore, the presence of natural dynamics are preferable'. From Hüsken (2020) and VER (2015) the different goals incorporating the usage of soft edges in the design are the following:

- Protection by an edge on which natural processes, like erosion and sedimentation occur, are allowed. Although the protective function of the edge should be enough during extreme conditions
- Using the removed silt as a construction material in and around the natural system
- The lessons learnt during the initial 'innovative' phase, about for example building with silt, contribute to an efficient construction in the next phases of the Marker Wadden project and other future projects
- Ideally a robust and self-maintaining system is created
- Understand and develop new ways of creating natural habitats with silt or other fine sediments

However, the usage of soft edges creates a problem, as this approach is very innovative and not much applied yet. Not so much is known about the usage of sand and silt as a natural protection in a lake environment. That is why an additional objective was added to the programme of requirements: *learning, monitoring of effects and innovate* (De Rijk et al., 2018). In light of this the Kennis- en Innovatieprogramma Marker Wadden (KIMA) was founded. The parties involved include: Rijkswaterstaat, Natuurmonumenten, Deltares and EcoShape. The three main research topics of KIMA are (KIMA, 2018):

1. Building with silt and sand
2. Ecosystem with value
3. Adaptive governance

From this follows the main interest for the soft edges: *How do the cross-shore and longshore profiles develop under influence of the local hydrodynamic loading (currents and waves)?* (Hüsken, 2020). Which immediately states the relevance of this thesis as more insight is needed in the dynamics of the soft edge and the beach-like protection in a lake environment (*Building with silt and sand*). Furthermore, the 'lessons learnt' and obtained knowledge can be used in the maintenance stage of the Marker Wadden project (*Adaptive governance*).

Erosion Noordstrand

The urge of a better understanding can also be understood if one looks at images of the development of the Noordstrand (figure 2.1). The amount of erosion is substantial, underlining the need for a nourishment only a couple of years after construction of the beach was finished. Whereas the first nourishment was only planned 10 years after final commissioning. Plus knowledge on this kind of low-energy and fetch-limited systems is limited (chapter 3), more research is needed (Jackson et al., 2002; Nordstrom and Jackson, 2012; Steetzel et al., 2017; Ton et al., 2019).

For the construction of the Marker Wadden some research has been performed in the form of pilot- and 'natuurstand' project Houtribdijk. Although this artificial beach near the Houtribdijk has provided some useful insights; its orientation, profile and initial development differ significantly from the Noordstrand. Making the Noordstrand an entirely different and stand-alone project. Recent research by Ton et al. (2020) primarily focused on nearshore processes at the Zuider- and Recreatistrand (beaches in the left bottom half of figure 1.1, right plot). The development of these beaches show more resemblance to the Pilot Houtribdijk. This creates the need for an additional research project solemnly focusing on the Noordstrand.

The uncertainty of the development of the Noordstrand, the missing pieces of the puzzle of the hydro- and morphodynamic processes at this beach and the desire to use this kind of soft edges as a coastal protection more often, underlines the importance of more research into this system of hydrodynamic and morphodynamic processes near the Noordstrand.

2.1.2 Broader perspective

In the past few years sandy protections, in not-so-straight-forward locations (not directly facing high-energy seas or oceans), have been designed and constructed. An example is the reinforcement of the Prins Hendrikzanddijk at Texel. The application of sand instead of normally used 'hard' material has led to a true metamorphosis of the landscape. The current sandy system of the Prins Hendrikzanddijk project is related more to the natural system present in this kind of environment (Hoogheemraadschap Hollands Noorderkwartier, 2020). This dynamic protection has to protect the South Eastern border of Texel for the coming decades. Another project can be



Figure 2.1: Development of the Noordstrand, 26th of July 2018 (left) and less than 2 years later: 10th of April 2020 (right). The beach profile in 2018 looks smooth, creating a wide beach face. The situation in 2020 shows a smaller beach with on the left side a cliff more than 2 meters high. (pictures taken by Anne Ton)

found closer to the Marker Wadden: the partial reinforcement of the Houtribdijk by sand instead of the usually applied rip-rap. The sandy protections have a dual function: provide protection from wave energy and water level fluctuations and on the other hand create room for plants and animals, contributing to the enhancement of the biodiversity in the Markermeer. This reinforcement includes a side-project, showing significant similarities with the Marker Wadden: the creation of the nature reserve Trintelzand. Albeit smaller than the Marker Wadden, the concept and purpose of Trintelzand is similar to that of the Marker Wadden: provide a habitat for numerous fish and bird species. For the reinforcement of the Markermeerdijken, located on the western side of the Markermeer (right plot, figure 1.1), the design includes (partly) sandy edges, enabling a dynamic link between the lake and land system.

These projects already show the potential of sandy protections outside the context of high-energy (direct contact with seas or oceans) systems. Sandy protections in low-energy systems can provide space for recreation, flora and fauna, and above all provide protection of the hinterland. Knowledge is still limited, but plans for similar projects are numerous, creating a need for knowledge as these protections need to be designed, monitored and maintained as efficiently as possible. As in the past the focus has been on the development of beaches with a perpendicular orientation with respect to dominant wind or wave direction, in a low-energy lake system. The big 'unknowns' are found when considering beaches with a deviating orientation. Some presumed development can be derived from literature, but this has never been verified or explored further. This need for knowledge is translated into the main research question of this thesis and 5 subquestions (section 2.2).

Building with Nature

Putting the previous paragraph in a larger perspective, this Marker Wadden project is an example of a *Building with Nature* project. This design approach is still novel as only a couple of Building with Nature projects have been realised: for instance the Sand Engine and Hondbossche and Pettemer Zeewering. The potential of this kind of projects is recognised world-wide especially in light of increased interest in sustainability and threat regarding climate change. According EcoShape (2021b): 'The guiding principle of Building with Nature is to work with nature, not against it. It uses system understanding and the inclusion of natural processes as core of its solution.' The usage of sandy protections and the main to understand the natural system creates a true Building with Nature project.

In addition to the engineering project this thesis aims to link the technical knowledge with other skills such as project- and asset management as these are to be implemented correctly for a successful Building with Nature project. To consider the Building with Nature approach we use the *System Engineering* approach. This approach is particularly valuable for multi-disciplinary and complex projects. The Marker Wadden project is an excellent example of such a project: different stakeholders and their wishes, different project aspects and innovative developments come together. This leads to an additional reflection in the discussion of this project:

Building with Nature: A System Engineering Approach

2.2 Research Questions

Using the analysis of the previous paragraphs we can define the main research question and divide this main question into five subquestions which are used as guidance throughout our research. In front of each question a summarising term can be found.

Which processes steer the morphological development of high-angle beaches with non-equilibrium orientation in low-energy lake environments? How do they influence morphology? Can our understanding be used for future maintenance (if needed) and construction of this kind of beaches?

(1)
System Identification

Which hydrodynamic processes could steer the (large-scale) behaviour of a beach in a lake environment like the Marker Wadden?

(2)
System Understanding

What is our current understanding of low-energy lake systems?

(3)
Link

Can the morphodynamics of a low-energy beach in a lake system, with non-equilibrium orientation, be linked to hydrodynamic processes? If so, in what way?

(4)
Equilibrium

Is an equilibrium position of the shoreline and cross-shore profile possible?

(5)
Lessons Learnt

How can the previous findings help during development and maintenance of beaches in this low-energy lake system?

2.3 Methodology

The methodology to answer the previous stated research questions is drawn up in the preparation phase with the help of some background and site-specific information and in analogy with the problem definition and research scope. We continue by an analysis of existing literature regarding low-energy systems and systems-specific research concerning the Markermeer, Marker Wadden and Pilot Houtribdijk. Next available hydrodynamic and morphodynamic data obtained near the Noordstrand is analysed. To be able to link these to the observed beach development we adapt an existing Delft3D model to the Marker Wadden Model to fill the missing gaps. All the results are combined to formulate the conceptual system description of the development Noordstrand which links the hydrodynamic and morphodynamic processes. This system description is further discussed when considering shoreline equilibrium, monitoring and maintenance of the beach.

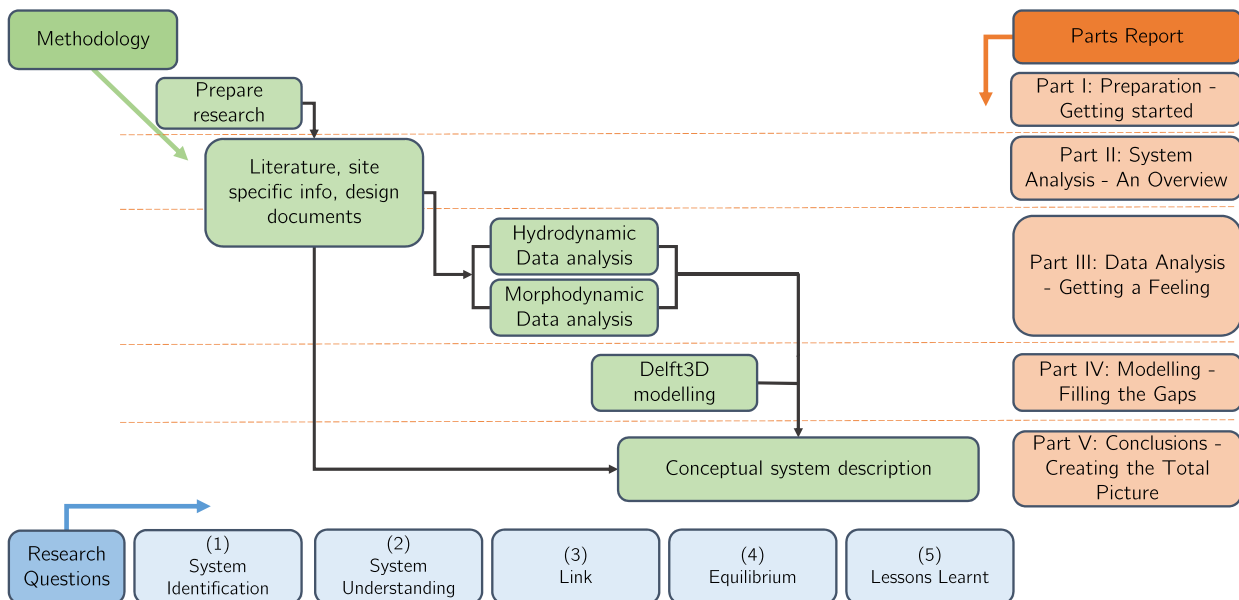


Figure 2.2: Visualisation of the methodology (green) of this research, the corresponding research questions (blue) and to which part of the document the part of the research framework belongs (orange).

2.4 Research Scope

This research project has a limited duration and to avoid scope creep, the scope of this thesis needs to be clearly defined. The items below summarise the main scope of this project and its boundaries:

- The focus of this thesis is primarily on the hydro- and morphodynamic processes in low-energy lake environment using the Noordstrand of the Marker Wadden as a case study. Finding can be used to broaden our understanding of low-energy lake systems in general.
- The focus is on Noordstrand with a non-equilibrium shoreline orientation, sometimes beaches with other orientations or the system as whole (Marker Wadden or Markermeer) needs to be considered for the correct context.
- The main part of the Noordstrand is considered in this thesis, running from the hard edge in the southwest to the start of the sandy prolongation of the beach approximately 1300 meters to the northeast, soft edge. The development of this sandy extension in the northeast is not considered during the analyses (figure 2.3).
- The main focus is on *hydrodynamic and morphodynamic* processes near the waterline. Other processes, such as aeolian transport, are considered but not part of the analyses.
- The data obtained at and around the Marker Wadden in the period of 2019 till 2021 is the main focus of the data processing part of this thesis. The hydrodynamic data analysis focuses on data obtained by FL66 (figure 2.4) from April 2019 till November 2020.
- The proposed and executed GPS measurement plan to monitor changes after the nourishment of the Noordstrand in winter 2020 only provides preliminary results and will not be part of the main focus.
- The data available for the analyses and the corresponding measuring devices are described in subsection 2.4.1.

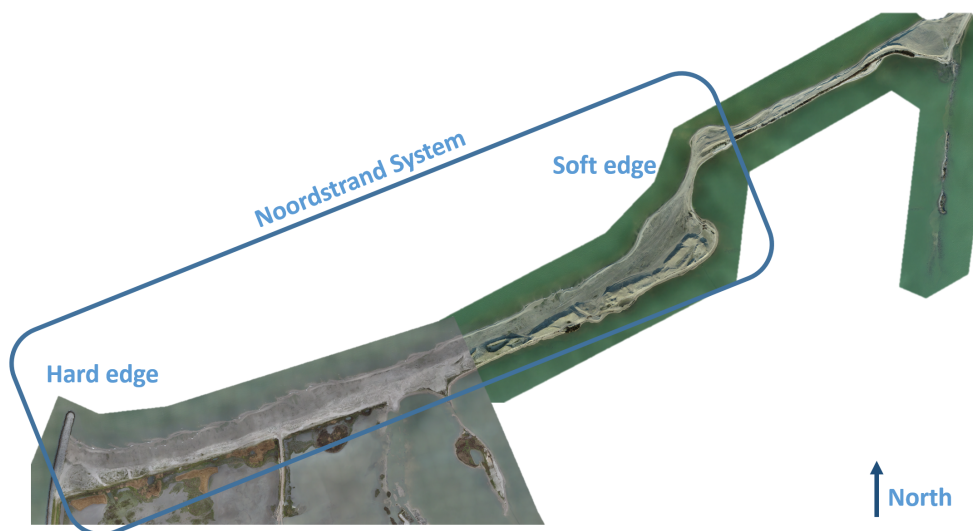


Figure 2.3: Aerial photographs of the Noordstrand (original photos by Surveying Team Boskalis). The blue box shows the part of the Noordstrand that is considered in this thesis: the *Noordstrand system*, starting in the southwest corner with the hard edge (rip-rap breakwater) and the soft edge in the northeast (sandy protection).

2.4.1 Available data

The Marker Wadden and the Houtribdijk are closely monitored by Rijkswaterstaat, providing ample amounts of data. offshore poles are installed to measure wave heights (STB) and current profiles (ADCP) at fixed locations (figure 2.4). Smaller offshore measuring platforms are installed at a specific location for a limited period of time, after which they are removed and re-installed at a new location. These three platforms measure bottom levels (ALTI), currents and wave heights (ADV and AQD) (figure 2.4). The combination of the offshore pole and three measuring platforms create insight in the development of waves and currents nearing the shoreline.

According the initial planning the three measuring platforms would be installed at the Noordstrand in December 2020. However, due to the nourishment of the beach during the same period the installation of these poles was no longer possible. This means only the data of offshore pole FL66 is available for the Noordstrand.

To summarise, the following data is available for this thesis (for more information, see appendix A):

- Data offshore pole FL66 (figure 2.4).
- Topography and bathymetry data of the Noordstrand from 2018 till 2020, measuring differing transects every 3 months.
- Wind data from measuring KNMI stations Houtribdijk and Berkhout (from Royal Netherlands Meteorological Institute (KNMI) (2020)).

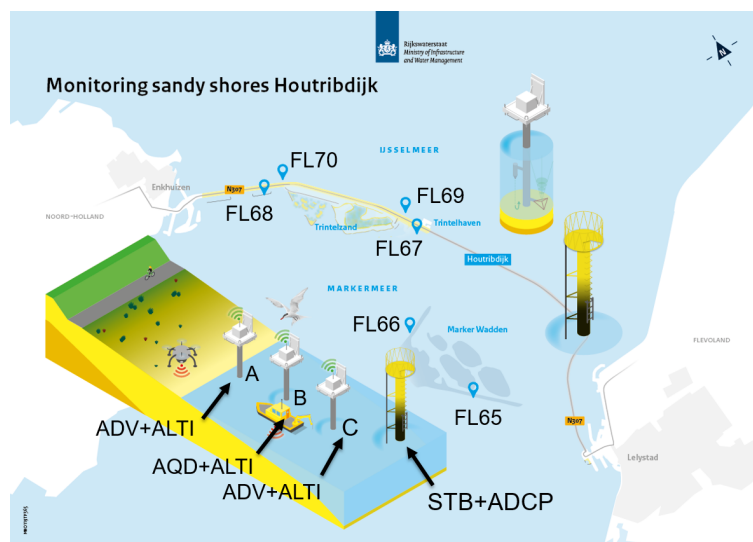


Figure 2.4: Overview of the monitoring campaign at the Houtribdijk and Marker Wadden. The FL locations indicate the permanent offshore poles mounted with a STB and ADCP. A, B and C are smaller measuring platforms, installed at one location for a finite time duration after which they are moved to the next location. They include an ADV, ALTI and AQD. The permanent offshore pole near the Noordstrand is marked *FL66*. The smaller measuring platforms have been installed in the vicinity of the Noordstrand as preferred location of the platforms and the additional nourishment coincided. (Figure adapted from Vuik et al. (2019))



System Analysis - An Overview

3

Literature Review

In this chapter the answer to the first subquestion of the main research question is sought. A literature study is performed to gain insight in the hydro- and morphodynamic processes expected in a lake environment. The main question, regarding **System Identification**, of this chapter is:

Which hydrodynamic processes could steer the (large-scale) behaviour of a beach in a lake environment like the Marker Wadden?

Using the following questions to enable us to answer the main question:

- (a) What are the differences between the lake and sea environment?
- (b) Which hydrodynamic processes occur in this kind of lake environment?
- (c) Which morphodynamic developments do we expect in this kind of lake environment?

This first question (a) is discussed in section 3.1. Question (b) about the hydrodynamic processes is elaborated upon in section 3.2. This is followed with information concerning the morphodynamic processes, question (c), in section 3.3. The conclusion of this literature review is given in section 3.4. The reference to the problem statement can be found in section 3.5.

3.1 Lake Environment

In coastal engineering the primary focus is on ocean and sea environments, followed by estuary and river systems. The sea environment, most of the time a 'high' energy coastal system, is mainly influenced by waves and water level fluctuations caused by tidal variations and surge. The energy density spectrum of the occurring waves varies between very low frequency waves and (short) wind waves (Verhagen and Schiereck, 2019; Bosboom and Stive, 2015). The increased amount of energy in the system is caused by the connection with oceanic waters. Here the circumstances are ideal for creating high-energy conditions: large areas, deep water and unlimited fetch. In a lake environment this connection is missing, resulting in a less energetic system: often called *low-energy*. Nonetheless, this does not mean nothing exciting happens in these systems!

3.1.1 *Low-energy environment*

In general much more is known about 'high' energy coastal environments compared to 'low' energy environments (Cooper et al., 2007; Jackson et al., 2002; Nordstrom and Jackson, 2012; Ton et al., 2019; Vila-Concejo et al., 2020). Even though the total length of low-energy shorelines around the world exceeds the length of the high-energy shorelines (Cooper et al., 2007).

In a lake environment the most important hydrodynamic processes include wind waves, water level fluctuations and for a small part ship waves. Tide and run-off velocities are neglected (Verhagen and Schiereck, 2019). This is also the case for the Marker Wadden. The Noordstrand of the Marker Wadden is not near a harbouring or manoeuvring location for vessels, and as a result the effect of ship waves can be neglected. The main focus

of this research is on hydrodynamic processes in a lake environment caused by natural processes. This includes wind-driven waves and currents, with the wind being the main supplier of energy in the lake system.

Using the terminology described and summarised by Vila-Concejo et al. (2020) and data collected by Ton et al. (2020) we can assess if the Noordstrand of the Marker Wadden is indeed a low-energy environment. The area of lake Markermeer has already been described as a low-energy environment and the beaches of the Marker Wadden were depicted as low-energy beaches (Steetzel et al., 2017; Ton et al., 2019, 2020). This was primarily based on the location, the Markermeer being separated from high-energy environments by the Houtribdijk and IJsselmeer. We find that the characteristics of the Noordstrand are approximately equal to the upper threshold values for the classification of low-energy (table 3.1). As other papers use higher thresholds for the classification of a low-energy beach: $H_b < 1.0m$ (Hegge et al., 1996) and $H_S \approx 0.45 - 0.5m$ (Aagaard, 1988); we deem the slight surpassing of the threshold values acceptable. The Noordstrand is indeed a low-energy beach as was expected from its topographical point of view.

Table 3.1: Comparison of low-energy environment conditions as described by Vila-Concejo et al. (2020) with the prevailing conditions of the Noordstrand at the Marker Wadden, as described by Ton et al. (2020) (using the period of April 2019 till September 2019, taking the 95-percentile H_{m0} as the governing H_S during storm conditions).

Condition low-energy From: Vila-Concejo et al. (2020)	Situation Noordstrand From: Ton et al. (2020)
1 Non-storm significant wave heights are minimal (<0.25 m)	Mean H_{m0} : 0.26 m
2 Significant wave heights due to strong onshore winds are low (<0.50 m)	95-percentile H_{m0} : 0.53 m
3 Beach face widths are narrow (≈ 20 m in microtidal environments (tidal range < 0.25 m))	≈ 20 m (Google Earth; April 2019)
4 Morphologic features include those inherited from higher energy events	True (Steetzel et al., 2017; Ton et al., 2020)

3.1.2 Fetch-limited environment

Other terms used for low-energy systems include 'fetch-limited' or 'sheltered' beaches (Vila-Concejo et al., 2020). Both terms describe a low-energy system, but two significantly different types, although a combination of fetch-limited and sheltered is a possibility (Jackson et al., 2002). The biggest difference between the two is the influence of nearby (high) energy systems, for instance in the connection to a nearby sea in the case of an estuary. In sheltered environments higher energy waves can still penetrate to the beach, but have lost most of their energy due to dissipation and refraction. This beach is thus subject to local and non-local waves. In a fetch-limited environment there is no influence of other high-energy systems. This implies only locally generated wind waves can create energy in the system. The magnitude of the produced energy depends on the wind speed and duration, fetch distance and basin dimensions. In vast basins (which are no longer a fetch-limited environment), for instance the Atlantic Ocean or the North Sea, the wind duration is the limiting factor. This is not always the case for smaller systems such as lakes and estuaries, in which the basin dimension and thus fetch distance becomes equally important. In the case of fetch-limited systems the fetch distance opposed to the wind duration is the limiting factor of wave growth, hence the name (Jackson et al., 2002; Nordstrom and Jackson, 2012).

Lakes and enclosed lagoons are in principle not sheltered: non-locally generated waves are not possible. As the basin dimensions are relatively small, the energy of the existing local waves depends not solely on wind duration, but also on fetch distance. In most fetch-limited systems the fetch is less than 25 kilometres (Cooper et al., 2007). This is also the case for the Noordstrand: the fetch over the Markermeer from the Noordstrand to the northwest (perpendicular to shoreline) is approximately 10 kilometres (Google Earth). For the other beaches on the Markerwadden, the Zuidstrand and Recreatistrand, the fetch increases to 35 kilometres (Google Earth) perpendicular to the shoreline. The fetch of these three beaches is comparable with the fetch distance of other fetch-limited beaches (Jackson et al., 2002). Taking the aforementioned into consideration we can categorise the Markermeer as a low-energy, fetch-limited system; and thus classify the Noordstrand a low-energy, fetch-limited beach.

3.1.3 Depth-limited environment

Lastly, it is important to consider the influence of depth-limitation in the case of the Noordstrand. The Markermeer is relatively shallow with a depth (h) of approximately 4 meters (table 1.1). Using the wave steepness relation, wave height over wave length: $\frac{H}{L}$ and a wave steepness s of 0.05 (characteristic for 'fresh' wind waves (Verhagen and Schiereck, 2019)), we can find a characteristic wave length. Using the 95-percentile and normal mean H_{m0} of 0.26 and 0.53 meter respectively (table 1.1), we find a corresponding wave length L of 5.2 meter and 10.6 meter. We can now calculate the water depth to wave length ratio: $\frac{h}{L}$. The smaller wave height, H_{m0} , results in a ratio of 0.77, meaning 'deep water waves' ($\frac{h}{L} > 0.5$ (Bosboom and Stive, 2015)). The bigger, 95-percentile H_{m0} , results in a ratio of 0.38. Being between the limits for 'deep water waves', $\frac{h}{L} > 0.5$, and 'shallow water waves' $\frac{h}{L} < 0.05$: thus 'intermediate water waves'. These waves do 'feel' the bottom and energy dissipation due to bottom friction plays a role in the development of these waves. If the fetch is short, wave height is still developing, the waves are not depth limited. However as the fetch distance increases, the waves become depth-limited and the effect of depth-limitation has to be considered. As stated by Young and Verhagen (1996): 'With increasing fetch, the effects of the finite depth become more pronounced. The total energy is smaller than would be expected in deep water and the peak frequency higher. With a further increase in fetch, a point is eventually reached where further spectral development ceases. At this point both the non-dimensional energy and peak frequency become depth limited.' Other research underlines the fact that initially, when fetch distance is small, the waves behave as deep water waves (Johnson, 1998). Considering the aforementioned findings and the fact that the depth of the Markermeer decreases even more towards the Noordstrand we have to take into consideration that the waves are also depth-limited.

It is important to realise a depth- or fetch-limited beach is not a scaled-down ocean system beach (Nordstrom and Jackson, 2012). The hydrodynamic and morphodynamic processes taking place can differ significantly, this is discussed in the next section.

3.2 Hydrodynamic Processes

The main hydrodynamic processes of a low-energy and fetch-limited beach include: (locally generated) wind waves and water level fluctuations (with differing origins) (Jackson et al., 2002; Nordstrom and Jackson, 2012; Vila-Concejo et al., 2020). Whereas these papers also discuss the influence of tidal variations, these are neglected in the case of the Marker Wadden as it is a non-tidal environment (Steetzel et al., 2017; Ton et al., 2019). As a consequence tidal reshaping does not play a role at the Noordstrand.

3.2.1 Waves

The main energy source in this lake system are locally generated wind waves. The wave height and period of these waves is determined by the duration, fetch and strength of the wind forcing (Vila-Concejo et al., 2020). Also bottom friction, linked to the dimensions of the lake, plays a role in the dissipation of energy (Jackson et al., 2002; Nordstrom and Jackson, 2012). The orientation of the beach to the dominant wind direction determines the potential of possible wave-energy (Nordstrom and Jackson, 2012). In our case this might indicate a different response between the Zuider- and Recreatiestrand, and the Noordstrand to this wind and wave forcing. The first two beaches face the dominant wind and wave direction, but the latter is oriented in parallel direction (a 90° difference in orientation of the Noordstrand and Zuider-/Recreatiestrand, figure 3.1).

Fetch-limited waves generally have low wave heights and short wave periods (Nordstrom and Jackson, 2012). The significant wave height in non-storm conditions typically does not exceed 1 meter (Jackson et al., 2002). This complies with the situation at the Noordstrand (table 3.1). The direction of the discussed waves can have a high impact on the dynamics of the beach (Cooper et al., 2007). As a result of the short wave length, there is little refraction when these waves propagate towards the shoreline. This results in waves arriving not perpendicular at the beach, but under an (large) angle. Hence the name high-angle beach. This process can have a significant effect on erosion, as these obliquely incident waves can cause enlarged longshore transport rates (Jackson et al., 2002; Nordstrom and Jackson, 2012). Due to the considerable difference in orientation of the Noordstrand opposed to the other beaches of the Marker Wadden this effect is worth investigating.

The local wind climate is thus the primary driver of the wave climate, alternating between higher energy storms

3.3 Morphodynamic Processes

The shaping of fetch-limited beaches is primarily influenced by locally generated wind waves (Cooper et al., 2007). This hydrodynamic phenomenon was discussed in the previous section. As the waves depend solely on the local wave climate we can distinguish conditions varying between storms, (high-energy events) and calm conditions (low-energy events) (Jackson et al., 2002). This difference is important as the morphological evolution of low-energy and fetch-limited beaches depends mainly on storm events (Vila-Concejo et al., 2020). The wave energy during non-storm weather conditions is often too low to reshape the beach (Cooper et al., 2007). This implies the beach cannot recover from cross-shore storm erosion, the energy is just too low. This is opposed to the recovery of a cross-shore beach profile after a storm in an exposed and high-energy environment. Tidal variations and higher wave energy reshape the cross-shore beach profile and bring back the dynamic equilibrium (Bosboom and Stive, 2015). This means the long-term morphological shape of a low-energy beach reflects the different storm events of the past. However, not only limited wave-energy for the reshaping of the beach can cause slow recovery: also the lack of available sediment. This is the case if longshore and cross-shore transport are enhanced, either driving away the available sediment for reshaping or transport the eroded sediment so far offshore that it is lost behind the 'wave base'. The 'wave base' indicates the depth to which the wave causes motion at the sea bed.

Bars and rips are generally not present on a low-energy beach and using the description as described for high-energy beaches, the low-energy beach can be classified as 'reflective' or 'dissipative' (Jackson et al., 2002; Bosboom and Stive, 2015). These are two completely different beach states. As the driving hydrodynamic processes and the resulting morphodynamics of a high-energy beach are significantly different compared to low-energy, we refrain from describing the Noordstrand as either 'reflective' or 'dissipative'.

3.3.1 *Cross-shore and longshore transport*

For simplicity cross-shore transport, longshore transport, and the beach profile development are considered separately. In case cross-shore transport is dominant, this results in an exchange of sediment between the beach face, upper shoreface and lower shoreface. In high-energy environment this cross-shore cyclic behaviour attributes to the recovery of the beach profile after storm events. In low-energy environments this cyclic behaviour is missing and the exchange is solely from the beach face to the upper shoreface. Sediment might be lost below the wave base, if it is transported even further offshore to the lower shoreface. The connection with the wave base could lead to the development of a submerged platform in the case of low-energy microtidal beaches (see next section).

Changes in wind direction and approaching wave angle cause longshore transport. This can be linked to parallel shoreline retreat or advance and the cross-shore slope might not change significantly if longshore transport is dominant (see right image of figure 3.2). The dominance of either cross-shore or longshore transport depends on the shoreline orientation with respect to the dominant wind direction, the associated fetch distance and sediment traps in the environment such as breakwaters or headlands (Jackson et al., 2002).

An increasing wind angle relative to the shoreline indicates a shift from cross-shore to longshore transport. This development on low-energy beaches was already observed by Nordstrom and Jackson (1992), although their findings describe a low-energy meso-tidal beach (figure 3.2). The location of the platform in the case of cross-shore dominance is a function of the tidal range (location relative to high tide (HT) and low tide (LT) in the figure).

Although considered separately, the process and development of a beach is generally a combination of cross-shore and longshore transport. This could mean the shoreline retreats in parallel form due to longshore erosion, but still shows step-like development due to cross-shore erosion and deposition (a combination between the two images of figure 3.2 would arise). Furthermore, the morphological development is much more intricate due to the complex interaction of beach shape, wave processes and local variations in morphology (Lorang and Stanford, 1993).

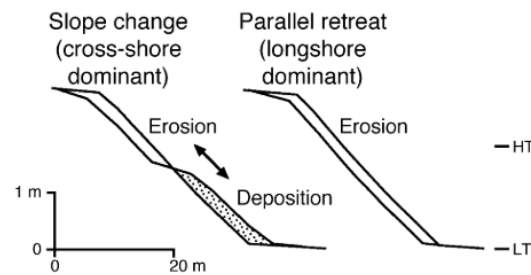


Figure 3.2: Changes in beach profiles for low-energy beaches, specifically for meso-tidal (see high tide (HT) and low tide (LT) level to the right) estuarine beaches from Nordstrom and Jackson (1992). The left image indicates a slope change, occurring in the case of cross-shore transport and the right image shows parallel shoreline retreat caused by longshore transport.

3.3.2 Beach shape

The previously discussed link between the water level variation and wave height influences the beach shape, as it affects the wave base (see previous section). This relation has already been found at the location of the Pilot Houribdijk (north western part of the Marker Wadden). The results describe the formation of a submerged platform (Steezel et al., 2017). More recent research included the analysis of the beaches of the Marker Wadden, at these locations this platform was also recognised (Ton et al., 2019, 2020). A correlation between dimensionless fall velocity, platform width and platform elevation has been established by Ton et al. (2019): 'Wider and deeper platforms are induced by higher wave energy and associated sediment mobility'. The same research found that sediment sorting plays a role in the development of the platform.

Recently the elevation of the platform has been linked to Hallermeier's depth of closure (related to the wave base) and it has been concluded that if the depth of closure has been reached, the platform development remains nearly stable (Ton et al., 2020). This indicates an equilibrium level for the platform elevation is possible for a low-energy beach, based on the depth of closure. The same research found that not only the cross-shore transport is responsible for the platform formation, but that it is a combination of both cross-shore and longshore transport. The beach face erodes during high-energy events and brings sediment from the beach face to the upper shoreface. There the sediment is further distributed by both cross-shore and longshore processes, diluting it over the platform and the lower shoreface. Ton et al. (2020) also found that the elevation of the platform might seem stable but the widening of the platform is still continuing, there is no sign this development is going to halt in the nearby future.

Platform development is also observed in other low-energy environments (Jackson et al., 2002; Allan et al., 2002). Although different names are used for the same phenomena: platform, terrace, plateau, etc. In meso- and macrotidal areas a similar platform can be found and is referred to as low tide terrace. This low tide terrace is in some ways similar to the submerged platform discussed before, as the elevation of the terrace is linked to the tidal ranges and thus to water level variations (Nordstrom and Jackson, 1992). About the complex processes driving the platform development and other morphological features in a low-energy environment a lot is still unknown.

3.4 Conclusion

First, we categorised the Noordstrand as a *low-energy, depth- and fetch-limited, high-angle beach*. Second, we interpreted the hydro- and morphodynamic processes as described by literature in this environment. The most important hydrodynamic processes are: locally generated wind waves and water level variations. Especially the link between the two is important and should always be considered. It is expected that beaches in a fetch-limited, low-energy environment are mainly shaped during high-energy events (storms) and are not or only partly reshaped during normal (quiet) conditions.

The following conclusions regarding the Noordstrand are drawn from this literature review:

- The orientation of the Noordstrand is significantly different compared to the orientation of the Recreatie- and Zuidstrand. It is expected that the enlarged wind and wave angle approach induce additional longshore transport rates.
- The dynamics during low-energy and high-energy events are different and it is expected that high-energy events primarily shape the beach in a lake system. The beach shape should show remnants of previous storm events.
- Most research near the Marker Wadden focuses on the cross-shore profile development, which includes the formation of a submerged platform. This platform formation is a combination of cross-shore and longshore transport (Ton et al., 2020). Nonetheless literature indicates the longshore currents cannot be neglected upon first glance.
- If it is true that the profile is not reshaped and the eroded sediment is lost, this volume loss should be measurable and arises the question: where is the eroded sediment going?
- Detailed understanding of low-energy, depth- and fetch-limited environments is missing. Specific research regarding the Noordstrand is limited. This creates a knowledge gap about these systems and the situation of the Noordstrand in particular. This is discussed in the next section.

3.5 Link Problem Statement

As stated by Nordstrom and Jackson (2012): 'Relatively little attention has been paid to erosion along small inland lakes, reservoirs, and estuaries, but erosion rates in these environments can be great despite low wave energies.' Some research on shoreline erosion in lakes has been performed, but this has been rather site-specific (Lorang and Stanford, 1993; Kirk et al., 2000; Allan et al., 2002). So our knowledge on low-energy, depth- and fetch-limited systems is limited and more research is needed (Jackson et al., 2002; Nordstrom and Jackson, 2012; Steetzel et al., 2017; Ton et al., 2019).

In the Netherlands additional research on the specific case of the Pilot Houtribdijk and Marker Wadden beaches has been performed (Steetzel et al., 2017; Ton et al., 2019, 2020). However, the main focus has been the Pilot Houtribdijk as this project has a longer lifetime and has been monitored for a longer period of time. The morphological development of the soft edges of the Marker Wadden do show some resemblance to the Pilot Houtribdijk, though more research is required (Steetzel et al., 2017). Some analysis has been performed on the beaches of the Marker Wadden. The shoreline orientation of the Recreatie- and Zuidstrand is perpendicular to the dominant wave and wind direction. Resulting in important findings for the cross-shore development of these beaches, such as platform development (Ton et al., 2019, 2020). In the past the situation of the Noordstrand has been assessed in light of the developments observed at beaches with a perpendicular orientation.

However, the Noordstrand is the odd one out: the shoreline orientation is not perpendicular but parallel to the dominant wind and wave direction. This, in combination with short obliquely incident waves arriving at the Noordstrand, might drive additional longshore transport rates (Jackson et al., 2002; Nordstrom and Jackson, 2012). This means the hydrodynamic and morphological development of this beach differs significantly from the other Marker Wadden beaches. Better understanding of the processes of the Noordstrand is needed, and could prove to be beneficial for the maintenance of the beach and for future projects including a 'soft' edge as protection. This research is meant to contribute to the decrease of the knowledge gap of this kind of environments, focusing on the situation in the Markermeer and near the Noordstrand.

4

System Understanding

In the previous chapter several literature sources concerning low-energy systems were discussed, the Noordstrand of the Marker Wadden was analysed in their context. To be able to further investigate the current 'gaps of knowledge' and formulate areas of interest for the remainder of this research, we need to consider the development of knowledge of this system: **System Understanding**. By doing this we can construct the correct context in which the Marker Wadden, were designed and verified. Furthermore, we can add new research, performed after construction of the Marker Wadden. By performing this analysis we form the foundation for current understanding and identify the unknowns. This chapter answers the question:

What is our current understanding of low-energy lake systems?

Using the following subquestions as a guidance:

- (a) How has our knowledge on this kind of systems evolved over time?
- (b) On which part of this knowledge is the design of the Marker Wadden based?
- (c) What are the current 'knowledge' gaps?

Our aim is to create a time line of our knowledge of sandy beaches in low-energy lake environments. In preparation the available literature, as used in chapter 3, is shortly discussed in section 4.1. Question (b) is answered in section 4.2 providing the knowledge framework which was accessible and used for the design of the Marker Wadden. The follow-up and monitoring of this and other projects has resulted in new research, discussed in section 4.3. The evolution of our knowledge in time is summarised in a time line, answering question (a). Combining all the above, this leads to our current understanding of the system, discussed in section 4.5, which concludes by stating the main knowledge gaps (answering question (c)).

4.1 Available Literature

In general a lot of research has been carried out for different coastal systems, mainly focusing on high-energy systems. Information about low-energy systems is also available, but is very specific. A low-energy, lake environment with artificially created sandy beaches is a niche and a whole different story compared to low-energy estuaries or sheltered barrier island beaches.

Generic literature and research concerning this kind of low-energy systems can be used to categorise different systems and give some direction as to predict the development of beach profiles. However, site-specific literature, research and measurements are needed to gain a more in-depth system understanding, as the interaction between different processes is very complex and depends on system characteristics (sections 3.2 and 3.3).

4.2 Design Marker Wadden

No other archipelago was constructed in the Netherlands on this scale before. Expertise and experience concerning this type of 'structure' is thus rather limited. Initially other projects, part of the 'Zwakke schakelprojecten', were used as reference. This included the Delflandse kust, the Sand Engine near Kijkduin and the Hondbossche and Pettemer Zeewering. All three are connected to the North Sea and are high-energy systems. For the Marker Wadden, the state of the system differing this much from other projects, a more relevant test location was created to provide more insight in the development of sandy beaches in a low-energy environment. The construction and development of the artificially created beach, Pilot Houtribdijk, was closely monitored. This pilot provided a great deal of data specifically targeting the development of a sandy beach in a lake environment as stated by the data report: Vuik et al. (2019).

The results of this pilot provided the main input for the verification of the design of the sandy edges of the Marker Wadden (Van Santen, 2016). This design with sandy edges was innovative, but also the design process was novel. Normally requirements 'shape' the design. However, in case of the Marker Wadden project, landscape architects first designed the archipelago and beach dimensions, which were verified in the next step. This verification included modelling different scenarios, to assess whether or not this design met the requirements as drawn up by the client. The assumptions and limitations of the design of the Marker Wadden are discussed in the next sections.

4.2.1 Assumptions design

The masterplan design of the Marker Wadden as designed by Vista landscape architects, was verified by Arcadis (Van Santen, 2016) mainly using different modelling agents (CROSMOR, LONGMOR and XBeach) and results of the research performed in light of the Pilot Houtribdijk. The final verified design included the following, as taken from Boskalis Nederland (2015):

- Focus on natural and ecological restoration of the biodiversity and habitat formation for birds and fish
- Smooth sandy dunes are created under the influence of water and waves
- The cross-shore profile is based on an equilibrium profile plus an additional wear layer. The profile of the Noordstrand is somewhat steeper (1:20 compared to 1:25) as less severe wave conditions are expected
- The longshore profile (orientation of the shoreline) is perpendicular to the dominant wind and wave direction. However, this is not the case for the Noordstrand. This situation is not discussed in depth during the verification, indicating an uncertainty in the design
- The sandy beaches are 'enclosed' by a hard edge or sandbuffer. The Noordstrand is on the northwest side protected by a hard edge and on the northeast side by a wider and higher sandbuffer (soft edge) (figure 2.3). The sandbuffers are designed to act as 'sand engines' providing the system with additional sediment.
- Stronger currents are expected around the northwestern top of the Marker Wadden (northeast of Noordstrand)
- Initial erosion is compensated with wear layers on top of the design profile and sandy buffers located at the edges of the beaches
- No maintenance is expected for the first 10 years, after these first 10 years there is no maintenance expected for the client for the following 10 years

4.2.2 Limitations design

The limitations of the design are numerous, which is not surprising considering the innovative location, design and design approach. The limitations are recognised and acknowledged by Van Santen (2016) during the verification process. As a result the design includes an extensive risk-management plan to deal with the limitations and uncertainties. Furthermore, one should not forget the development of the Marker Wadden is closely monitored and researched to be able to reduce limitations and uncertainties in future maintenance and design.

Modelling

One part of the limitations of the verification can be found in using high-energy models to verify a design in a low-energy environment. The models used for verification include CROSMOR, LONGMOR and XBeach. The question arises if these models give a correct representation of this entirely different system. Additionally an existing Delft3D-SWAN model is used to assess the uncertainties of the wave climate as calculated with the Brettschneider approach (Van Santen, 2016).

Furthermore for these modelling agents input parameters, for example water depth and sediment size, are needed. For these parameters assumptions are used, based on field observations, measurements and expert judgement. Deviations from the real in-situ values are very much possible and can potentially be the origin of processes which behave differently compared to expectations based on model runs.

In addition the different processes accountable for shaping a beach are regarded more or less separately in the design. The morphological stability of the beach profile in cross-shore and longshore direction is considered individually. For optimal understanding and representation the combined processes need to be considered, as the evolution and development of a beach is an intricate interaction between the different processes. Even bigger and smaller beach features can enhance overall or location-specific development.

Orientation

The design of the Marker Wadden and the prediction of morphological behaviour of its beaches is primarily based on the knowledge obtained by the project Pilot Houtribdijk. This project has resulted in numerous insights in low-energy beach development, but has one major limitation: namely its orientation. The shoreline of the Houtribdijk beach is oriented perpendicular to the dominant wind and wave direction. Therefore, this is not a correct reference case for the Noordstrand as it has a completely different orientation: parallel to the dominant wind and wave direction. The used assumption that the processes at the Noordstrand behave roughly the same as the perpendicularly oriented beaches might be too straightforward.

To the best of their knowledge the designers have considered the accountable processes and development of the contrary case of the Noordstrand. The knowledge of this kind of systems is limited, the particular case of a non-equilibrium orientation even more so.

Disturbance

The construction of the Marker Wadden introduced a major disturbance of the natural processes in the Markermeer lake. It is unknown how this system is going to respond to this disturbance and which processes are enhanced, reduced or not affected over time. The timescale in which the natural system restores its equilibrium is unknown.

4.3 New Research

In the past years new results of the Pilot Houtribdijk have been analysed and have created new insights. Furthermore the first results of research conducted at the newly constructed Marker Wadden are presented. Both help in our understanding of these sandy protections in low-energy systems. The most important findings (as already summarised in chapter 3) include: more perceptions in the link between platform development and combined hydrodynamic forcings such as water level and wave height, and the influence of high-angle waves on the formation of three-dimensional features such as beach cusps.

4.4 Time Line

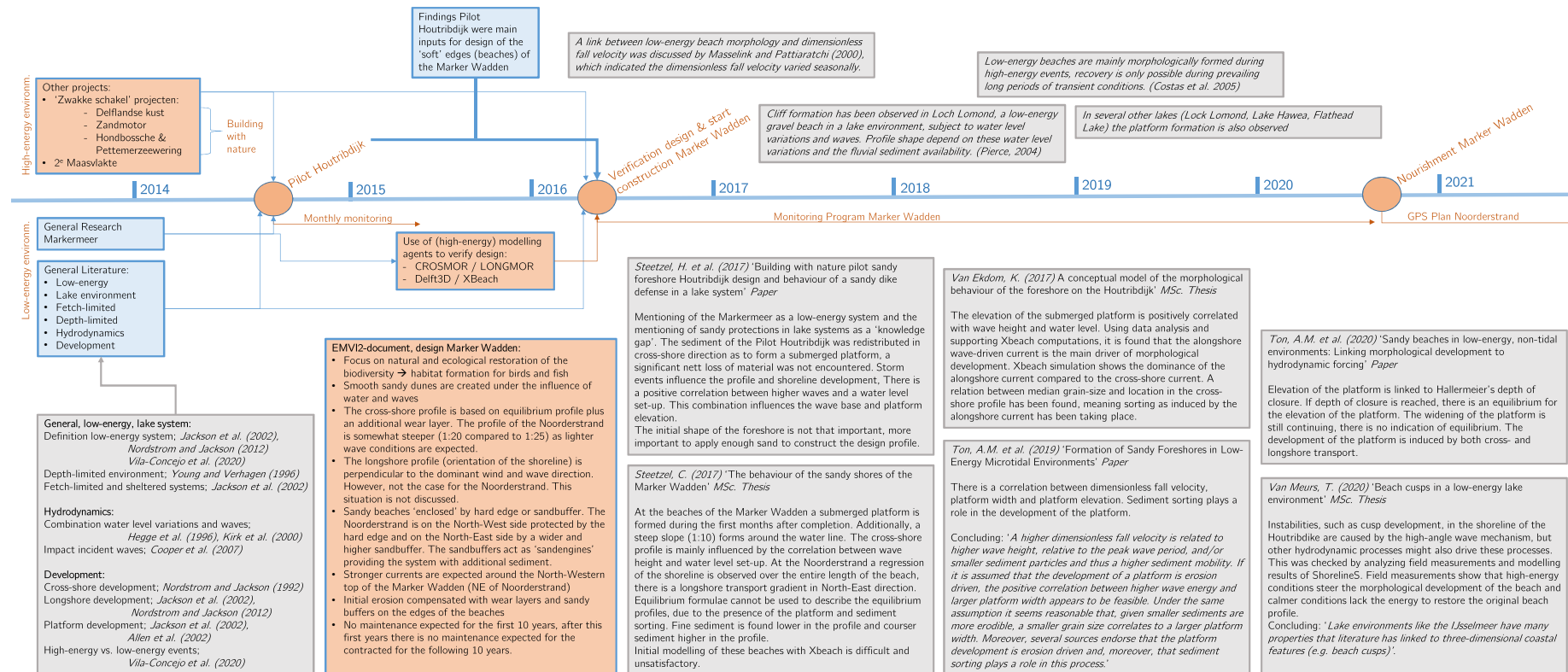


Figure 4.1: Timeline of our knowledge concerning low-energy lake systems. Some sources are specifically used as input for the Marker Wadden design (orange boxes). Larger orange dots on the timeline indicate main events concerning the Marker Wadden design, verification, construction and maintenance. Relevant literature formed by research conducted at Pilot Houtribdijk, Marker Wadden and other low-energy (lake) environments are summarised in the light grey boxes.

4.5 Conclusion

To summarise our understanding of the low-energy lake system and its hydro- and morphodynamics the following section gives the main take-aways from research up until now (figure 4.1). The last section indicates the present 'gaps of knowledge', to be used as stepping stones for the focus of this research.

4.5.1 *Current state*

It is mainly the interaction between cross-shore and longshore transport that drives system development in low-energy lake environments. Most research focused on beaches with an equilibrium shoreline orientation relative to the dominant wave direction.

Low-energy (lake) environment/system:

- Fetch- and/or depth-limited system
- High incident waves experience little refraction and thus enhance longshore currents
- High-energy events cause morphological changes
- Low-energy events do not have sufficient energy to reshape profiles after storms, although prolonged transient periods can induce some recovery
- Three-dimensional features at the beach are possible
- Formation of an offshore submerged platform is possible. At less exposed beaches the shape of the platform is more profound and the beach face is steeper and narrower

Disturbance

In case the natural system is significantly disturbed, we can conclude the following:

Beaches in this system with equilibrium shoreline position:

(perpendicular to dominant wind and wave direction)

- Design/initial profile not that important if available sediment is enough to form the natural profile
- Redistribution of sediment in cross-shore direction, no net loss of sediment over the cross-shore transects
- Shoreline regression
- Submerged platform is formed
 - Platform elevation linked to depth-of-closure (Hallermeier)
 - * Elevation linked to water depth and wave height
 - * Elevation stable (in equilibrium)
 - Platform width is still developing
 - Formation and development of platform linked to cross-shore and longshore transport
- Sediment sorting can occur
- Correlation water level and wave height if both are high this results in more erosion

Beaches in this system with non-equilibrium shoreline position:

(parallel to dominant wind and wave direction)

- Shoreline regression
- Submerged platform is formed
 - Platform elevation linked to depth-of-closure (Hallermeier)
 - * Elevation linked to water depth and wave height
 - * Elevation stable (in equilibrium)
 - Platform width is still developing
 - Formation and development of platform linked to cross-shore and longshore transport

4.5.2 Visualisation

The previous findings are summarised in an 'infographic' (figure 4.2).

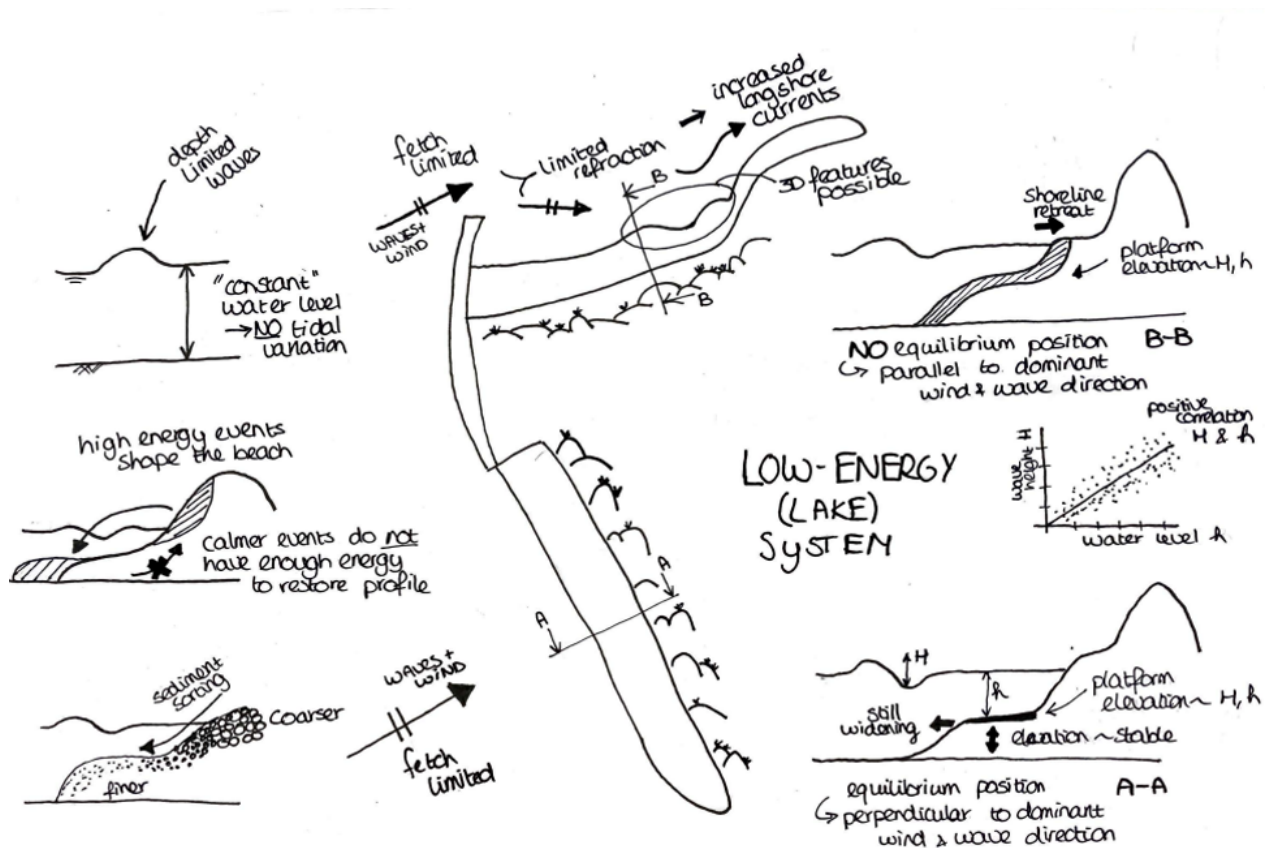


Figure 4.2: An infographic of our understanding of low-energy lake systems, showing the main findings from literature and other relevant projects (Pilot Houtribdijk, Marker Wadden). The shape of this system resembles the Marker Wadden, but can be used to explain any low-energy lake system with varying shoreline orientation.

4.5.3 Knowledge gaps

Overall the hydrodynamic and morphological processes in a low-energy system are not yet understood. Most focus has been paid to beaches with an equilibrium shoreline orientation with respect to the dominant wind and wave direction. This has led predominantly to insights in the cross-shore development of the beach profile.

The main knowledge gap is associated with the unknown development of a beach with non-equilibrium shoreline orientation, in a low-energy system.

The uncertainty of the development of a beach with this orientation also incorporates the unknown coupling between cross-shore and longshore processes, responsible for beach development as a whole. One should avert from considering cross-shore and longshore processes separately, but regard and research the beach and its processes as a whole.



Data Analysis - Getting a Feeling

5

Methodology - Data Processing

This chapter discusses the methodology applied during the data processing part of this thesis. The chapter starts with section 5.1 which discusses the time frame for the data selection. The last part is split into the two main parts of the data analysis: hydrodynamics (section 5.2) and morphodynamics (section 5.3).

5.1 Considered Period of Time

To be able to investigate the link between different processes at the Noordstrand an undisturbed measuring period is desirable. External factors, such as construction works and maintenance of instruments, influence the data and should be terminated. As morphological features develop in months to years (Bosboom and Stive, 2015), a significantly long period of undisturbed data is preferable.

The monitoring program of the Markermeer, Marker Wadden and Houtribdijk started already in 2018 (Vuik et al., 2019). Offshore measuring station FL66 near the Noordstrand was only fully operational in April 2019 (Ton, 2020). April 1, 2019 is therefore chosen as the starting date. Due to ongoing erosion near the Noordstrand additional nourishments near the Noordstrand started in November 2020, to be finished in December 2020. As a consequence the end date of the 'undisturbed' period of time is marked by the start of the nourishment. Before the nourishment work started the ADCP at FL66 malfunctioned, changing the end date to 19 November 2020. Concluding, the time period from April 2019 till November 2020 is used in the hydrodynamic and morphodynamic data analysis.

After the nourishment of December 2020 the morphological development of the beach is monitored monthly (appendix G) Due to previously stated malfunctioning of the ADCP end of November 2020, the removal of FL66 in February 2021 due to bad weather conditions and the end of the measuring campaign in March 2021, hydrodynamic data at the Noordstrand after the nourishment is very limited and insufficient to be linked to morphological measurements (topography and bathymetry changes).

Primary focus on time period:
1 April 2019 - 19 November 2020

5.2 Hydrodynamics

The hydrodynamic data is retrieved from a Data Management System (DMS) controlled by HKV, as discussed by Vuik et al. (2019). After retrieval of the data the main processing includes: finding water level fluctuations at FL66, performing a peak-over-threshold method to identify high-energy events and analysing individual events.

5.2.1 Water level fluctuations

The step gauge (STB) at FL66 measures the water level relative to NAP, which fluctuates during the year (figure 6.3). We are interested in periods of set-up or set-down to be able to link this to other phenomena such as wind, waves and current. The following options are considered:

1. No processing, work with water level relative to NAP.
2. Remove rolling average from water level measurements, different time frames for the rolling average are investigated: 7 days, 10 days, 20 days and 30 days.
3. Using water level differences between FL66 and FL67, the latter is located near the Houtribdijk (figure 2.4). Positive values indicate a set-up, negative values a set-down.

A link between wind direction and set-up was already discussed in chapter 3. Wind directions directly facing the Houtribdijk, parallel to the Noordstrand shoreline orientation, significantly influence set-up or down values. Therefore the wind directions are split into four segments: 20°-110°, 110°-200°, 200°-290° and 290°-20° (same segments as are used in further analysis: figure 6.1). A higher correlation between parallel oriented wind directions with respect to the shoreline and set-up/down is expected. Splitting the data into segments gives a better representation of the correlation. From preliminary data plotting a second order polynomial fit is presumed better than a linear fit. Python's *np.polyfit* function is used to fit a second order polynomial ($p(x)$) to the data, minimising the squared error (E). The residual error is normalised using the variance (σ^2). The closer this normalised residual is to zero, the better the fit.

$$E = \sum_{j=0}^k |p(x_j) - y_j|^2$$

$$\sigma^2 = \sum_{j=0}^k (y_j - \mu)^2$$

From option 2, remove a rolling average, the 10-day rolling average proves to be best. Compared to option 1 (water level relative to NAP, figure B.1a) and option 3 (water level difference between FL66 and FL67, figure B.1b), option 2 has the smallest normalised residual (figure 5.1). This method is thus chosen to find the water level fluctuations. The latter can be found by subtracting the 10-day rolling average based on the water level relative to NAP from the water level points relative to NAP. Analysis of the other 2 methods can be found in section B.1.

Furthermore it is interesting to note that the correlation between wind speed and water level fluctuation is higher if the wind is coming from 200°-290° (normalised residual of 0.48, figure 5.1), compared to the other parallel direction 20°-110° (normalised residual of 0.61, figure 5.1). Winds from the other segments show almost little to no correlation (bottom two plots, figure 5.1). It is worth noting that winds from 200°-290° seem correlated with positive water level fluctuations: set-up, and winds from 20°-110° with negative water level fluctuations: set-down.

Comparing wind conditions and water level fluc. (10-day average removed)

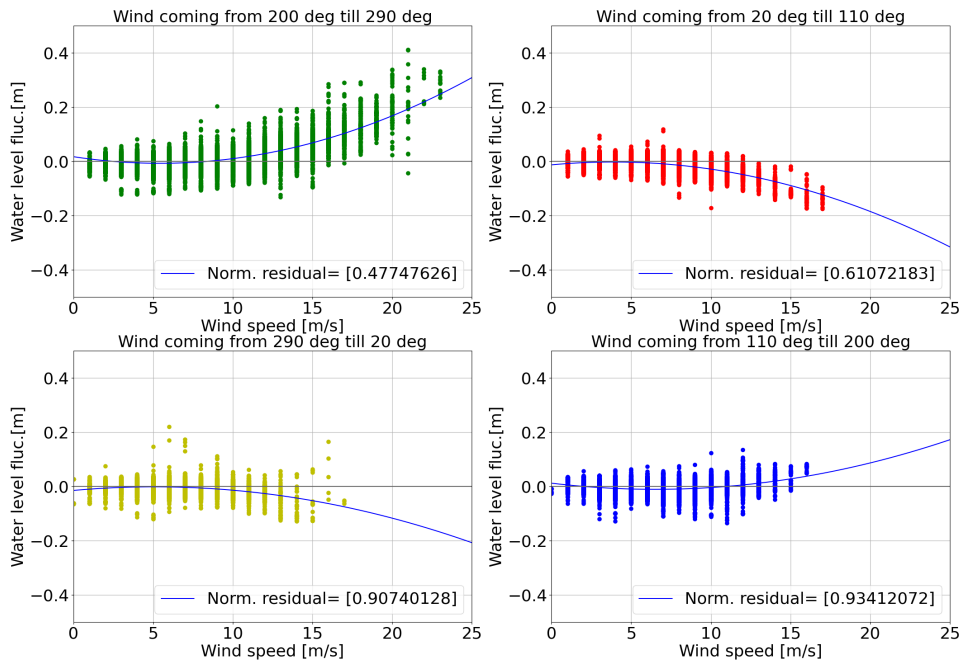


Figure 5.1: Four different plots, each representing a different segment based on wind direction (see figure 6.1): hourly averaged wind speed versus water level fluctuations (obtained by removed a 10-day rolling average on the water level points). A second order polynomial (blue line) is plot through the data points and the normalised residual of the least squares method is shown in the lower right. The closer to zero, the better the fit of the polynomial to the data.

5.2.2 Peak-over-threshold - waves

The classification of high-energy events is based on wave height, as this categorisation is used in papers on low-energy beaches and other research focusing on the Markermeer. The threshold is set to 0.5 meter, right on the boundary of the low-energy classification (Aagaard, 1988; Vila-Concejo et al., 2020). Ton et al. (2020) has also used 0.5 meter as a threshold for the identification of high-energy events in the Markermeer. Alternatively, water level fluctuations or water level differences between FL66 and FL67 can also be used to find peak events (section B.5).

Using Python's `scipy.signal.find_peaks` peak-over-threshold tool we are able to classify peak events (using the input as described in table 5.1). This results in 146 high-energy events (figure 6.9). Using water level fluctuations or difference in water level at FL66 and FL67 we find fewer peak events (51 and 12 respectively, when using 0.1 meter as a threshold value). The 12 peak events found whilst comparing the water level at FL66 and FL67 correspond with the peak events identified when using the water level fluctuations at FL66 only (figure B.27), indicating that high set-ups to the Houtribdijk correspond to high water level fluctuations near FL66.

Table 5.1: Input for peak-over-threshold method to identify high-energy (peak) events, *based on waves*.

Peak-over-threshold parameter	Setting	Unit	Source (if relevant)
Threshold	0.5	meter	Aagaard (1988); Vila-Concejo et al. (2020) Ton et al. (2020)
Minimum distance between peaks	12	hours	Engineering judgement
Prominence	0.3	meter	Ton et al. (2020)

5.2.3 Selection events

Three high-energy events from the identified peaks are selected to be analysed individually based on interesting phenomena (official storms) and availability of data. Two calm periods are added to the list. All events are summarised in table 5.2.

Table 5.2: Summary of individually considered events: high-energy and calm periods. If applicable interesting information considering the period of time is noted in the column *Notes*. The section in which the event is discussed is noted in the last column *Section*.

Event nr.	Description	Start event	End event	Notes	Section
1	High-energy	5 June 2019	14 June 2019	-	Section B.4.2
2	High-energy	7 February 2020	19 February 2020	Storm Ciara and Storm Dennis; max. wind gust measured	Section 6.2.2
3	High-energy	24 August 2020	30 August 2020	Highest significant wave height measured	Section B.4.3
4	Calm	5 April 2020	12 April 2020		Section B.4.4
5	Calm	11 July 2020	18 July 2020		Section B.4.5

5.3 Morphodynamics

The data for the morphodynamic analysis is composed of GPS measurements obtained in various ways (section A.2). The retrieval dates and availability of data at certain locations varies (also section A.2).

The raw data is first filtered and next interpolated on a grid covering the Noordstrand. This method enables us to produce general overviews of the development of the beach, mainly in longshore direction. Different transects are analysed to understand the development of the beach in cross-shore direction.

5.3.1 Projection and interpolation on a grid

The raw data is filtered by applying a filter pass on the data for which error measurements are available. If the error exceeds 0.10 meter, the data is removed from the dataset. Next a polygon covering the area of the Noordstrand is created (shown in red in figure C.1). Only data within this polygon is interpolated on the grid to save computation time.

The data is interpolated on a grid composed of 500 meter long transects evenly spaced every 20 meters (grey grid shown in figure 5.2). Later specific transects can be considered for the cross-shore analysis (transects 100 meter apart are analysed later, see coloured transects in figure 5.2). For the interpolation Python's *scipy.interpolate.griddata* function is used. Using the *linear* method of interpolation, we create a smoother resolution opposed to the *nearest* method (the latter takes less computation time, but the data is interpolated step wise instead of linearly). The threshold for the interpolation is set to 10 meters, meaning if the closest data point is more than 10 meters away a NaN (Not a Number) value is placed on the grid.

5.3.2 Transects

The interpolated data is rotated with 23.5° and processed to display vertical and horizontal distance to the reference point (the reference point is shown as the green dot, one of the corners of the polygon; figure C.1). This to enable the comparison of different transects during the transect analysis.

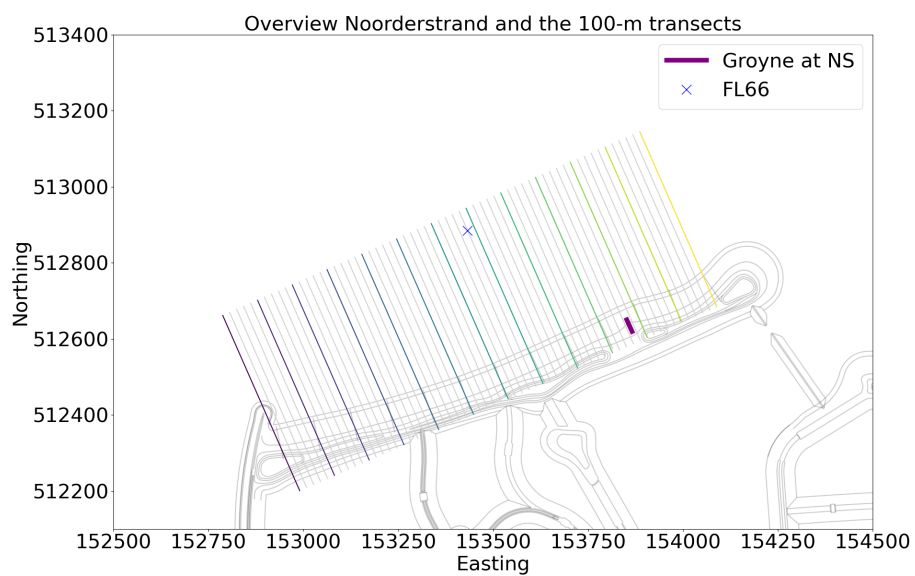


Figure 5.2: Overview of the Noordstrand showing the transects of the grid (grey lines) and the transects used for the cross-shore analysis in chapter 7: 100 meters apart. The offshore measuring station FL66 and the groyne are also shown as a blue cross and purple line respectively.

6

Hydrodynamics

This chapter discusses the data analysis performed using the hydrodynamic data available at FL66 and wind data measured by the KNMI. The data-processing method is discussed in chapter 5. For additional information and extensive graphs the reader is referred to appendix B. First, general overviews of the data are presented in section 6.1. Followed by the analysis of high-energy events and using the data obtained during storms Ciara and Dennis (February 2020) as a representation of what happens during a peak (high-energy) event, in section 6.2. Conclusions based on the hydrodynamic data analysis are given in section 6.3.

Main considerations to keep in mind while reading this chapter:

- Only data obtained in the period *April 2019 till November 2020* is considered (section 5.1)
- Available data: KNMI weather data obtained at the Houtribdijk, step gauge and ADCP data from offshore measuring pole FL66 near Houtribdijk (more information on instruments and data: appendix A)
- For data points concerning directions (either wind or current) the plotted angle is the direction the wind or current is *coming from*, relative to the north
- The *names* of the four coloured parallel lines in figures, indicate where the wind or current is *going to*

6.1 General Data Analysis

This section is split into the four main hydrodynamic processes of the Markermeer lake-system: wind, water level variation, waves and current. The wind is the main driver of the other 3 processes in a low-energy lake environment (section 3.2). Four sections relative to the orientation of the Noordstrand are identified, which proves to be useful in the analysis of wind and current direction (figure 6.1). This rose is shown on top of imagery of the Noordstrand and Markermeer in figures B.2a and B.2b respectively.

6.1.1 Wind

Wind measurements are obtained near the Houtribdijk (Royal Netherlands Meteorological Institute (KNMI), 2020) and analysed to create a wind rose for the period April 2019 till November 2020 (figure 6.2). The average hourly wind speed during the considered period is 7.4 m/s. The primary wind direction is southwest (coming from). The maximum measured wind gust occurred on the 9th of February 2020 at noon (during storm Ciara) and equalled 32 m/s. A critical remark considering the wind speed obtained at station Houtribdijk has to be given to the reader: due to the set-up of the station on the dike the wind speeds are slightly overestimated. This overestimation is noted, but considered acceptable for the hydrodynamic data analysis. For the modelling part the wind speed is adjusted (section 8.3).

Around high-energy (peak) events (classification of these events, section 5.2.2) the direction the wind is coming from changes slightly to the western segment. Hourly averaged wind speeds can increase up to 20 m/s (figures B.3a and B.3b). During high-energy events wind from the northwestern to southern segments is negligible, although this is also an indirect result of the used classification of peak events. The fetch and thus build-up of waves is longer if wind originates from the southwestern to western direction and as a result these occasions are more likely to be classified as peak events.

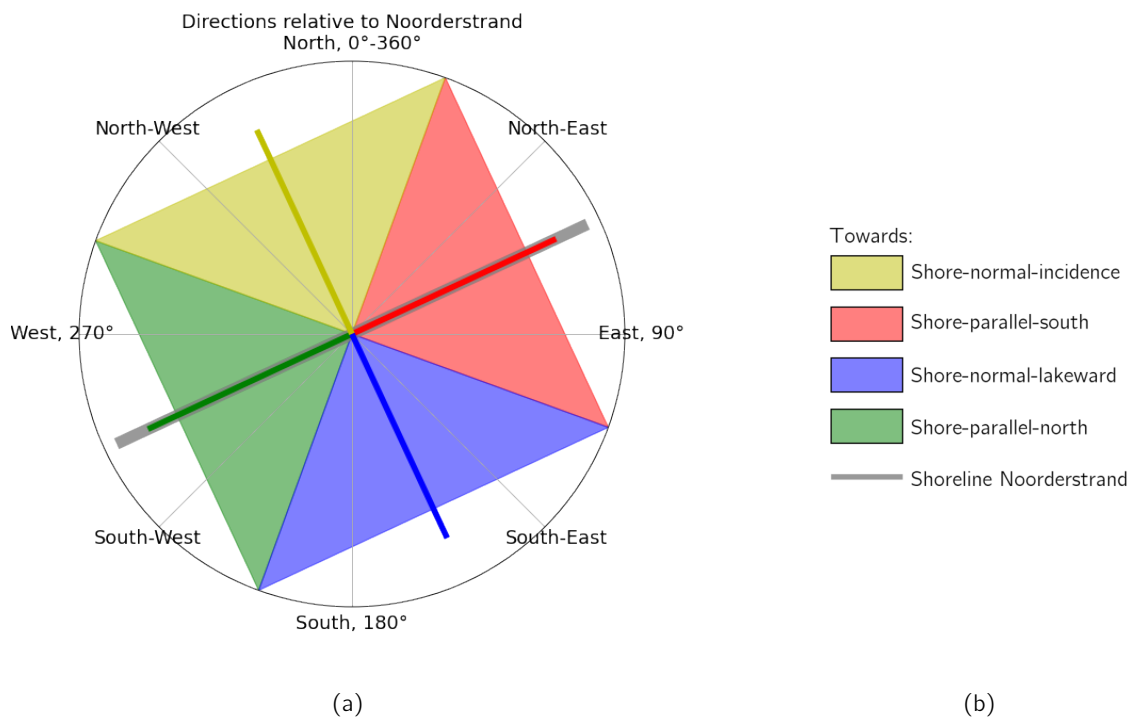


Figure 6.1: (a) Rose divided into four sections all relative to the Noordstrand orientation. The beach heading is 245° (shoreline is the grey line underneath shore-parallel-south/north). The angle of the wind or current data shown in graphs is the direction the wind or current is *coming from*. (b) The colours indicate the direction the wind or current are *going to*. 4 parallel coloured lines can be found in graphs with directions and correspond to this description.

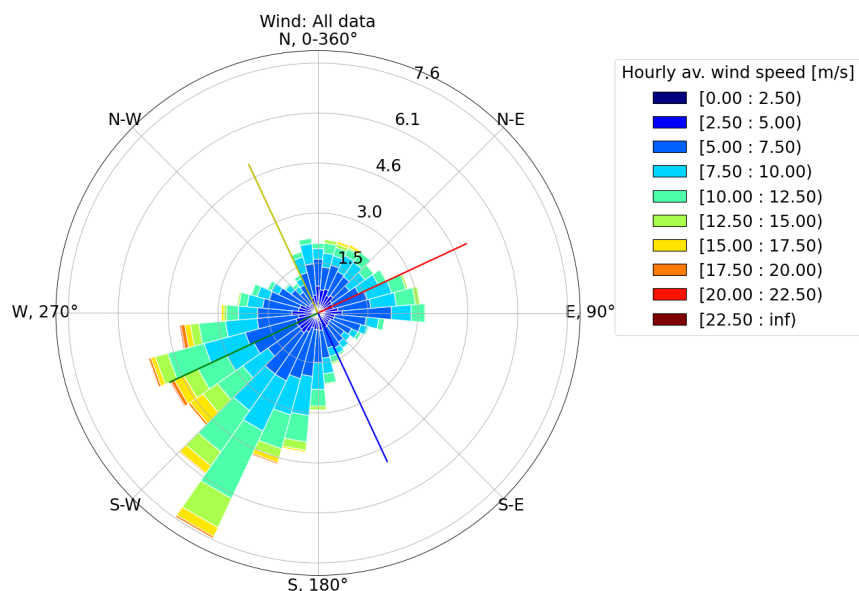


Figure 6.2: Wind rose of data from April 2019 till November 2020. The four coloured lines correspond to the different directions relative to the Noordstrand (figure 6.1). The colours of the bars indicate the hourly average wind speed in m/s. The bars are normalised, meaning the length of the bar corresponds to the relative frequency of occurrence. The angle is the direction the wind is *coming from*.

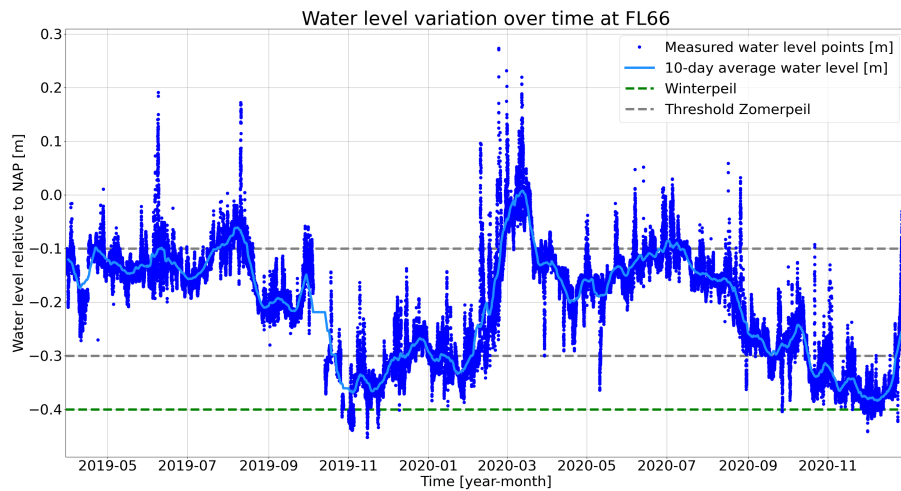


Figure 6.3: Time series of water level variation in meter relative to NAP as measured by the step gauge at FL66. Darker blue are individually measured water level points, the light blue line is the 10-day average water level relative to NAP. The grey and green lines show the 'zomerpeil' and 'winterpeil' respectively.

6.1.2 Water level variation

The water level relative to NAP in the Markermeer oscillates during the year. Rijkswaterstaat (2018) has prescribed a lower limit for the water level in winter of -0.4 meter NAP (green line, figure 6.3) and during the summer the water level is controlled to fluctuate between -0.3 and -0.1 meter NAP (grey lines, figure 6.3).

During individual events, in duration ranging from hours to days, the water level can significantly deviate from its 10-day average water level (figure 6.3). Wind 'pushes' the water to the Houtribdijk, creating a set-up over the Markermeer. Especially increased wind speeds from the southwestern direction, which are quite common (figure 6.2), can create set-ups as high as 0.4 meter (figure 6.5).

6.1.3 Waves

The significant wave height (H_{m0}) is calculated from measurements made by the step gauge (STB). The highest wave height measured occurred on the 23rd of February 2020 and was 1.2 meter high. This is quite significant considering an average water depth of 4 meter in the Markermeer.

A clear link between wind speed and wave height is evident. Coupling of water level fluctuations (mostly positive set-up) and wave height in the Markermeer was already shown by Steetzel et al. (2017) and Ton et al. (2019). The same links are evident when comparing wind speed, wave height and water level fluctuations measured at FL66 (figure 6.4). A positive linear relation between wind speed and wave height is visible: higher wind speeds lead to higher water level fluctuations. The highest waves do not occur simultaneously with maximum wind speeds, some delay between increase of wind speed and build-up of waves is expected. Set-up is faster to respond to increased wind speeds and maximum set-up occurs at almost the same instant as maximum wind speeds (dark red dots at the far right in figure 6.4).

When adding wind direction, one can see that winds coming from the southwest (250°) result in increased wave heights and higher set-ups (yellow to red dots, figure 6.5). This is especially evident if higher wind speeds are present (size red dots, figure 6.5). Winds from the shore normal direction ($\approx 150^\circ$) never result in wave heights higher than 0.2 meters nor is high set-up expected. An interesting finding is the combination of increased wind speeds from the north to northeast direction ($\approx 20^\circ$) leading to a set-down in combination with higher waves (orange and red dots in the lower left corner, figure 6.5).

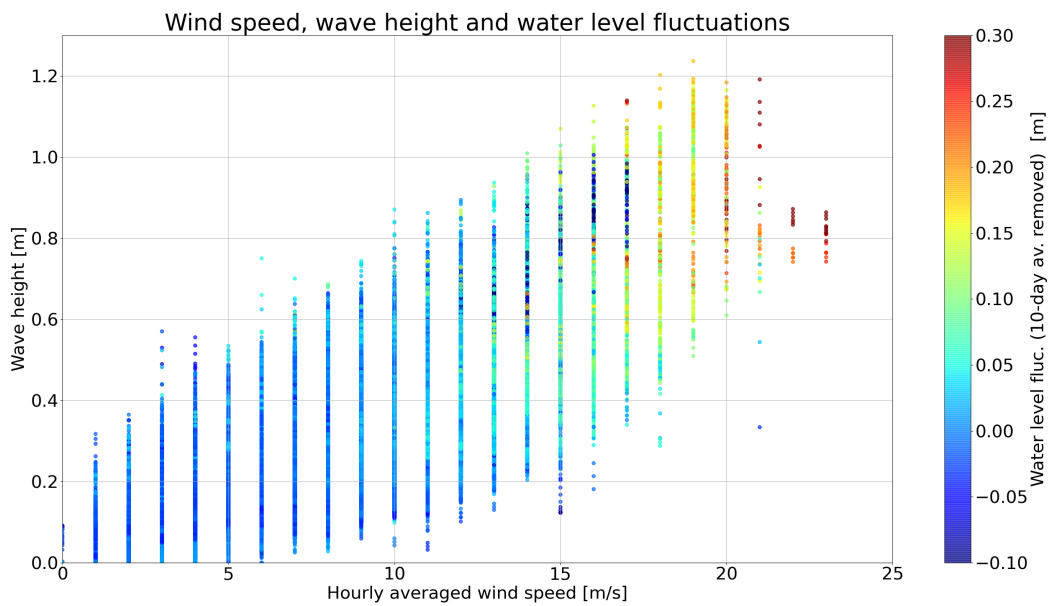


Figure 6.4: Hourly averaged wind speed in m/s plotted against wave height in meter, the colour of the dots indicate the water level fluctuations (10-day average removed).

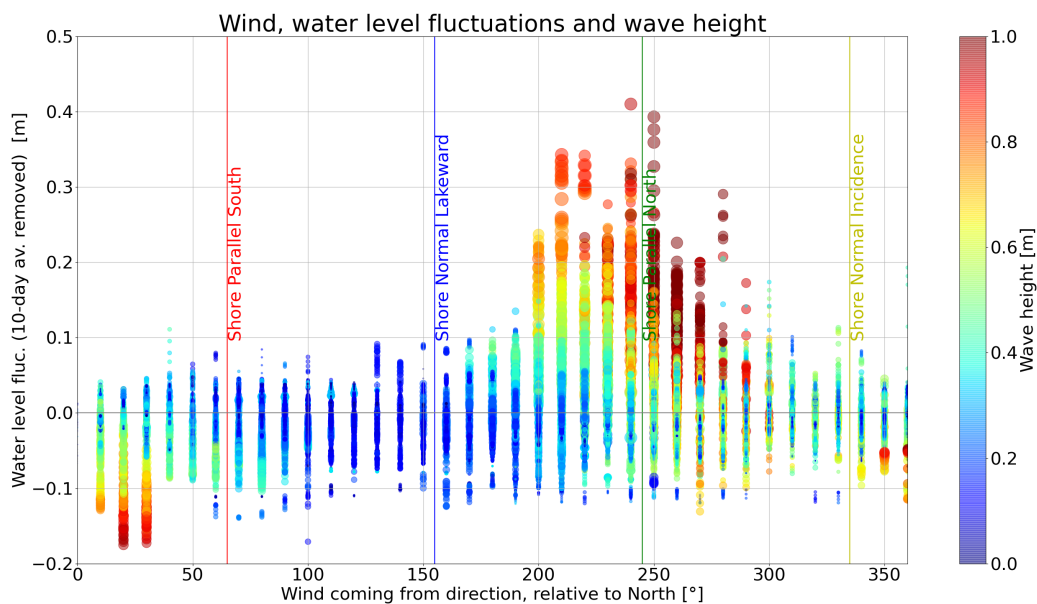


Figure 6.5: Wind direction (coming from) in ° plotted against water level fluctuations (10-day average removed). The colour of the dots indicate the wave height in meter, legend shown on the right. The size of the dots corresponds to the hourly averaged wind speed squared (FH^2), meaning the larger the dot the larger the corresponding wind speed in m/s. The four vertical lines are linked to the different directions relative to the orientation of the Noordstrand as shown in figure 6.1.

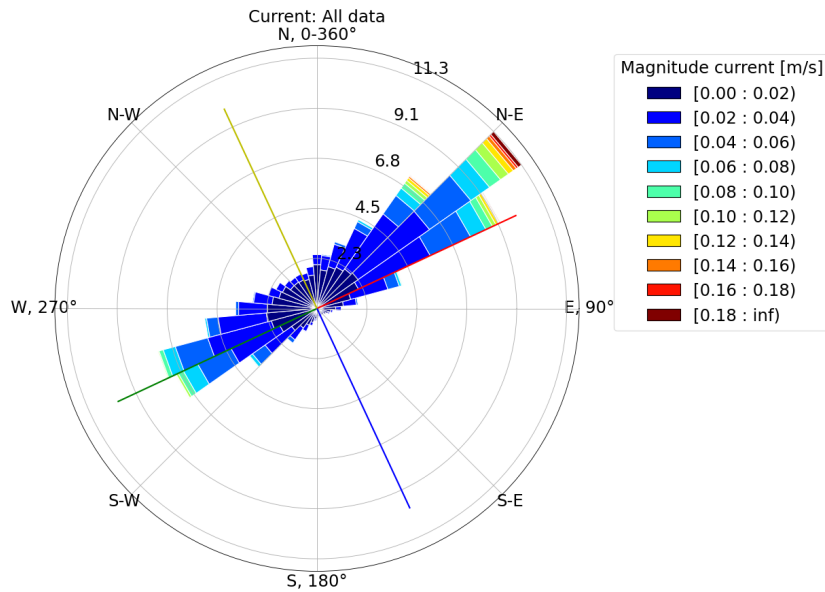


Figure 6.6: Current rose of data from April 2019 till November 2020. The four coloured lines correspond to the different directions (figure 6.1). The colours of the bars indicate the depth-averaged current magnitude in m/s. The bars are normalised, meaning the length of the bar corresponds to the relative frequency of occurrence. The angle is the direction the current is *coming from*.

6.1.4 Current

An ADCP (Acoustic Doppler Current Profiler) measures the current profile at FL66. This data is depth-averaged to be able to analyse the general current magnitude and direction. Limitations of the ADCP and the effects on the measured current profile are described in appendix A. The biggest limitation is the lack of data in the top of the water column ($\approx 1\text{ meter}$), missing information regarding the current near the surface.

As the location of FL66 is outside the shoaling zone, the current at depth is believed to be unaffected by waves. In general the depth-averaged current flows parallel to the shoreline orientation (most bars close to green and red line. figure 6.6). The northeast direction is a more common origin of currents compared to the west or southwest. The magnitude of the current can increase up to 0.14-0.18 m/s and the measured maximum is 0.38 m/s. This range of magnitudes is only common around and during peak events (figures B.4a and B.4b). During high-energy events the current is mainly from the northeast direction thus flowing in shoreline parallel southern direction, opposite to the wind direction (figure B.4a).

Currents from the northwest, perpendicular to the shoreline orientation, are small (bar around yellow line in figure 6.6) and negligible during peak events (figure B.4a).

The highest current magnitude occurs if the origin of the current is approximately 50° , flowing to the shore parallel south. This is not exactly parallel to the shoreline (red dots next to the red 'shore parallel south' vertical line. figure 6.7), however it is linked to a wind coming from the west to southwest. The higher the wind speed, the higher the magnitude of the current (size dots in figure 6.7). Also an increase in current magnitude can be expected if the current flows shore parallel north and originates from 250° (west to southwestern direction), this is linked to more southern to eastern wind directions (green and blue dots on the green vertical line, figure 6.7).

Incorporating water level fluctuations give the same conclusions: higher current magnitudes occur if the current flows parallel to the shoreline orientation (red and yellow dots on the red and green vertical lines, figure 6.8). Now we can see increased magnitudes correspond to higher water level fluctuations (redder dots appear higher, figure 6.8). Nonetheless increased negative water level fluctuations can also occur simultaneously with increased magnitudes of the current (red dots at -0.1 meter water level fluc., figure 6.8). Currents perpendicular to the Noordstrand shoreline orientation, either towards or away from the beach, are not significant in magnitude.

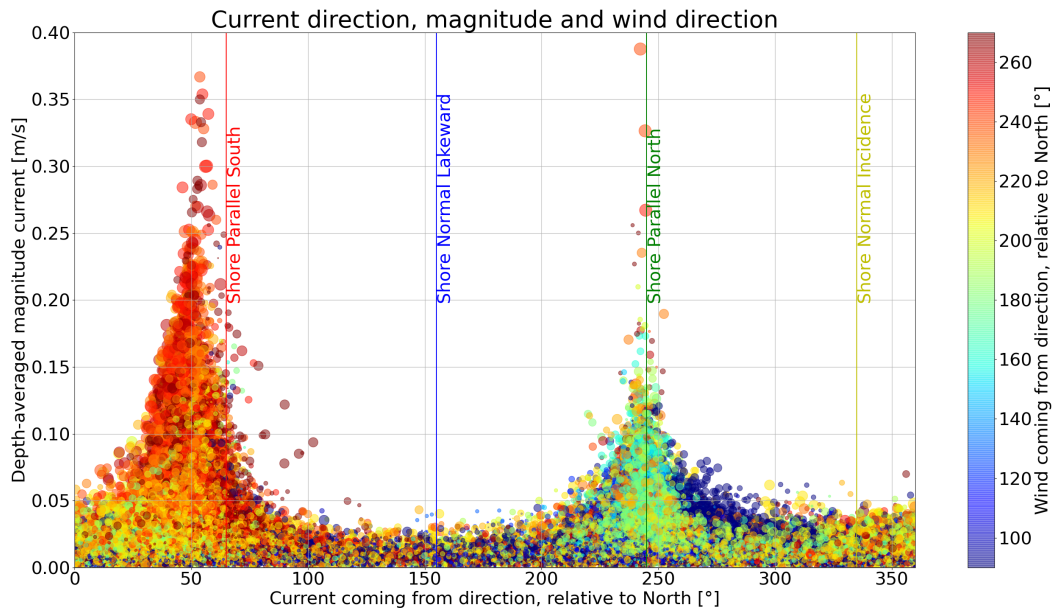


Figure 6.7: Current direction (coming from) in ° versus the depth-averaged current magnitude in m/s. The colour of the dots indicates the direction the wind is coming from, colourbar legend shown on the right side. The size of the dots corresponds to the hourly averaged wind speed squared (FH^2), meaning the larger the dot the larger the corresponding wind speed in m/s. The four vertical lines are linked to the different directions relative to the orientation of the Noordstrand as shown in figure 6.1.

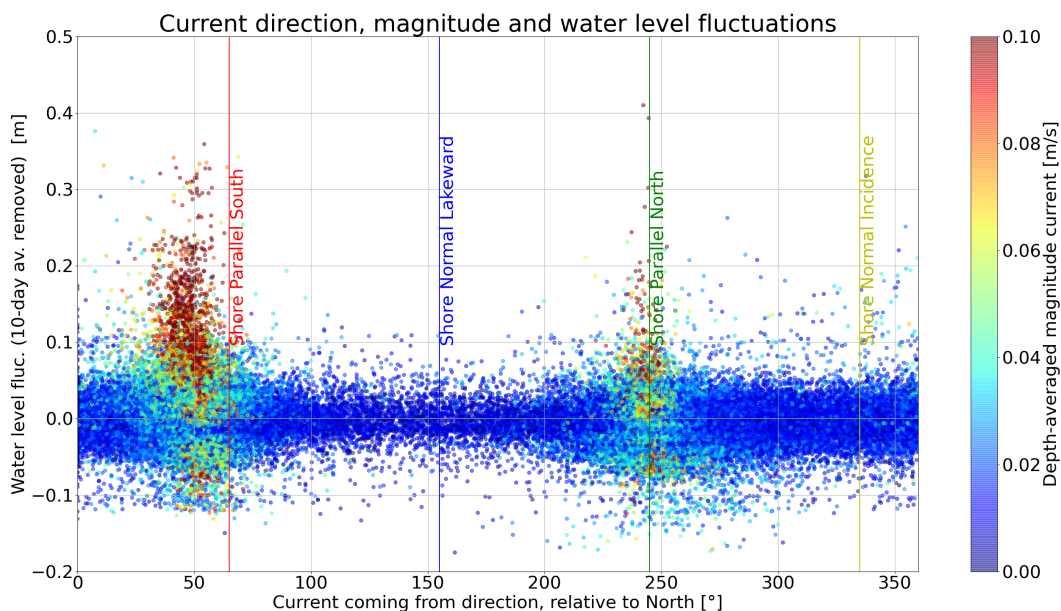


Figure 6.8: Current direction (coming from) in ° against the water level fluctuations (10-day average removed), the colour of the dots corresponds to the depth-averaged magnitude of the current in m/s. The four vertical lines are linked to the different directions relative to the orientation of the Noordstrand as shown in figure 6.1.

6.2 High-Energy Events

High-energy (HE) or peak events are categorised using a peak-over-threshold (PoT) method based on wave height (section 5.2.2). 146 high-energy events are found in the period from April 2019 till November 2020, exceeding the 0.5 meter significant wave height threshold (figure 6.9). The peak-over-threshold method is also used to classify high-energy events based on water level fluctuations at FL66 and by comparing the water level difference between FL66 and FL67 (location Houtribdijk), see section B.5.

As discussed in the literature review, different high-energy events can shape the low-energy beach. The effect on the development of the Noordstrand can be influenced by the frequency or intensity of the high-energy events, or a combination of both. Using the identified HE events and a measure for the energy we are able to analyse this (section 6.2.1).

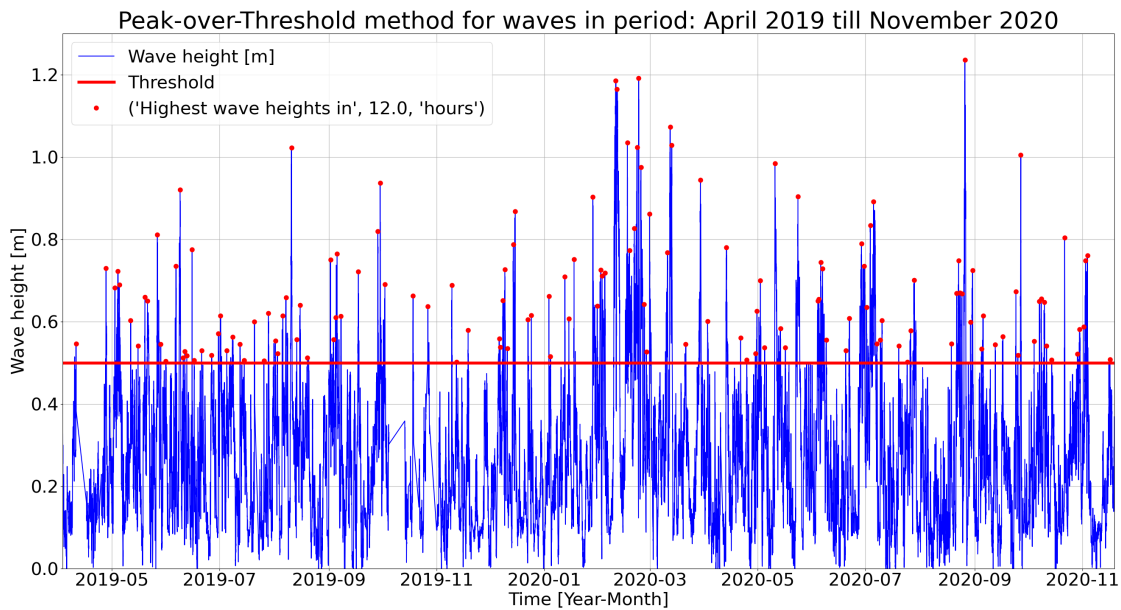


Figure 6.9: Time series of wave height data at FL66, used to identify peak-over-threshold events (or high-energy events). In red the threshold value set to 0.5 meter (for other input values for the peak-over-threshold method see section 5.2.2). The red dots indicate individual peak events, in total 146 events are found in the period from April 2019 till November 2020.

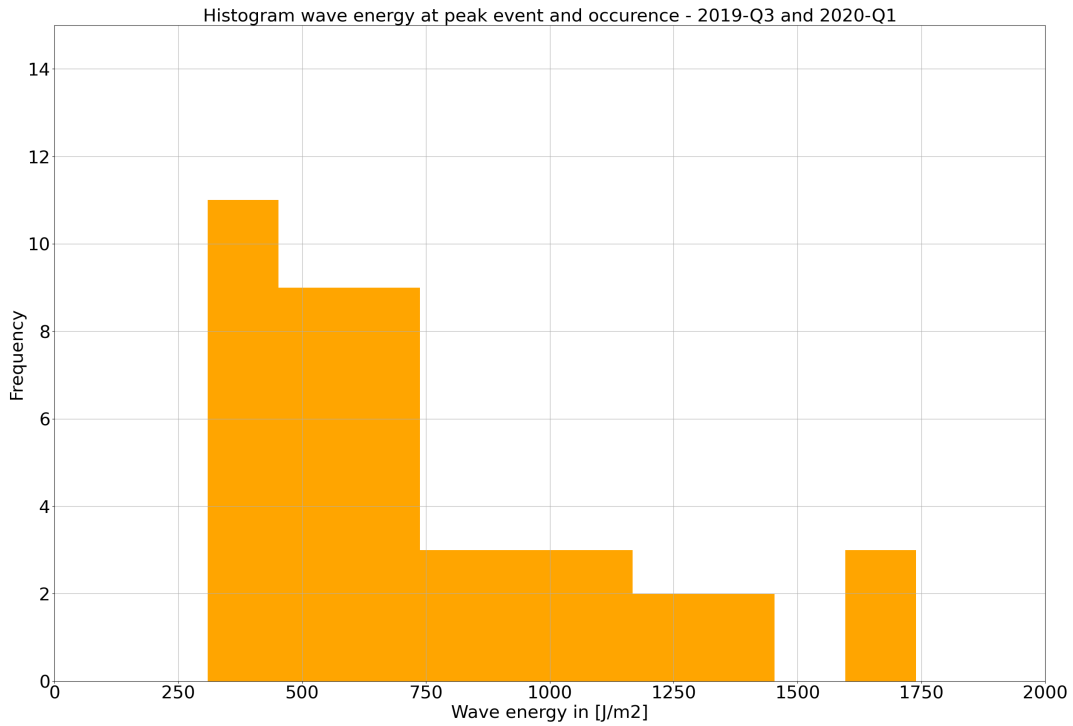
The high-energy event from 7 till 19 February 2020 is presented in this section (chosen from table 5.2) representing processes occurring during a high-energy event. Similar results are observed during other high-energy events (for the analysis of the other high-energy events, see sections B.4.2 and B.4.3). An identical analysis is performed for two calm periods (table 5.2) and is shown in sections B.4.4 and B.4.5 respectively.

6.2.1 High-energy events: frequency versus intensity

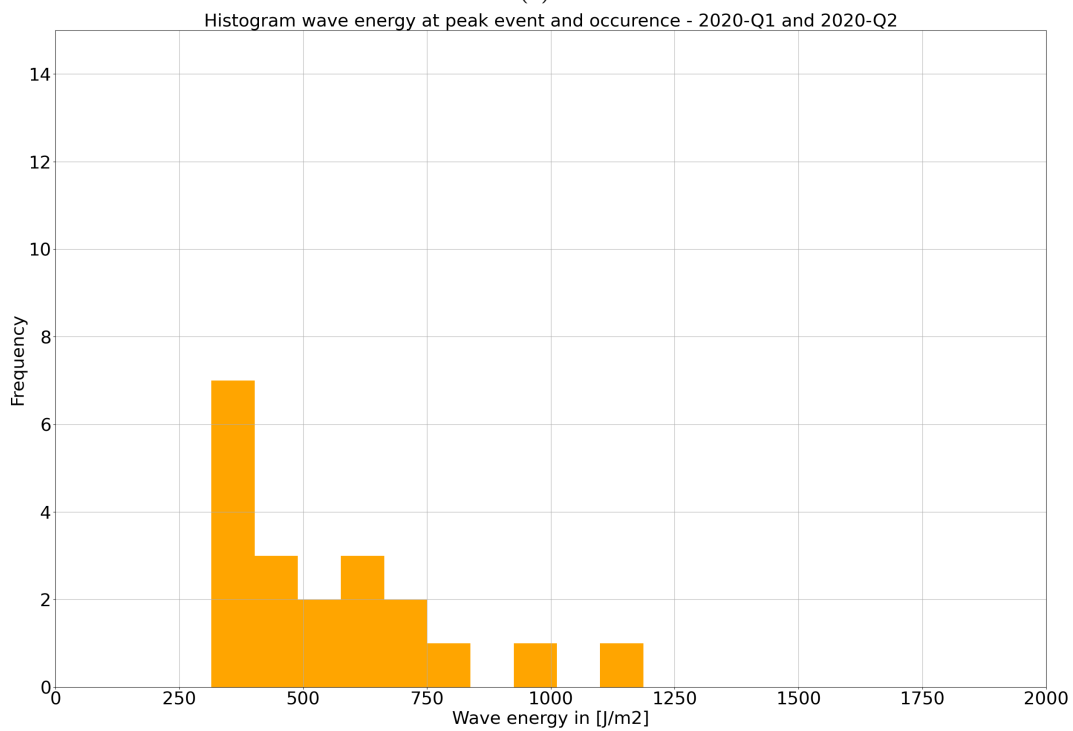
To assess the frequency of high-energy events in a certain period, we can count the amount of peak events identified by the PoT method. Furthermore we can estimate the energy of a peak period using a simple relation between wave height and wave energy (linear wave theory, equation 6.1). For this formula we only consider the wave height at the peak of the storm, *we do not take into consideration the duration of the high-energy event*. We acknowledge the fact that this analysis is therefore not complete, but for now it is deemed sufficient for an exploratory analysis.

$$E = \frac{1}{8}\rho gH^2 \quad (6.1)$$

We consider two different periods: **period 1: 2019 Q3 - 2020 Q1** (September 9, 2019 till April 10, 2020) and **period 2: 2020 Q1 - 2020 Q2** (April 10, 2020 till July 7, 2020). In period 1, which is approximately twice as long as period 2, in total 45 high-energy events are identified. This results in an average of 7.5 high-energy event per month. In period 2 a total of 20 high-energy events are found, giving a mean of 6.7 events per month. The amount of high-energy events are thus approximately equal. On the other hand if we compare the wave energy during the peak events we observe noticeable differences (figures 6.10a and 6.10b). Considering period 1, we notice a reasonable amount of high-energy events in which the wave energy exceeds 750 J/m^2 (figure 6.10a). In this period the average wave energy per peak event is equal to approximately 750 J/m^2 . Looking at period 2 we observe only 3 high-energy events exceeded a wave energy of 750 J/m^2 (figure 6.10b). Although there is some bias as this period is shorter, the average wave energy of 560 J/m^2 in this period does show a real difference. The frequency of high-energy events in both periods might be the same, the intensity of these events is not: in the period from 2019 Q3 till 2020 Q1 has been more energetic than the period from 2020 Q1 till 2020 Q2.



(a)



(b)

Figure 6.10: Histogram of wave energy (equation 6.1: $\frac{1}{8}\rho g H^2$) using the wave height of the identified high-energy event for periods: (a) **Period 2019 Q3 - 2020 Q1**; (b) **Period 2020 Q1 - 2020 Q2**; It is important to note that the duration of the high-energy event has not been taken into consideration.

6.2.2 High-energy event: 7 - 19 February 2020

This event is a representation of what happens during periods of high-energy near the Noordstrand. This specific period of time, February 2020, includes storm Ciara and storm Dennis (Musch, 2020).

Four peak events are identified in this period, two around storm Ciara (11th of February) and two later during storm Dennis (17th of February) (peak events are indicated by thicker markers in figures B.5, B.6 and B.7). Positive correlations between water level relative to NAP and wave height; and set-up/down compared to the Houtribdijk and water level fluctuations are visible (figure B.5 and figure B.6 respectively). All peak events include winds from southwestern to western direction and occur simultaneously with currents in shore parallel southern direction (coming from 50°), the peak events do not necessarily match maximum current magnitudes (top right plot, figure B.7). One can see a link between increased hourly averaged wind speeds and increased current magnitudes (bottom right plot, figure B.7).

The water level fluctuations (10-day rolling average removed) at FL 66 show a similar trend when compared to the set-up/down with respect to FL67 (Houtribdijk) (figure B.6). Although the water level fluctuations range between -0.1 and more than 0.3 meter and the set-up/down compared with FL67 remains smaller (between 0.0 and 1.0 meter). This can be caused by the way in which the step gauge is installed and how it obtains measurements (section A.1.1).

When hourly averaged wind speeds in- or decrease the water level fluctuations, wave heights and current magnitude in- or decrease correspondingly (figure 6.11). The water in the Markermeer only needs a few hours to 'react' to increased wind speeds and create a water level set-up with respect to the Houtribdijk (FL67), which is also observed as water level fluctuations offshore of the Noordstrand (FL66). Once the water level fluctuation reaches its maximum, it only takes the current magnitude a few hours to increase and also reach its maximum (second plot, figure 6.11). When wind speeds decrease after a peak occurrence, so does the water level fluctuation and current magnitude. The latter needs more time to adjust and reduces more slowly compared to water level fluctuations.

During periods of increased wind speeds (>15 m/s, 7 Bft or higher) from western to southwestern direction, water level fluctuations become positive and the depth-averaged current starts to flow from northeastern direction (50°), flowing in shore normal southern direction (top plot, figure 6.11). If hourly averaged wind speeds are lower (<10 m/s) the current tends to come from the same direction as the wind, although this depends on the exact orientation of the wind and the influence of the geometry of the Marker Wadden. Currents in the shore parallel direction are more common in the dataset than currents perpendicular to the shoreline orientation, probably due to the proximity of FL66 to the beach. Especially currents perpendicular to the shoreline flowing in lakeward direction are negligible. Currents oriented towards the beach (shore normal incidence) are negligible in magnitude but can occur (top right plot, figure B.7).

An exponential relation between hourly averaged wind speeds and water level fluctuations is evident (figure 6.12). Wave height is slower to respond to increased wind speeds (red dots are individual data points 12 hours before and after peak event), and maximum wave heights (peak events, shown as green diamonds) do not occur simultaneously with maximum wind speeds (figure 6.12). Set-up is quicker to respond to an increase in wind speed than wave height.

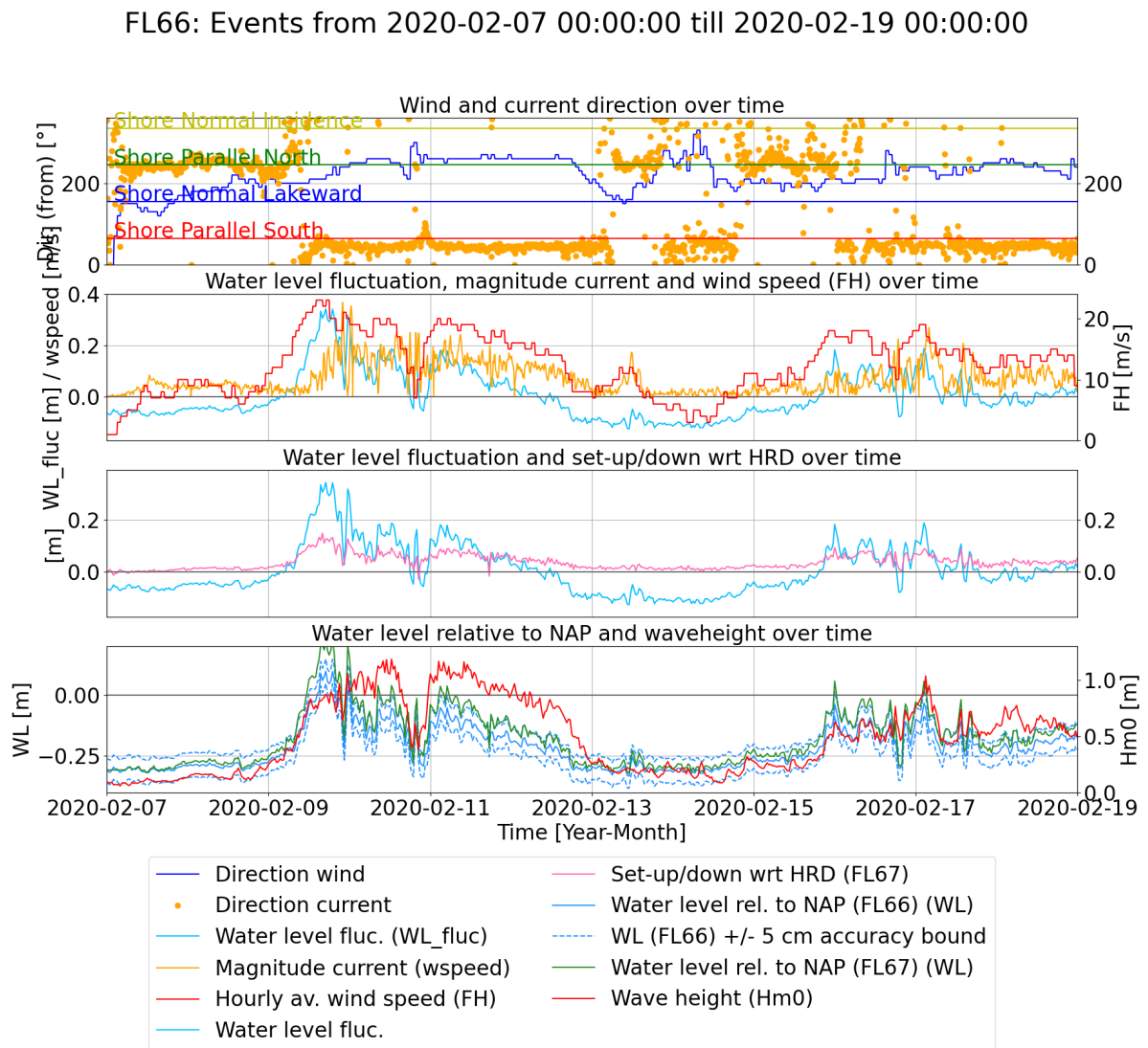


Figure 6.11: **7 - 19 February 2020**; overview plot of all conditions. From top to bottom: (1) Wind and current direction (coming from), coloured vertical lines link to directions as specified in figure 6.1. (2) Water level fluctuations at FL66, magnitude current and hourly averaged wind speed. (3) Water level fluctuations at FL66 (obtained by removing 10-day average water level) and set-up/down compared with FL67 (Houtribdijk). (4) Water level relative to NAP at FL66 and its 5 cm accuracy bounds, water level relative to NAP at FL67 and wave height.

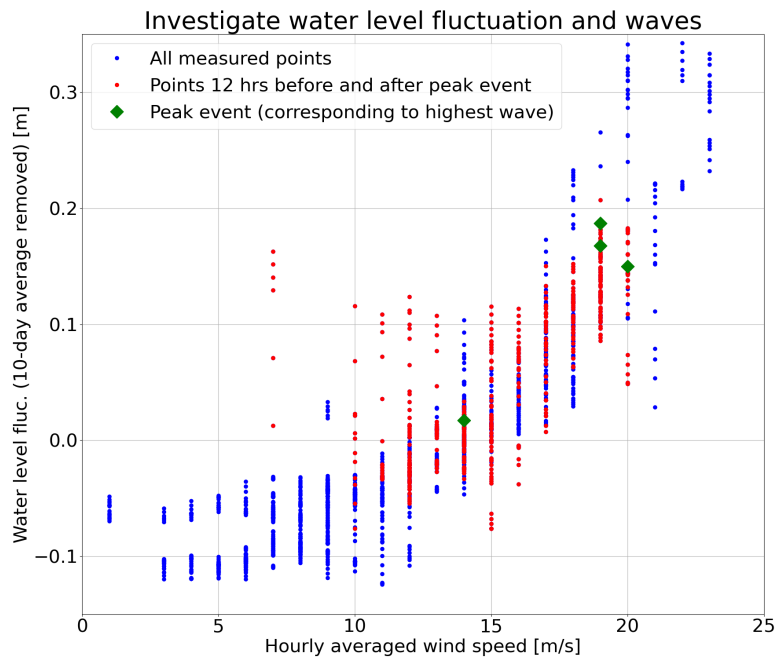


Figure 6.12: **7 - 19 February 2020**; Hourly averaged wind speed against water level fluctuations at FL66. The blue points are all the data points measured in this period. The red dots highlight the measurement 12 hours before and after a peak event. The individual peak events are shown as green diamonds, these corresponds to the identified peak event using the peak-over-threshold method on significant wave height.

Current profile over depth

In the previous sections the depth-averaged current is considered, we now zoom in to look at the current profile over depth. Different profiles are analysed during high-energy events. At the moment during which the current magnitude is maximum (figure 6.13 (a)), the current profile is almost depth-uniform. A small linear gradient can be found in the u-component of the current, being maximum nearer to the surface and reducing in magnitude towards the bottom (from 0.3 m/s to 0.24 m/s, left plot 6.13 (a)). Some hours before this occurrence the current followed the shore parallel northern direction, but shifted towards shore parallel southern direction (figure B.7). Meaning the build-up to maximum current magnitudes can occur in a matter of a 3-6 hours (depending on forcings such as wind speed, direction and corresponding water level fluctuations).

Figure 6.13 (b) shows the current profile over depth during a period in which the depth-averaged direction of the current has remained unchanged for at least 24 hours. With winds coming from the west to southwestern direction and a significant increase in water level (and fluctuations) (figure 6.11) we expect a linear gradient in the current magnitude over the vertical: the current direction following the direction of the wind forcing in the top of the water column and resulting in a return flow at the bottom. The latter compensating the water level set-up against the Houtribdijk (mass balance). This analysis has shown that this is not the case. Other periods of time have also been considered and show comparable results. Only ADCP measurements at FL66 are available, the current profile over depth can be entirely different in other parts of the Markermeer.

Non-uniform profiles over depth are possible occasionally with a magnitude difference between surface and bottom current magnitude of 0.15 m/s (an example is visible in figure B.16). This linear gradient in current magnitude can occur if hourly averaged wind speeds are low (<10 m/s).

6.2.3 *Calm period*

During calm periods wave height, water level fluctuations and current magnitude are small (figures B.18 till B.20 (April 2020) and figures B.23 till B.25 (July 2020)). In general the current direction tries to mimic the direction of the wind, but is influenced by the geometry of the Markermeer and presence of the Marker Wadden. As a result, even in calm conditions the current has a preference for the shore parallel direction (figures B.17 and B.22), although to some extent influenced by the governing wind direction. The current profile over depth is mostly uniform, with some deviations in which the linear gradient of the magnitude is relatively small (<0.05 m/s) (figure B.21). As a consequence also in calm conditions a depth-averaged current seems a reliable representation.

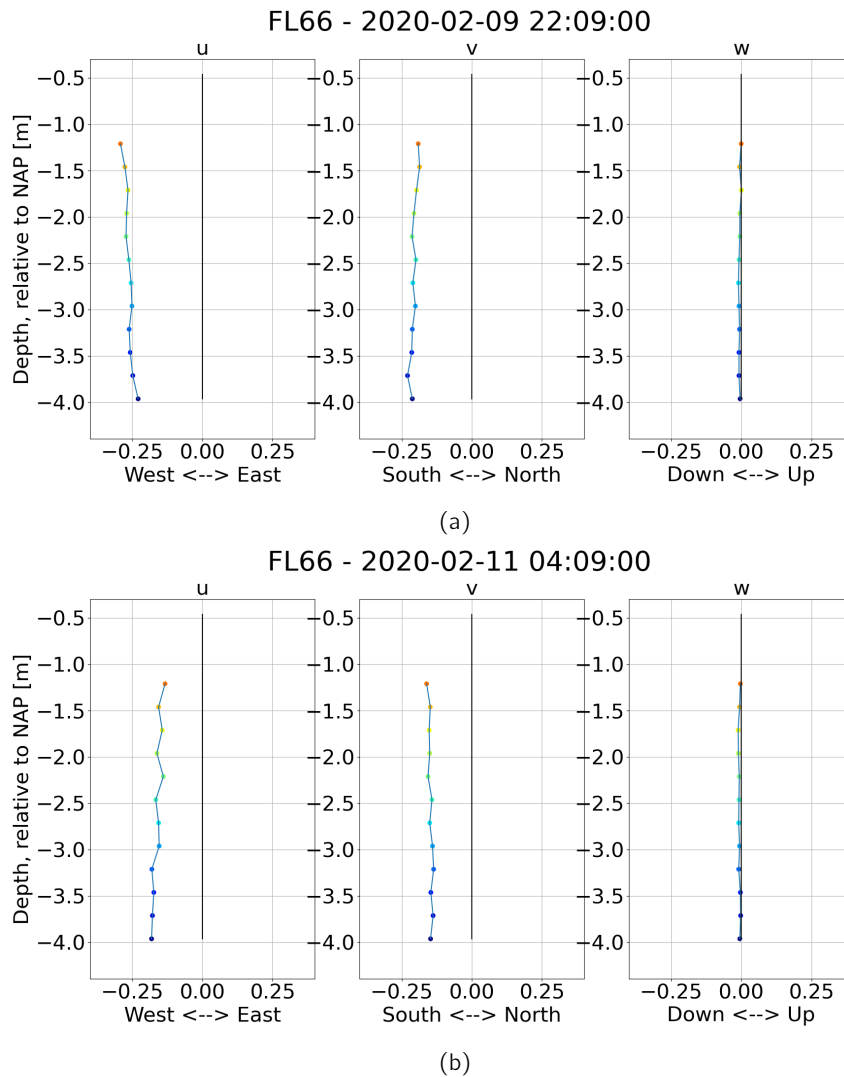


Figure 6.13: Current profile over depth, showing current magnitude in the three main directions in three different plots. The coloured dots indicate the layer levels as measured by the ADCP. The bottom of the graphs indicate the bottom level of the lake. The top of the graphs indicate the elevation of the water level. Shortcomings of the ADCP measurements near the bottom and surface are discussed in more detail in section A.1.2. (a) Current profile over depth at 9 February 2020, 22:09:00; during storm Ciara. Current magnitudes at this time are maximum during the considered high-energy event. (b) Current profile over depth at 11 February 2020, 04:09:00. *Data-processing script courtesy of Anne Ton*

6.3 Conclusions

The results of the hydrodynamic data analysis lead to the following conclusions:

- Water level fluctuations (10-day rolling average removed) give a good indication of set-up or down over the Markermeer. These water level fluctuations are linked to increased wind speeds. Correlation between wind speed and water level fluctuation is higher if wind originates from 200°-290° compared to the other shoreline parallel direction (20°-110°). Winds coming from 200°-290° have a high occurrence and their fetch distance over the Markermeer is maximum. This means these winds are also linked to increased significant wave heights and set-up against the Houtribdijk. The latter is faster to respond to increased wind speeds than the significant wave height. Maximum set-up is measured simultaneously with maximum wind speeds.
- As a result of water level fluctuations (set-up/down) a general flow pattern in the Markermeer arises, resulting in a measurable current near FL66. Higher current magnitudes occur if the current flows parallel to the shoreline orientation. Highest current magnitudes occur if the current originates from approximately 50°. This is not exactly parallel to the shoreline but close to flowing to the 'shore parallel south'. This little deviation is hypothesised to be caused by the geometry of the Marker Wadden and its location in the Markermeer. The described situation occurs if wind is coming from 200°-290° (west to southwestern direction) and wind speeds are higher than 10 m/s. Depth-averaged current magnitudes as high as 0.38 m/s are possible.
- Increased winds from 20°-110° result in negative water level fluctuations (set-down) in combination with higher waves. Higher current magnitudes are also expected, originating from 250° (west to southwestern direction), flowing in shore parallel northern direction.
- The current profile at FL66 is mainly uniform over depth, deviations are possible during calm conditions depending on wind speed and direction. However the gradient of the vertical is negligibly small. This means a depth-average current can be considered in further analyses for both high-energy events and calm periods. Currents perpendicular to Noordstrand shoreline orientation, either towards or away from the beach, are not significant in magnitude.
- During high-energy events we see a linear link between water level fluctuations and set-up/down with respect to the Houtribdijk. Water level fluctuations occur simultaneously with an in- or decrease in water level relative to NAP. An exponential link between hourly averaged wind speeds and water level fluctuations is observed during high-energy events. The delay between increased wind speeds and water level fluctuations (set-up or -down) is only a couple of hours, likewise the wind causes an increase in wave height during high-energy events.
- During the analysed peak events the current mainly originates from 50° and flows in shoreline parallel southern direction. Currents from this direction are linked to set-up. Before the peak event, the current tries to mimic the wind direction, but as wind speeds increase (>15 m/s), water level fluctuations become positive. When the set-up of water level against the Houtribdijk continues to increase and the hourly averaged wind speed remains roughly above 10-15 m/s, the current changes direction, from following the wind direction to flowing oppositely. When wind speeds reduce after the peak event, this is followed by a decrease in water level fluctuations first and as a consequence the current magnitude decreases too. The latter takes longer to die out.
- During calm periods the current tries to follow the direction of the wind, but wind and current direction are not always similar. The current near the Noordstrand is part of the larger wind-induced lake current is thus speculated to be influenced by the geometry of the Marker Wadden and the location in the Markermeer.

The hydrodynamic analysis has shown the influence of different hydrodynamic processes. Their influence on the hydro- and morphodynamics nearshore is difficult to deduct as only offshore measurements are available. We need to link the offshore measurements with the nearshore development of the beach. A preview for this is discussed in section 7.3.1. In this section the need for modelling hydrodynamic processes off- and nearshore is explained as the combination can lead to a better understanding of the main hydrodynamic and morphodynamic processes near the Noordstrand.

7

Morphodynamics

In this chapter the morphodynamic data analysis concerning the Noordstrand is discussed. This starts with a more general data analysis using elevation data in section 7.1, followed by the analysis of a specific high-energy period in section 7.2. This high-energy period includes the storms Ciara and Dennis (part of the hydrodynamic data analysis, section 6.2.2). The summary of the conclusions can be found in section 7.3, which includes the link to the hydrodynamic data analysis of chapter 6 and anticipates the need for a model of the system (chapter 8). The chapter ends with a section showing the results of the exploratory morphodynamic analysis of the fieldwork data in section 7.4.

The main considerations to keep in mind while reading this chapter are:

- One should note the availability of 100 meter transects is very limited, only the datasets of 2019 Q3 and 2020 Q1 include 100 meter transects and thus provide us with data around the waterline. The other datasets focus on bathymetry, topography and KIMA elevations only, lacking crucial measurements around the waterline.
- An impression of the groyne (shown as a purple line in the overview figures) can be found in figure 7.1.



Figure 7.1: Groyne at the Noordstrand, looking from the northeastern edge of the beach towards the groyne and rest of the beach. Picture taken during the field trip of December 10, 2020.

7.1 General Erosion

An overview of the available GPS data for the morphodynamic data analysis is presented in table A.1. Focus remains on the same period as used in the hydrodynamic analysis: April 2019, **2019 Q1**, till July 2020, **2020 Q2**. For the last part of the considered period the data of Q2 is used instead of Q3, as in Q3 the works for the new nourishment already started, thus affecting the measurements.

When looking at the general erosion of the Noordstrand between April 2019 and July 2020 the following is observed (figure 7.2):

- 100 meter transect measurements are missing for 2019 Q1 and 2020 Q2, little information about the elevation near the waterline is available. The KIMA section (section A.2), horizontally 600 to 800 meters from the reference point, does contain elevation data near the waterline.
- In general erosion of the beach face is observed, which can be quite significant, up to 3 to 4 meters in some locations (figure C.2). The erosion of the beach face is more profound from 0 till 600 meters to the reference point horizontally, near the southwestern part of the Noordstrand, close to the hard edge. Another erosion hot spot can be found 100 meters to the west of the groyne. At this location the decrease in elevation is highest. At the location of the KIMA measurement section we observe less erosion of the beach face.
- In general we recognise sedimentation a little lakeward of the submerged platform (elevation platform taken from Ton et al. (2020), see grey dashed line in map figures). Sedimentation rates are higher near the northeastern side of the Noordstrand (900 to 1200 meters horizontally from the reference point).
- Initially, the beach face eroded and the entire region below the offshore platform showed an increase in elevation (plot (a) of figure C.3). During later months ongoing erosion at the beach face is still observed, but also some positive changes in elevation right next to the erosion hotspots are visible. During this later period an extension of the offshore platform is noticed, but more offshore the positive elevation changes have diminished and even some erosion is recognised.

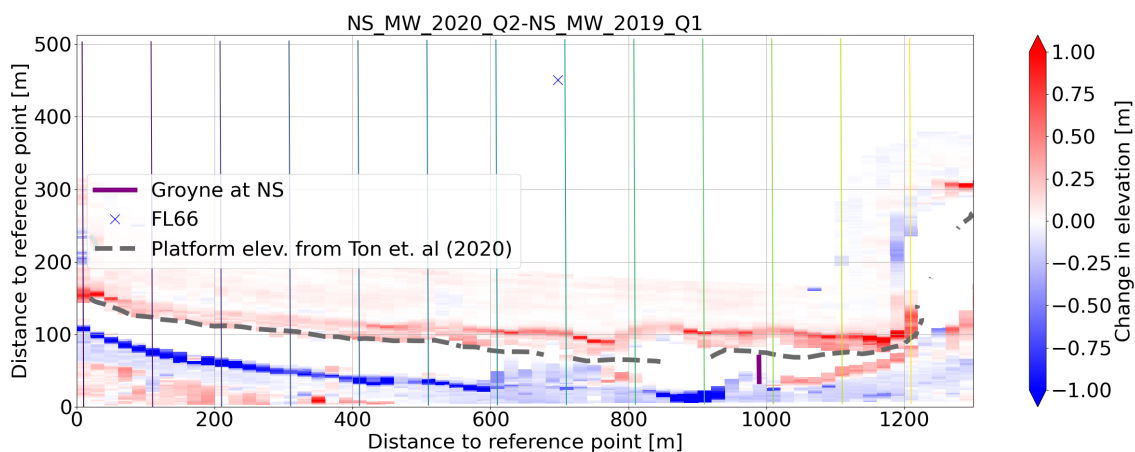


Figure 7.2: **General overview:** Total changes in elevation when comparing measurements at the start of the interesting period (2019 Q1) with the end (2020 Q2). Positive changes in elevation are shown in red and are associated with sedimentation. Negative changes are shown in blue and indicate erosion. The offshore measuring station, FL66, is visible in the centre top of the graph (blue cross). The groyne is shown as a purple line at approximately 1000 horizontal meters from the reference point (impression of the groyne in figure 7.1). Measurements around the waterline are missing as only topography and bathymetry data are available for this period of time, this area is therefore white. White coloured areas indicate an absence of data (so not a 0 m change in elevation as the colourbar might suggest). The coloured vertical lines indicate the 100 meter transects - which are not available for this data. The KIMA section does show some measurements near the waterline. The dashed grey line indicates the location of the offshore platform at an elevation of -1.11 meter relative to NAP (from Ton et al. (2020)) using the data at the start of the mentioned period to show the development of the platform offshore.

7.2 Analysis High-Energy Period

Datasets 2019 Q3 (obtained in September-October 2019) and 2020 Q1 (obtained in April 2020) contain 100 meter transect measurements to link topography and bathymetry around the waterline. During this period (roughly 6 months) from **2019 Q3 till 2020 Q1** 47 of the total 146 peak events were identified, including storms Ciara and Dennis (section 6.2.2). During this period the Noordstrand changed significantly during high-energy events according visual observations (Island Wards Natuurmonumenten, 2021). This combined with the fact that more data is available around the waterline make it an interesting period to analyse.

One can see how erosion is common around the beach face and has been more severe in the southwestern part of the Noordstrand and 100 meters west of the groyne (figure 7.3). Some changes in elevation are as high as 4 meters, at these locations significant volumes of sand vanished. This explains the cliff formation as described by several observers (an impression of severe erosion and cliff formation is shown in figure 2.1, taken during the measurement campaign of April 2020).

It looks like erosion extends from the beach face to the offshore platform (grey dashed line in figure 7.3). Beyond the location of the platform we notice some sedimentation at different parts of the beach. Near the hard edge there are some positive elevation changes lower than the offshore platform. In between 100 to 400 meters horizontal to the reference point one observes negligible elevation changes. From 600 to 1200 meters sedimentation rates below the platform elevation are more common and significant, reaching its maximum near the link of the main beach to the soft edge. This might indicate a change of transport rates.

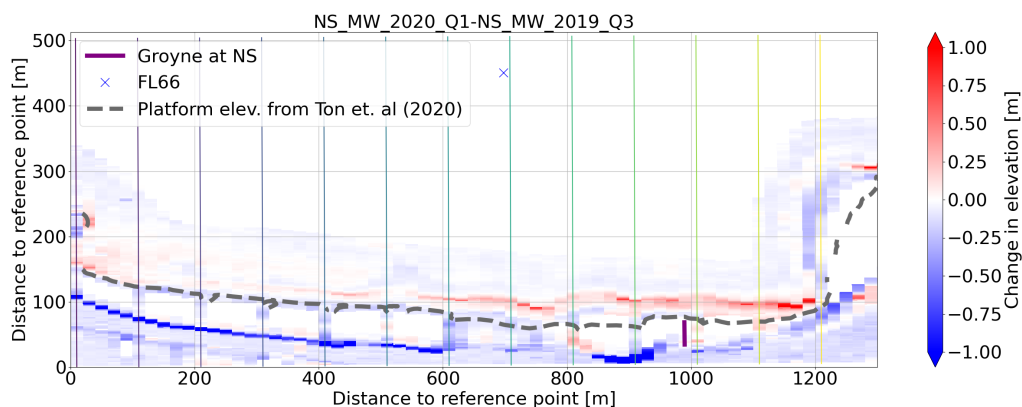


Figure 7.3: **Period of HE events:** Changes in elevation when comparing measurements at the start of the considered high-energy period (2019 Q3) with the end (2020 Q1). Positive changes in elevation are shown in red and are associated with sedimentation. Negative changes are shown in blue and indicate erosion. White coloured areas indicate an absence of data (so not a 0 m change in elevation as the colourbar might suggest). Measurements around the waterline are available every 100 meter - transects visible as coloured vertical lines. The location of the offshore platform (dashed grey line at -1.11 meter relative to NAP (from Ton et al. (2020))) is shown using the data at the start of the mentioned period to show the development of the platform offshore.

7.2.1 Link: frequency versus intensity

We can see how the erosion rates have dropped in just 3 months (2020 Q2 vs Q1, figure C.3). Consider the discussion on frequency versus intensity of high-energy events of the previous chapter (section 6.2.1) as the shown periods of the morphodynamic analysis match. Morphological development of period 1 (2019 Q3 - 2020 Q1) is shown in figure 7.3, period 2 (2020 Q1 - 2020 Q2) can be found in figure C.3. The relative frequency of high-energy events in both periods match, but the intensity of the first period was much higher.

In period 2: 2020 Q1 till 2020 Q2, sedimentation occurs next to the location of the offshore platform over the entire length of the beach. The beach seems to have recovered somewhat from the high-energy period (period 1) before or sediment has arrived from elsewhere. In this particular case it seems that intensity opposed to frequency of high-energy events has more influence on the morphological development of the beach.

7.2.2 Analysis transects

We now look more closely at the development of the thirteen different transects during the period 2019 Q3 and 2020 Q1, each 100 meter apart (figure 7.4). Information on all transects can be found in appendix C.3.2. Four different transects are highlighted and analysed. The findings are summarised below:

- **Transect 300 meter:** At this location erosion along the entire transect was observed. This transect is in the middle of the southwestern part of the beach near the hard edge, representing the area from 0 to 500 meters (relative to the reference point). Erosion seems to have been more severe in this area, we observe little sedimentation (figure 7.4). Erosion is common over the entire transect (bottom plot, figure 7.5a). The highest water level measured in this period reaches the dune face, coinciding with the increased erosion at this location (top plot, figure 7.5a). The offshore platform elevation has decreased a little.
- **Transect 700 meter:** This location in the middle of the Noordstrand experienced erosion of the beach face and sedimentation near the offshore platform. It is located within the KIMA section (figure 7.4). It represents the area ranging from 500 meters to 1200 meters (relative to the reference point). We observe erosion near the dune and beach face, but sedimentation at the location of the offshore platform (top and bottom plot, figure 7.5b). Erosion around the average water level is very limited, but more severe near the highest measured water level. The platform progresses towards the lake and its elevation has decreased.
- **Transect 900 meter:** Here we observe large erosion rates at the beach face near the dunes and some sedimentation at the location of the submerged platform. The presence of the groyne could have been an influencing factor (figure 7.4). At this part of the beach the dune elevation has more than halved with an elevation change of more than -4 meter (top plot, figure 7.6a). This drastic change in topography is underlined by visual observations of Natuurmonumenten and might be linked to the high-energy period in February 2020. Not all sediment in this transect is lost, the platform has progressed lakeward and increased in height over a length of 50 meters (bottom plot, figure 7.6a). At this location the elevation of the platform has increased instead of decreased.
- **Transect 1000 meter:** At this location, being relatively close to the groyne, we observe erosion of the upper beach face and sedimentation just offshore of the location of the average waterline and offshore platform (figure 7.4). At the beach face we notice relatively small erosion rates (bottom plot, figure 7.6b). Near the submerged platform we observe positive changes in elevation, the platform has grown lakeward and its elevation has increased (top plot, figure 7.6b). Sedimentation compensates more than is eroded along this transect, indicating sediment from elsewhere has settled in this region.

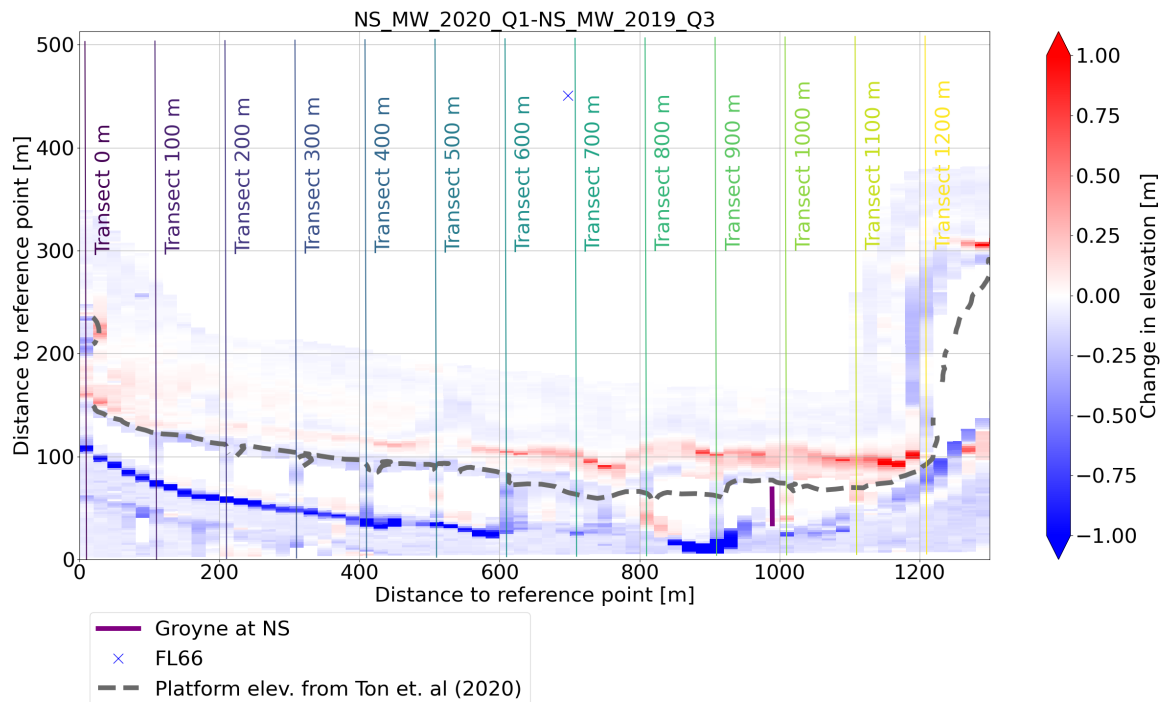
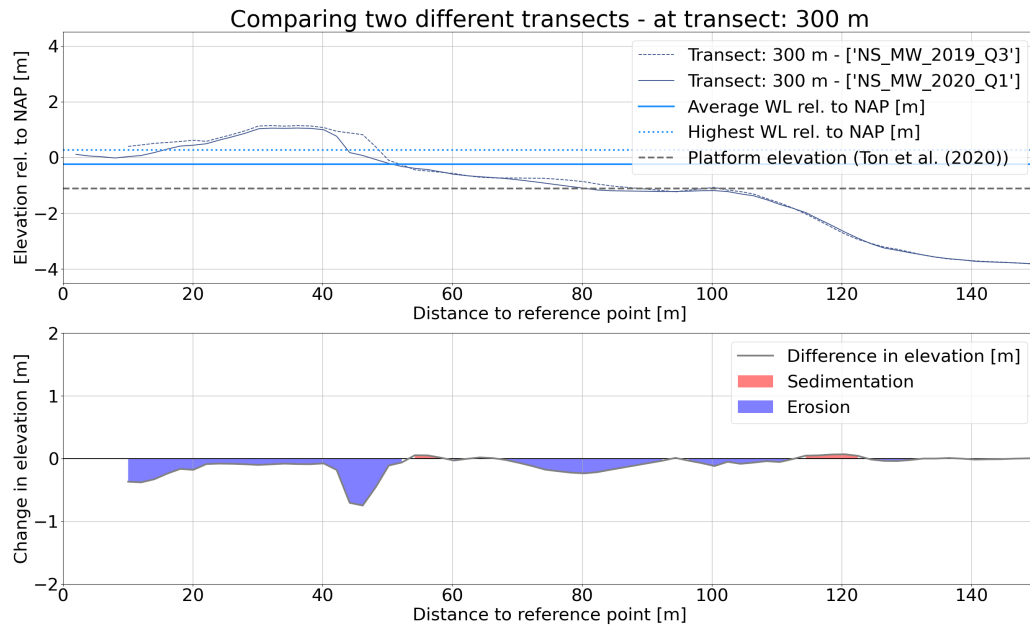


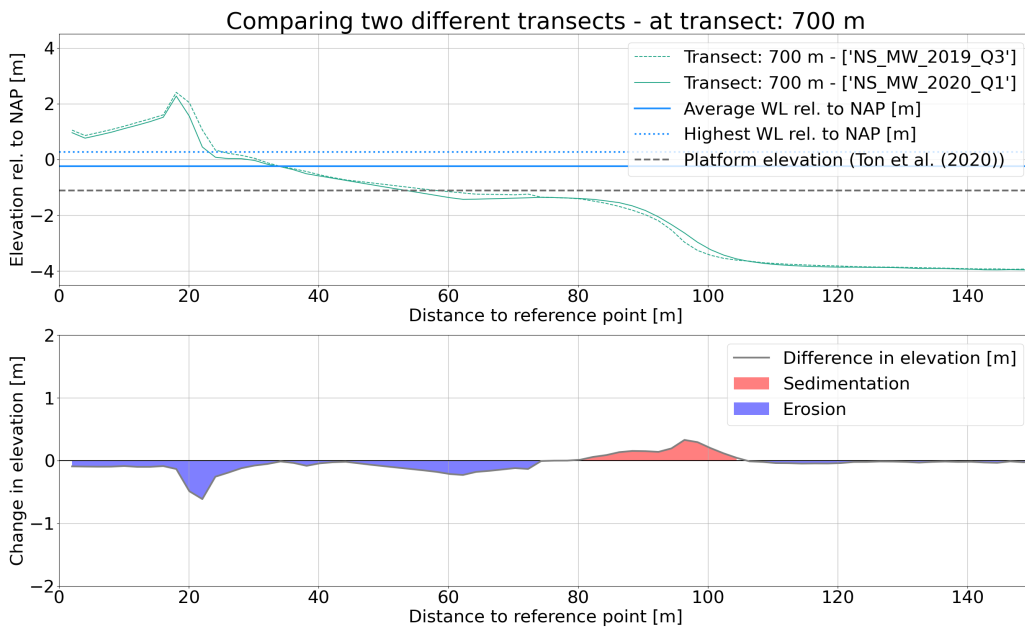
Figure 7.4: Figure 7.3 is now shown with the available 100 meter transects on top. The colours correspond to the transects plotted in figure C.4. White coloured areas indicate an absence of data (so not a 0 m change in elevation as the colourbar might suggest). Transects 0 and 1200 meter include the elevation of the hard and soft edge respectively.

Analyses of all available transects (appendix C.3.2, figures C.6a till C.12) support the idea that the (upper) beach face is eroding, whilst sedimentation is limited to the area lakeward of the submerged platform. Erosion rates can be especially severe at the upper beach face: cliff formation at the location of the dunes is principally observed at transects 100, 200, 300, 400, 500 and 900 meter. If negative changes in elevation exceed 1 meter (figure 7.3) this is linked to the formation of cliffs. Cliffs mainly appear near the hard edge in the southern-western part of the Noordstrand and 100 meters southwest of the groyne. It is important to note that *the highest water level observed during the measured period coincides with the locations of most severe erosion in the cross-shore transects and the location of the 'newly formed' cliff*. Other locations, mostly those in the northeastern part of the Noordstrand, show sedimentation around the average waterline.

The platform seems to be growing in offshore direction. This growth is more profound near the soft edge in the northeast of the Nooderstrand. Transects 0 till 500 meter show little sedimentation near the platform. From the 600 meter transect onward positive changes in elevation cover approximately 20 meters in width, with an exception near the 1100 meter transects where an area with a width of 50 meters is subject to sedimentation.

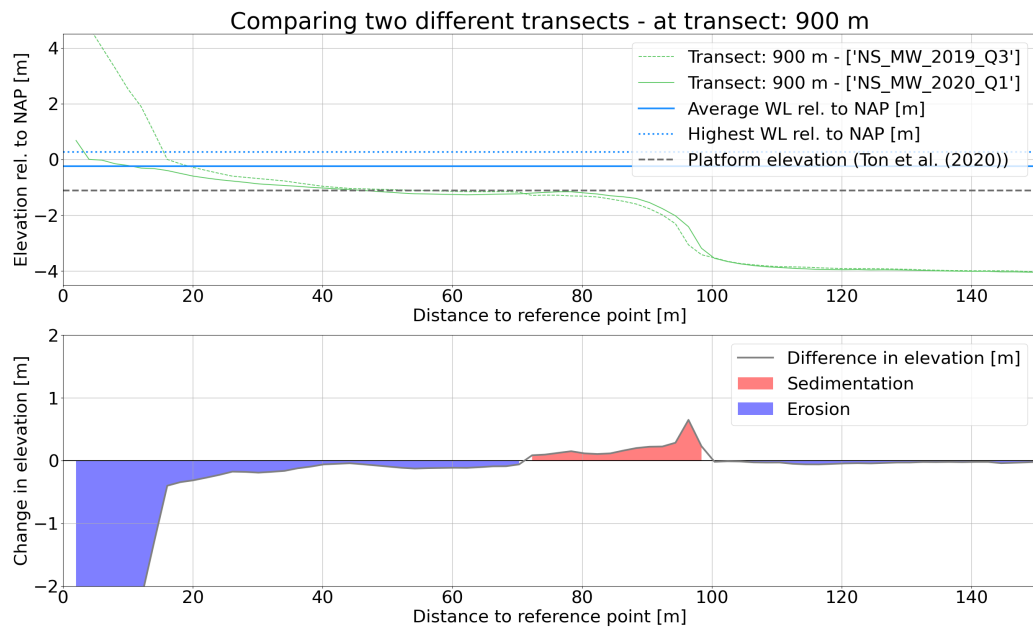


(a)

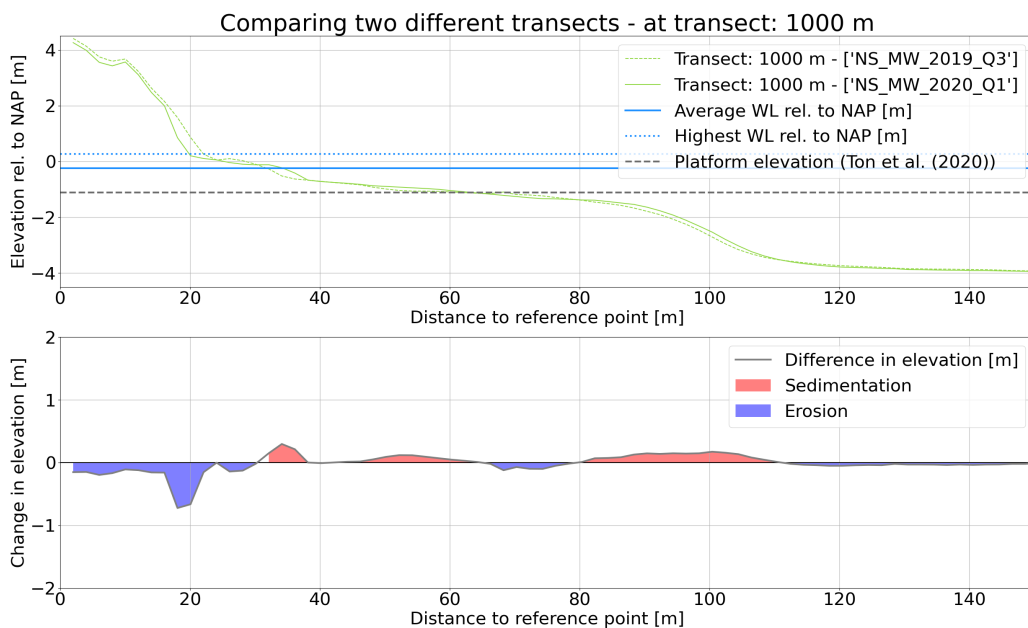


(b)

Figure 7.5: (a) Transect 300 meter; (b) Transect 700 meter; Comparing two different transects, 2019 Q3 (dotted line) to 2020 Q1 (solid line). Top plot: The colour of the transect plot corresponds to the colour of the transect indicated in figure 7.3. The solid blue horizontal line is the average water level relative to NAP in the considered period, with the dotted blue horizontal line being the maximum water level relative to NAP in the same period. The elevation of the platform is represented as a grey dashed line (elevation taken from Ton et al. (2020)). Bottom plot: difference in elevation (2020 Q1 - 2019 Q3), sedimentation given in red and erosion given in blue. The distances are relative to the reference point.



(a) Change in elevation at 10 meters distance to the reference point: -4.7 meter



(b)

Figure 7.6: (a) Transect 900 meter; (b) Transect 1000 meter; Comparing two different transects, 2019 Q3 (dotted line) to 2020 Q1 (solid line). Top plot: The colour of the transect plot corresponds to the colour of the transect indicated in figure 7.3. The solid blue horizontal line is the average water level relative to NAP in the considered period, with the dotted blue horizontal line being the maximum water level relative to NAP in the same period. The elevation of the platform is represented as a grey dashed line (elevation taken from Ton et al. (2020)). Bottom plot: difference in elevation (2020 Q1 - 2019 Q3), sedimentation given in red and erosion given in blue. The distances are relative to the reference point.

7.3 Conclusions

The previous analyses lead to the following conclusions concerning the morphodynamics of the Noordstrand:

- Erosion of the upper beach face is observed over the entire length of the Noordstrand. Erosion rates are higher near the hard edge in the southwestern part of the beach (0 to 600 meters) and one other erosion hotspot located 100 meters west of the groyne is identified. In the middle of the beach, the KIMA section, we observe significantly less erosion.
- Erosion of the entire beach was relatively high during the high-energy period of 2019 Q3 till 2020 Q1. At locations with cliff formation, the highest water level measured coincides with the location of most severe erosion. This could lead to 'slumping' of the dunes, creating cliffs (Sallenger, 2000). In these regions the elevation of the platform decreased. Linking to the analysis of frequency versus intensity of the high-energy events in the hydrodynamic data analysis (section 6.2.1), we hypothesise the intensity of the peak events has more influence on the morphological development of the Noordstrand.
- Positive elevation changes are more rare compared to negative changes. Sedimentation rates mainly occur lakeward of the submerged platform and are higher near the northeastern, soft edge of the beach (900 to 1200 meters). This indicates a change in transport rates. In this part of the beach some positive changes in elevation are observed around the waterline. At locations closest to the soft edge, the platform elevation has increased: sedimentation rates outweigh erosion rates, indicating arrival of sediment from elsewhere.
- When considering erosion cumulatively over the analysed transects, it is much more than the total sedimentation. This can indicate loss of sediment over the different transects and could enhance structural erosion of the beach. This cannot be stated with certainty due to the lack of periodical measurements around the waterline. Still the following question arises: *where is the lost sediment now?*

7.3.1 Linking hydrodynamics and morphodynamics: need for modelling

In this and the previous chapter we have analysed the available data, focusing on the hydrodynamic processes and the morphological development of the Noordstrand. In both the hydrodynamic and morphodynamic data we have observed the results of the combined action of different processes. Due to limitations regarding measuring devices, location in the field and frequency of measurements we are unable to identify the individual contribution of each hydrodynamic process (wind, waves, wind-driven and wind-induced current). To be able to assess the influence of each process individually the usage of a simulation program is beneficial, especially if this program enables us to model wind- and wave-driven flow separately. For a correct description of the system we need to consider the system of the Noordstrand, Marker Wadden and Markermeer as one. As a consequence we can look at the effect of the larger lake circulation, the location of the Marker Wadden in the Markermeer and the Marker Wadden geometry on the processes near the Noordstrand. Are the hydrodynamics only enhanced locally or are they part of a bigger - lake general - system?

In our previous data analysis we are limited to the offshore hydrodynamic data measurements of FL66. We cannot link this correctly to our elevation data obtained closer to the Noordstrand. The simulation program, a computational model, can bridge the divide between our offshore measurements and the nearshore development: *filling the gaps* which are left by the data analysis. Another solution would be the installation of nearshore measuring devices as was done at other location in the Markermeer (figure 2.4). Albeit this is impossible regarding the timespan of this research, using a modelling agent creates other benefits. By using a computational model we can look at different locations individually: overall lake circulation and the situation near the Noordstrand. Furthermore we can enhance or reduce certain processes by changing parameters within the model: making it possible to assess the influence of different factors on the beach hydro- and morphodynamics.

In the end we need to consider the fact that a model is always an approach to describe the real world and one should remain critical towards model outcomes. The previous analyses have not been for nothing, we are now better able to judge the model results. Not to mention the hydrodynamic and morphodynamic data analysis have resulted in some suggestions regarding the model. First, the waves and current are quite fast to respond to changing wind forcing, we do not need to model several days to weeks to see changes in the hydrodynamics. Second we have identified the interesting wind directions in light of their frequency of occurrence and impact on offshore hydrodynamics. Last, we have found an almost depth-uniform current profile at FL66: meaning the usage of a 2DH (depth-averaged) model is acceptable (the 3D situation should be checked in a sensitivity run).

7.4 Exploratory Morphodynamic Analysis - Fieldwork Data

After the nourishment of the Noordstrand was finished in December 2020 we organised monthly field trips in which we measured the Noordstrand elevation. These measurements are needed to investigate the initial development of the beach after the nourishment. The GPS measuring plan is discussed in appendix G and appendix H gives an overview of the obtained data. In this research we do not analyse our own field data in detail, but here we present an exploratory morphodynamic analysis of this data.

To assess the initial development of the beach we combine our GPS data with the topography and bathymetry measurements of Boskalis for the periods 2021 Q1 and 2021 Q2. The raw data is first filtered and next interpolated on the grid covering the Noordstrand (same method as used in the main morphodynamic analysis, chapter 5). The measurements of period 2021 Q1 are taken approximately one month after the nourishment is finished. Boskalis indicated the increased level of sediment 'fines' in the nourishment, starting with the measurements one month after completion means most fines have been washed out. This is beneficial as we consider the coarser sediment (diameter $\approx 350 \mu\text{m}$) in regard to beach development.

Observing the general development of the Noordstrand in the first 3 months we notice increased rates of sedimentation lakeward of the submerged platform and main erosion around the waterline (figure 7.7). The erosion and sedimentation rates are similar along the entire length of the beach. Unfortunately information around the waterline is only available every 100 meters, making the development around the waterline subject to uncertainty. These measurements every 100 meters make transect analysis possible. In the transects we observe erosion around the waterline and most sedimentation offshore of the submerged platform, meaning the platform width has increased at least a couple of meters (figure 7.8).

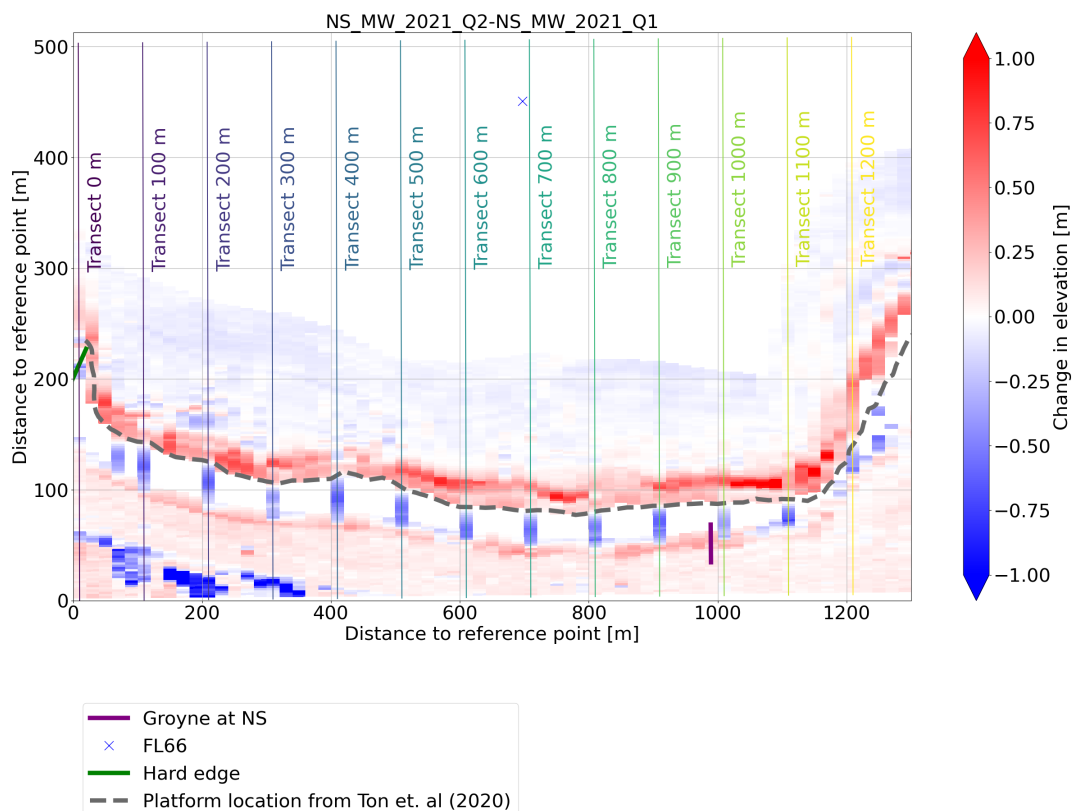


Figure 7.7: Changes in elevation: 2021 Q2 - 2021 Q1. Positive changes in elevation are associated with sedimentation (red) and negative changes indicate erosion (blue). White coloured areas indicate an absence of data (so not a 0 m change in elevation as the colourbar might suggest). Measurements around the waterline are only available every 100 meter - the transects visible as coloured vertical lines. The dashed grey line indicates the location of the offshore platform using an elevation of -1.11 meter relative to NAP (from Ton et al. (2020)) using the 2021 Q1 data to show the development of the platform offshore.

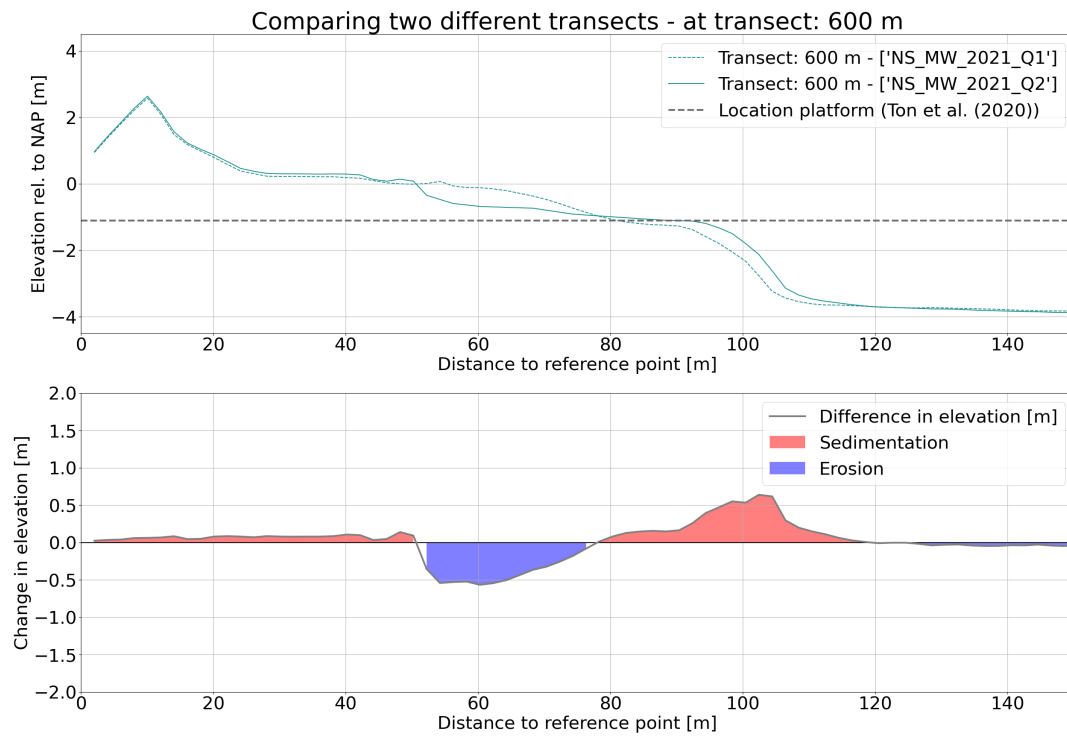


Figure 7.8: Transect 600 meter; Comparing two different transects, 2021 Q1 (dotted line) to 2021 Q2 (solid line). Top plot: The colour of the transect plot corresponds to the colour of the transect indicated in figure 7.7. The elevation of the platform is represented as a grey dashed line (elevation taken from Ton et al. (2020)). Bottom plot: difference in elevation (2021 Q2 - 2021 Q1) with sedimentation given in red and erosion given in blue. The distances are relative to the reference point.

IV

Modelling - Filling the Gaps

8

D3D Model Marker Wadden

Using the Delft3D (D3D) Marker Wadden model we want to investigate the hydrodynamics near the Noordstrand of the Marker Wadden. Following the data analysis of the two previous chapters we want to find the 'missing gaps' in our knowledge on how the system behaves during different events. Therefore we want to focus on:

- Understanding the hydrodynamic system near the Noordstrand: as far offshore as FL66, but focusing on the situation more nearshore. How do different events contribute to the hydrodynamic processes observed near the beach. Can this be linked to measured erosion patterns?
- Can the current direction, opposite to the wind direction at FL66, in case of high-energy events be explained?
- What part of the natural system is susceptible to waves and which part to the wind-induced lake current? What is the influence of the waves versus the influence of the wind-induced current?
- What is the behaviour of different hydrodynamic processes over time?
- Can these findings be translated to a better understanding of the hydrodynamic and morphodynamic system of the Marker Wadden?

This chapter starts with a small introduction of the modelling software used: Delft3D, in section 8.1. Followed by an explanation of the used D3D Marker Wadden model in section 8.2. Section 8.3 discusses the calibration and validation of the model. The modelled scenarios, including the idealised wind schematization runs and sensitivity runs, are discussed in section 8.4.

8.1 Delft3D

The Delft3D software can simulate free surface flows using numerical approximations. The D3D modelling suite consists of different modules, for this research we focus on the Delft3D-FLOW and Delft3D-WAVE components (version Delft3D 4.04.01). A small introduction of the flow, waves and numerical modelling components of Delft3D are given in section D.1.

8.2 Marker Wadden Model

The used Marker Wadden model is derived from the original Markermeer model. This model was initially created by WL Delft Hydraulics (Deltares) to investigate the hydrodynamics and silt/sediment movement in the Markermeer. A description of this initial model is given by Hulsbergen and Kuijper (2007). This model has been redefined multiple times for different purposes, an example is the investigation of silt traps as mitigation measures for turbidity by Vijverberg (2008).

This is not the first research using a D3D model to investigate hydrodynamic and morphodynamic processes in the Markermeer. Some extensive changes to the original model were already made by Ton (2020) to create the Marker Wadden model. That Marker Wadden model is the basis of the model used in this analysis. As this research focuses on finding the missing gaps in our understanding of the hydrodynamic processes near the Noordstrand some smaller changes to the Marker Wadden model are made to create the correct context for the modelling of the Noordstrand. The following changes are incorporated whilst going from the Markermeer model to the Marker Wadden model, focusing on the Noordstrand:

- A 2DH (depth-averaged) model is used instead of the original 3D model, to suppress computation time. Calibration runs run by Ton (2020) have shown that 2DH model results correspond to field data obtained at the offshore measurement locations in the Markermeer. Furthermore, data analysis has shown that the current profile over depth is mostly uniform (section 6.2.2). One should take into consideration that the obtained depth-profile near the Noordstrand is located offshore (FL66), therefore we cannot with full certainty conclude that the current profile is uniform over depth more nearshore. At other locations current profiles over depth (FL65 and FL67, figure 2.4) were measured nearshore and also showed uniformity over depth. To highlight the importance of the uncertainty in the current profiles close to the Noordstrand, an additional 3D model run is created to compare the results to (section 8.4.3).
- The 2DH model is calibrated by Ton (2020) using field data obtained by on- and offshore measuring stations as shown in figure 2.4. Extra calibration runs, covering two high-energy event and one calm period, are performed to show the similarity between the D3D model results and data obtained at FL66 (section 8.3).
- The Marker Wadden model is comprised of two submodels: the *total model* and *nested model*, a nested grid is used to be able to create higher resolution results near the beaches of the Marker Wadden.
- Accurate bathymetry and topography measurements of Boskalis are used to create a reliable representation of the depth near the Marker Wadden beaches in the model. This includes the locations and depth of sand extractions pits in the proximity of the Marker Wadden.
- For this research only the hydrodynamic part of the Marker Wadden model is considered, initially no morphodynamic runs are performed (*Sediment processes is switched off*).
- Output of the FLOW part of the model is saved as a NetCDF file, making post-processing of the model data in Python possible. Unfortunately this type of output is not supported by the currently installed WAVE-module on Civil Engineering cluster and thus outputs D3D .dat files.

The following sections deal with the flow, waves and domain characteristics of the Marker Wadden model in more detail.

8.2.1 Flow

The physical processes selected for the Marker Wadden model (both *total* and *nested*) are wind and online wave coupling with Delft3D-WAVE. The wind is the only forcing for both the flow and wave processes. An input file providing time-series of wind direction and speed is added to the master definition file. The wind drag coefficient, c_d (equation D.4), is related linearly to the wind speed (equation 8.1). The coefficients forming c_d are calibrated for the Markermeer by comparing flow patterns with field data.

$$c_d = 0.0013 + 0.0000593U_{10} \quad (8.1)$$

For bottom roughness the *White-Colebrook* formula is used in both models, this formula is chosen as it is also used in the original Markermeer model. This makes the calibration of different parameters easier, as an initial guess for different parameters is available from the older model. The equivalent roughness height, k_s , in U

and V direction is a uniform value of 0.05. D3D uses the Chézy friction coefficient in the depth-averaged flow calculations (equation 8.2) (Deltares, 2021a). Bottom stress formulation due to waves is set to *Fredsøe, 1984*. All settings are calibrated by comparing the outcome of different model runs with field data. The parameters that result in the best representation of reality are chosen.

$$C = 18 \log_{10} \left(\frac{12H}{k_s} \right) \quad (8.2)$$

8.2.2 Waves

The Delft3D-WAVE module is coupled to the Delft3D-FLOW module using online coupling. The coupling interval is set to 60 minutes, meaning every hour a new wave computation is performed. This computation uses the input from FLOW and its output updates the FLOW module in return with the wave information (figure 8.1).

For the *total model* a circular directional space is defined with 36 directions, for the *nested model* the amount of directions is enlarged to 108 (same value as used in the preliminary Marker Wadden model). This direction resolution is suitable for swell waves (The SWAN team, 2020b) and enlarging the circular directional space prevents the 'Garden Sprinkler Effect' (Booij and Holthuijsen, 1987). For both models the physical parameters are set to default. The used Marker Wadden model is calibrated using only the extension of the wind to the WAVE module (*wind: use and extend*). The *nested model* makes use of boundary conditions specified using the output of the *total model*, saved as 2D wave spectra information at the specified boundary points (figure 8.4: vel_1 till $wlev_6$). Output is written for the FLOW grid every 30 or 60 minutes (depending on the model run). The *nested model* makes use of hotstart files to decrease the computation time.

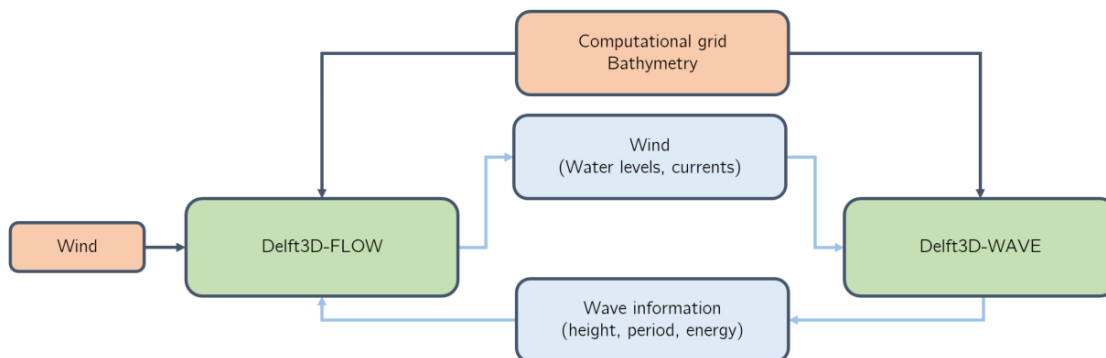


Figure 8.1: Online coupling of Delft3D-FLOW and Delft3D-WAVE as used in this research. Green boxes indicate the two modules, the orange boxes the input of the modules and the blue boxes the information that is shared between the two modules.

8.2.3 Domain, grid and bathymetry

This section discusses the set-up of the model: the considered domain, computational grids and the used bathymetry for the depth points of the model. As discussed before, the Marker Wadden model consists essentially of two models: *Total* and *Nested* (differences are summarised in table 8.1). Simply put the resolution of the *nested* model is nine times smaller than the *total* model. This refinement is a trade-off between resolution and computational time: the chosen refinement gives an adequate resolution of the Noordstrand whilst computation time is acceptable.

Table 8.1: Differences between *Total model* and *Nested model*; NS is Noordstrand.

Comparison	Total model	Nested model
Grid points in M direction	197	623
Grid points in N direction	206	884
Average gridsize at NS	150 m x 150 m	16.5 m x 16.5 m
Refined (compared to total model)	1x	9x
Time step	2.5 min	0.75 min
Average computation time	30-60 min	12 hours

Domain & Grid

All model boundaries are land boundaries, as we are modelling a lake. The IJmeer, Gooimeer and Eemmeer are part of the model and connected to the Markermeer in the south. The addition of these water bodies is needed for a correct representation of the hydrodynamics in the Markermeer. The land boundaries are closed, meaning there is no exchange of water with the outside. In reality there is in- and outflow of water at several locations (e.g. at the Buiten-IJ, Nijkerkersluis, Krabbersgat and some location along the Houtribdijk). The influence of these discharges is negligible compared to the large scale lake circulation we are investigating. Especially considering the fact that we are looking at the hydrodynamics near the Noordstrand for a few hours to a couple of days, as a result we neglect these discharges.

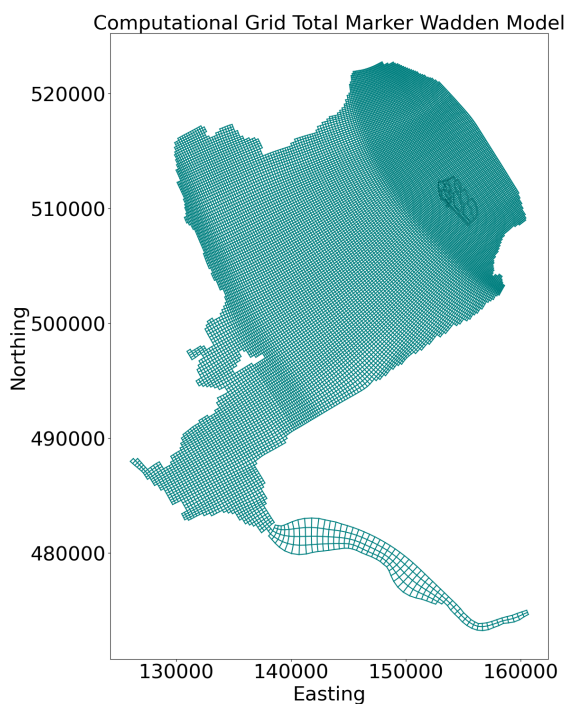


Figure 8.2: Computational grid of total model, showing the Marker Wadden in the top right.

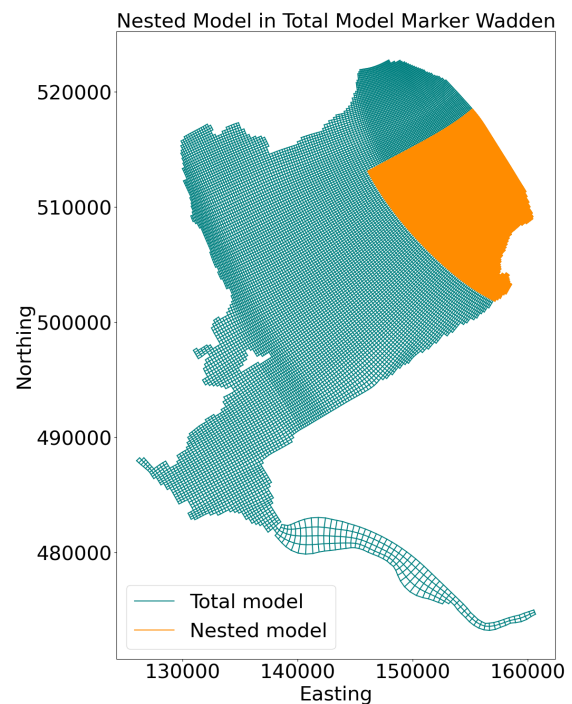


Figure 8.3: Computational grid (blue) with the nested grid on top (orange).

Inside the *total model* an additional D3D model is nested: *nested model* (figures 8.2 and 8.3 showing the nested model in orange), to provide a higher resolution near the Noordstrand. The models are connected using water level boundaries in the south and velocity boundaries in the north of the nested model (figure 8.4). This combination of boundary conditions for the nested grid is chosen as to create a well posed problem (a unique solution exists), only water level or velocities boundary conditions would not suffice. In this Marker Wadden model the choice of velocities on the northeastern boundary and water levels on the southwestern boundary is made without considering the direction of the wind. This is not completely appropriate, for winds from southwestern direction it is better to set velocity boundaries on the southwestern border and water levels on the other. For more northern winds this set-up should switch. For this research we keep the set-up as the original model (as shown in figure 8.4) as the Noordstrand is quite far from the model boundaries (no direct influence expected), *total* and *nested* model show the same general lake circulation patterns and calibration runs show acceptable results near FL66.

The nesting process means the total model must be run first, writing model output at the observation points as set by the *Nesting(1)* tool of D3D. Using *Nesting(2)* of the D3D toolbox the data obtained at the observation points in the total model is translated to boundary conditions for the nested model (Deltares, 2021a). Wave information is provided as 2D spectra output at the same observation points and is stored in .sp2 files for the total model. Using a Matlab script the .sp2 files are combined and the format is edited so it can be used as 2D spectra input for the nested model.



Figure 8.4: *Nested model* showing a gradation of bathymetry in blue (darker blue means larger depth, notice the sand extraction pits on the western side of the Marker Wadden). The boundaries in the north are comprised of velocity measurements, created by data output of the *total model*. In the southwest the boundaries are formed using water level measurements. The eastern boundary is a closed land boundary. In yellow the thin dams within the nested model are visible, representing obstacles which block the flow.

Bathymetry

For our model bathymetry data is interpolated on the computational grid (bathymetry visible in figures 8.5 and D.2 for the *total* and *nested model* respectively). For the *nested* Marker Wadden model measurements as obtained by Boskalis in Q3 2019 are used in the interpolation for the depth points at the Noordstrand. This time period is chosen as the rest of the depth points are based on data obtained in the same period. This dataset includes topography, bathymetry and 100 meter transects GPS measurements. Thus providing a higher and better resolution near the waterline of the Noordstrand (figure 8.6). Even taking into consideration these measurements there is a low sample density around the waterline: only a few depth measurements for every 100 meters of beach. Subsequently data is interpolated using a *triangulation method* (Deltares, 2021c). During the computational modelling of a scenario the depth values are specified in grid cell corners, the cell centre values are computed using the mean of the value in the adjacent grid cell corners.

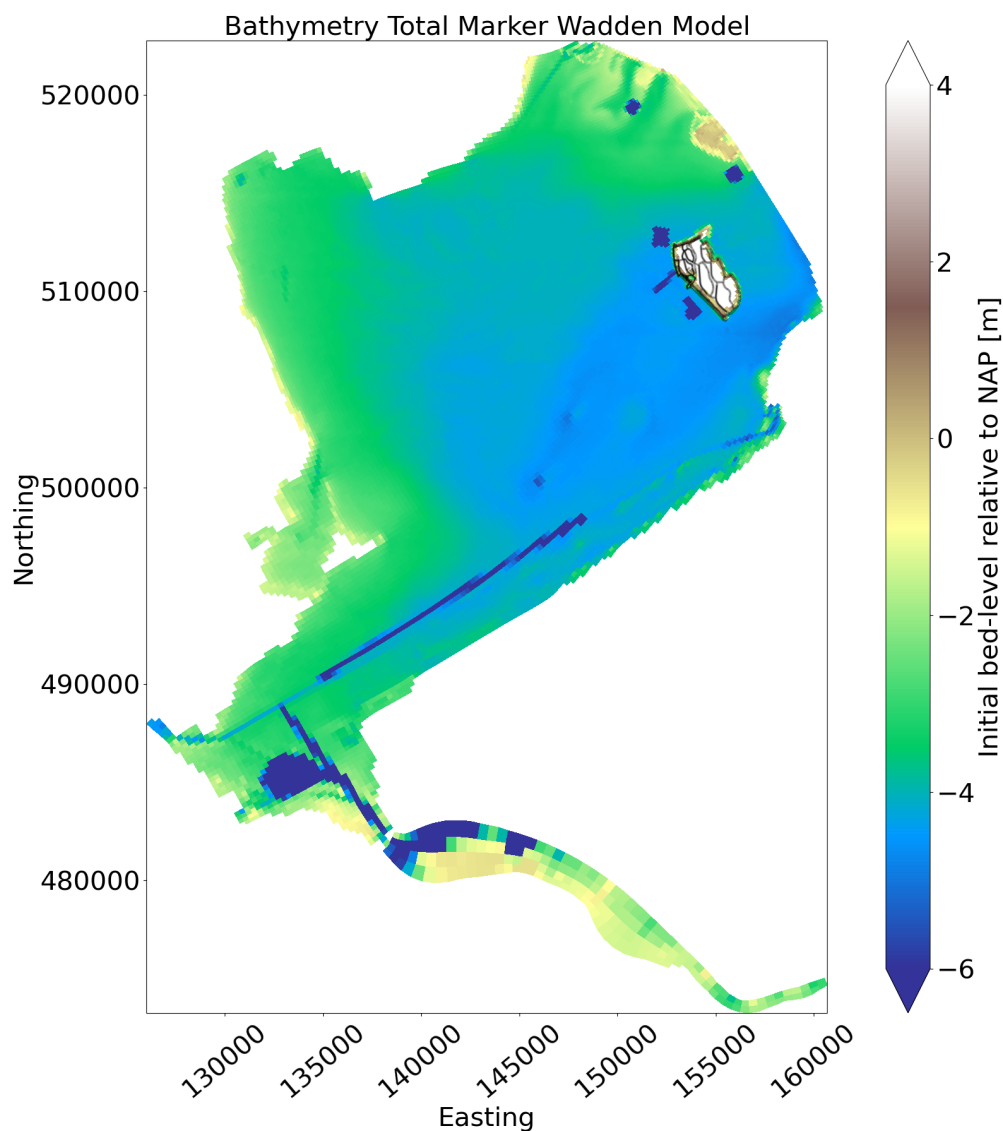


Figure 8.5: Bathymetry of the *total model*. Dark blue depicts the deeper areas: shipping channels and sand extraction pits and light brown and white areas correspond to dry land.

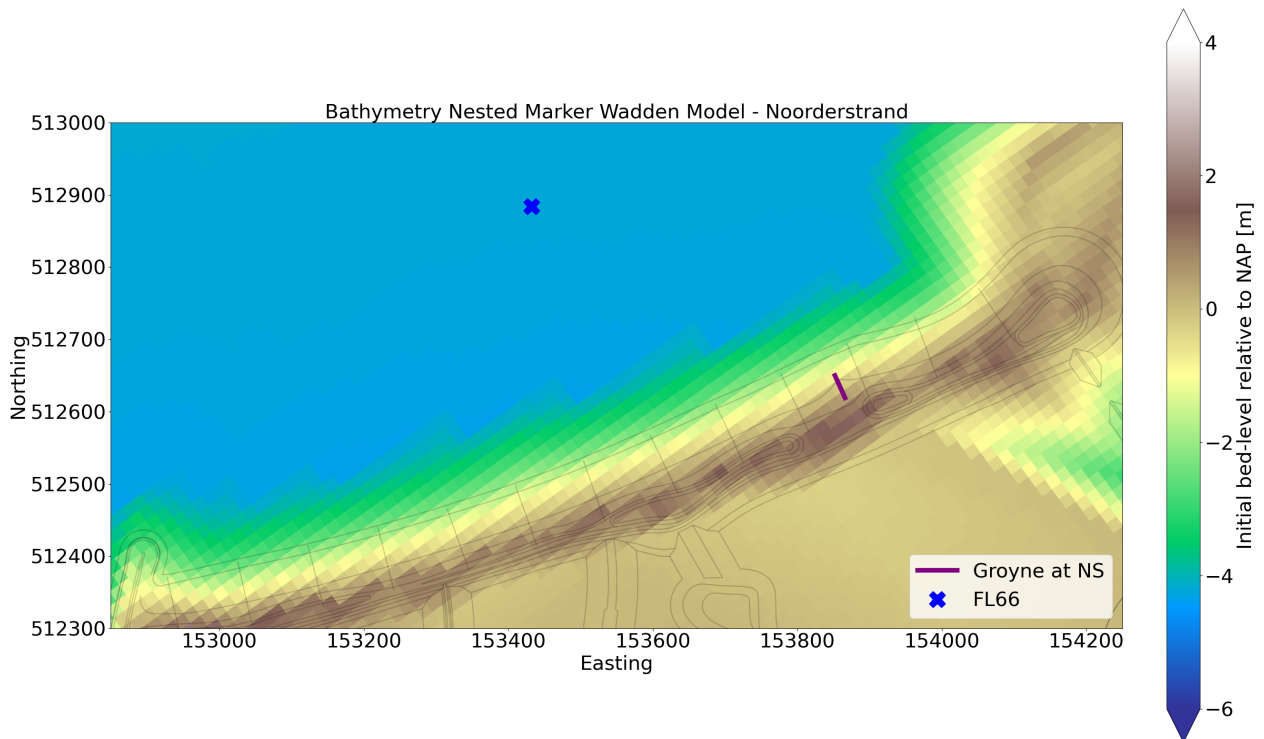


Figure 8.6: Bathymetry of the *nested model* near the Noordstrand, an overview can be found in figure D.2. A smooth, but quite steep transition of the dunes to the lake bottom is observed. The bathymetry is based on the 2019 Q3 data provided by Boskalis, the platform is *not* included in the bathymetry.

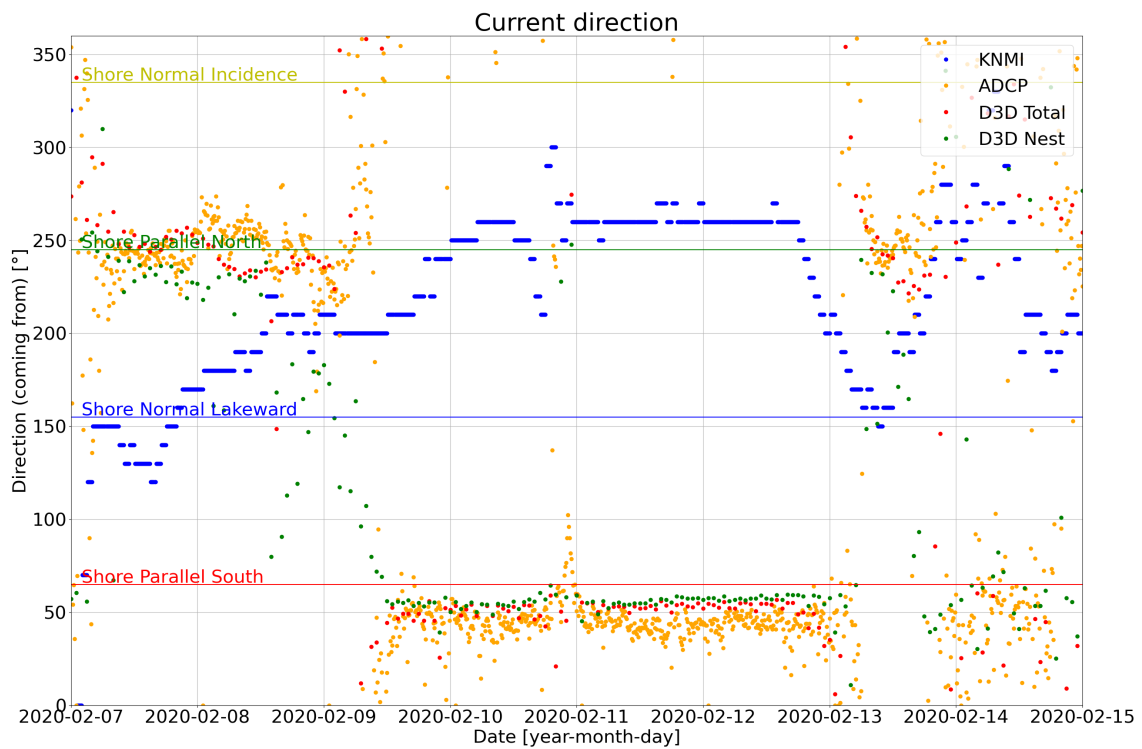
8.3 Calibration and Validation

The D3D has been calibrated by Ton (2020), by comparing model output and real data obtained by the off- and nearshore stations in the Markermeer (figure 2.4). To show the validity of the model, the results of the total and nested model runs are compared to the data obtained at FL66 by the STB and ADCP.

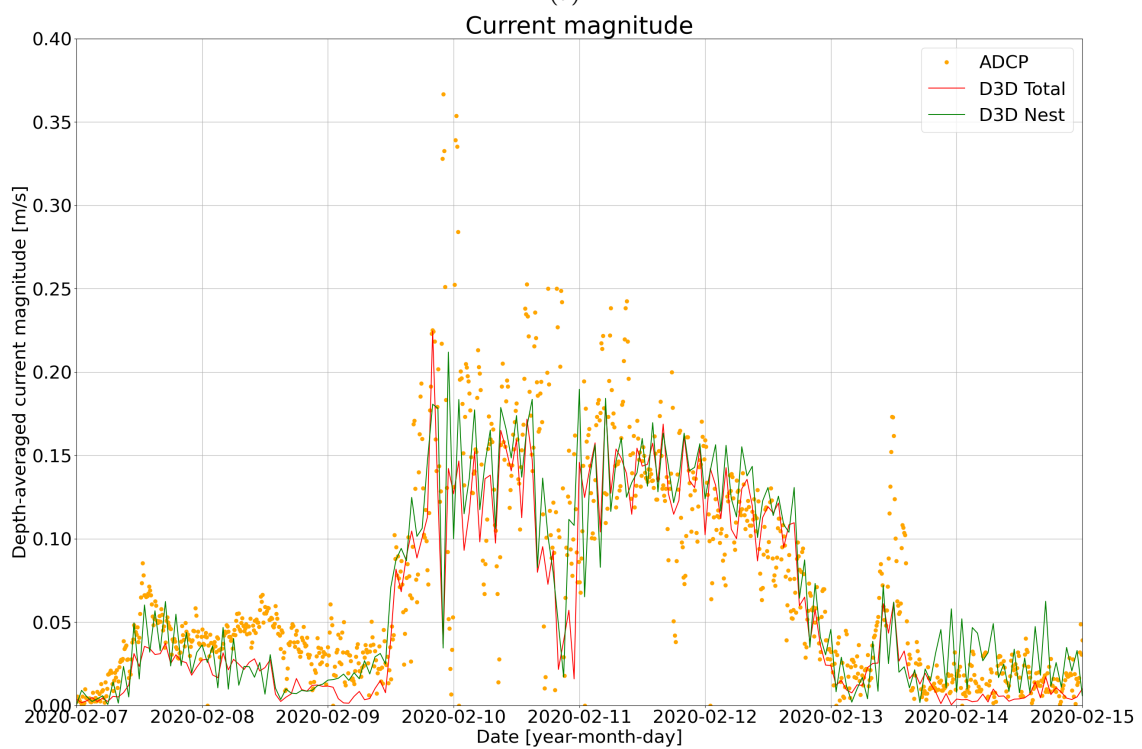
Figures 8.7a and 8.7b show the comparison of D3D model output and ADCP data. The former shows current direction: the models, both total and nested, show good correspondence to the direction measured by the ADCP. Both models show less spreading of the current direction compared to the ADCP data. Figure 8.7b shows the current magnitude, both the D3D total and nest results are within acceptable range of the ADCP measurements. Some high outliers are not found in the D3D model results (e.g. around 2020-02-10) and at some occasions the current magnitude as predicted by the model deviates more than 0.1 m/s from the ADCP data. The *nested model* results in slightly higher current magnitudes than the D3D *total model*. For this calibration run the wind direction measured at KNMI station Houtribdijk was used. The wind speed of station Berkhout was used as the Houtribdijk wind speed data is slightly overestimated due to the location of the station on top of the dike.

A negative offset of 0.03 meter in water level for both models is observed (figure D.6b) when comparing model outcomes and water level obtained by the stepgauge at FL66. The models simulate a lower water level relative to NAP, but the overall development of set-up and set-down matches. Some 0.1 to 0.2 meter difference between significant wave height as computed by the models and the STB are observed (figure D.6a), both models underestimating the significant wave height during the storm. The *nested model* is somewhat more reliable especially after the peak of the storm has vanished. The underestimation of the significant wave height can be caused by the usage of the Berkhout wind speed, no open water correction is applied (for other models Deltares adds a 7% open water correction, which is not applied in this model).

Visualisation of the calibration runs of the other periods can be found in section D.3 of the appendix. Model runs of June 2019 and April 2020 show higher wave heights than measured (figures D.8a and D.5a) as the wind speed at the Houtribdijk was not corrected (wind speed of station Houtribdijk was used). The wind direction does not need to be corrected and the current direction subsequently shows good correspondence to the measurements. For the run of February 2020 the wind speed was corrected, showing a better representation of both wave height and current magnitude, proving the wind speed data of Berkhout is more reliable.



(a)



(b)

Figure 8.7: Two figures showing ADCP measurements obtained at FL66 (orange dots) *total model* results (red dots) and *nested model* results (green dots): (a) Current direction at observation point FL66; (b) Current magnitude at FL66.

8.4 Scenarios

Different scenarios can be used as input for the D3D models. As we want to focus on the development of waves and the wind-induced current we create idealised wind schematization runs. These modelled scenarios are discussed in more detail in the next section.

8.4.1 Model runs

In the model we work with idealised wind schematization runs: we create an idealised setting for the wind, the main forcing of the hydrodynamic processes. For each run we set the direction the wind is coming from and stepwise in- and decrease the wind speed (figure 8.9). The modelled wind directions are all relative to the Noordstrand (figure 8.8), focusing on winds parallel and perpendicular to the shoreline orientation. We add a model run using the main wind direction as found in the data analysis (225°) for completeness.

From the data analysis we know the hydrodynamic processes respond to a changing forcing within a couple of hours, therefore we only model a short period of time. This also reduces the computation time of the model. The model includes three hours during which the wind speed is 0 m/s before increasing the wind speed (figure 8.9); model runs have shown these three hours are enough to account for the spin-up time of the model.

Simulation time:
1 January 2019 00:00:00 - 2 January 2019 19:00:00

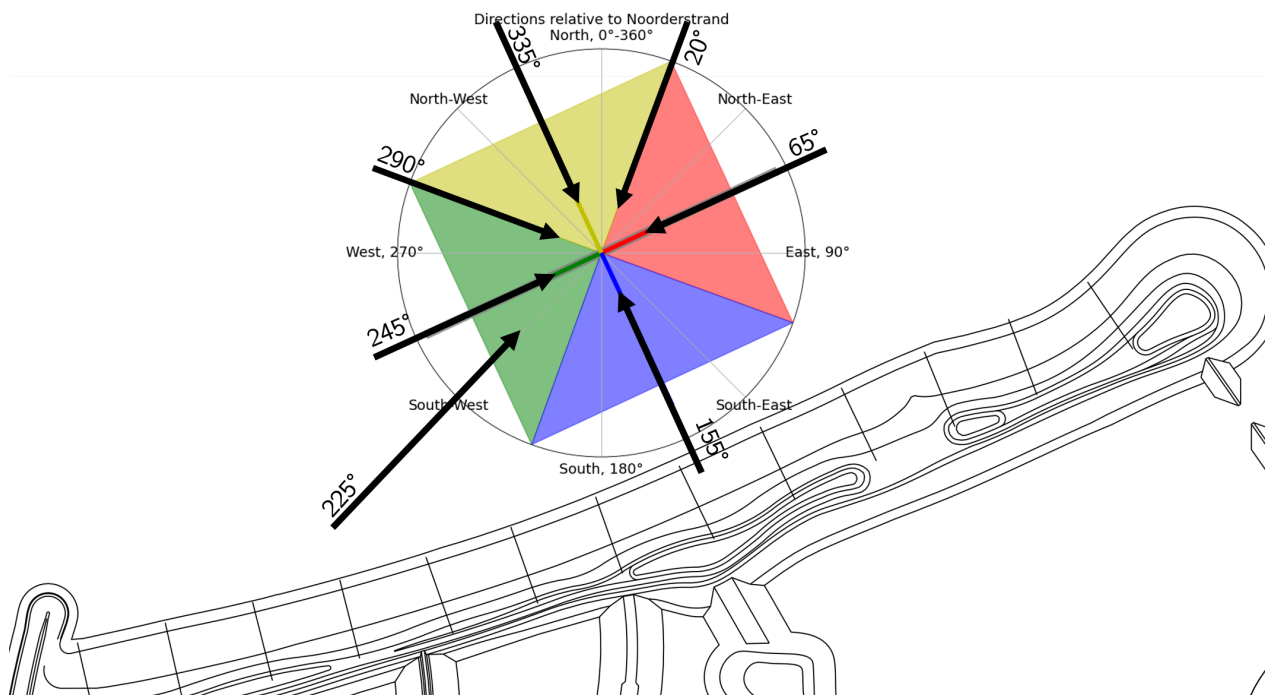


Figure 8.8: The seven wind directions used for the idealised wind schematization runs, all chosen relative to the Noordstrand. 65° and 245° indicate the shoreline parallel direction. 335° means the wind is blowing perpendicular to the shoreline orientation of the Noordstrand. For completeness the most frequent wind direction from the KNMI data is added: 225° (general southwestern winds).

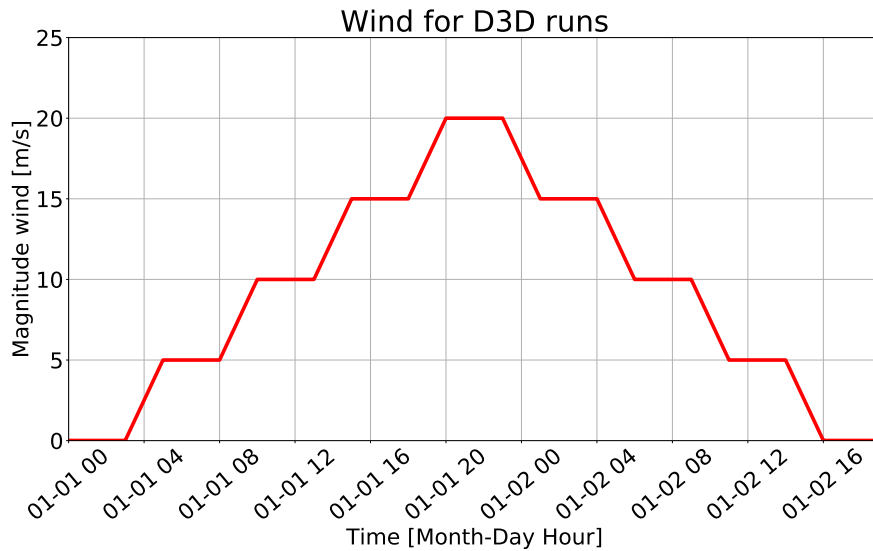


Figure 8.9: Schematization of in- and decrease of the wind speed for the idealised model runs. Every build-up of 5 m/s takes 2 hours until a maximum wind speed of 20 m/s is reached. It remains at the maximum for 3 hours after which the wind speed decreases again with 5 m/s every step.

8.4.2 Observation points

Nine observation points are included in the *nested model* runs to be able to observe specific parameters at these locations (figure 8.10). Results at these observation points are stored in the *trih*-file every 30 minutes. Station FL66 A is so far nearshore that it remains dry during all the modelled scenarios.

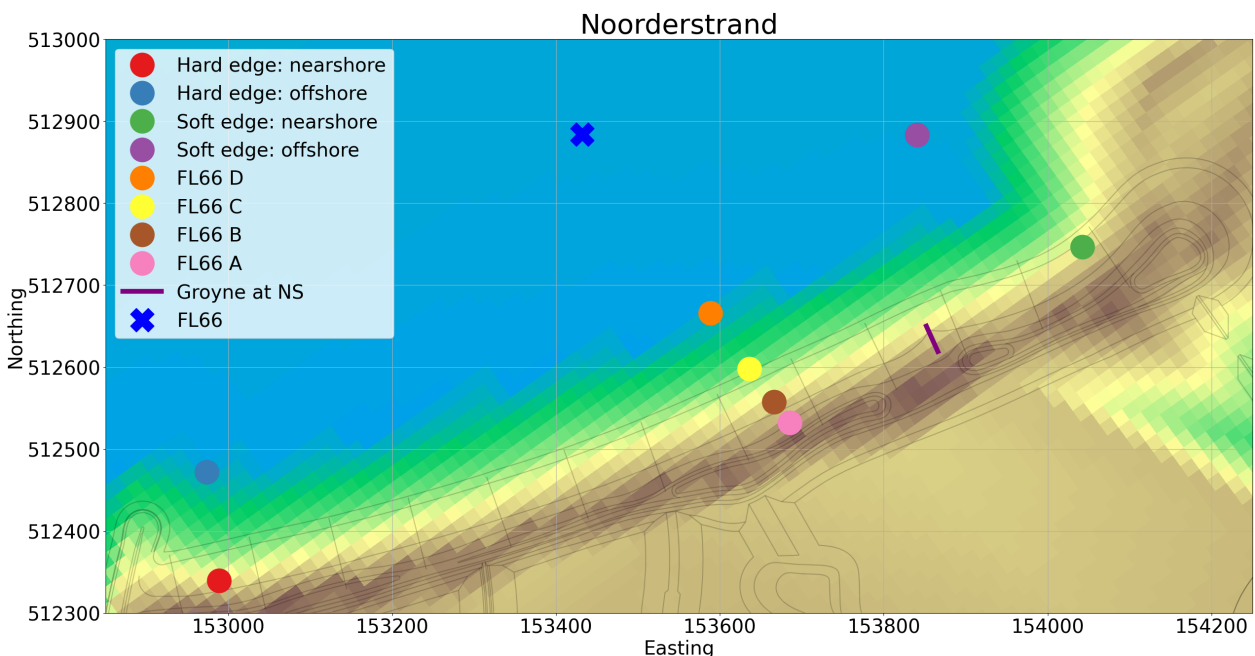


Figure 8.10: Observation points as set in the D3D *nested* model. The dark blue cross corresponds to the location of FL66. From this offshore station to the dunes of the Noorderstrand, 4 stations are included: FL66 D (orange), FL66 C (yellow), FL66 B (brown) and FL66 A (pink), from offshore to nearshore. FL66 A is so far nearshore that this location shows minimal results (mostly a dry cell). In addition two observation points near the edges of the Noorderstrand are included of which two offshore (bottom depth -4.23 m NAP) and two nearshore (-0.95 m NAP).

8.4.3 Sensitivity and exploratory model runs

Additional model runs to investigate other possible influences are performed next to the idealised wind schematization runs. The following runs focus on the influence of local bathymetry or topography:

- *Influence of submerged platform*: the offshore platform as observed at the Noordstrand (chapters 3 and 7) is smoothed out by the depth interpolation process in QUICKIN. Therefore we manually include a submerged platform in the bathymetry, with an elevation of -1.1 meter NAP, according to Ton et al. (2020). This allows us to investigate the influence of the platform on the hydrodynamics.
- *Influence sand extraction pit*: initial model runs show the 'flow' attraction of the sand extraction pits. To investigate the influence of the northern sand extraction pit we remove it from the Marker Wadden model and compare the results with the previous model outcomes.
- *Influence hard edge*: primary model runs show the creation of a rotation cell due to the presence of the hard edge (rip-rap breakwater, figure 2.3) in the southwest of the Noordstrand. We remove the thin dams, the model representation of the breakwater, from the model to investigate the relation between the presence of the breakwater and the rotation cell.

The sensitivity runs include:

- *3D model run*: the calibrated model is depth-averaged, only considering one layer in the vertical. The importance of adding multiple layers in the vertical model direction is explored by running the *total model* in 3D mode and comparing the outcome with the Marker Wadden model.
- *Wind and current, use and extent*: in the Marker Wadden model the FLOW-module updates the WAVE-module using wind data (so waves can be created by SWAN using the specified wind input). In this case not only the wind is used and extended from FLOW to WAVES but also the current (in between brackets in middle blue box, figure 8.1). In this way the effect of waves on the general current is accounted for (forcing, enhanced turbulence and bed shear stress) and vice versa (set-up, current refraction and enhanced bottom friction) (Deltares, 2021b).
- *Influence drying and flooding criterion*: the first model runs show certain flow patterns in the grid cells close to the waterline. These grid cells are subject to drying and flooding, a difficult process to model correctly (also discussed in section 10.4). By changing the drying and flooding threshold value we investigate the influence of these grid cells on the general nearshore flow.

All parameters of the sensitivity and exploratory model runs, except for the setting to be investigated, remain unchanged and similar to the original Marker Wadden model. For these runs we use the schematized wind input as shown in figure 8.9 and simulate two different wind directions: 245° and 335° (shoreline parallel and from dominant direction; and perpendicular to the shoreline orientation).

9

D3D Model Results

This chapter presents the main results of the D3D Marker Wadden model, the set-up of this model is discussed in the previous chapter. Most important model outcomes are discussed in this chapter, starting with the results of the idealised wind schematization runs, modelling flow and waves, in section 9.1. The outcome of the wave analysis is discussed in subsection 9.1.4. For two of the seven scenarios we additionally perform flow only computations, section 9.2. This is followed by the analysis of the sensitivity and exploratory model outcomes in section 9.3. The main findings are summarised in the last section, section 9.4. Additional model output and figures can be found in appendix E.

As an offline coupled total and nested model are used, it is important that general flow patterns in both models match. Considering this requirement the outcomes of both models are compared after each run. If the flow patterns in both models are not consistent, the results are considered unreliable and thus rejected. All scenarios considered in the D3D model analysis showed matching flow patterns between the total and nested model.

9.1 Idealised Wind Schematization Runs

To investigate the hydrodynamics near the Noordstrand idealised wind scenarios are run using the Marker Wadden model. Seven different scenarios are considered, corresponding to the seven wind directions chosen relative to the orientation of the Noordstrand (figure 8.8). The wind speed is increased to a maximum, 20 m/s, in stages and later decreased to 0 m/s (figure 8.9).

Section E.1 of the appendix shows for all seven scenarios the outcome of the *nested model* run, presenting the main circulation around the Marker Wadden islands, the flow patterns near the northern part of the Marker Wadden and the situation near the Noordstrand. The results near the Noordstrand are presented in this section (figure 9.2).

9.1.1 Delay hydrodynamic processes

All scenarios show a short delay between maximum wind speed and maximum occurring current magnitudes near the Noordstrand. The duration of the delay depends on the location of the observation points (for considered observation points see figure 8.10). More offshore locations show a difference between wind and current maximum of 30 minutes (dark blue, purple and light blue lines in top plot, figure 9.1). The current is faster to respond in more nearshore regions (e.g. brown line top plot, figure 9.1). Nonetheless this differences between offshore and nearshore can also be the result of the exact locations of the observation points: the offshore locations being closer to the transition zone and nearshore locations placed in high current magnitude hotspots. Some delay corresponds to the observed lag between wind and current measurements obtained by the ADCP.

The exact delay between wind speed and wave height maximum cannot be determined with certainty due to the coupling process between the *FLOW* and *WAVE* module. In Delft3D- *WAVE* (SWAN) wave generation by wind uses the user defined U_{10} for the friction velocity u_* (equation 9.1). This friction velocity returns in both the initial wave growth term, α , and the exponential wave growth term, β , of the energy source term used for the computation of waves (equation 9.2). When a wave computation is started (every 60 minutes, a quasi-stationary approach) the prevailing wind speed is taken from the *FLOW* input file and is used as input for

U_{10} . As we are only looking at the exponential wave growth term, β , in our quasi-stationary approach, the initial wave growth term, α , is not considered in our computations. Wave parameters are calculated and written to the output files. This means the flow is modelled every 0.75 minutes (table 8.1) and the waves only every 60 minutes. This results in a step-wise development of the wave height (lower plot, figure 9.1). For a complete overview of equations for wind generation in SWAN the reader is referred to Holthuijsen (2019) and The SWAN team (2020a).

$$u_*^2 = C_D U_{10}^2 \quad (9.1)$$

$$S_{in}(\sigma, \theta) = \alpha + \beta E(\sigma, \theta) \quad (9.2)$$

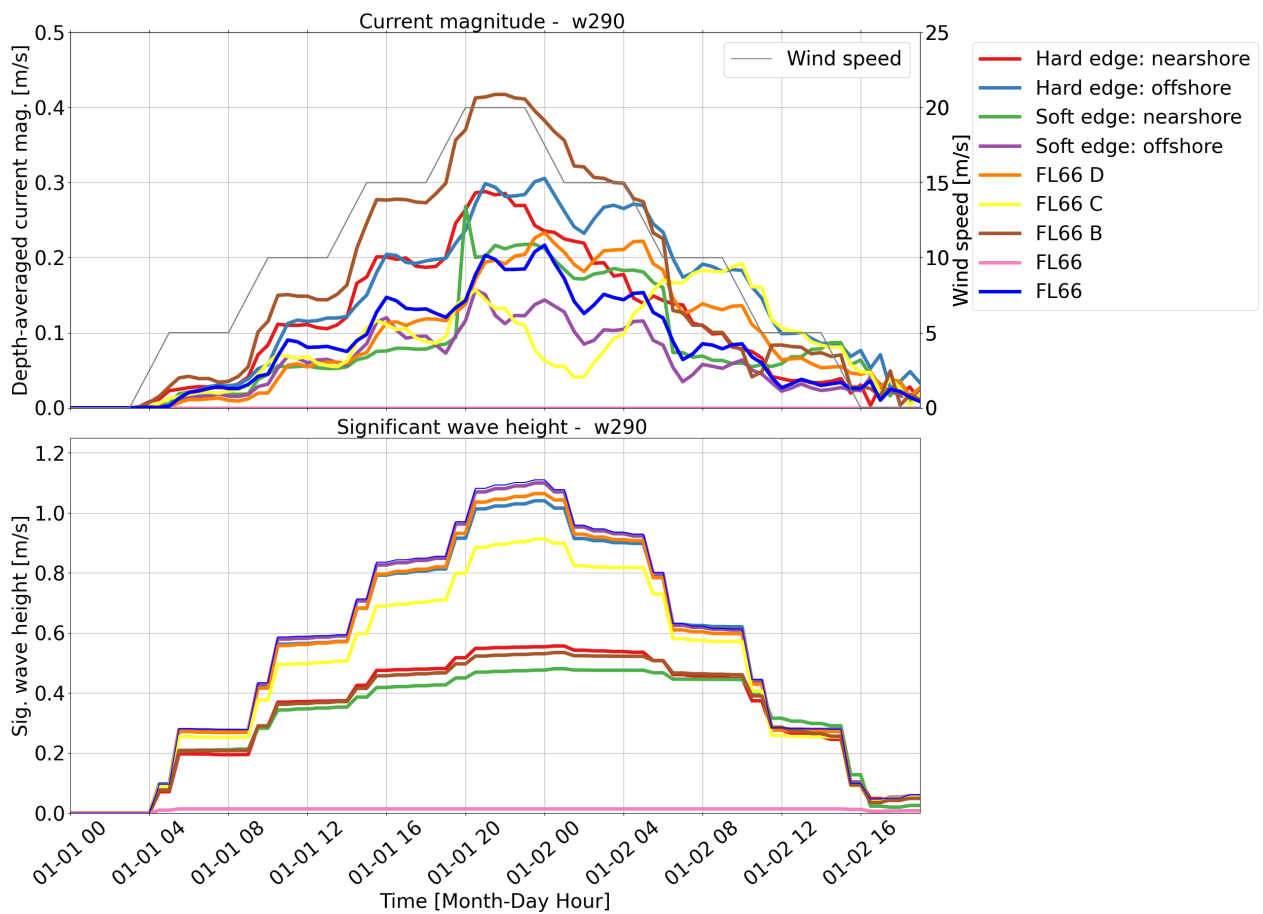


Figure 9.1: Current magnitude (top) and significant wave height (bottom) in the observation points for wind coming from 290°. The development of the wind speed is shown in grey in the top figure. Colours of the lines correspond to the locations as shown in figure 8.10.

9.1.2 Current direction and magnitude

When current magnitudes are maximum in the proximity of the Noordstrand six out of seven scenarios show a nearshore current direction which is opposite to the current direction offshore (figure 9.2). In the 20° scenario the current magnitude at FL66 is close to 0 m/s, whilst close to the beach current magnitudes as high as 0.27 m/s are observed going in shoreline parallel southern direction (w20, figure 9.2). No opposite flow patterns near- and offshore are observed in this particular case.

Scenarios in which the wind is coming from southwestern to northern direction (225°, 245°, 290° and 335°), result in a flow parallel to the Noordstrand going to the northeast (towards the soft edge). At FL66 the flow direction is opposite: going to the southwest. This is hypothesised to be the result of the larger lake circulation which is more profound offshore. Water flows towards the Marker Wadden from the northwest, but confronts the Marker Wadden: the flow is deflected to the southwest. The scenarios 225° and 245° show similar results: very high current magnitudes occur near the beach and upper shore face (w225 and w245, figure 9.2). Current magnitudes for the 245° scenario are slightly larger, exceeding a depth-averaged current of 0.3 m/s along more than 80% of the beach shoreline. This difference is explained by the Noordstrand orientation: the beach is more sheltered if winds are coming from a more southern direction. For both scenarios the region in which current magnitudes are negligible is located slightly more nearshore than the Markermeer bottom contour (-4.0 meter NAP) around a water depth of 2.5 meter.

The 290° and 335° show a jet-like current at the transition of the Noordstrand into the soft edge (w290 and w335, figure 9.2). Current magnitudes are high, more than 90% of the nearshore experiences current magnitudes higher than 0.3 m/s, before deflecting offshore in the jet-like current. This jet-like current seems to be the result of a northeastern going current along the Noordstrand converging with the southwestern going current arriving from northern part of the soft edge (figures E.13a and E.14a). Due to the convergence and acceleration of the flow we deem the description: *jet-like* fitting. The exact location of the jet-like current seems to depend on the magnitude of both currents. In case of a stronger southwestern going current entering the Noordstrand from the soft edge in the northeast the location of the jet-like current is 'pushed' towards the Noordstrand (scenario 335°).

Similar strong current magnitudes, but in opposite direction, are found when winds arrive from northeastern directions (20° and 65°). Especially in the case of a shore parallel wind direction, 65°, current magnitudes exceed 0.3 m/s along more than 70% of the shoreline (w65, figure 9.2). For a wind coming from the southeast, 155°, the Noordstrand is sheltered from direct wave attack: as a result negligible current magnitudes are observed near the beach (w155, figure 9.2).

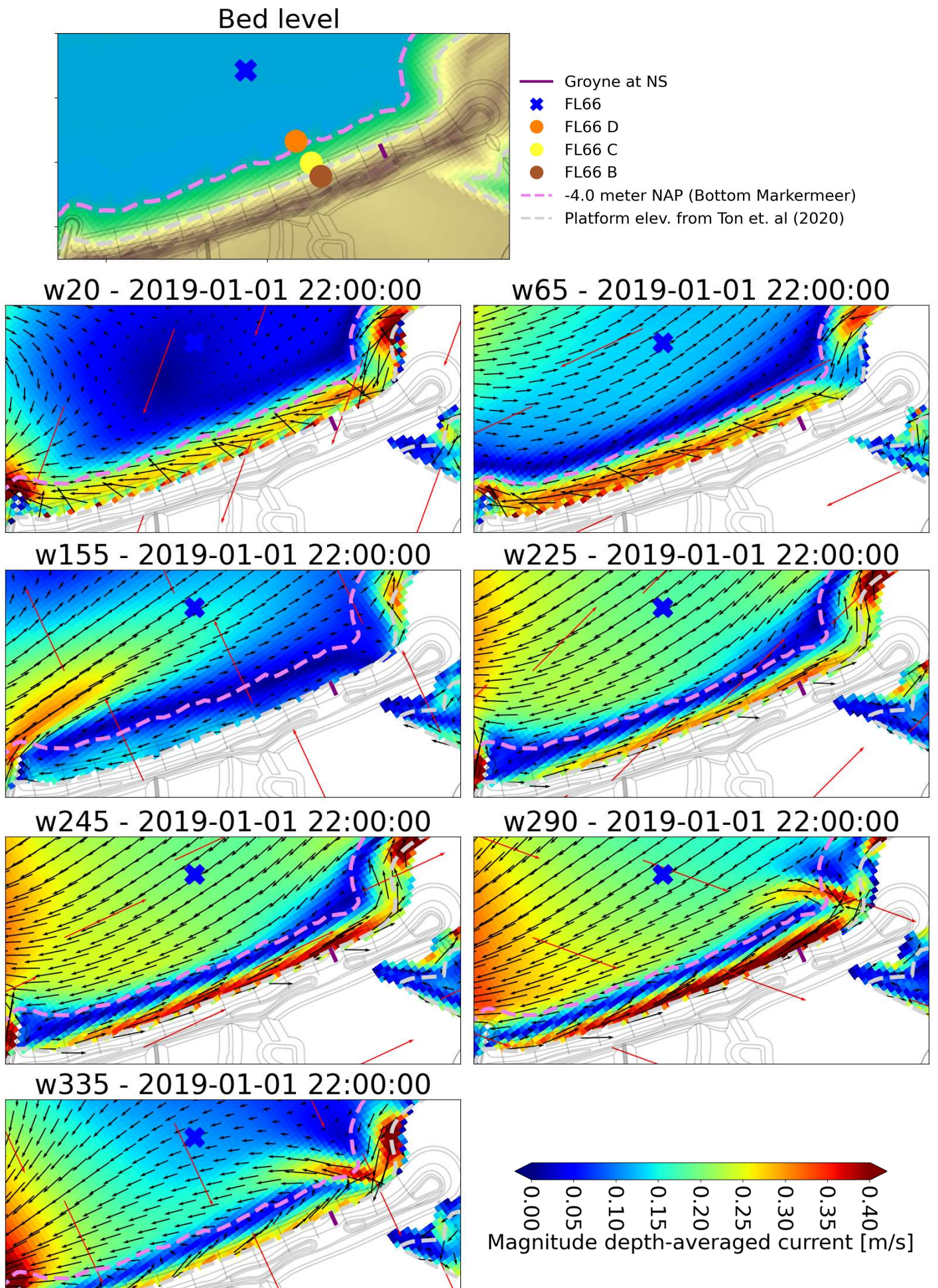


Figure 9.2: Overview current direction (black arrows) and magnitude (colourbar) for each schematised wind direction (red arrows) at the moment of maximum wind speed. Top plot shows the topography and bathymetry.

9.1.3 Influence topography and bathymetry

Next we analyse the influence of the local geometry, topography and bathymetry, looking at:

- Influence of submerged platform
- Influence hard edge
- Influence sand extraction pit

Influence submerged platform

The depth interpolation of the bathymetry on the computational grid in QUICKIN has removed the platform completely. As a result of the smoothing a linear depth profile is created. For this scenario the submerged platform is added manually to the bathymetry data. Platform formation as observed near the Noordstrand was already discussed in section 3.3.2. Due to the implementation of the platform the -1.1 meter NAP contour line (depth of the platform) shifts offshore (white striped line, insertion platform, figure 9.6). The width of the platform is somewhat exaggerated compared to the real width, to be better able to assess its influence on the hydrodynamics. It is important to note that we did not extent the width of the platform beyond the length of the hard edge.

In the presence of the submerged platform, the area width over which large, shore parallel, currents occur is increased (figure 9.6). The same is observed when considering the data obtained at the observation points in the model. FL66 C, was in case of no platform close to the region in which current magnitudes decreased. Now this observation point is situated in the region with maximum flow velocities. Due to the presence of the platform the current direction at FL66 C remains towards the northeast for a longer period of time (yellow crosses, figure E.23a). The submerged platform also increases the current magnitude at this location (figure E.23b), showing similar build-up and values as encountered at FL66 B.

Influence hard edge

The presence of the soft and hard edge do seem to influence the flow pattern. Both edges can cause acceleration and deceleration in the region of the upper shoreface depending on the wind direction. In case of the soft edge, located in the northeast, the curvature of the beach facilitates the jet-like current (scenarios 290° and 335°) or an area in which the flow parallel to the beach decelerates (other directions) (figures 9.2).

The hard edge (breakwater) located in southwest of the Noordstrand (figure 2.3) is modelled using thin dams. According Deltares (2021a): 'Thin dams are infinitely thin objects defined along the grid lines, which prohibit flow exchange between two computational cells at the two sides of the dam without reducing the total wet surface and the volume of the model. The purpose of a thin dam is to represent small obstacles (e.g. breakwaters or dams).' This thin dam blocks the flow and can as a result influence flow patterns. Remember, due to wind set-up or -down wind-induced lake circulation currents arises in the Markermeer. If this results in a general southwestern going current in the offshore region of the Noordstrand, this flow partly collides with the breakwater. Part of the flow goes around the hard edge and continues in southwestern direction, the other part of the flow will change direction under influence of the breakwater and continues more nearshore in northeastern direction, a *rotation cell* is formed (figure 9.3). A flow opposite to the general lake current is formed in the nearshore. Along the length of the shoreline the current magnitude is further enlarged by the wave-induced current present in the breaker zone. This combined current continues in northeastern direction and, depending on the prevailing wind direction, shoots offshore in a jet-like manner or continues around the soft edge. The initial acceleration in the proximity of the hard edge might increase longshore transport rates in the southwestern part of the Noordstrand.

The influence of the hard edge on the flow is analysed by removing the thin dams from the Marker Wadden model. We now observe that for similar conditions the rotation cell is no longer present (figure 9.6). In this new situation high flow velocities around the outer edge of the Marker Wadden are found, result of the wind-induced lake circulation. The flow travels in northern direction, it follows the geometry and turns to the northeast to follow the edge of the Noordstrand. The current direction nearshore remains unchanged (going in shoreline parallel northern direction), but the development of the current is completely different. Minimal acceleration is observed in the southwestern part of the beach (figure 9.6). However, by removing the breakwater the outermost southern edge would be subject to enlarged current magnitudes and could be a potential erosion hotspot especially in case of southwestern winds (w245, figure 9.6 and zoom-in figure 9.4).

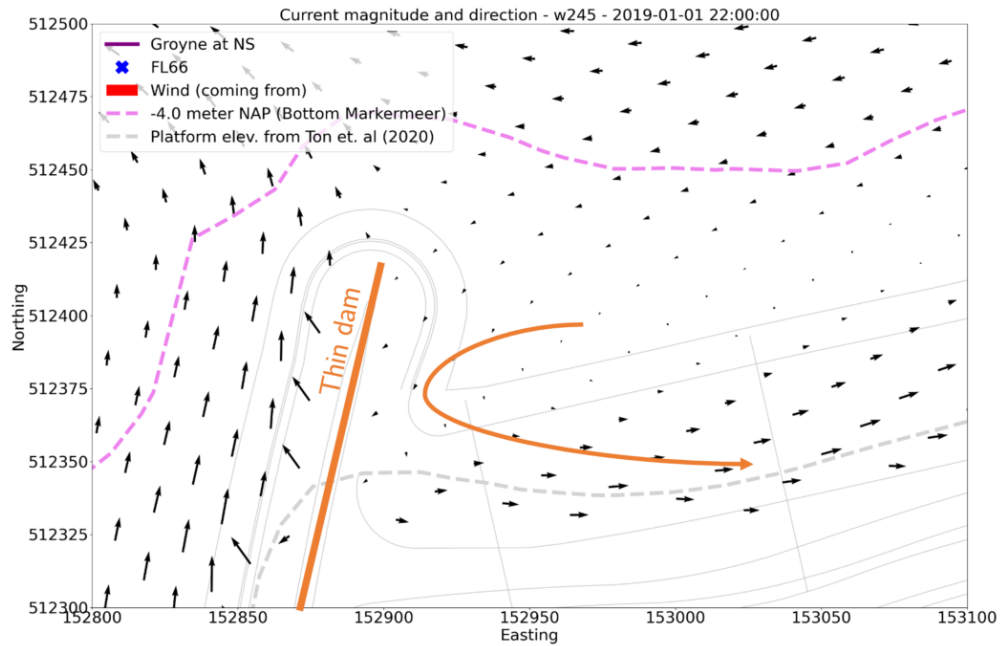


Figure 9.3: Rotation cell near the hard edge of the Noordstrand, for a wind coming from 245°. The orange line is a linear representation of the thin dams modelled in D3D. The orange arrow indicates the direction of the flow. A rotation cell is formed in the proximity of the hard edge.

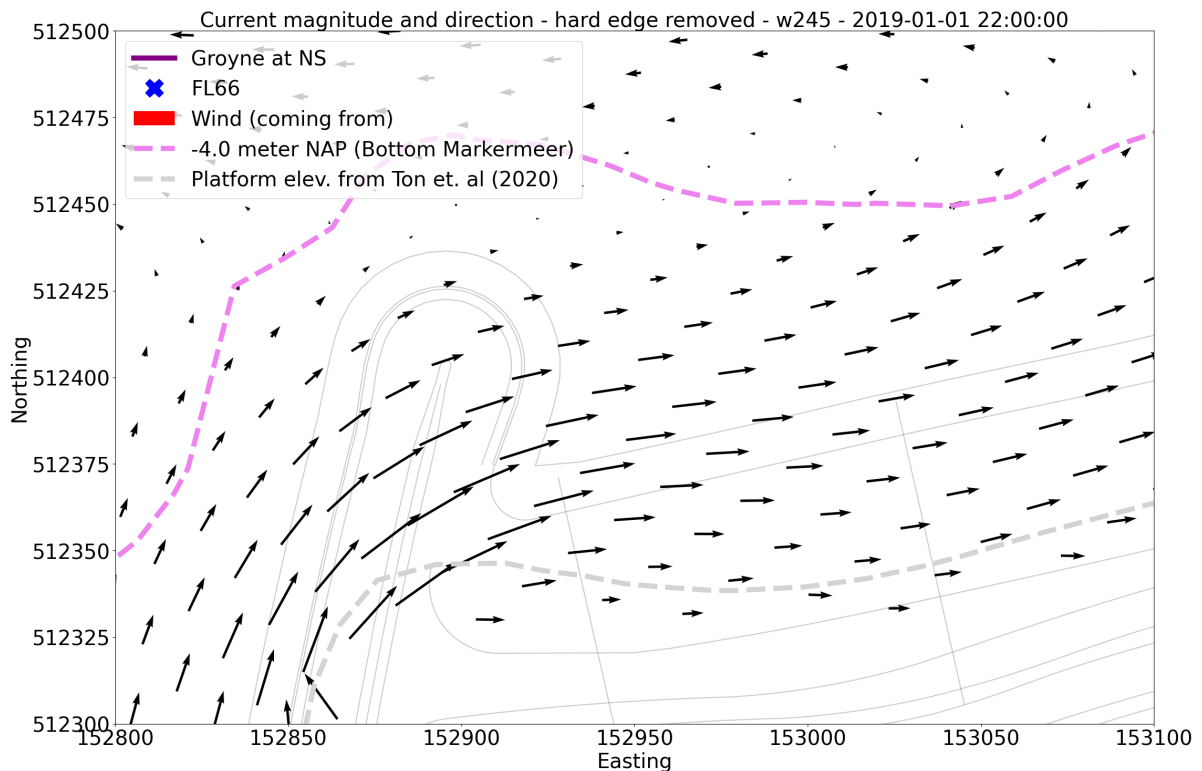
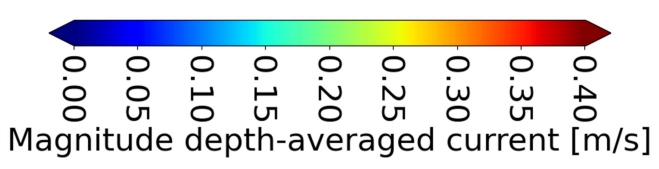


Figure 9.4: Hard edge is removed from the Marker Wadden model, meaning flow is possible where first the breakwater was located. Black arrows indicate current magnitude and direction. Wind is coming from 245°. Zoom out is visible in plot w245 of figure 9.6.

Influence sand extraction pit

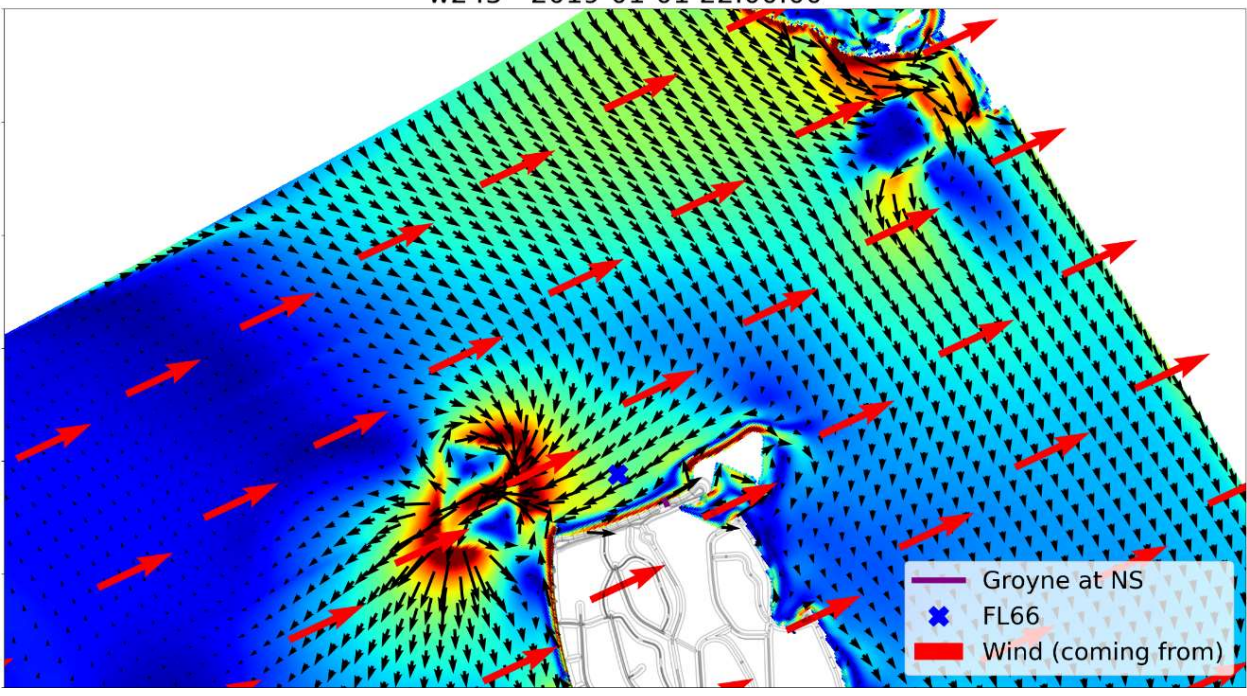
All model runs show the attraction of flow and enlarged flow velocities in the sand extraction pits around the Marker Wadden (dark red patches in figures of section E.1). The acceleration can be biased due to the 2DH numerical modelling as depth increases vastly in these pits, but the acceleration of flow over a navigational channel is physically possible (Van Rijn, 1986; Jensen et al., 1999). The sand extraction pits are not completely similar to navigational channels, but the same physical processes might appear. One of the pits is located very close by the hard edge of the Noordstrand. This might influence the flow patterns observed at the Noordstrand, therefore we investigate the removal of this pit on the nearshore processes.

The general lake circulation patterns do not change when removing the sand extraction pit from the model. We observe how the sand extraction pit has an influence on the magnitude of the general flow, but only in the proximity of the pit (figure 9.5). Removing the sand pit does not change the current directions and magnitudes much near the Noordstrand (figure 9.6). More offshore locations, hard edge (offshore) and FL66, show a minor decrease in magnitude (≈ -0.02 m/s). It seems the sand extraction pit only has a minor influence on the flow pattern offshore, its influence on the nearshore current direction and magnitude is negligible.



- Groyne at NS
- ✖ FL66
- - -4.0 meter NAP (Bottom Markermeer)
- - - Platform elev. from Ton et. al (2020)

w245 - 2019-01-01 22:00:00



Removal sand pit - w245

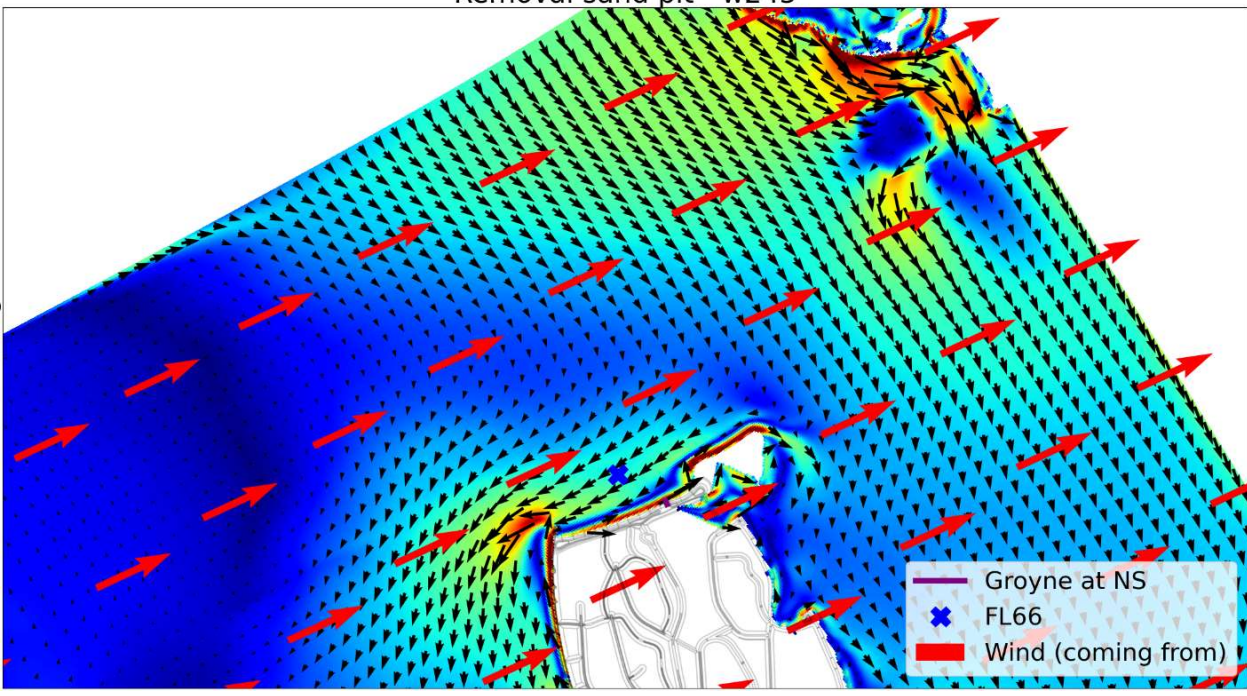


Figure 9.5: Overview current direction (black arrows) and magnitude (colourbar) for the runs with (top plot) and without (bottom plot) sand extraction pit near the Noordstrand due to parallel (245°) wind forcing (red arrows), showing the entire northern part of the *nested model*.

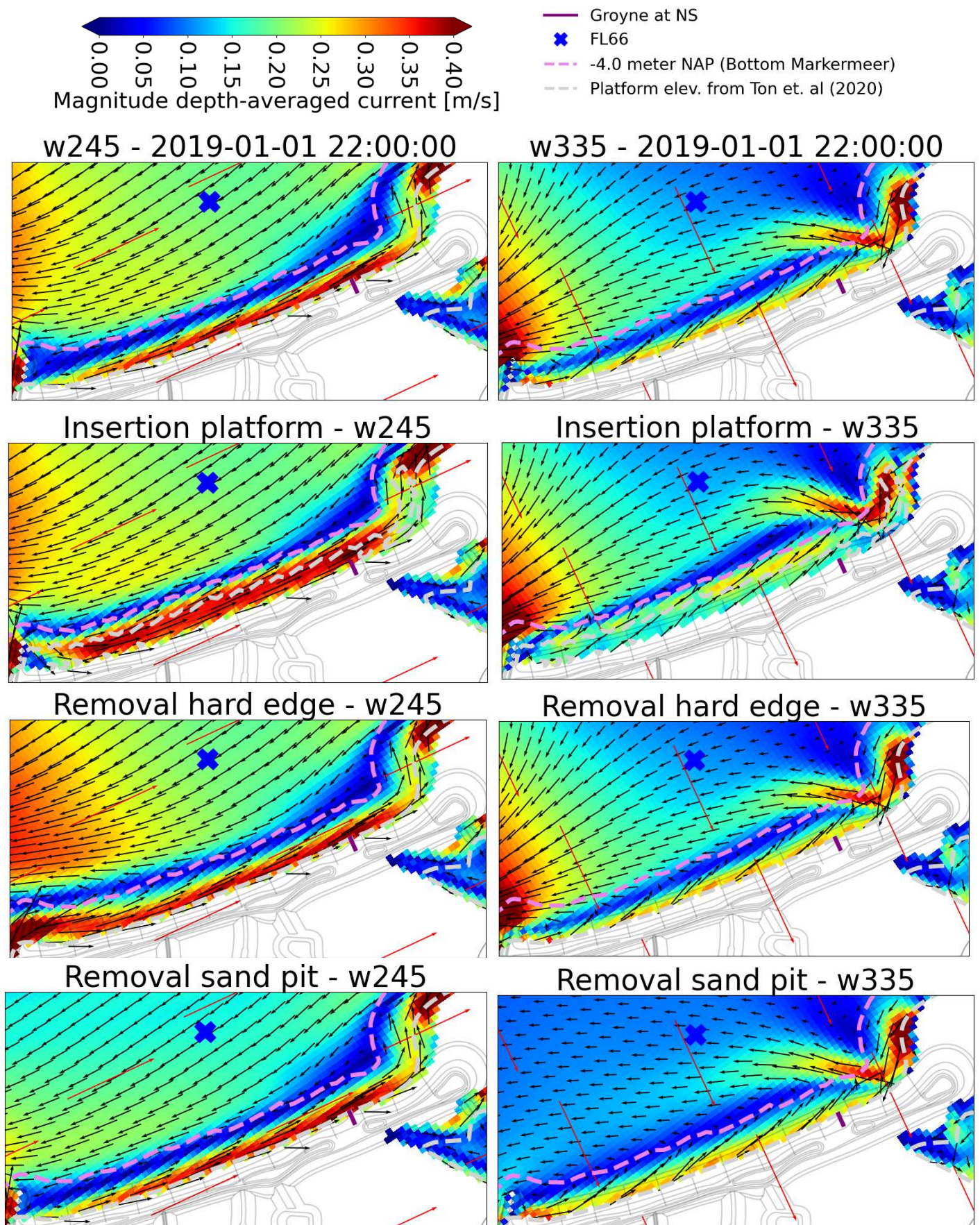


Figure 9.6: Overview current direction (black arrows) and magnitude (colourbar) for the runs investigating the influence of local features: removal of the hard edge, insertion of a submerged platform and removal of the sand extraction pit. The original results (no adaptations) are the top two plots. These runs use the parallel (245°) and perpendicular (335°) oriented wind directions (red arrows) as input.

9.1.4 Waves

For all the idealised wind schematization runs the wave direction and wave height is considered offshore and nearshore. In all model runs considering obliquely incident waves near the Noordstrand the refraction is limited (figure 9.7), meaning high-angle waves arrive at the shoreline. This was already expected based on the literature review (chapter 3) and the observation of 3D features, such as beach cusps, at the Noordstrand during field trips. Additionally, these high-angle waves contribute to an increase in the longshore current in the surfzone, influencing longshore transport rates.

In case waves arrive perpendicular at the beach, wind coming from 335°, there is no refraction not even near the edges (w335, figure 9.7). In that scenario significant wave heights are in the order of 1 meter due to the fetch distance. In case of northeastern winds (65°), wave heights offshore do not exceed 0.8 meter (w65 figure 9.7). In the 155° scenario the Noordstrand is completely sheltered from wave attack and the wave height nearshore is negligible (w155, figure 9.7).

Winds from a more southwestern to northwestern direction have a higher occurrence. We observe how winds from these directions can cause enlarged wave heights offshore due to the increased fetch distance (w225, w245 and w290, figure 9.7). In case of more southwestern winds, which have the highest occurrence, the southwestern part of the beach is a little more sheltered due to the local geometry of the beach in combination with the breakwater. In the proximity of FL66 the offshore significant wave height is roughly 1.0 meter and the wave height decreases nearshore to 0.5 meter. In case of northwestern winds (290°) the wave impact is more direct and this results in larger wave heights nearshore (w290, figure 9.7). In the other three scenarios, 225°, 245° and 290°, we notice little refraction and as a result high-angle waves are observed near the shoreline of the Noordstrand (w225, w245 and w290, figure 9.7).

Influence topography and bathymetry

We have analysed the influence of changing specific features of the local geometry on the flow. In case of the inclusion of a submerged platform and the removal of the hard edge we have also analysed the influence on the waves. The removal of the sand extraction pit on waves was checked, but no differences were observed.

By inserting a submerged platform we see how the wave height on top of the platform decreases significantly compared to the runs without a platform. Instead of an incoming wave height of 0.7 meter the inclusion of the platform reduces the significant wave height to 0.4 meter nearshore (broader blue band nearshore in *insertion platform* plots, figure 9.8). This means the presence of a submerged platform reduces wave energy near the beach face. However, during events with an increase in water level (mostly coinciding with high-energy events) the influence of the platform on wave breaking reduces.

The breakwater is not long enough to influence the nearshore wave climate at the Noordstrand significantly, only right next to the breakwater the wave height is reduced (bottom two plots, figure 9.8). Furthermore, most sheltering in case of a southwestern wind is caused by the entire southwestern border of the Marker Wadden and the relative 'hidden' position of the Noordstrand. The diffraction process was not activated in our Marker Wadden model, so this cannot be analysed.

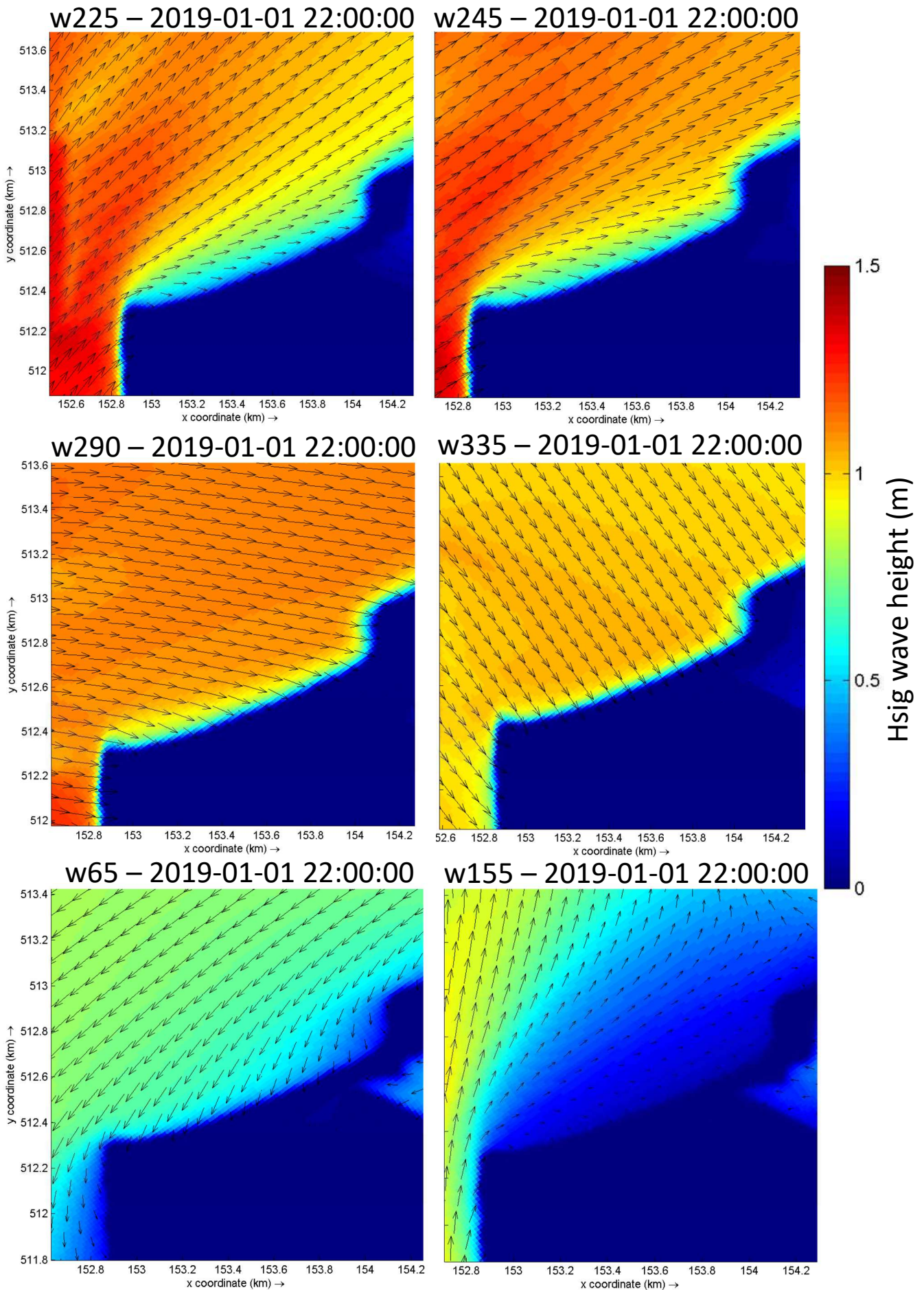


Figure 9.7: Overview wave direction (black arrows) and magnitude (colourbar) for each schematised wind direction at the moment of maximum wind speed shown at the Noordstrand. Scenario 20° is not shown, but looks similar to w65.

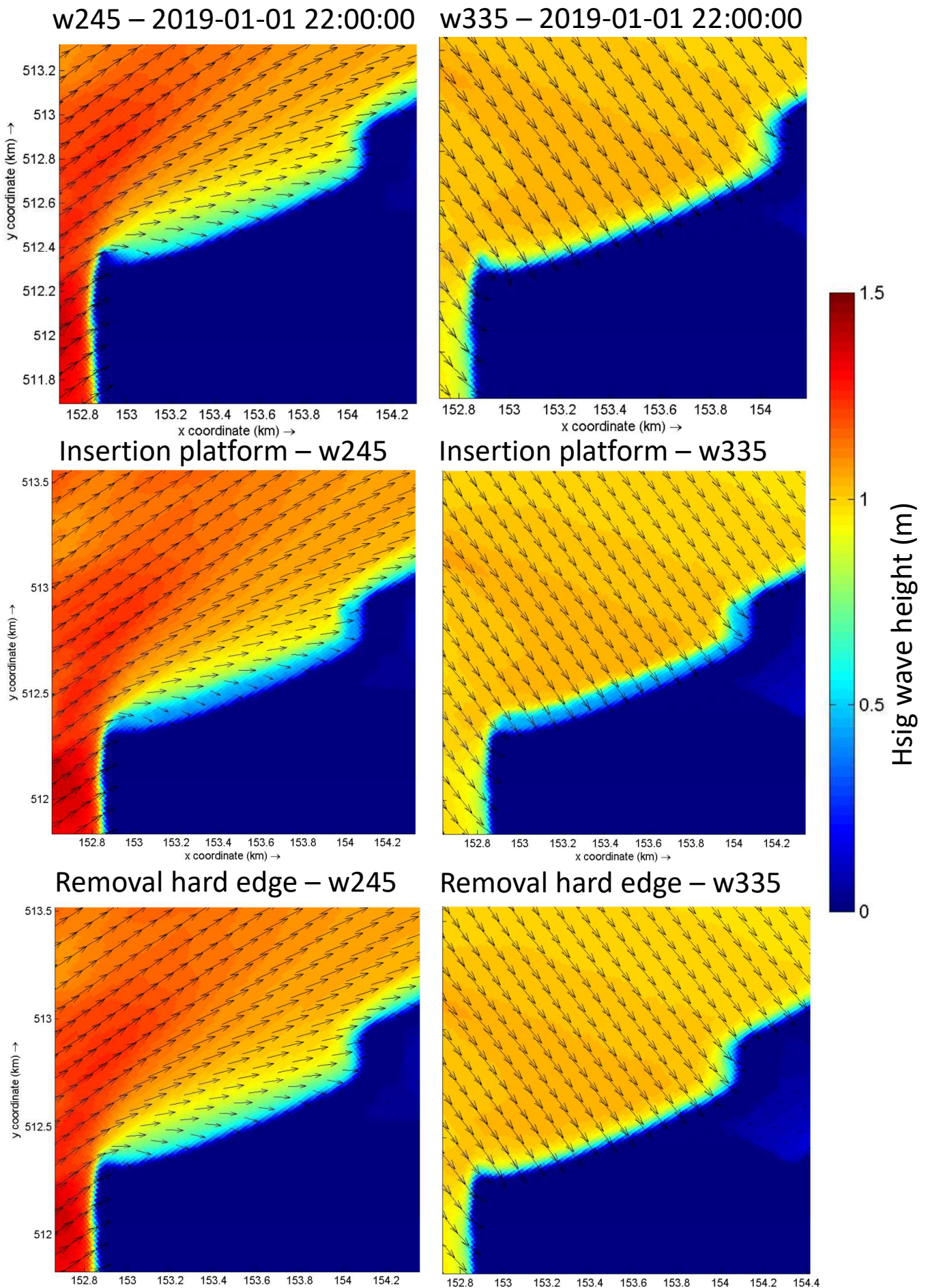


Figure 9.8: Overview wave direction (black arrows) and magnitude (colourbar) for the runs investigating the influence of local features near the Noordstrand on wave propagation: removal of the hard edge and insertion of a submerged platform. The original results (no adaptations) are the top two plots. *Note: for original no adaptation runs (top) the .mdw file was updated to include a segment of obstacles: additionally blocking the propagation of waves at the hard edge (other original runs (figure 9.7) are not updated to include this feature).* These runs use the parallel (245°) and perpendicular (335°) oriented wind directions as input.

9.2 Comparing Flow & Waves to Only Flow

The wave module is turned off (Delft3D-WAVE is not used) and as a result wave generation and dissipation processes are not considered. These additional *flow only* runs enable us to investigate wind-induced processes (focusing on the wind-induced circulation in the lake and near the Noordstrand). For the flow only scenarios we focus on the wind directions 245° and 335° solely. As they represent the critical incoming wind directions: 245° shoreline parallel (southwestern winds are much more frequent than northeastern winds) and 335° causing normal incident waves with respect to the Noordstrand shoreline orientation. Upon first glance the flow only patterns do not really differ, however when looking in more detail minor but important differences can be distinguished.

For both wind directions the highest current magnitudes are measured earlier in time. If waves are included the timing of this maximum is delayed, but the period of enlarged current magnitudes is extended (figures E.17a and E.17b). Additionally, the waves enlarge the observed current magnitudes. Even in the flow only model run the jet-like current is present. Waves do also enlarge the magnitude of this jet-like current (w335, figure 9.9).

Waves seem to 'push' the region with enlarged current magnitudes towards the waterline (w245, figure 9.9), this situation persists even when wind speeds drop (figures E.15b and E.16b). Current magnitudes of the wind-induced current only can still be significant near the beach: along a length of 1000 meters the magnitude of the depth-averaged current exceeds 0.3 m/s (figure 9.9). In this case the wind-induced current definitely has an impact on the nearshore hydrodynamics. During one of our field trips we encountered an enlarged longshore current on top of the submerged platform near the soft edge, making it more difficult to navigate through the water. The weather conditions were relatively calm, no real waves were present. Could this be an indication of the enlarged wind-induced current along the Noordstrand?

For the 335° wind scenario we observe two major influences of the waves: namely an increase in the longshore current and the current direction changes more towards the offshore in case of waves (w335, figure 9.9), indicating increased cross-shore velocities. The latter can be explained by the normal incidence waves approaching the beach during these wind conditions, resulting in larger cross-shore velocities and potentially increase cross-shore transport. For the flow only computation with wind from 245° we observe smaller current magnitudes near the middle of the beach (w245, figure 9.9). This is not observed when waves are included, it seems the influence of waves 'spreads' the effect of the wind-induced current along the beach.

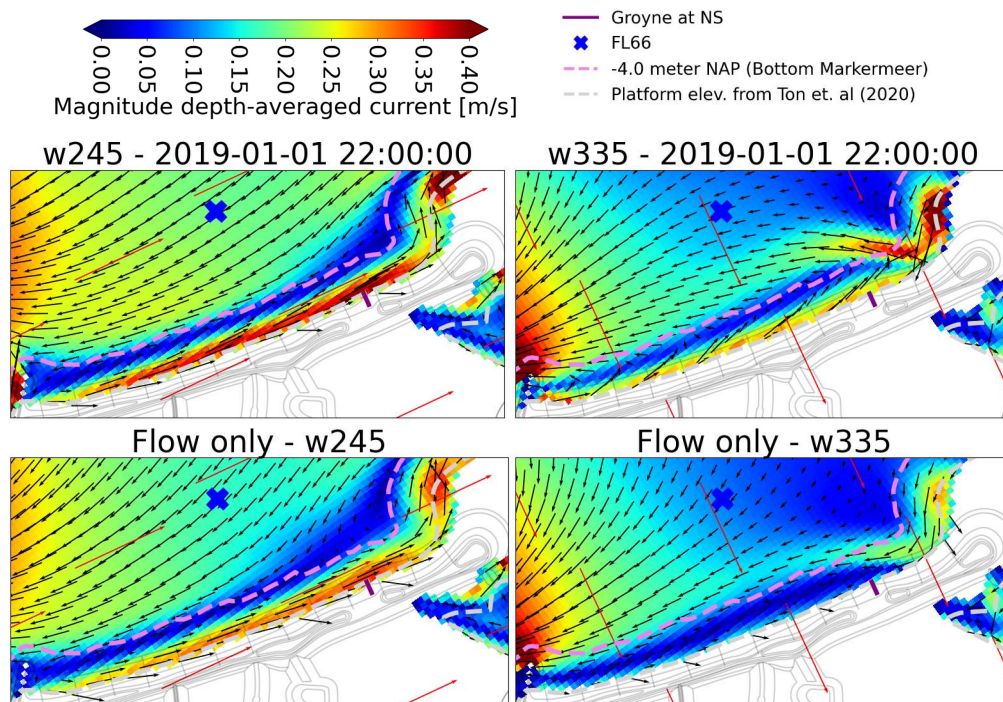


Figure 9.9: Overview current direction (black arrows) and magnitude (colourbar) for the flow & waves (top two plots) and the flow only (bottom two plots) runs, for different wind directions (red arrows).

9.3 Sensitivity and Exploratory Model Runs

This section includes the results of the sensitivity and exploratory model runs (set-up discussed in section 8.4.3) focusing on the following:

- 3D model run
- Wind and current: use and extent
- Influence drying and flooding criterion

9.3.1 3D Model

The Marker Wadden *total model* is extended from a 2DH to a 3D model, to investigate the velocity profile over the vertical: is depth-averaging an acceptable representation of reality? Delft3D-FLOW uses the σ -grid: the number of layers is constant and the layer thickness is relative to the water depth. In the 3D Marker Wadden model we introduce 20 layers, each having a layer thickness of 5% of the water depth. The original Markermeer model included only 7 layers, in our opinion not sufficient to evaluate the velocity profile over depth. A (background) vertical eddy viscosity of $1e^{-5}$ is added to the model, using the $k-\epsilon$ model for the 3D turbulence modelling. Wind directions 245° and 335° are considered and the development of the wind speed is similar to the idealised schematization runs (figure 8.9).

Figures 9.10a and 9.10b show current profiles over depth for both wind scenarios (245° plot(a) and 335° plot (b)). The shown current profiles are the situations in which *the profile deviates the most from uniform flow over depth* during a model run, meaning in this profile we observe the largest gradients over u, v and current magnitude over depth in the considered period of time. In case of wind coming from 245° the direction of the current over depth in u and v direction is uniform (southwest), the highest current magnitudes are found at a water depth of 2.3 meter. A depth-averaged current magnitude (red line in right plot of figure 9.10a) overestimates the current magnitude at the surface (difference > 0.1 m/s) and at the bottom (difference ≈ 0.1 m/s). Consequently it underestimates the maximum occurring current magnitude with a value of ≈ 0.05 m/s (present slightly deeper than mid-depth). The 335° scenario does show a deviating current profile over depth for the v component (middle plot, figure 9.10b). In the upper part of the water column flow is towards the south, similar to the direction of the wind (although influenced by the Marker Wadden geometry). In the bottom part of the water column the flow is in the opposite direction: going north. Water is 'pushed' onto the Noordstrand by the perpendicular oriented wind (compared to the Noordstrand shoreline orientation), creating a return current in the bottom part of the water column towards the north. This results in the observation of a wind-driven current. The difference between the maximum southern and northern component of the v-velocity is less than 0.2 m/s. The depth-averaged current matches the horizontal magnitude over the vertical (profile vs red line, figure 9.10b). Vertical velocities in both 3D models are small (order $10^{-6} - 10^{-5}$) and thus negligible.

Wind from 245° causes a water level set-up to the Houtribdijk, resulting in a larger water depth for increasing wind speeds at FL66 (blue line, figure E.20). Wind coming from 335° does result in a small local set-up in front of the Noordstrand (with a resulting return flow in the lower part of the water column). However, when considering the effect of the wind forcing on the entire Markermeer we observe a set-down at FL66 (orange line, figure E.20).

Comparison 2DH and data ADCP

Looking at the results of the 3D model we can conclude depth-averaging is acceptable. The current direction does not change much over depth, only in case of a perpendicular oriented wind compared to the shoreline orientation. Nonetheless, in that case the gradient over the vertical is small and the current magnitudes near the Noordstrand are not significant (≈ 0.1 m/s, figure 9.10b and w335, figure 9.2). In case of wind coming from 245° , the 2DH model slightly overestimates the current in the top and bottom part of the water column and underestimates the current magnitude in the middle. This difference is deemed acceptable as we consider the general magnitude of the current in this research instead of looking into the exact build-up of the current over the vertical. We can compare the u and v components of the 245° model run (figure 9.10a) with the ADCP measurements of February 2020 (figure 6.13). The resemblance is striking: during this energetic period wind was primarily from southwestern direction matching the 245° wind forcing of the model. Both, the 3D model and ADCP data, show a more or less uniform current profile over depth.

It is important to note that only the vertical velocity profile at FL66 is considered. It could well be that velocity profiles over depth in other parts of the Markermeer do not show the same uniformity. For now this is not further investigated, but could be an interesting case for a follow-up study.

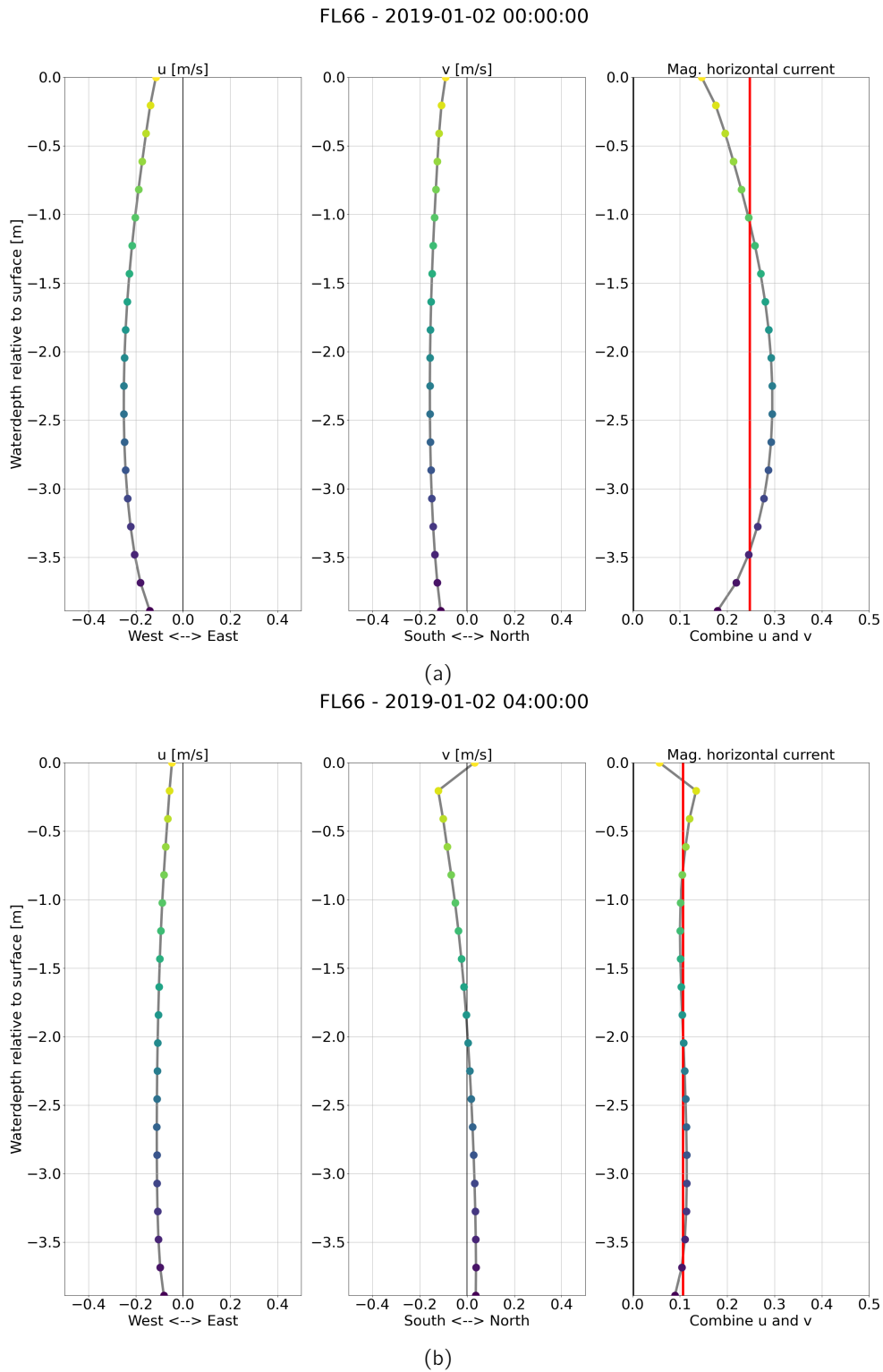


Figure 9.10: Velocity profile over water depth at FL66: u and v direction of the current in the horizontal plan (two left plots). The right plot is the horizontal current magnitude over the vertical ($\sqrt{u^2 + v^2}$), with the depth-averaged current magnitude (red line). The coloured dots represent the layers of the D3D model; (a) **Wind coming from 245°**; (b) **Wind coming from 335°**

9.3.2 *Wind and current: use and extent*

Extending the coupling between Delft3D-FLOW and Delft3D-WAVES from only wind to wind and current, did not noticeably change the earlier observed flow patterns (comparison figures E.22a and E.22b). This could be influenced by the fact that SWAN does not solve the wave-induced current (The SWAN team, 2020a), but gives Delft3D-FLOW the gradient in radiation stresses as source for the momentum equations of the shallow water equations. Therefore, the wave-induced current is already taken into consideration when only extending the *wind* for the FLOW to the WAVE module. In return the wind-induced current does not seem to influence the dynamics of the waves much. Even the effect of the current on wave height and direction, is negligible. This is not surprising as the current magnitudes in this system are rather limited compared to tidal currents present in high-energy environments. Tidal currents exceeding 1 m/s are possible near the Dutch coast (Rijkswaterstaat, 2021), in our case we are looking at general current magnitudes ranging between 0.2 and 0.4 m/s. This could mean the influence of currents on the propagation and breaking of waves is rather limited.

9.3.3 *Influence drying and flooding criterion*

The information in the outer grid cells, near the waterline, is difficult to assess. These cells are subject to the drying and flooding process in Delft3D. A grid cell is flooded if the water depth exceeds the specified *threshold depth* and is dry when the water depth is smaller than the half of this value (Deltares, 2021a). In the schematised model runs we use the default value for the threshold depth: 0.1 meter. However, in our case the bathymetry nearshore changes approximately 0.5 meters over the length of one grid cell, possibly influencing the drying and flooding process. Besides, if the water depth is smaller than 0.05 meter but non-zero, the grid cell is considered dry and water is 'lost' from the mass balance. If this occurs in multiple grid cells, this can influence the model outcome. To assess this effect we change the threshold depth from 0.1 to 0.01 meter.

Analysing the outcome of this sensitivity run (flooding and drying crit., bottom two plots, figure 9.11) we observe current patterns and magnitudes matching the original model run (top two plots, figure 9.11). We notice the lower threshold depth has an influence on the model: lower laying grid cells behind the Noordstrand dunes have flooded, a flow to the northeast has commenced. In addition to this 'flood' we find another breach near the soft edge of the Noordstrand.

Looking at this sensitivity run we conclude the effect of changing the drying and flooding threshold depth does not significantly influence the model outcome. The nearshore current is an effect of the hydrodynamic processes rather than a numerical artefact of the modelling of drying and flooding grid cells. It also seems the mass balance is not influence significantly by the set threshold depth, still we consider the model outcomes in the outer grid cells with care.

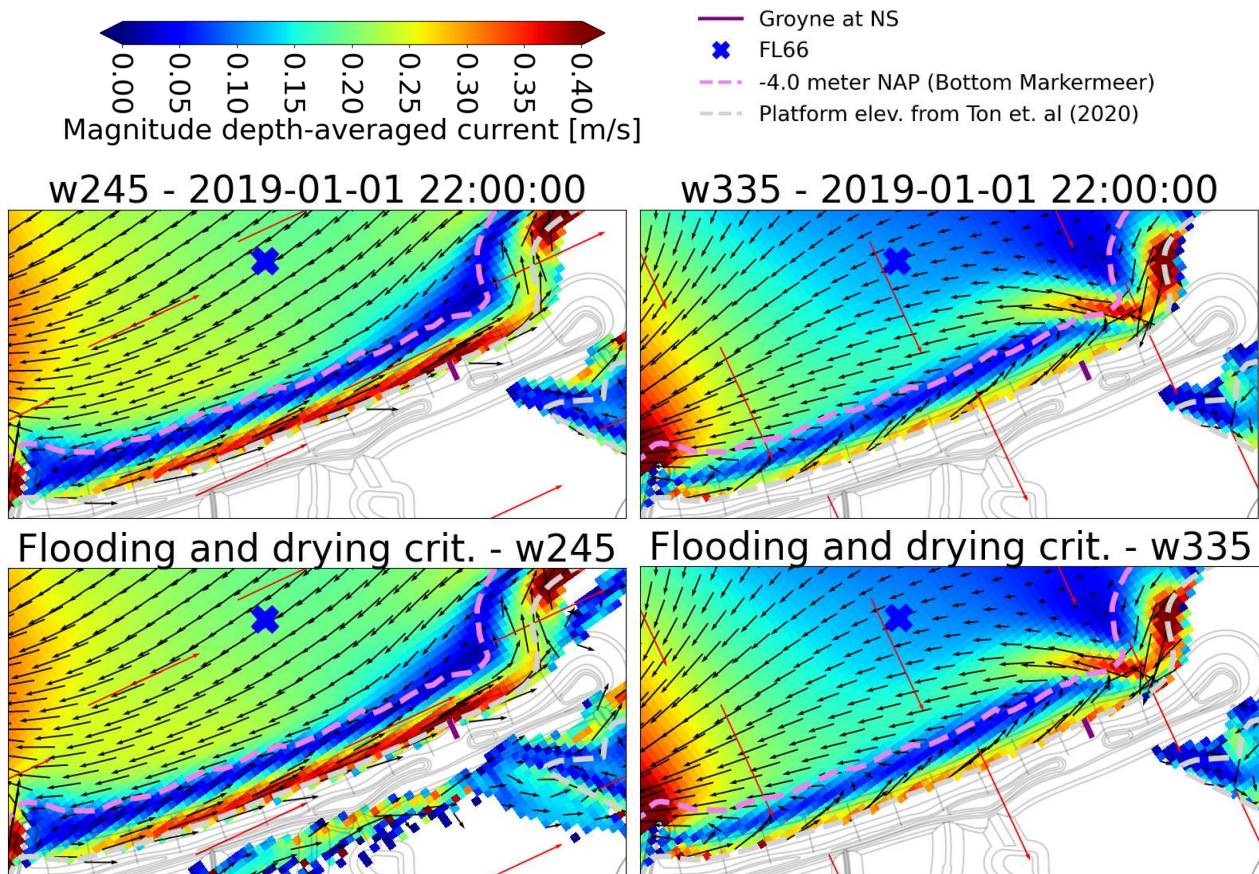


Figure 9.11: Overview current direction (black arrows) and magnitude (colourbar) for the sensitivity runs regarding the drying and flooding threshold depth for different wind directions (red arrows). The default value of 0.1 meter (top two plots) and the adapted value of 0.01 meter (bottom two plots) are used for the threshold depth.

9.4 Conclusions

Using the D3D Marker Wadden model to investigate the hydrodynamic processes near the Noordstrand we can conclude the following:

- An additional model run using a 3D model has shown only minor differences in current magnitudes over depth, underlining the validation of the depth-averaged (2DH) model. This has been validated for other measuring stations in the Markermeer.
- In general the wind-induced current is fast to respond to changes in wind speed. As a set-up or -down of water level is created over the entire Markermeer, a larger lake circulation is created. The direction of this current depends on the location, wind forcing and geometry of the Marker Wadden. Winds from southwestern to northern direction (225°, 245°, 290° and 335°) result in a flow parallel opposite to the wind direction offshore (going in southwestern direction), closer to the beach the nearshore flow is in the opposite direction (going towards the northeast). This is the result of a rotation cell which is caused by the proximity of the hard edge (bullet point four). In case of a northeastern wind direction (20° and 65°) directions are reversed, still an opposite flow direction between off- and nearshore is observed.
- For some wind directions (290° and 335°) a jet-like current is formed near the soft edge, created by the convergence of the longshore current along the Noordstrand and the wind-induced lake current along the soft edge. This jet-like current behaviour could potentially bring sediment offshore, where it is transported with the general wind-induced lake circulation along the offshore contours of the Noordstrand. In the region of the beach where the jet-like current occurs, acceleration or deceleration of the general flow is observed in most of the considered wind scenarios. It could be a potential location of erosion or sedimentation depending on the prevailing wind direction.
- Sensitivity runs show the influence of the hard edge on the flow pattern: a rotation cell is formed in which flow velocities gradually increase along the southwestern part of the Noordstrand. If the breakwater is removed the rotation cell is no longer present. The nearshore current direction remains the same, but acceleration of the current along the Noordstrand is minimised.
- Waves enlarge the current magnitude close to the beach when the wave-induced longshore current and nearshore wind-induced current are in the same direction. The waves do not change the direction of the nearshore current. Waves do cause a decrease of the width of the nearshore region in which the current is significant (larger than 0.2 m/s). This makes the area in which the current flows opposite to the general offshore lake current smaller.
- The wind-induced current on itself can create current magnitudes exceeding 0.3 m/s near the upper shoreface of the Noordstrand, but only if the wind forcing is from southwestern directions causing a set-up to the Houtribdijk. This wind-induced current can be further enhanced by the wind-driven current (formed by the wind shear stress at the surface) in relative shallow areas (e.g. on top of the submerged platform). Even in case of only wind-induced and wind-driven flow a rotation cell is present near the hard edge, causing an acceleration of the flow along the southwestern part of the beach. A northwestern wind direction does not create wind-induced current magnitudes near the Noordstrand which are significant. However, if waves are included this results in higher current magnitudes, exceeding 0.25 m/s near the upper shoreface.
- One should keep in mind to remain critical towards information displayed in the outermost grid cells, representing the waterline. The drying and flooding procedure in combination with a relatively coarse grid can give unreliable results. A sensitivity run in which the drying and flooding threshold depth was decreased showed similar flow patterns, underlining the result of the other model runs. Noteworthy is the influence of the sand extraction pit, its attraction of flow can be both physical and numerical. Removing the sand extraction pit near the Noordstrand does not change the observed current direction and magnitudes significantly and therefore its direct influence on the Noordstrand can be neglected. Nonetheless the sand extraction pits do influence the general circulation in the lake in the D3D model.



Conclusions - Creating the Total Picture

10

Discussion

In this chapter we present a conceptual system description of the general system (Markermeer) and how this influences our local system of the Noordstrand. For the latter this includes a hypothesised description of how the hydro- and morphodynamic processes interact and influence beach development. This means we ought to find the **Link** between hydro- and morphodynamic processes and use this information to assess if an **Equilibrium** situation is possible at the Noordstrand. We want to identify the **Lessons learnt**, useful for the monitoring and maintenance of the Marker Wadden beaches and low-energy beaches in general. Concluding, we use the outcomes of the hydrodynamic, morphodynamic and D3D model analysis to answer the last three research questions.

Section 10.1 describes the processes in the total system which are linked to the local system description in section 10.2. In this section we present the three main scenarios possible at the Noordstrand, based on the main forcing: wind. This helps answering the following two research questions:

Can the morphodynamics of a low-energy beach in a lake system, with non-equilibrium orientation, be linked to hydrodynamic processes? If so, in what way?

Is an equilibrium position of the shoreline and cross-shore profile possible?

We link our conceptual description of the system to the monitoring and maintenance strategy in section 10.3. Answering the last research question:

How can the previous findings help during development and maintenance of beaches in this low-energy lake system?

Section 10.4 discusses critical remarks concerning the presented conceptual system description and the research approach of this thesis. Exploratory research is presented in section 10.5. We place this research in the bigger perspective considering the Building with Nature principles in section 10.6, using a system engineering approach.

10.1 Getting the Total Picture

During the different investigations of the processes near the Noordstrand, one finding immediately stood out:

The situation of the Noordstrand cannot be understood without looking at the situation in a larger, lake-general perspective.

Certain local hydrodynamic processes are influenced by more general processes in the Markermeer. The key is to find the link between offshore and nearshore processes. Therefore we believe it is important to first consider the more general system of the Markermeer.

10.1.1 Processes Markermeer

The Markermeer has been identified as a low-energy, depth- and fetch-limited system (section 3.4). The main energy input in this system is the wind: creating waves, water level set-up or -down and wind-induced currents.

Wind

In the Markermeer the combination of wind speed and direction drives the hydrodynamic processes. Highest waves, result of longest fetch distances, and maximum set-up of water level against the Houtribdijk are the result of winds originating from south to southwestern directions. These wind conditions are more common especially in combination with increased wind speeds (figure 10.1). Considering the occurrence of high-energy events the bias towards higher wind speeds of station Houtribdijk is compensated when considering the hourly averaged wind speeds instead of the maximum wind gusts.

Using the KNMI data acquired from April 2019 till November 2020 we notice the high occurrence of these south to southwestern winds (170° to 290°). In general, the corresponding wind speeds range between 5 and 15 m/s. Periods with hourly averaged wind speeds up to 15 m/s (≈ 7 Bft) occur occasionally. Periods with wind speeds exceeding 20 m/s (9 Bft) are exceptional.

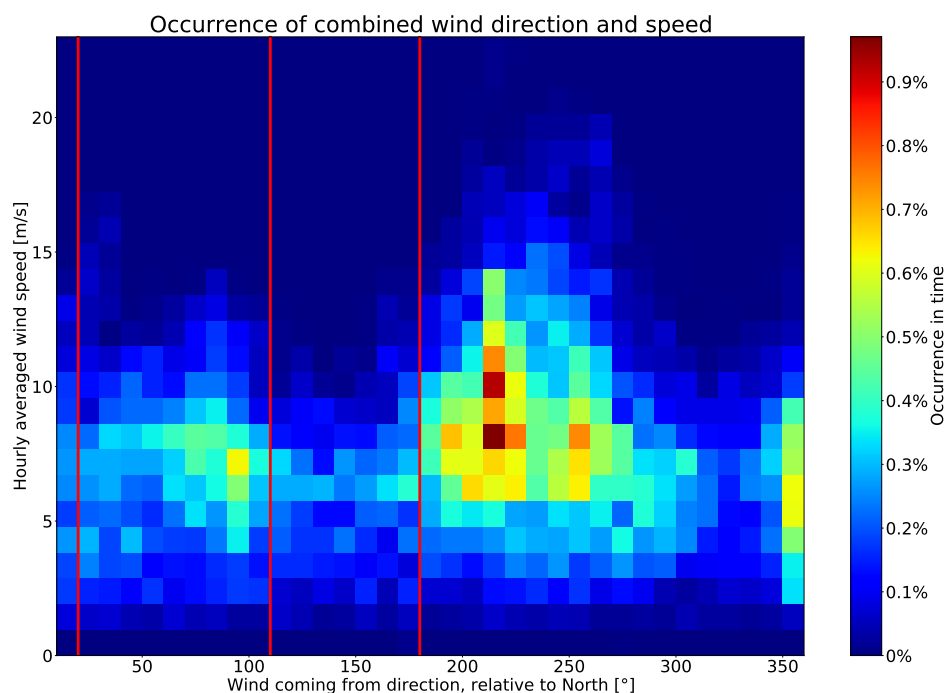


Figure 10.1: Double histogram of the wind direction (coming from, in $^\circ$) versus hourly averaged wind speeds (in m/s) at station Houtribdijk. The colourbar indicates the occurrence of the combination of wind speed and direction in percentages. The data of the time period from April 2019 till November 2020 is considered. The red lines are used in the scenario identification in section 10.2: scenario 1: sheltering (winds from 110° to 180°), scenario 2: set-down (winds from 20° to 110°) and scenario 3: set-up (winds from 180° to 20°).

Water level set-up and set-down over the lake

We have found that hourly averaged wind speeds exceeding 10 m/s cause water level fluctuations near FL66. A clear relation between wind speed from southwestern direction (wind direction 200° - 290°) and a set-up is observed in the data (figure 5.1), meaning increased wind speeds almost immediately cause a water level set-up against the Houtribdijk (left plot, figure 10.2). The higher the wind speed and the longer the duration of increased wind speed, the larger the set-up. Even average wind speeds (≈ 7 m/s) already cause some water level differences over the Markermeer. Winds from the northeast (20° - 110°) correspond to a water level set-down near the Houtribdijk (right plot, figure 10.2). The set-up and -down are also observed in the D3D model runs. For

southwestern winds the water level set-up between the Noordstrand and Houtribdijk can exceed 10 cm (w245, figure 10.3). A set-up near the Houtribdijk results in an increase in water level near the Noordstrand (FL66).

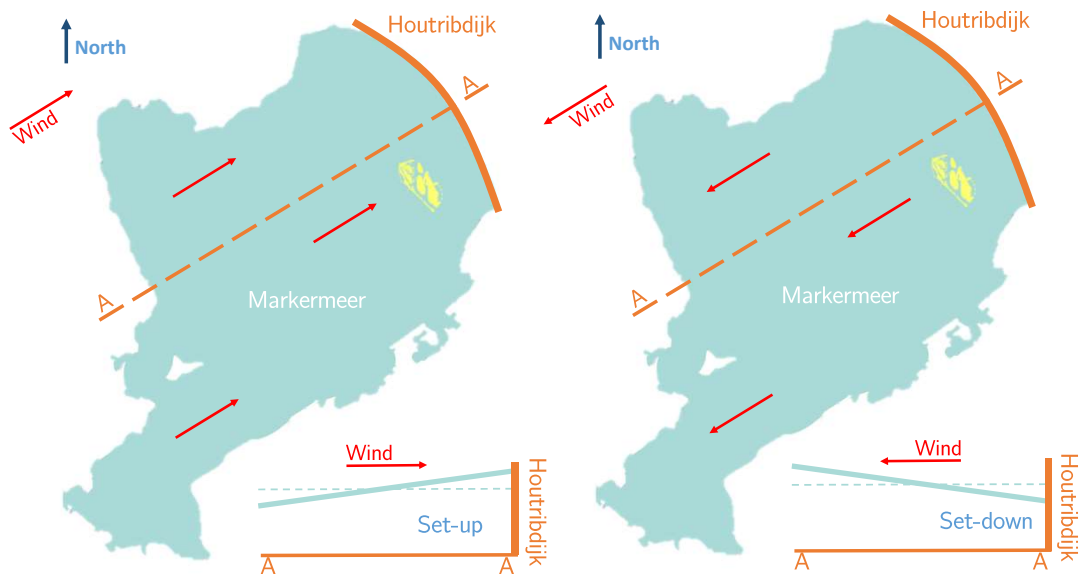


Figure 10.2: Visualisation of set-up (left) and set-down (right) at the Houtribdijk. Winds from mainly southwestern directions result in set-up, winds from the northeastern direction in set-down.

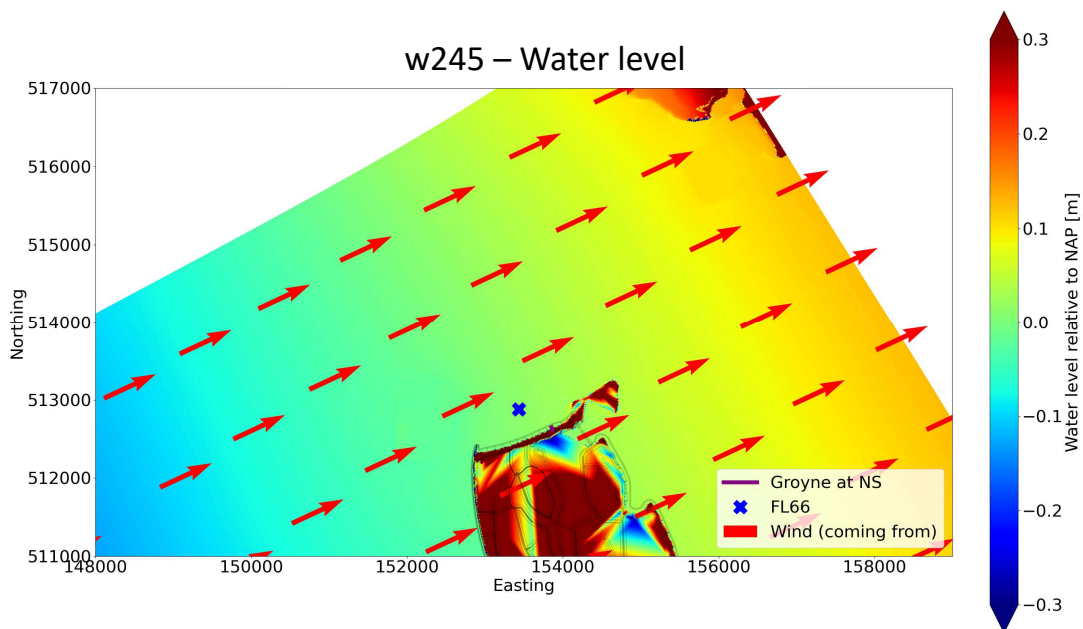


Figure 10.3: D3D *nested* model run showing the set-up of water level against the Houtribdijk in case of southwestern winds (245°) with a speed of 20 m/s (maximum in idealised run). Water level is shown by the colourbar, the red arrows indicate wind direction. Differences in water level within the Marker Wadden islands are due to the coarse topography used in the D3D model and information displayed here is not a correct representation. As a result one cannot use this D3D model to model the hydrodynamics inside the Marker Wadden islands. The topography and results near the Noordstrand are checked and give a correct representation of the hydrodynamics near the beach.

General wind-induced (lake) circulation

In response to a water level set-up or -down over the lake, return currents are formed due to mass continuity (water cannot continue to pile up on one side of the Markermeer). This return current near the middle and the bottom of the water column, is basically an indirect wind-driven current and goes in opposite direction with respect to the wind (bottom middle plot, figure 10.4). The current in the top of the water column is directly influenced by the wind shear stress and is in the same direction as the wind forcing: the wind-driven current.

Due to the prevailing wind conditions a set-up near the Houtribdijk is more common. The wind-driven and return current in the vertical profile due to the set-up, influence the general lake circulation. As a result the set-up drives, indirectly formed, wind-induced currents in the Markermeer. We do not consider this wind-induced current over the vertical, but regard this current in the horizontal plane. An example: the set-up drives an offshore current close to the Noordstrand. This wind-induced current, is part of the general lake circulation pattern and is locally influenced by other factors such as the geometry of the Marker Wadden and local obstacles. Concluding, we observe a certain circulation in the horizontal plane of the Markermeer based on general levels of set-up or -down near the Houtribdijk. The offshore wind-induced current, part of the larger lake circulation pattern, is measured by the ADCP near the Noordstrand. Hourly averaged wind speeds exceeding 10 m/s, which was the case for 24% of the considered time, already resulted in a measurable wind-induced current at this location. This means the presets for an enlarged general wind-induced offshore current are present quite often. For these wind speeds the depth-averaged current direction at FL66 is approximately opposite to the direction of the wind and seems to be slightly reflected by the soft edge located in the north of the Marker Wadden.

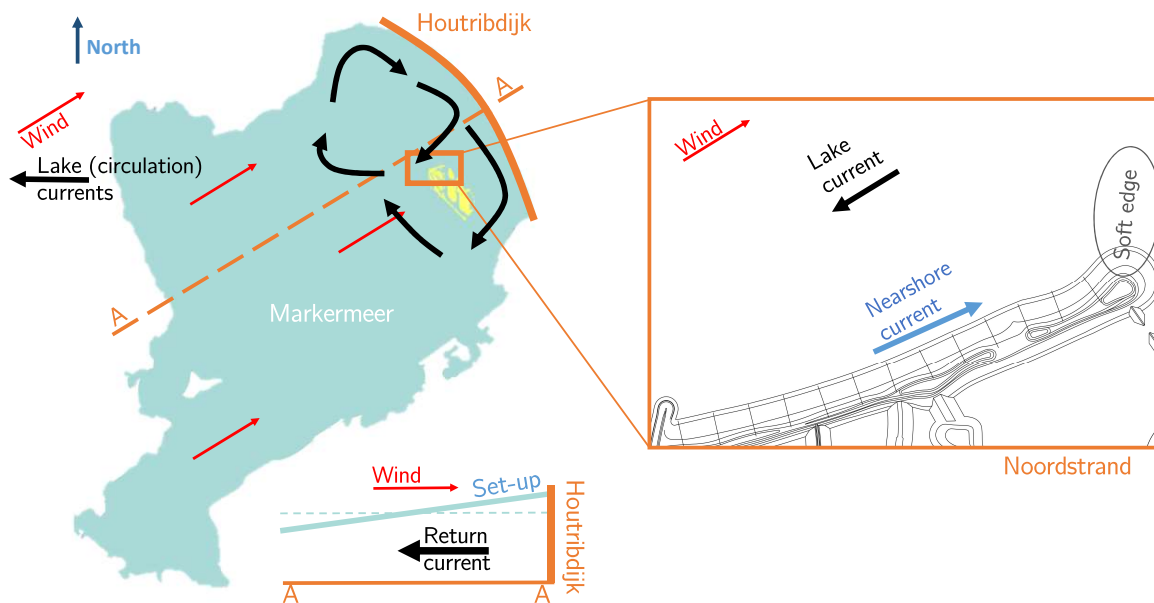


Figure 10.4: Schematization of the formation of a (wind-induced) lake circulation current due to water level set-up against the Houtribdijk (left plot). The water level set-up indirectly drives general wind-induced currents in the horizontal plane of the Markermeer. A mismatch in offshore and nearshore current is found, thought to be caused by (local) geometry and the interaction of offshore and nearshore processes (right plot).

Location and geometry Marker Wadden

The location and geometry of the Marker Wadden in the Markermeer influence the general lake circulation patterns observed in the lake, by causing local accelerations or decelerations. Other processes such as local water level fluctuations and certain obstacles also influence the general flow patterns. In our D3D modelling we have observed how the presence of the soft edge (northeastern corner of the Marker Wadden) causes increased flow velocities locally if wind originates from a southwestern direction. If winds originate from the southeast the Noordstrand is completely sheltered from waves and enlarged offshore wind-induced currents. If, in the hypothetical case, the Marker Wadden were placed in another part of the Markermeer the resulting lake circulation pattern and its influence on the Marker Wadden beaches, would have been completely different.

The Marker Wadden create a feedback mechanism with the Markermeer system: the islands influence the hydrodynamics of the lake, which in return changes the hydrodynamics near the Marker Wadden beaches.

Mismatch offshore and nearshore wind-induced current

Combining the FL66 data and the results of the D3D model we can investigate the link between off- and nearshore processes. The most important conclusion being:

The direction of the offshore wind-induced (lake) current and the wind- and wave-driven nearshore current is opposite, hypothesised to be caused by the (local) geometry and the interaction of offshore and nearshore processes.

We hypothesise the offshore areas, FL66 in this case, are less influenced by the local geometry of the beach compared to the nearshore region (figure 10.4), although this depends on the exact wind direction (e.g. southern winds result in almost complete sheltering of the Noordstrand nearshore and offshore areas). As a result offshore processes and measurements cannot be translated to an understanding of the nearshore processes directly.

Waves

Winds from the west to southern direction (200°-290°) create the highest waves near the Marker Wadden due to the maximum fetch distance. As this wind direction is more common, enlarged waves near the Marker Wadden occur regularly. This explains why only days with a wind force of 3 Bft or less are sufficient for our waterline measurements at the Marker Wadden beaches during our field trips. Due to their relative short wave length and limited bottom depth, there is little refraction: resulting in high-angle waves approaching the beach even during mild conditions. This is confirmed by the outcomes of the Marker Wadden D3D model runs (section 9.1.4). As a result the wave-driven part of the nearshore current is enlarged.

10.2 Development Noordstrand

Having created the correct context we can now consider the development of the Noordstrand. Its non-equilibrium orientation, with respect to dominant wind and wave direction, mean nearshore processes can behave completely different compared to beaches with an equilibrium orientation. For completeness the beach development as observed during the analysed period is shown in figure 10.5.

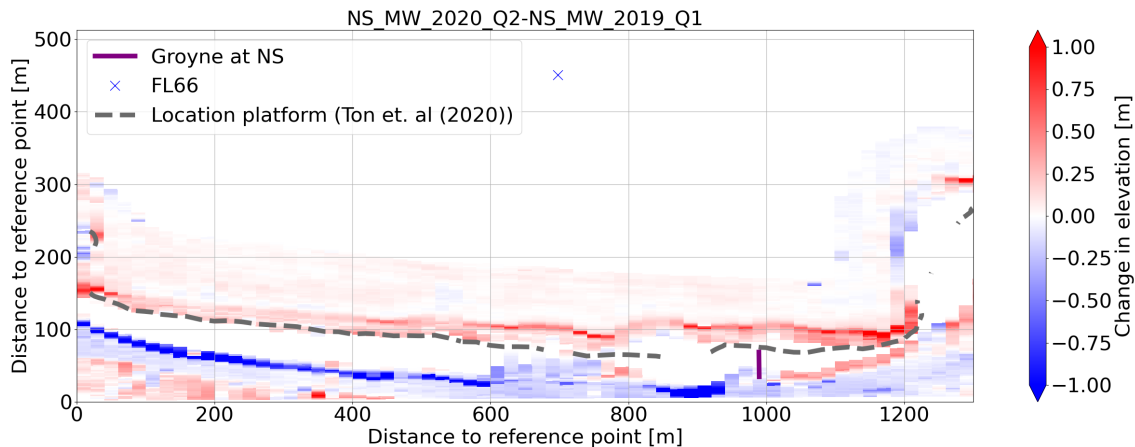


Figure 10.5: General development of the Noordstrand: from 2019 Q1 - 2020 Q2 (identical to figure 7.2). Sedimentation (red), erosion (blue) and lack of data (white) are shown.

10.2.1 Cross-shore and longshore transport

Due to the posed research questions (regarding the global development of the beach), the non-equilibrium orientation of the Noordstrand and conclusions from our previous analyses we focus on coastline change and corresponding longshore transport rates. Considering the general change of the Noordstrand in the past we can conclude the following:

When considering the Noordstrand, erosion rates significantly outweigh sedimentation rates: indicating increased gradients in longshore transport and the general loss of sediment. Sedimentation is limited to the area lakeward of the submerged platform and near the inner curve of the soft edge (northeastern end of the Noordstrand).

This indicates the 'loss' of sediment from the cross-shore profile which can be caused by losing sediment underneath the wave base (depth-of-closure) or it is moved away by the longshore transport. Literature already suggested the impact of high-angle waves on increased longshore transport (Jackson et al., 2002; Nordstrom and Jackson, 2012). We consider the general coastline change of the Noordstrand: '*Coastal change occurs in the case of spatial transport gradients and/or in case of sinks and sources*' (Bosboom and Stive, 2015). A simple formula for longshore transport includes the effect of combined wave and current sediment stirring and transportation of the sediment by the longshore/nearshore current (equation 10.1, from Bosboom and Stive (2015)).

$$\langle S_y \rangle = \underbrace{m_2 \langle u^2 + V^2 \rangle}_{\text{sediment load stirred by wave-current motion}} * \underbrace{V}_{\text{longshore current responsible for transport}} \quad (10.1)$$

For our conceptual system description we divide the Noordstrand processes into three scenarios based on governing wind conditions, their influence on the Noordstrand hydrodynamics and ultimately their impact on beach development.

10.2.2 Identification scenarios

The three defined scenarios are:

- **Scenario 1: Sheltering;** occurring if winds are from a direction of 110° to 180° . This scenario is not so common, especially not in combination with increased wind speeds (figure 10.1, region between 110° to 180°). The Noordstrand is sheltered from direct wind and wave attack.
- **Scenario 2: Set-down;** in this scenario winds originate from 20° to 110° resulting in water level set-down near the Houtribdijk. These wind directions occur regularly but rarely in combination with high wind speeds (figure 10.1, region between 20° and 110°).
- **Scenario 3: Set-up;** this includes wind from a wider range: 180° to 20° , resulting in a water level set-up against the Houtribdijk and increased water levels at the Noordstrand. This is most evident for southwestern winds (200° - 290°), which have a high occurrence and are linked to enlarged wind speeds (region after red line at 180° in figure 10.1). Correspondingly this scenario includes the high-energy events.

The time period of 20 months considered for the calculation of wind occurrence is similar to the analysed period of the hydrodynamic data analysis (April 2019 till November 2020). It is important to note that the development of the Noordstrand is the result of the combined action of all scenarios and all occurring wind conditions. However due to the deviating occurrence of different wind conditions and varying effects on the hydrodynamic processes, one scenario might have a bigger attribution on the beach development than others. In light of system understanding we consider the different scenarios and their effect on beach development separately.

The different terms used in the explanation of the scenarios are summarised in the List of Terms. Additionally an overview of the different processes and how they are depicted in the schematization figures of the scenarios is shown in figure 10.6.

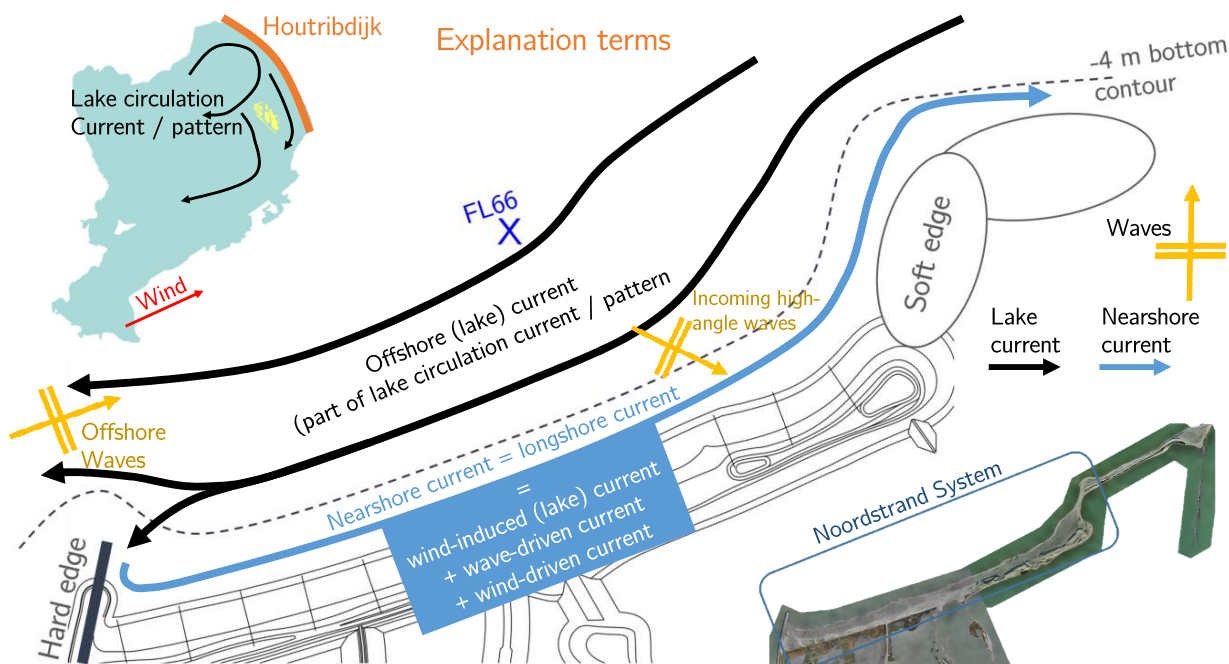


Figure 10.6: Explanation different terms used in our Noordstrand data analyses and system description. The lower right shows the considered area for our *Noordstrand system* (see also figure 2.3). The colours of the different processes and their description match. Note: we have used the current pattern and wave direction from scenario 3: set-up - general, the offshore and nearshore current patterns and wave information is different in every scenario.

10.2.3 Scenario 1: Sheltering

Wind directions of 110° to 180° do not occur often (15% of the considered time period), especially not in combination with high wind speeds: no high-energy events are expected in this scenario (figure 10.1). Offshore, the wind-induced lake current (part of the Markermeer circulation pattern) is dominant, no significant nearshore currents develop as the Noordstrand is sheltered (figure 10.7). As a result we can neglect the influence of this scenario on the Noordstrand development.

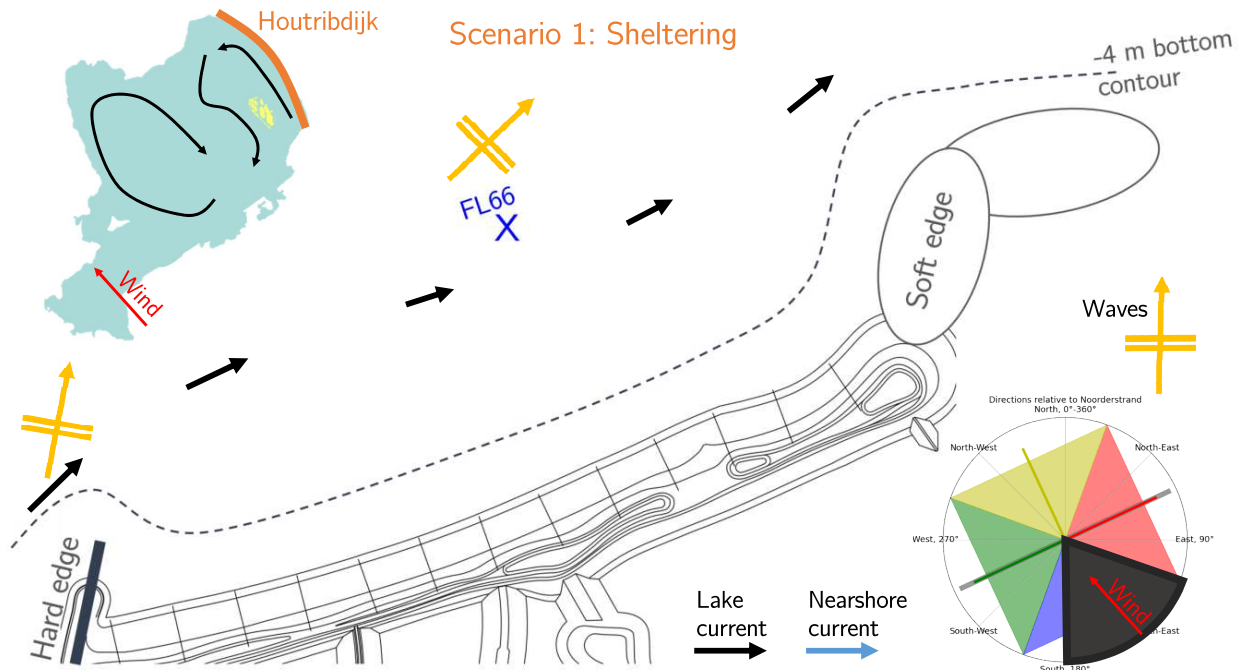


Figure 10.7: Scenario 1: Sheltering. Winds originate from 110° to 180° (grey region in wind rose, lower right), no high wind speeds or high-energy events are expected. In this case the Noordstrand is sheltered from waves (yellow arrows) and significant nearshore currents. We observe a general wind-induced current in the offshore region part of the larger lake circulation pattern, which is mainly unaffected by the Noordstrand (black arrows).

10.2.4 Scenario 2: Set-down

This scenario with winds from 20° to 110° occurs 25% of the considered time. Wind speeds are moderate (5 to 10 m/s) and no high-energy events are expected. A set-down in water level near the Houtribdijk is formed, influencing the general lake circulation currents. Near the Noordstrand this results in an offshore wind-induced current towards the northeast. We find a nearshore current going in opposite direction: southwest. The area close to the soft edge is sheltered from direct wave attack. High-angle waves can arrive at other parts of the beach and enlarge the nearshore current in the breaker zone. Near the hard edge the longshore current decelerates before passing around the breakwater. This scenario is visualised in figure 10.8.

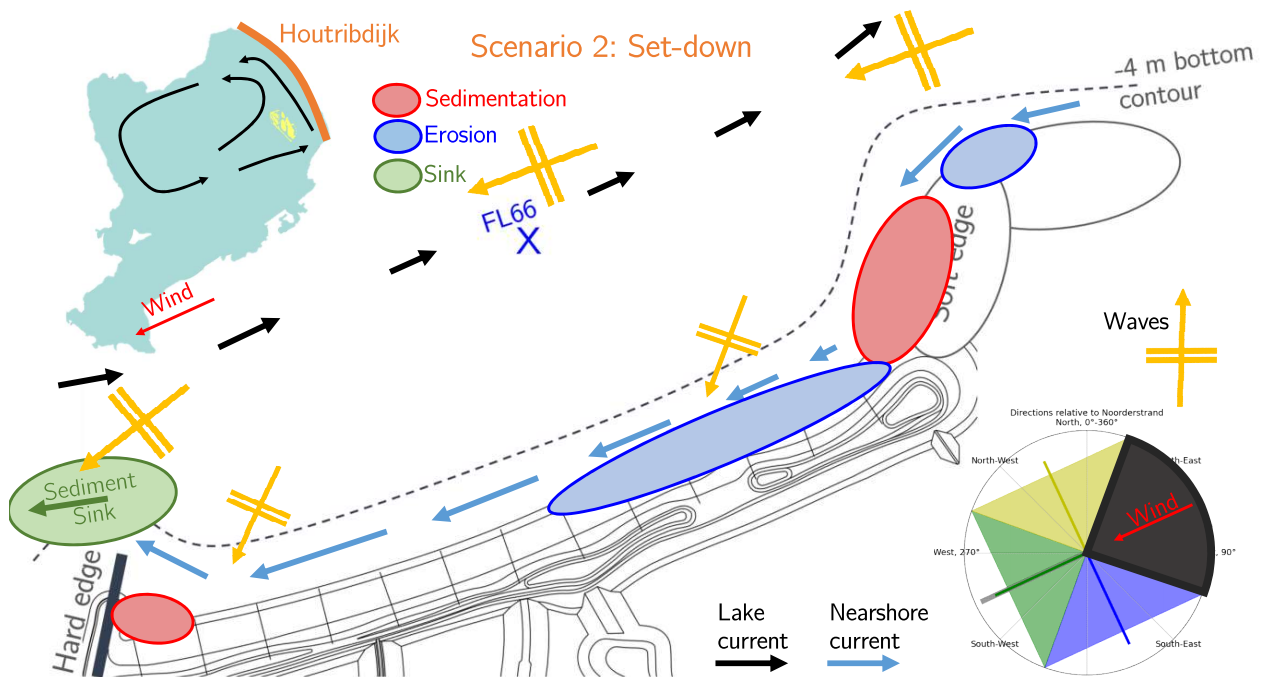


Figure 10.8: Scenario 2: Set-down; hydrodynamics and link to morphodynamics. Winds originate from 20° to 110° (grey region in wind rose, lower right), no high wind speeds or high-energy events are expected. In this case an offshore wind-induced current to the northeast is present (black arrows) and an opposite longshore current is found nearshore (blue arrows). This nearshore current is enlarged along its course due to incoming high-angle waves (yellow arrows) and local geometry. Changes in the nearshore hydrodynamics cause gradients in the transport rates, resulting in erosion (blue) and sedimentation (red). Notice how, based on this scenario, we expect erosion near the soft edge (northeast) and sedimentation near the hard edge (southwest).

What will happen? - Hypothesised development

To link the scenario to coastline development we need to consider gradients in longshore transport and any sources or sinks. Sediment arriving from the northern part of the soft edge is a possible source, sediment leaving the beach around the hard edge a sink (top right corner and bottom left corner respectively, figure 10.8). We expect a positive gradient in longshore transport around the soft edge as the nearshore current accelerates due to the geometry of the beach (blue circle, top figure 10.8). Once the current arrives on the main part of the beach it decelerates as it is more sheltered from wave attack and the flow diverges: a possible location of sedimentation (red circle on the right, figure 10.8). Along the main stretch of the Noordstrand the longshore current accelerates due to increased wave impact and the influence of both the wind-induced and wind-driven current (u and V in equation 10.1). An increase in longshore transport rates is the result, erosion occurs (longer blue oval in figure 10.8). The flow decelerates in the proximity of the hard edge, decreasing its transport capacity. Some sedimentation might be expected in this location.

Can it really happen? - Link to prevailing wind conditions

Significant acceleration and deceleration as described above only occur for wind speeds higher (15 m/s) than the normally observed (5-10 m/s) in case of this wind direction (20° to 110°). During normal conditions the wave heights near the beach are approximately 0.25 meter and nearshore current magnitude does not exceed 0.1 m/s. Instead of sedimentation near the hard edge we observed erosion, making the occurrence of this scenario less likely (figure 10.5). Combining this with a limited possibility of high-energy conditions, we conclude this scenario did not significantly influence the development of the Noordstrand.

10.2.5 Scenario 3: Set-up

This last scenario includes the broadest range of wind directions: 180° to 20°, which are more common: 60% of the considered time. These directions show a clear link with increased wind speeds and include all the observed high-energy events. A water level set-up is formed against the Houtribdijk, resulting in: an offshore wind-induced current (part of the larger lake general circulation pattern) going to the southwest (figure 10.4) and an increase in water level at the Noordstrand. The longer fetch distance results in increased wave heights. The nearshore current which is formed is in the opposite direction: northeast (figure 10.9).

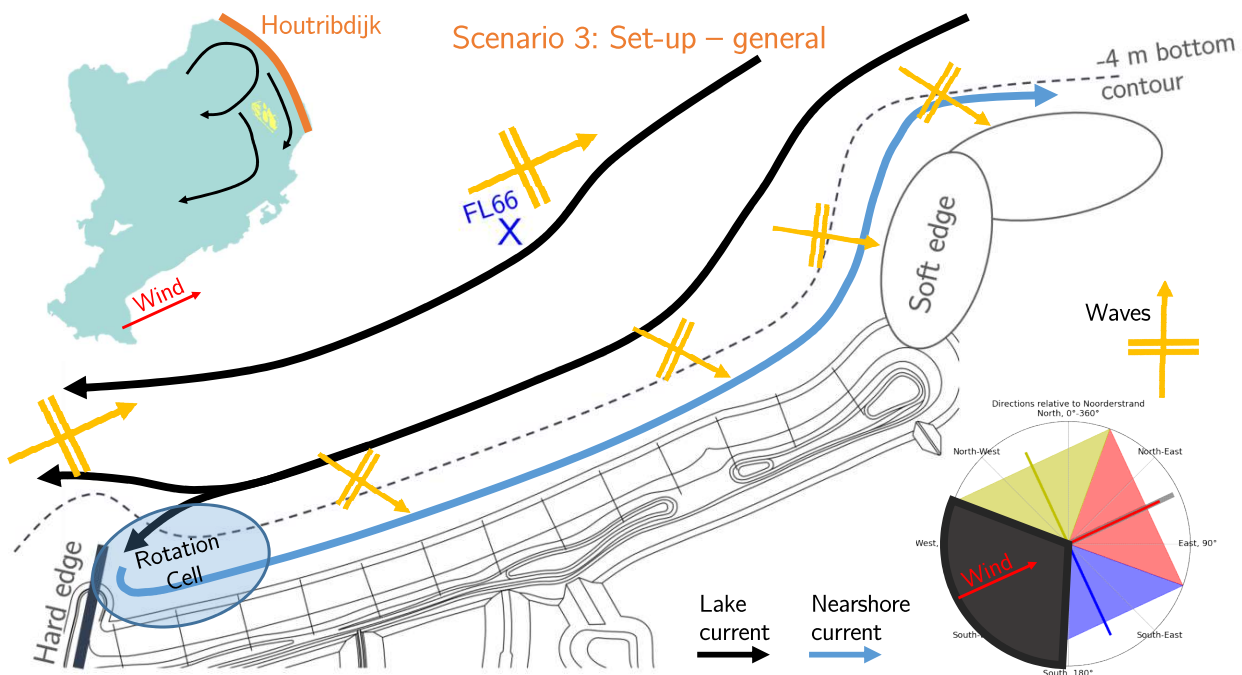


Figure 10.9: Scenario 3: Set-up - general; hydrodynamics. Winds originate from 180° to 290° (grey region in wind rose, lower right). In this case an offshore wind-induced current to the southwest is present (black arrows) and an opposite longshore current is found nearshore (blue arrow) linked by a rotation cell next to the hard edge. This current is enlarged along its course due to incoming high-angle waves (yellow arrows) and local geometry. The longshore current leaves the proximity of the Noordstrand in the northeast.

What will happen? - Hypothesised development

We believe the nearshore current is a combination three different factors: the nearshore component of the wind-induced current which is influenced by local geometry (its direction is opposite to the direction of the offshore wind-induced current), the wave-driven current formed by incoming high-angle waves breaking in the breakerzone, and the wind-driven current which is enhanced by the relative shallowness nearshore due to the presence of the submerged platform. As the hard edge partly blocks the offshore wind-induced current, a nearshore rotation cell is formed, leading to the gradual acceleration of the nearshore current near the southwestern part of the beach. This longshore current is further enhanced by breaking waves as the sheltering effect of the breakwater diminishes further away from the hard edge. Local bathymetry and the submerged platform seem to be influencing

factors, as the region in which the longshore current is present is limited to the region from the waterline to the Markermeer bottom contour (runs with and without submerged platform, section 9.1.3). Also this relative shallow depth on top of the platform increases the influence of the wind-driven component of the longshore current and this submerged platform decreases the nearshore wave height. Near the soft edge the longshore current decelerates and, depending on the wind direction, continues north or is deflected offshore in a jet-like current manner (figure 10.11).

The discussed gradients in longshore current V and increased high-angle wave impact u (in case of more western wind directions, see section 9.1.4) cause increased longshore transport rates (S_y increases) and thus erosion is observed over a stretch of approximately 600 meters northeast from the hard edge. Waves 'reduce' the area accommodating the longshore current, further enhancing flow velocities. The indirect result of the rotation cell is erosion along the southwestern part of the beach (blue oval lower left corner, figure 10.10). Even without waves, so solemnly considering the wind-induced and wind-driven current, the acceleration due to the rotation cell can be significant.

Closer to the soft edge the longshore current decelerates, forming a region of sedimentation as transport gradients decrease (red circle top right, figure 10.10). Furthermore near the soft edge the shoreline rotates and the incoming waves arrive no longer under a high angle but now arrive more perpendicular to the shoreline. The wave-driven component of the longshore current decreases, but the transport caused by waves in cross-shore direction increases. This could indicate a shift from transport in longshore direction to more transport in cross-shore direction: the waves transporting the eroded sediment lower in the beach profile and offshore. Thus this is a possible location of a sediment sink (green circle, figure 10.10). The offshore oriented transport near the soft edge is also observed in the D3D morphological runs (section 10.5).

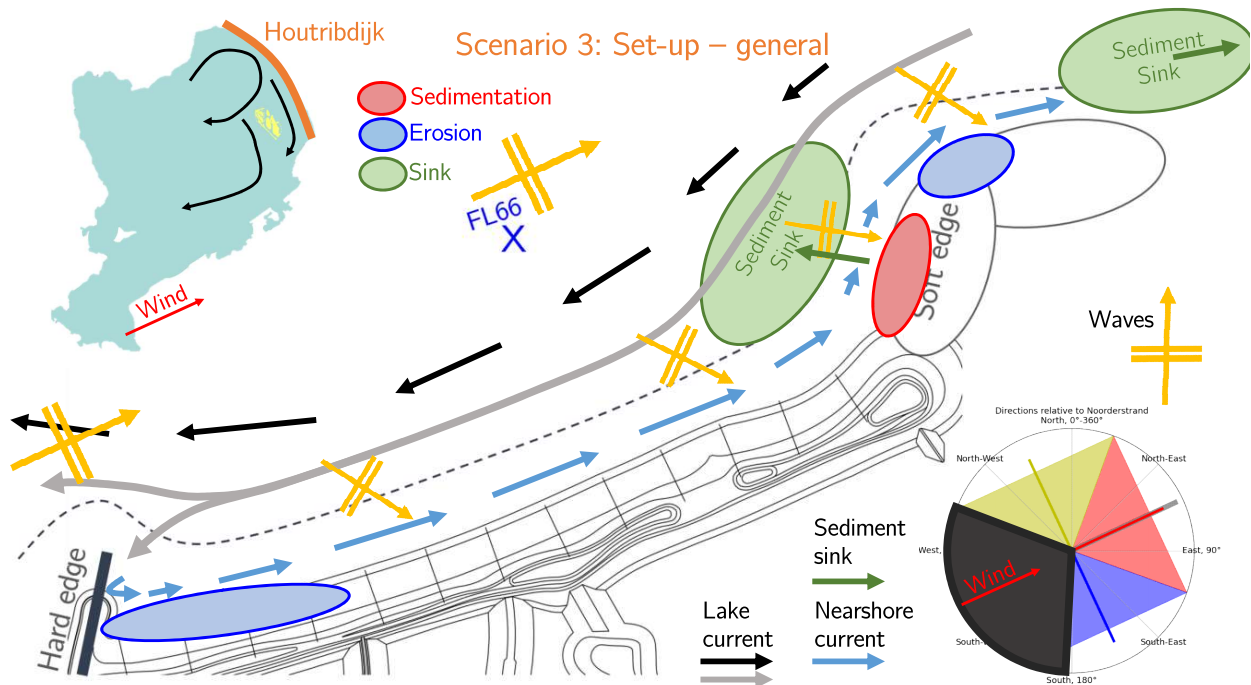


Figure 10.10: Scenario 3: Set-up - general; hydrodynamics (similar to figure 10.9: main offshore wind-induced current shown in grey; offshore (black) and nearshore (blue) current now show gradients) and link to morphodynamics. Changes in the nearshore hydrodynamics cause gradients in the transport rates, resulting in erosion (blue) and sedimentation (red). Notice how in this scenario we would observe erosion near the hard edge, along the southwestern part of the beach and little sedimentation near the soft edge. Most eroded sediment leaves the Noordstrand (sinks: green): the system is not 'closed'.

Near the outer bend of the soft edge the nearshore flow converges and accelerates again: another location of erosion (blue circle top right, figure 10.10). Based on our results we hypothesise the increase of the transport rates along the Noordstrand is significantly more than the decrease, meaning most eroded sediment is lost (sediment sinks, green circles figure 10.10). The longshore current carrying the eroded sediment is either deflected offshore in a jet-like manner near the soft edge (see next section) or is transported around the soft edge. In both cases sediment is lost from our system: this means our system is not 'closed', an indication of structural erosion.

Exploratory morphological runs in D3D (section 10.5) have shown sediment transport over the entire width of the platform and even next to the platform. This transport seems to be diminish lakeward of the Markermeer bottom contour. The transport on top and right next to the platform is even present during mild conditions (wind speed 10 m/s, figure 10.17).

This *general* scenario occurs 67% of the all the considered scenario 3 conditions. A jet-like current is formed in 33% of the scenario 3 cases, see next section.

Jet-like current

If winds confront the beach more perpendicular the longshore current is deflected offshore in a jet-like manner near the soft edge (figure 10.11). This jet-like current is formed by the convergence of the northeastern going longshore current from the Noordstrand and a southwestern going current arriving from the northern edge of the beach, believed to be the nearshore component of the general lake circulation pattern influenced by the Markermeer set-up and geometry of the Marker Wadden. Once both currents converge the flow accelerates, transport gradients increase and we expect erosion, in severe cases a gully could be formed. The jet-like current transports suspended sediment offshore, where it is either 'lost' (sink) or it is transported with the offshore wind-induced current in southwestern direction. Sensitivity runs have shown a potential region of deceleration offshore and thus settling of sediment next to the submerged platform is possible (the region between the Markermeer bottom depth and platform elevation contour, figure 10.12). As a result the platform will widen. This means sediment returns in the cross-shore profile with a *detour*. This is underlined by the exploratory morphological D3D model runs, as they show transport next to the platform (figure 10.17). This is an interesting case for a point of attention in a follow-up study.

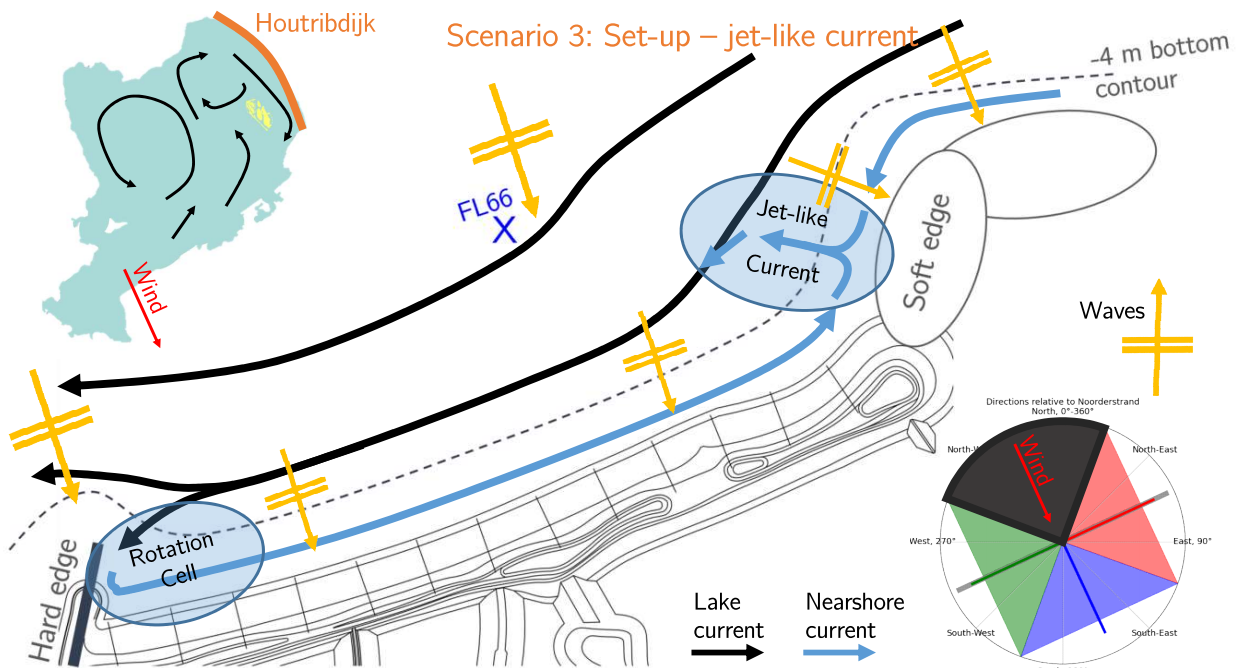


Figure 10.11: Scenario 3: Set-up - jet-like current; hydrodynamics. Winds originate from 290° to 20° (grey region in wind rose, lower right). In this case an offshore wind-induced current to the southwest is present (black arrows) and an opposite longshore current is found nearshore (blue arrow) linked by a rotation cell next to the hard edge. This current is enlarged along its course due to incoming high-angle waves (yellow arrows) and local geometry. The longshore current leaves the system in jet-like manner near the soft edge.

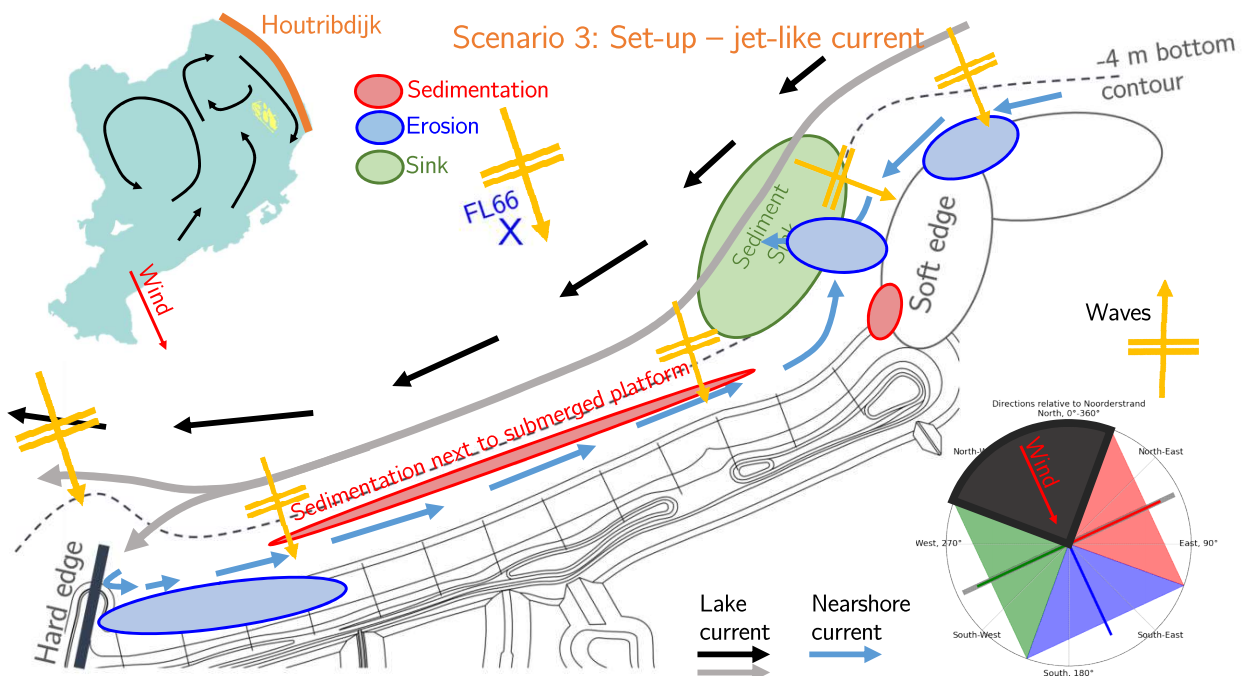


Figure 10.12: Scenario 3: Set-up - jet-like current; hydrodynamics (similar to figure 10.11: main offshore wind-induced current shown in grey; offshore (black) and nearshore (blue) current now show gradients) and link to morphodynamics. Changes in the nearshore hydrodynamics cause gradients in the transport rates, resulting in erosion (blue) and sedimentation (red). Notice how in this scenario we would observe erosion near the hard edge and the location of the jet-like current. Sediment is transported offshore where it is either lost (sediment sink: green) or could potentially settle next to the submerged platform.

Can it really happen? - Link to prevailing wind conditions - High-energy conditions

This scenario includes all high-energy events and according literature these events mainly influence beach development in low-energy systems (Vila-Concejo et al., 2020). In case of high-energy events we need to include the influence of set-up over the Markermeer and thus increased water levels at the Noordstrand. Hegge et al. (1996) already suggested how storm surge can have a profound influence on erosion. We have found that the location of most severe erosion and maximum measured water level in the beach profile coincide. Due to slumping of the dune face, small amounts of wave energy are already enough to erode large volumes of sediment. We also found a link between increased wave height and set-up of water level against the Houtribdijk in case of high-energy events, as was already observed by Steetzel et al. (2017) and Ton et al. (2020). This means that during high-energy events we are not dealing with small amounts of wave energy, but with enlarged wave energy: a great deal of sediment is stirred by the combination of slumping and increased wave energy (the first term in equation 10.1 increases). Additionally, as a result of high water level set-up the offshore and nearshore wind-induced currents in the Markermeer and in the proximity of the Noordstrand are larger. This longshore current is further enhanced by wave breaking (increase of the second term in 10.1), especially as the relative protection of the breakwater diminishes along the beach length, and by the wind-driven current on top of the submerged platform. Transport gradients increase: eroded sediment is immediately transported away by the enlarged longshore current. Based on this scenario we expect severe erosion in the southwestern part of the beach in case of high-energy events, which is only partly compensated by sedimentation in the northeast of the Noordstrand. Thus we expect most sediment is lost from the Noordstrand system.

The described development has been observed in the rather energetic period from 2019 Q3 till 2020 Q1. One should take into consideration that these kind of high-energy event do have a large impact on beach development but do not occur often (hourly averaged wind speeds only exceeded 15 m/s during 3% of the considered period of time), therefore we should also consider the influence of milder conditions on beach development.

Can it really happen? - Link to prevailing wind conditions - Milder conditions

15% of the time wind speeds between 10 and 15 m/s (6-7 Bft) occur with wind directions considered in this scenario: meaning milder conditions are much more common than very high energy events. The stepwise increase in wind speed in our D3D model allows us to additionally investigate these conditions. In the nearshore observation point we find for milder conditions a significant nearshore current magnitude (≈ 0.25 m/s) in combination with a wave height of approximately 0.3 meter. The occurring maximum are thus lower. The evolution of the longshore current remains unchanged: accelerating along the southwestern part of the beach due to the rotation cell and only partly decelerating near the soft edge. This means we still expect gradual erosion along the length of the beach, although less severe. All three components forming the longshore current are in the same direction: the wind-induced nearshore current is opposite to the offshore wind-induced current (part of the general lake circulation pattern) going in northeastern direction, the high-angle waves increase the longshore current component in northeastern direction and the wind-driven current on top of the submerged platform follows the direction of the wind and is also going towards the northeast. These three components together can be quite significant especially as they are all in the same direction.

The previous statements are underlined by the morphodynamic data analysis, which shows a constantly eroding upper beach face over the entire length of the Noordstrand and only little sedimentation in some locations (lakeward of the submerged platform and close to the soft edge, figure 10.5).

So, what is happening?

Due to the governing wind directions and link to increased wind speeds we expect *scenario 3: set-up* has had the most influence of the observed development of the Noordstrand. Combining the development during high-energy and mild conditions we come up with the summarised conceptual system description:

It is important to consider that the development of the Noordstrand is the result of the combined action of all scenarios and all occurring wind conditions, but for now we focus on the scenario we believe has had the most influence in the observed development of the Noordstrand.

Erosion rates are most severe during high-energy events, showing erosion over the entire beach face. This is hypothesised to be caused by the combination of obliquely incident waves, with increased wave heights, reaching the upper shoreface. There the shoreface erodes and the nearshore current transports the eroded sediment from the cross-shore transect to other parts of the beach.

The nearshore current is essentially a combination of three phenomena. One: the offshore wind-induced current 'hits' the hard edge, creates a rotation cell and an indirectly wind-induced nearshore current along the Noordstrand is formed (thus the indirect result of the general lake circulation formed by the set-up against the Houtribdijk and influenced by local geometry). Two: the longshore current formed by the obliquely incident (or high-angle) waves breaking in the breakerzone. Three: the wind-driven current which is enlarged due to the relative shallowness on top of the submerged platform. In case all three currents are in the same direction they enhance one another and create a significant nearshore current: this is the case for wind conditions linked to scenario 3.

During high-energy events this nearshore current is combined with increased water levels. This combination can lead to slumping of the duneface as most eroded sediment is immediately lost from the cross-shore transect and erosion of the beach profile will continue. This can even lead to the creation of cliffs in severe cases.

Most eroded sediment is transported offshore near the soft edge or around the soft edge by the longshore current. The offshore transport is caused by the decrease in the angle of incidence of the waves near the soft edge: the longshore transport component decreases and the cross-shore transport component increases, transporting sediment offshore, below the depth-of-closure. In both cases most eroded sediment is lost from the Noordstrand system.

Even during milder conditions the described processes occur although transport rates and corresponding erosion are much smaller. Due to the higher occurrence of milder conditions the erosion is more gradual but still substantial. The combination of high-energy events and mild periods contribute to the development of the Noordstrand.

10.2.6 Testing conceptual system description - Fieldwork data

An exploratory morphodynamic analysis of the obtained fieldwork data in the period 2021 Q1 till 2021 Q2 shows erosion near the waterline and main sedimentation lakeward of the submerged platform (figure 10.13). We are considering the development of the beach in the first months after completion of the Noordstrand nourishment of December 2020. Looking at the wind conditions measured in the same period we observe a high occurrence of western and northern winds, of which the latter is more common. By linking these wind conditions to our conceptual system description and comparing the outcome with the actual development of the beach, we can test our conceptual system description.

Based on the observed wind conditions we hypothesise scenario 3: set-up (winds from 180° to 20°) has been the governing factor in beach development (figure 10.14). Different from the wind conditions in the previous period considered (April 2019 till November 2020) is the higher occurrence of northern winds in this case compared to (south)western winds in the previous period. Furthermore in this considered period the amount of high-energy events (hourly averaged wind speeds > 15 m/s) is only 93 hours compared to 422 hours in the period April 2019 till November 2020. This difference is expected as the analysed period after the nourishment is much shorter.

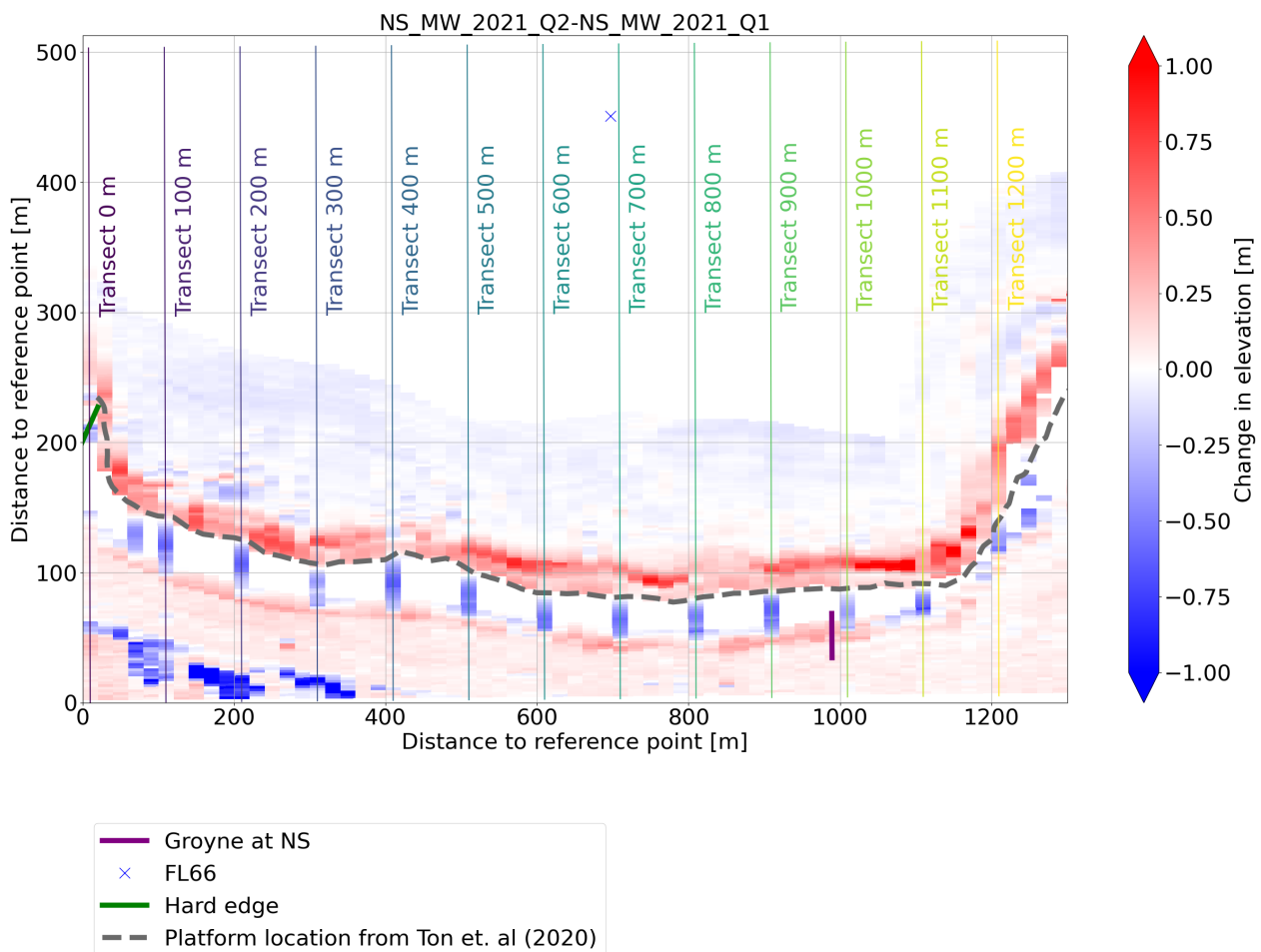


Figure 10.13: Changes in elevation: 2021 Q2 - 2021 Q1 (identical to figure 7.7). Positive changes in elevation are associated with sedimentation (red) and negative changes indicate erosion (blue). White coloured areas indicate an absence of data (so not a 0 m change in elevation as the colourbar might suggest). Measurements around the waterline are only available every 100 meter - the transects visible as coloured vertical lines. The dashed grey line indicates the location of the offshore platform using an elevation of -1.11 meter relative to NAP (from Ton et al. (2020)) using the 2021 Q1 data to show the development of the platform offshore.

Based on scenario 3, set-up, we would expect more erosion of the upper shoreface in the southwestern part of the Noordstrand. This erosion is not observed in the actual development. On the other hand in this period relatively more northern winds occurred, resulting in normally incident waves. We would expect a more cross-shore development of the beach profile and this is what we recognise in the general development of the beach (see also figure 7.8). This cross-shore development can also be caused indirectly: the beach erodes near the waterline, the longshore current transport this sediment along the length of the beach and is brought offshore near the soft edge. There it follows the offshore current part of the general lake circulation pattern and can (thus indirectly) settle next to the submerged platform. This development is part of the hypothesised scenario 3: set-up - jet-like current, thought to be the result of more northern winds. Based on the observed higher occurrence of northern winds this indirect cross-shore development is possible.

To conclude we do not observe increased erosion in the southwestern part of the beach as is expected from our conceptual model. The deviations can be the result of the lack of high-energy periods in the first three months after the nourishment, as these greatly impact the beach development. Moreover other processes could have been dominant in the initial months after the nourishment: the constructed profile of the nourishment quickly develops to include the submerged platform, its presence which was also observed before the nourishment was applied. This initial test highlights the knowledge gaps in our conceptual system description and underlines the need for future monitoring, measuring and researching.

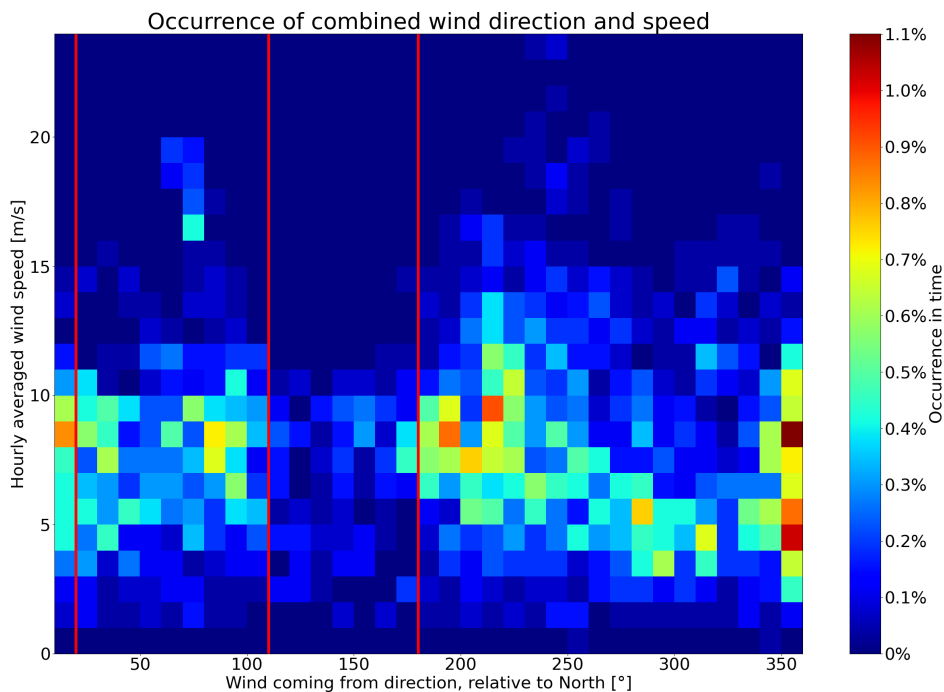


Figure 10.14: Double histogram of the wind direction (coming from, in $^{\circ}$) versus hourly averaged wind speeds (in m/s) at station Houtribdijk. The colourbar indicates the occurrence of the combination of wind speed and direction in percentages. The data of the time period from January 2021 till April 2021 is considered. The red lines are used in the scenario identification in section 10.2: scenario 1: sheltering (winds from 110° to 180°), scenario 2: set-down (winds from 20° to 110°) and scenario 3: set-up (winds from 180° to 20°).

10.2.7 Equilibrium

The cross-shore profile development has not been the main focus of this study but combining literature, results of our data analysis and the conceptual description from the previous paragraphs we can conclude the cross-shore profile of the Noordstrand is not (yet) in equilibrium. The duneface and upper shoreface are subject to erosion during mild and high-energy events. Some eroded sediment arrives lower in the beach profile and helps widen the platform. This underlines the finding of Ton et al. (2020) that the platform width is still developing. Not all eroded sediment is used to widen the platform, most sediment leaves the cross-shore transect. It is also possible sediment arrives near the platform following a *detour*, facilitated by a jet-like current (see paragraph: *jet-like current*).

We believe the longshore current is governing in determining both the cross-shore and longshore development of the beach. However as described in our identified governing scenario, sediment is ultimately lost from our Noordstrand system either offshore or around the soft edge. This structural erosion leads to the conclusion that an equilibrium shoreline position is not possible in this system.

Future development

If wind conditions remain similar to the analysed period and no maintenance is performed at the Noordstrand we believe a general regression of the shoreline is observed in the coming years. This regression will be more severe near the hard edge and less severe near the soft edge. The submerged platform will continue to expand offshore, most noticeable near the soft edge. If other wind conditions not linked to *scenario 3: set-up* occur more often the development of the beach can be different. Depending on the exact conditions the regression of the shoreline could be reduced by processes transporting sediment in the opposite direction compensating erosion (e.g. higher occurrence of *scenario 2: set-down*).

10.3 Monitoring and Maintenance

The first five islands of the Marker Wadden, including the Noordstrand, are now in the maintenance phase. In this section we shortly discuss how our findings can be used in the maintenance and adaptation strategy of the Noordstrand.

10.3.1 Maintenance

The maintenance strategy depends on what the client prefers: in our case we consider the protective and recreational function of the beach. The client (Natuurmonumenten) prefers a wider beach making the area accessible and attractive for the public. Based on our conceptual system description an equilibrium shoreline is not possible, meaning the width of the foreshore will decrease over time. To fulfil its recreational function the eroded sediment has to be compensated with nourishments.

Location nourishment

As the erosion is most severe next to the hard edge and along the southwestern part of the Noordstrand this is an obvious location for a nourishment. Adding sediment in the area influenced by the rotation cell would create a local 'sandmotor' transporting sediment along the length of the beach. Ultimately the nourishment is eroded completely and regression of the shoreline continues until a new nourishment is applied.

The nourishment can best be placed near the duneface, creating a buffer for high-energy events, and partially in the region of the upper shoreface creating a wear layer for gradual erosion. Placing sediment below the elevation of the platform will not have an effect as most erosion takes place near the waterline and duneface: the elevation of the submerged platform is essentially the wave-base (or depth-of-closure, Ton et al. (2020)). There is not enough energy in this system to distribute sediment below the platform elevation to higher parts in the cross-shore transect. One could argue that making the submerged platform very wide will limit wave impact on the beach face and thus reduce erosion. However, the magnitude of the nearshore current does not solely depend on waves and the area of influence of this current is larger in case of a submerged platform (subsection 9.1.3). Greatly expanding the submerged platform is costly and its effects on local flow patterns is not completely understood, using our current understanding this does not seem to be a reliable solution.

The extend of this research is not sufficient to predict the expected timing and volume of the nourishments. We do acknowledge the importance of monitoring the Noordstrand development, especially during high-energy periods as individual events can significantly undermine the recreational function of the beach.

10.3.2 Adaptations & improvements design

Next to nourishments which compensate the loss of sediment (creating a source equal to S_y , from equation 10.1) one could decrease the gradient in longshore transport rates (decrease u or V) or remove the sediment sinks from the Noordstrand system.

The rotation cell caused by the hard edge is mainly responsible for the erosion of southwestern part of the beach. One could consider removing the breakwater, as a result the rotation cell will vanish and the acceleration of the longshore current will be limited (second term V in equation 10.1). Indeed this will decrease the transport rates in this part of the beach, but removal of the hard edge means wave and flow impact will be more severe near the northern edge of the Marker Wadden. This edge needs to withstand large flow velocities and needs to be redesigned for this purpose. For now removal of the breakwater does not seem a reliable and cost-effective solution. Additional research and model runs of how removal of the breakwater will influence waves and general flow patterns is needed.

Another possibility is the removal of the sediment sinks, we 'close' the system so to say. This can be achieved by prolonging the soft edge (or built an extended hard edge at this location) thus far that flow around the soft edge is minimal (blue arrows, figure 10.15). Eroded sediment from the beach will be deposited in front this new edge as transport gradient decrease. Slowly the shoreline orientation an equilibrium orientation with respect to dominant wind and wave conditions (orange line, figure 10.15). Erosion of the southwestern part of the beach continues if the rotation cell is still present. This extension of the soft edge could potentially influence offshore and nearshore flow patterns (as an exploratory morphological D3D run has shown, figure F.4). Additionally the transport of sediment from the northeast to the southwestern part of the beach in case of northeastern wind (scenario 2: set-down) is reduced or even completely blocked by this extension. The intricate combination of lake general and local processes make predictions concerning coastline development in this case unreliable. Furthermore the sediment sink formed by the offshore oriented transport near the soft edge, due to a change in the angle of incidence of waves, will still be present.

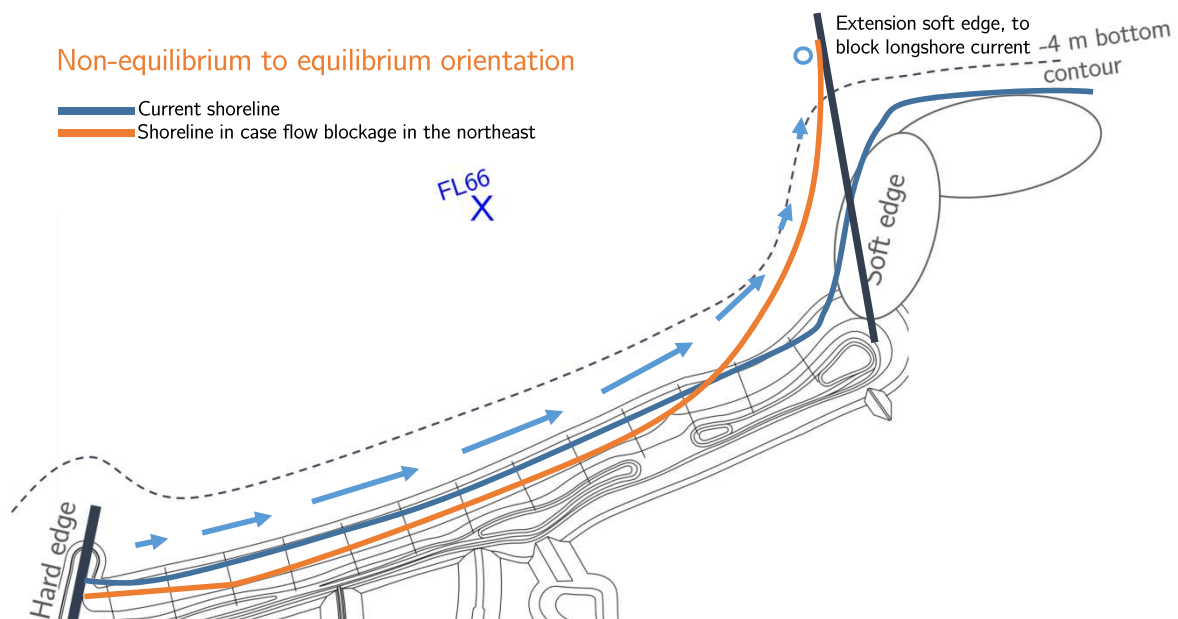


Figure 10.15: Hypothesised development (orange line) of the Noordstrand in case of a 'closed' system, the prolonged edge in the northeast blocks the longshore current. Notice how the orientation of the Noordstrand will change to an equilibrium shoreline orientation.

10.4 Critical Remarks

This section gives the critical remarks on our conceptual system description, the data and the research methods.

10.4.1 *Conceptual system description*

The basis of the conceptual system description of the Noorderstrand is our analysis using the available hydrodynamic, morphodynamic and D3D model data. Our critical remarks regarding this description are split into the link between offshore and nearshore processes, and the governing wind conditions versus beach development.

Link offshore and nearshore processes

Only offshore data near the Noorderstrand is available, which make the translation to the nearshore processes difficult. We have tried to link both using a Delft3D model calibrated using field data. The model has been used to assess different scenarios nearshore, however we cannot validate these results as no nearshore measurements near the Noorderstrand are available. One could argue nearshore measurements from other Marker Wadden beaches were considered in the calibration, but the Noorderstrand is the sole beach with a non-equilibrium orientation. This could potentially mean different processes play a dominant role in beach development.

We believe the usage of this model is acceptable for a first exploration of the system. Our findings need to be verified with additional nearshore measurements to assess whether the model correctly describes the nearshore processes and if our conceptual system description needs to be altered.

Governing wind conditions versus beach development

We based our conclusion of *no equilibrium* on a period of 20 months of wind and hydrodynamic data. The windrose used in the verification of the design of the Noorderstrand (left plot, figure 3.1) deviates from the windrose of our analysed data (figure 6.2). A 20-month period might seem significant but is actually not long enough to be linked to future development. An example: compared to the design windrose, which used representative wind speeds and directions, we have observed less northeastern events. This absence might explain the increased erosion in the southwestern part of the beach as northeastern events would lead to sedimentation near the hard edge (scenario 2: set-down). A higher occurrence of northeastern winds could lead to a more balanced sediment transport as these winds can (partly) compensate sediment transport occurring from southwestern winds. Therefore it is important to consider that the combination of different wind conditions and thus different scenarios 'shape' the Noorderstrand, the contribution of one scenario depends on the occurrence of the corresponding wind conditions.

For a preliminary understanding of our system we believe our analysis is sufficient, especially as we have aimed to explain the erosion observed in the considered time period. Nonetheless for a more complete understanding the wind, hydrodynamic and morphodynamic processes need to be monitored for a longer period of time.

10.4.2 *Data and analyses*

The different analyses and the related data are evaluated in this section, split into the three main parts of our research: hydrodynamic data analysis, morphodynamic data analysis and Delft3D modelling.

Hydrodynamic data analysis

Critical in the ADCP current data is the absence of information concerning the top 1-1.5 meter of the water column. We know the current profile is influenced by the wind drag in the top and the return current lower in the water column is formed by a combination of wind- and wave-driven processes, but the direct influence of wind and waves in the top of the water column cannot be observed.

Furthermore the location of FL66 is a point of attention. It is so far offshore that it mainly measures the general lake hydrodynamic processes (wind-induced current and propagating waves), but the measurements are influenced by the proximity of the Noorderstrand (main current direction is 50° not 65° which is exactly shore parallel southern direction). As a result it is impossible to completely split the observed measurements into an offshore and nearshore originating part.

Morphodynamic data analysis

The frequency and resolution of the morphodynamic data has been a limiting factor. The 3-monthly topography and bathymetry measurements made the assessment of the impact of individual high-energy events impossible. Elevation measurements near the waterline were even less frequent. Our work-around is the usage of linear interpolation to fill the missing gaps and project the data on a predefined grid. In this interpolation we did not account for the effects of consolidation and settlements of the sediment over the course of time, this could lead to a slight overestimation of erosion rates.

For an improved morphodynamic analysis with greater accuracy more and higher resolution measurements have to be obtained. We contributed to this by organising monthly field trips after the nourishment was finished in December 2020, during which we measured the elevation around the waterline in more detail and more often. This new dataset with elevation data obtained every month containing 50 meter transects is a potential start of a follow-up morphodynamic analysis.

Due to data availability and time constraints we have focused on the development of the main part of the Noordstrand, ranging from the breakwater in the southwest to the soft edge in the northeast. Our results indicate the influence of the soft edge on flow patterns and transport rates, accommodating the location of the sediment 'sinks' of our system. Therefore our analysis is essentially incomplete. Extending our Noordstrand system to include the northeastern extension might hold the answer as to where the eroded sediment is going.

Delft3D modelling

Multiple critical aspects of the modelling in Delft3D can be summed up: the lack of calibration data nearshore and depth-averaged (2DH) modelling are just examples. In this critical discussion we want to focus on the modelling of the nearshore processes present in only a small part of the computational grid as these processes are essential in the development of the beach, see the enumeration below. Some of the critical remarks have been translated to recommendations for additional and future research (section 11.2).

- The orientation of the real shoreline and computational grid are different, therefore the waterline shows a stepwise resolution along the beach, which is not a correct representation.
- In the cells near the waterline the water depth changes 4 meters in just 5-6 grid cells, which can influence the drying and flooding process. This phenomenon is already a difficult and challenging process to model as the chosen threshold depth can influence the principle of mass conservation and thus flow patterns, making the representation of the waterline less reliable. For a better representation one should (locally) refine the grid near the beach significant changes in bathymetry (for local refinement use Delft3D Flexible Mesh). We have investigated the influence of the threshold depth and reducing the threshold depth did not change the results much (section 9.3.3). We remain critical towards information displaced in the outer grid cells and use the collective information displayed by the collection of grid cells for our analysis.
- The SWAN model is a wave averaged model. This model cannot solve the wave-driven current separately, making it impossible to solely investigate the influence of waves on the longshore current. Furthermore we cannot assess the influence of single waves on the beach profile in case of high-energy events. For the response of the beach to a single high-energy event a different type of modelling agent is needed (for instance XBeach, even though XBeach does not resolve individual waves; it, unlike Delft3D, includes processes such as wave groups and infragravity waves which influence hydrodynamic processes such as water level and wave breaking). By accounting for additional processes in software such as XBeach the response of the beach can be modelled more accurately, creating additional insight into beach development during individual high-energy events.
- The boundary conditions imposed, water levels at one nested boundary and velocities at the other, in combination with the relatively small area (in case of the *nested model*) can have an influence on the nearshore results. This means the model result near the Noordstrand can be affected by the imposed boundary conditions, which is undesirable. To minimise the influence of the boundary conditions on the nearshore flow one could consider enlarging the computational domain or decreasing the grid size of the current domain. However, both will result in an increase in computational time. Additionally one can consider changing the imposed boundary conditions, however this also means the nesting procedure has to be adapted. In this case a Delft3D Flexible Mesh model might be interesting to consider, see section 11.2.

10.5 Exploratory Research

Two additional exploratory analyses have been done. First, we tried to link possible sedimentation areas to the data analysed in the morphodynamic data analysis. Second, we have done some morphological modelling in Delft3D. Both analyses show promising results, but as their application so far has been rather limited and the uncertainty towards the results is large, we choose to present these results in the discussion instead of in the main 'results' sections.

Extending Noordstrand system

In our conceptual system description we have noticed sediment is lost from the Noordstrand system. We identified a sediment sink: eroded sediment leaves the considered area with the longshore current around the outer bend of the soft edge. The question which remains is: *where is the eroded sediment going?* From an exploratory investigation we might be able to locate the possible location where (part of) the eroded sediment settles. The southwestern winds, responsible for high erosion rates, cause longshore current deceleration in the most Northern part of the extension of the soft edge (this is outside our predefined system borders, most northern corner of the Marker Wadden, top right outside blue box figure 2.3). As a result transport rates drop and we expect sedimentation in this location. Combining the flow patterns with morphological data (elevation data of 2019 Q3 compared with 2018 Q3), we observe a positive change in elevation (sedimentation) in the expected location (figure 10.16).

This is only an exploratory run showing how a deceleration area in our Marker Wadden model matches an observed sedimentation area. This could be a potential settling location of the Noordstrand eroded sediment and could partly answer the question of where the sediment is going. Identifying the specific locations of the sediment sinks help us in our general understanding of the Noordstrand development.

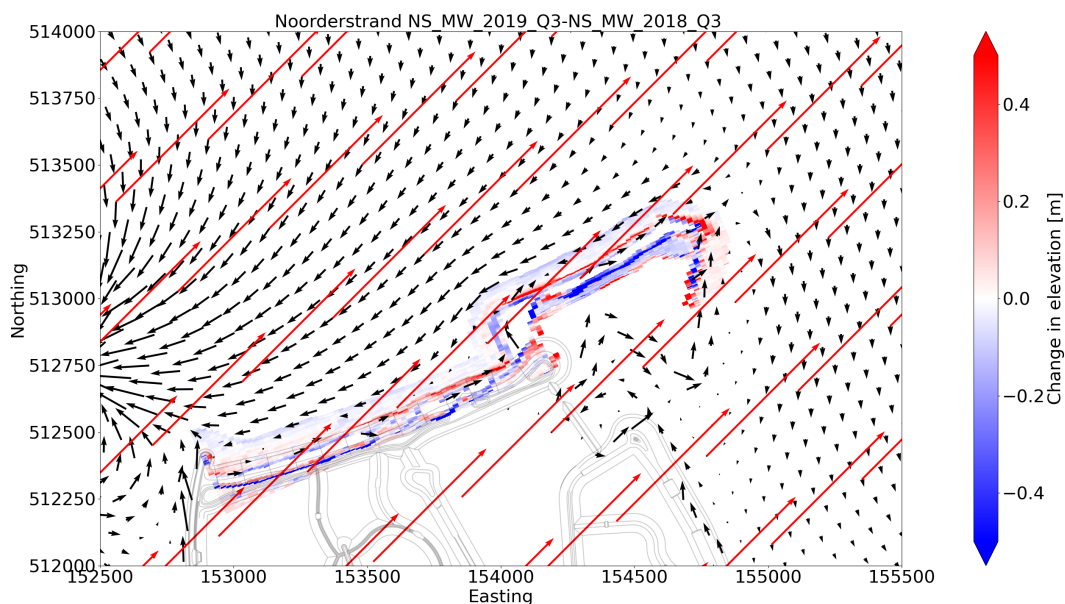


Figure 10.16: Elevation change (colourbar plot) together with D3D model results for wind coming from 225° (southwest, red arrows), showing current direction (black arrows). Sedimentation (red) and erosion (blue) rates are found by analysing the elevation data obtained by Boskalis in the period 2018 - Q3 till 2019 - Q3. Notice the patch of sedimentation (red) in the upper northern part of Noordstrand and Marker Wadden. In this location different currents merge resulting in deceleration, this could be a potential settling location of (part of) the eroded sediment from the Noordstrand system.

Morphological model runs

Appendix F shows the set-up of an initial try to model the morphodynamics near the Noordstrand using Delft3D. Figures F.1b, F.2b and F.3b show a snapshot of the transport magnitude and direction in the middle of the beach for a wind speed of 15 m/s. All three models show the general transport near the soft edge is directed offshore, an indication that the eroded sediment from the beach is deflected offshore possibly caused by the change in angle of incidence of approaching waves (as in scenario 3, see section 10.2.5).

For winds directly facing the Noordstrand (335°, figure F.3a) transport rates along the beach are higher compared to the situation in which the wind is parallel to the Noordstrand shoreline orientation (245°, figure F.1a) or winds in between (290°, figure F.2a). This is believed to be caused by the more direct wave impact on the beach in case of perpendicular oriented winds (335°), resulting in increased transport rates in cross-shore direction.

The general transport rates shown in the 290° morphological run, are smaller than for the 335° wind conditions (comparing figures F.2a and F.3a). The wind arriving from 290° results in increased transport rates near the middle to northeastern part of the Noordstrand, however the total magnitude of this transport is less than the total transport in case of directly incident wind (335°). The total transport magnitude is formed by both the cross-shore and longshore component. Southwestern winds result in a higher longshore component of the transport vector nearshore, indicating an increased transport in longshore direction, but the cross-shore component is smaller. Combined the contribution of the increased longshore component is not enough to even the increased transport magnitude in case of perpendicular oriented wind.

Based on the $S-\phi$ formulation (or CERC-formulation) we expected the largest transport magnitude for the 290° wind direction: obliquely incident waves with an angle of 45° relative to the shoreline occur (figure 9.7) resulting in the largest longshore transport rates compared to the scenarios concerning other wind directions. Nevertheless the largest transport magnitudes occur in case of 335° winds (perpendicular incident wind and waves), indicating most significant contribution to the total transport magnitude is caused by the cross-shore component (see also previous paragraph) and not the longshore component.

This mismatch between theory and model results indicate the need to properly calibrate and validate a morphological model. Different parameters relating hydrodynamic processes such as waves and currents to different components of the transport can be calibrated for this specific system, but the question arises if general transport formulas used for high-energy environments are also applicable in low-energy systems such as the Markermeer. The results are questionable, due to the uncertainty in the transport factors, but they do show the ability of further investigating the link between hydro- and morphodynamic processes using a morphological model.

Two additional morphological runs are analysed to observe the effect on transport in case of an extension of the soft edge (see figure 10.15) and in case of an extended submerged platform. For the former, extension of the soft edge, we expected less loss of sediment as the longshore current is decreased. We cannot give conclusions on this as only transport rates are available, but we can see how the extension influences the offshore and nearshore current patterns (red arrows, figure F.4). This shows the situation is much more complex than initially thought and underlines the importance of considering the larger context of the system and the corresponding processes. In this case a new 'rotation cell' is formed northeast of the extension of the soft edge, potentially make the beach to the northeast subject to increased erosion rates.

The inclusion of an extended submerged platform shows the presence of transport over the entire width of the platform even in case of milder wind conditions (wind speed is 10 m/s, figure 10.17). The relative shallowness of the area on top of the platform accommodates sediment transport. More importantly, this model run, for wind coming from 290°, shows transport is also observed next to the submerged platform (transport rates increase as the wind speed increases). The effect of waves offshore of the platform is more limited, indicating an influence of the wind-induced current on sediment transport. In extreme conditions (wind speed is 20 m/s) the transport rates next and on top of the platform increase especially in the northeastern part of the Noordstrand (figure F.5).

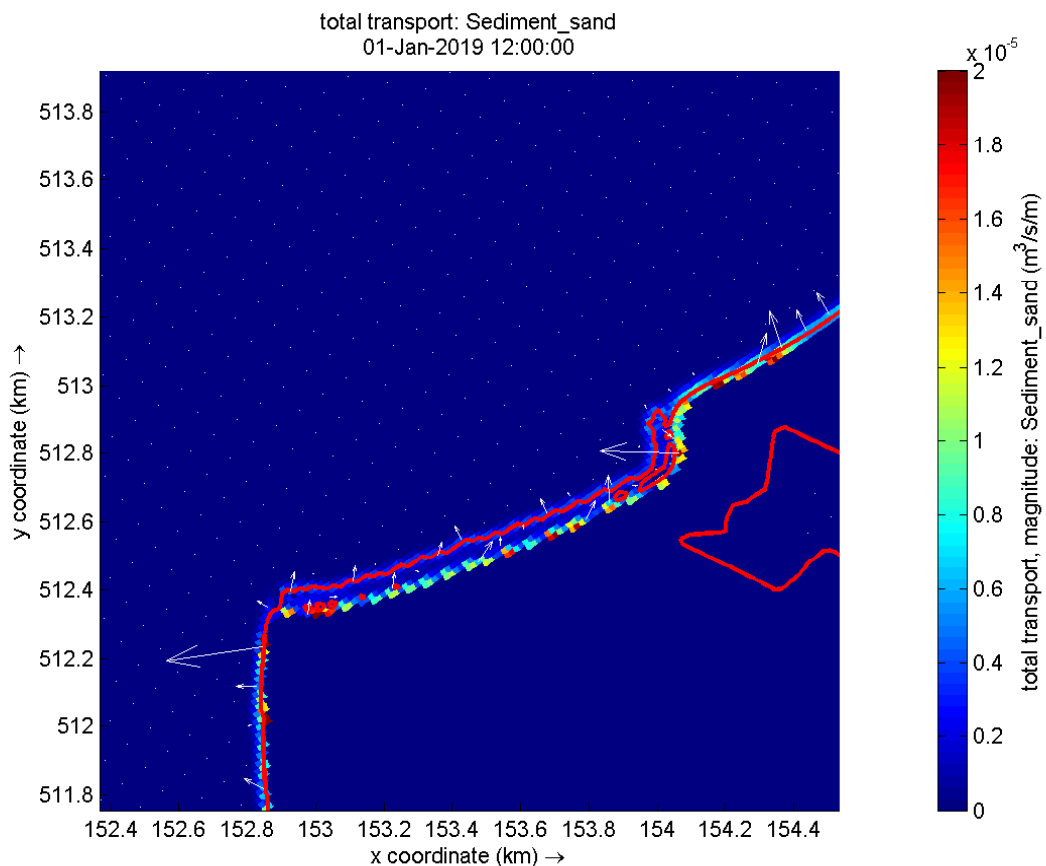


Figure 10.17: Total transport magnitude (colourbar) and direction (white arrows) for wind coming from **290°** in case an extended submerged platform is present, platform is shown as the -1.11 meter NAP depth contour (red). The shown transport is due to a wind speed of 10 m/s (5 Bft).

Linking to Hallermeier's depth-of-closure

The link between the submerged platform elevation and Hallermeier's depth-of-closure (or wave base) has been described by Ton et al. (2020). Whereas some might simply conclude nothing happens in the beach profile below the depth-of-closure, the exploratory morphological model runs show transport of sediment even next to the submerged platform (figures 10.17 and F.5). This underlines our previous conclusion that transport is not only caused by wave-induced motions, but other hydrodynamic processes play a role. An interesting follow-up study could include the breakdown of the wave-induced and current-induced components of transport. It could well be that the currents are not only capable of transporting the sediment, but are also responsible for the initiation of motion.

10.6 Building with Nature - a System Engineering Approach

We have identified three critical points of the Building with Nature approach: taking into consideration the development of the system after the final commissioning, uncertainties of innovative solutions and the understanding of an unknown system. This means the following key points of Building with Nature projects are regarded from a System Engineering perspective:

- Consider the project over a period of time rather than only the initial realisation of the project
- Consider the uncertainties and unknowns
- Consider the understanding of an unknown system

We use a System Engineering approach to find some points of attention and recommendations concerning these statements. The full analysis can be found in appendix I.

First we identified the importance of considering the entire life cycle of a system/project. The life cycle in case of Building with Nature projects can be uncertain as these projects are adaptive and innovative solutions. As a result it can be difficult to assess the different parts of the system life cycle. Therefore, we propose to select some TY's, from the system engineering view on *designing for TY's*, which are special points of attention during the different phases of the project and life cycle. We believe *reliability*, *maintainability* and *flexibility* are interesting TY's to consider in a BwN project. In the Marker Wadden project an additional focus on e.g. *flexibility* of the design can lead to less maintenance. Close cooperation and communication between all stakeholders is necessary to correctly implement these TY's.

Second, this project is an excellent example of a project which acknowledges its own uncertainty. *Learning*, *monitoring of effects and innovate* are key points of the Marker Wadden and any other BwN project. Increased system understanding is needed for correct integration and verification of different subsystems and components. Only if subsystems are understood in their smaller context they can be combined to form a more general system understanding. This has been shown in this research too: lake circulation patterns can have effects on the nearshore current and thus local beach development. The *integration and verification* of system processes can be improved in future projects, but for this we first need to learn, monitor, innovate and ultimately understand this system.

11

Conclusion & Recommendations

This chapter presents the answers to the research questions as stated in the research proposal (chapter 2) in section 11.1. Section 11.2 gives the main recommendations for the situation of the Noordstrand and future research regarding low-energy systems in general.

11.1 Conclusion

In the beginning we identified the main research question (blue box below). Using literature, hydrodynamic data obtained near the Noordstrand, morphodynamic data of the beach itself and the Marker Wadden D3D model we are able to give an answer in the context of the Noordstrand. The extent of some findings can be extended to low-energy beaches with a non-equilibrium orientation in general. The main research question is answered by giving the answer to the five subquestions, discussed in the next paragraphs.

Which processes steer the morphological development of high-angle beaches with non-equilibrium orientation in low-energy lake environments? How do they influence morphology? Can our understanding be used for future maintenance (if needed) and construction of this kind of beaches?

11.1.1 System Identification

Which hydrodynamic processes could steer the (large-scale) behaviour of a beach in a lake environment like the Marker Wadden?

The Markermeer has been identified as a low-energy (lake) system assessing different phenomena (Vila-Concejo et al., 2020; Hegge et al., 1996; Aagaard, 1988; Steetzel et al., 2017; Ton et al., 2019, 2020). According literature different processes can steer the behaviour of low-energy beaches, but most importantly low-energy lake systems cannot be simply described as scaled down high-energy systems (Nordstrom and Jackson, 2012). The following mechanisms were identified in literature first and later recognised in our Noordstrand system: the main forcing in the system is the wind, creating wind-induced currents, wind-driven currents and waves; due to limited refraction high-angle waves can cause enlarged longshore transport rates (Jackson et al., 2002; Nordstrom and Jackson, 2012); the evolution of the beach mainly depends on storm events (Vila-Concejo et al., 2020), during these events the combination of high water levels and high waves can cause severe erosion (Kirk et al., 2000); and little recovery is expected as low-energy events do not have enough energy to reshape the beach.

During our research we identified one other major process: the influence of general currents part of the larger lake circulation pattern formed by water level set-up or -down over the lake and influenced by the location and geometry of the islands. These currents can be significant in magnitude. In case of the Noordstrand this general wind-induced current is present offshore and nearshore, but are in the opposite direction. The nearshore component is confined to the nearshore bathymetry and can be accelerated or decelerated regionally due to local influences, impacting transport rates. The local geometry is an influencing factor: in case of the Noordstrand the hard edge creates a rotation cell, meaning its presence indirectly causes increased erosion.

11.1.2 System Understanding

What is our current understanding of low-energy lake systems?

Several researchers have highlighted our limited knowledge on low-energy systems and the need to extend our understanding (Jackson et al., 2002; Nordstrom and Jackson, 2012; Steetzel et al., 2017; Ton et al., 2019). Apart from the main processes described in the previous paragraph a naturally forming submerged platform has been identified at the Marker Wadden beaches and other low-energy systems (Jackson et al., 2002; Allan et al., 2002; Steetzel et al., 2017; Ton et al., 2019). A lot is still unknown about this development but some first steps in the explanation of platform formation are taken (Ton et al., 2020).

The design of sandy beaches to protect the hinterland in a low-energy lake environment is novel and innovative. To understand the design of the Marker Wadden beaches we have to place the design and development in the correct context of time and knowledge. The initial lay-out of these beaches is primarily based on our knowledge concerning sandy protections in high-energy environments (e.g. *Sand Engine, Hondsbossche and Pettemer Zeewering*) and includes a local pilot: Pilot Houtribdijk. However the orientation of the Noordstrand imposed a difficulty: its non-equilibrium shoreline orientation has no predecessor. Recent studies after construction of the Marker Wadden beaches (Steetzel, 2017; Ton et al., 2019, 2020) showed general shoreline regression and a link between the elevation of the submerged platform and Hallermeier's depth-of-closure, however their research primarily focused on beaches with an equilibrium shoreline orientation: Pilot Houtribdijk, Recreati strand and Zuidstrand. Combining the previous statements we found: *the main knowledge gap is associated with the unknown development of a beach with non-equilibrium shoreline orientation, in a low-energy system.*

We believe this low-energy system is not a scaled down high-energy system as the observed processes, their occurrence and importance in flow patterns and beach morphodynamics is different. Furthermore a beach with non-equilibrium shoreline orientation can behave totally unlike beaches with an equilibrium orientation, however the breakdown of the differences is difficult due to local influences. The answers to the following questions expand our knowledge a little and are hopefully a first step towards more research and an even better understanding.

11.1.3 Link: Conceptual System Description

Can the morphodynamics of a low-energy beach in a lake system, with non-equilibrium orientation, be linked to hydrodynamic processes? If so, in what way?

Combining literature, field measurements and D3D model runs we were able to create a conceptual system description for this non-equilibrium oriented beach. One needs to bear in mind that the combined action of all occurring wind conditions has resulted in the observed beach development. To increase system understanding we have simplified the observations and came up with three different scenarios describing the development of the Noordstrand together. One of these scenarios is thought to be mainly responsible for the Noordstrand development based on occurrence of wind conditions and agreement with observations (main scenario shown in figure 11.1).

The main indirect driver of beach development of this non-equilibrium oriented beach are winds from the south-western to northwestern segment (180° to 290°), as these wind directions have the highest occurrence. Likewise all high-energy periods are linked to these wind directions (dominant is the southwestern direction). With these winds higher wave heights due to long fetch distances and a water level set-up against the Houtribdijk are expected. As a result the latter drives the general lake circulation pattern even present during milder conditions (wind speeds between 5-15 m/s) (top, figure 11.1). Wave heights are still significant nearshore even in case of milder conditions (≈ 0.3 meter). Waves, during both high-energy and milder periods, stir the sediment at the upper shoreface and beach face. The longshore current is responsible for the transportation of this eroded sediment from the transect. This longshore current is formed by the nearshore wind-induced current (nearshore component of the lake circulation pattern), the wave-driven current and the wind-driven current on top of the submerged platform. Due to the acceleration of this longshore current and the increasing impact of waves along the stretch of the Noordstrand, transport gradients increase: leading to erosion along the entire shoreline. This is most evident in locations of rapid acceleration of nearshore velocities as is the case near the hard edge due to the presence of the rotation cell (figure 11.1).

This entire process is intensified during high-energy events, leading to increased stirring by enlarged waves and

increased transport rates due to a growth in longshore current magnitude. High-energy events are linked to increased water levels and consequently this could lead to slumping of the duneface, forming cliffs. Significant changes in the profile and the shoreline are expected during high-energy events, but gradual erosion during milder conditions has a powerful effect on the overall beach development too as these have a much higher occurrence.

Additional field measurements to validate nearshore model results and thus our conceptual system description are needed. Furthermore it is important to note that our conceptual system description is based on one governing scenario identified by analysing a short period of wind data. In the future other wind conditions might become more frequent, compensating or enhancing transport rates and thus influencing erosion and sedimentation patterns. To conclude it is the combined effect of all occurring wind conditions that shape the Noordstrand.

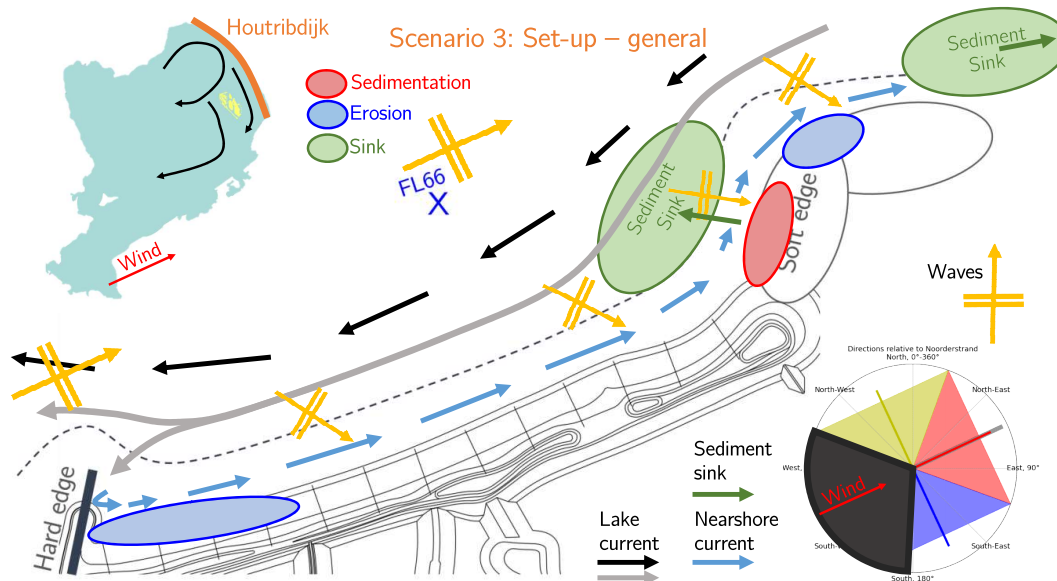


Figure 11.1: Scenario 3: Set-up - general; hydrodynamics and link to morphodynamics. Winds originate from 180° to 290° (grey region in wind rose, lower right). An offshore wind-induced current to the southwest is formed with a nearshore component in opposite direction. This current is enlarged along its course due to incoming high-angle waves and local geometry. Changes in nearshore hydrodynamics cause gradients in transport rates, resulting in erosion (blue) and sedimentation (red). In this scenario we observe erosion near the hard edge, along the southwestern part of the beach and little sedimentation near the soft edge. Most eroded sediment leaves the Noordstrand (sinks: green): the system is not 'closed'.

11.1.4 Equilibrium

Is an equilibrium position of the shoreline and cross-shore profile possible?

Based on our results an equilibrium position of both the shoreline and cross-shore profile is not (yet) possible. The duneface and upper shoreface erode, most significantly during high-energy period, but gradual erosion during milder conditions is believed to be of importance. The erosion is only partly compensated by sedimentation lakeward of the submerged platform. The sediment might have ended up here via a detour: the longshore current has transported the eroded sediment offshore where it follows the offshore wind-induced lake circulation current before it settles in the lower shoreface. When combining observations and our conceptual system description we believe there is structural erosion of the shoreline meaning that an equilibrium position of the shoreline is not possible when this design of the Noordstrand is exposed to the observed wind conditions.

One can speculate whether an equilibrium shoreline position is even possible at all for this beach. Our research is insufficient to be able to answer this, however we found local obstacles meant to, for instance, minimise wave impact can have negative secondary effects on general beach development. Therefore we suggest, in case of alterations of any existing beach or new designs in this kind of systems, to find a complete understanding of the general and local processes and their interaction. New designs and obstacles should be tested in models to prevent the overlooking of effects on erosion and decrease uncertainties in beach development.

11.1.5 Lessons Learnt

How can the previous findings help during development and maintenance of beaches in this low-energy lake system?

Based on our conceptual system description an equilibrium profile is impossible, meaning the beach will structurally erode due to the presence of sediment sinks. For the Noordstrand this means periodic nourishments are required. Measures to eliminate the sink, for instance halting the longshore current by prolonging the soft edge or removing the breakwater to eliminate the rotation cell, are quite costly, might result in unforeseen negative side effects and might not even be beneficial in stopping the structural erosion of the beach. We believe extensive monitoring of the Noordstrand by elevation and hydrodynamic measurements off- and nearshore could lead to a better understanding of the system and help future projects in similar systems. Obtaining both nearshore and offshore measurements could lead to a better understood link between both, enlarging our system understanding. Regarding the periodicity of the nourishment we believe this can be reduced if the recreational function, prescribing a certain width for the shoreface, does not need to be fulfilled the entire time. In that case the presence of cliffs is acceptable and a nourishment, preferably near the southwestern part of the beach near the dune or upper shoreface, is only needed if the beach can no longer fulfil its protective function.

For non-equilibrium oriented beaches in low-energy systems in general, we have found that these beaches are profoundly different from beaches in high-energy environments or sandy protections with an equilibrium shoreline orientation. Not only the effect of waves on the beach development should be taken into consideration when designing the beach, the effect of the general wind-induced lake circulation and local currents, such as the wind-driven current on top of the submerged platform, should be included. Only by regarding the entire system and understanding the link between different processes we can assess our beach design and development. This makes the usage of one-line models, based on the angle of incidence of waves solely, such as Unibest-CL+ unreliable. For an engineer designing this kind of protections in low-energy environments this means a more elaborate model must be used to assess shoreline development. Which in turn, again, underlines the importance of the understanding of the different hydrodynamic processes. This knowledge is needed to create a reliable model which can be used in the design process. All together this means an engineer cannot simply use the CERC-formulation to calculate transport rates (CERC only takes into account the wave-induced longshore current), but needs to ensure that no hydrodynamic process is disregarded upon first glance and next investigate what kind of model gives the best representation of the different processes.

Last, we have learnt that the processes are very system- and site-specific: the presented conceptual system description is only applicable for the Noordstrand. Adaptations or new designs for the Marker Wadden or other low-energy systems create entirely different systems with differing influencing processes. For understanding of these systems and implications of designs site-specific data and calibrated computational models resembling the system are needed and should be analysed. All combined this means we need to *change the current way of thinking* (see recommendations section below).

11.2 Recommendations

The recommendations are split into two parts: part one discusses the specific recommendations towards the situation of the Noordstrand of the Marker Wadden and part two considers the recommendations regarding scientific research of the low-energy beaches in general thus placing this research in a broader perspective. For both the list of recommendations could be endless, therefore we have chosen the recommendations that we believe are the best step forward in extending our understanding of the development of the Noordstrand and low-energy beaches.

11.2.1 *Situation Noordstrand*

We have combined our main recommendations regarding the Noordstrand into four different parts, taking into consideration the different aspects of this research (data analysis, modelling, implementing):

- Linking offshore and nearshore processes
- Extend Noordstrand system
- Updating Delft3D Marker Wadden model
- Morphological model runs

Linking offshore and nearshore processes

The link between offshore and nearshore processes, as explained in our conceptual system description, needs to be validated and verified by additional measurements. For an increased understanding of the Noordstrand system additional offshore and nearshore data is needed, obtained simultaneously for the best link between the general lake circulation and processes nearshore. We have seen the influence of the local geometry on the nearshore flow patterns and therefore one needs to consider the placement of these measurement devices. For the least biased measurements of nearshore flow a location somewhere in the middle of the Noordstrand needs to be considered. The offshore location could be FL66 and the nearshore location could be placed in line with FL66 but perpendicular to the shoreline orientation on top of the submerged platform (similar to the campaign at the other beaches as shown in figure 2.4). We suggest to install a step gauge (STB), to measure water level fluctuations and wave height, and an ADCP or ADV, for current magnitudes and directions. Additional measurements near the hard edge to validate the presence of the rotation cell could also be beneficial as we believe this is the main cause of erosion in this area. Measurements near the soft edge could provide insights into the hypothesised offshore transport at this location. The nearshore measurements can also be used to further validate the Marker Wadden model near a non-equilibrium oriented beach.

We advice to increase the resolution of the elevation data near the waterline (GPS measurements), to be better able to link the morphodynamic processes to the hydrodynamic processes. Decreasing the transect distance from 100 meter to 50 meter already gives a better view of the shoreline development of the Noordstrand. Most desirable are elevation measurements during the measuring period of the offshore and nearshore stations as in that case both can be linked and the interaction of hydrodynamic and morphodynamic processes can be investigated.

Extending Noordstrand system

We have showed some preliminary results of trying to link flow patterns and morphodynamic data obtained outside our Noordstrand system. This to answer one of the remaining questions: *Where is the sediment going?* We concluded we need to expand our system to include a larger area. This is endorsed by the general conclusion as we cannot consider the Noordstrand without considering the entire Markermeer system.

The possibility of sedimentation near the more northern part of the soft edge is an interesting case to check in morphology runs in Delft3D. The inclusion of this part of the Marker Wadden in the Noordstrand system is an important next step. It could also be beneficial to expand the bathymetry measurements further offshore to locate possible locations of offshore sediment sinks.

Updating Delft3D Marker Wadden Model

The Marker Wadden model can be improved by calibrating the nearshore hydrodynamics of the Noordstrand with field data (see paragraph: *Linking offshore and nearshore processes*). To remove or reduce numerical artefacts such as the stepwise shoreline representation and mass loss due to drying and flooding we suggest to refine the grid near the Noordstrand. Creating a Delft3D Flexible Mesh (FM) model of the Markermeer and Marker Wadden could be beneficial as local refinement is possible whilst limiting the computation time. By locally refining a total model, the need for *nesting* is omitted, as a result the boundary conditions of the *nested* model cannot influence the nearshore flow as the *nested* model and its boundary conditions are no longer needed. We also advise to investigate the current profile over depth at other locations of the Markermeer to see if depth-averaging (2DH model) is indeed acceptable at other locations or a 3D model is a better representation.

With an improved model one could study different phenomena. We suggest to include the morphology option of Delft3D (see next recommendation: *Morphological model runs*) and further investigate the link between offshore and nearshore processes. An interesting case is to extend the analysis on how the extension of the soft edge influences the general lake circulation and local longshore currents. A completely out-of-the-box model run would be to change the location of the Marker Wadden in the Markermeer and see how the flow patterns in the Markermeer change. This and other representative or exploratory model simulations can ultimately lead to a better understanding of how general and local processes interact and how man-made interventions influence both.

Morphological model runs

In the discussion of the results of the morphological D3D Marker Wadden model runs we had to remain very critical towards these exploratory runs as nearshore hydrodynamic processes and the morphological model itself are not calibrated. Furthermore the sediment transport formulas used by Delft3D are empirical and were fit to specific data sets. The latter mainly concern high-energy systems and therefore we have to remain critical if these empirical formulas describe the processes in our low-energy system correctly (more information in section F.1). Upon first glance some results match the observations and outcomes of the morphodynamic data analysis, but other results do not. Based on $s-\phi$ curves we expected higher transport rates for the obliquely incident wind and waves (290°) compared to the normally incident wind and waves conditions (335°), however the exploratory morphological runs showed the contrary when considering transport magnitudes.

For a better understanding of the Noordstrand and to verify our conceptual system description we advise to further develop the Marker Wadden morphological model. However, we believe it is beneficial to first look at the other recommendations before diving into the morphological model as the outcomes of the other recommended investigations can help significantly with the morphological modelling.

11.2.2 *Low-energy systems in general*

We have found that the hydrodynamic and morphodynamic processes depend on the system characteristics. Their occurrence and influence are not the same in every low-energy system. This research has shone light on the development of the Noordstrand and Marker Wadden system, but some results are beneficial for our understanding of low-energy systems in general.

Frequency versus intensity high-energy events

Literature stated the dependency of beach evolution on high-energy events (Vila-Concejo et al., 2020). We found an indication that intensity of high-energy events has more influence on beach development than the frequency of these events. The analysis of the frequency versus intensity of high-energy events in this research has been rather brief and we should remain critical towards the approach used: only the peak wave height was considered to calculate wave energy, the duration of the high-energy event was disregarded.

Further analysis is advised in which the duration of the storm is taken into account. Furthermore we advise to investigate a longer period of time. For the Noordstrand the only period in which hydrodynamic and morphodynamic overlap is already considered, meaning additional datasets are needed (see paragraph: *Linking offshore and nearshore processes*). Research linking erosion rates to intensity or frequency of high-energy events can be extended to include other Marker Wadden beaches or other low-energy systems.

Change current way of thinking

As previously stated low-energy systems cannot be compared to scaled down high-energy systems (Nordstrom and Jackson, 2012). We have for instance identified the importance of a nearshore wind-induced current created by water level set-up over the Markermeer and local geometry. During high-energy events current magnitudes can be significant, even if the effect of waves on the current is neglected. Main focus during the general design process of the Marker Wadden and other systems concerning sandy protections is the influence of waves. In case of high-energy systems such as the North Sea this has been a proven approach, but in low-energy systems governing processes could be entirely different. For instance: in case of the Marker Wadden the impact of the general lake circulation on the nearshore hydrodynamics has not been considered, however we have seen its influence on the longshore current enhances erosion. When designing a sandy protection in a low-energy system processes such as general wind-induced flow patterns due to lake circulation flows, nearshore currents and water level fluctuations should be part of the design process.

Therefore we need to change our *way of thinking and designing*. Instead of designing a beach profile and shoreline solemnly based on the wave climate, we need to consider the entire system. In this analysis the link between offshore and nearshore processes is crucial as to include the positive feedback mechanism between (local) geometry and the hydrodynamics. This recommendation is associated with the lessons learnt in section 11.1.5.

To conclude one should not underestimate the *energy* in low-energy systems. It is easy to dismiss beach development in a relative small system especially if the shoreline is not directly confronted by wind and waves. However, we know when looking at the situation of the Noordstrand and using our conceptual system description that the entire beach will vanish from the archipelago if no monitoring and maintenance is executed, leaving the northern part of the Marker Wadden unprotected.

Bibliography

- Aagaard, T. (1988). Nearshore bar Morphology on the Low-Energy Coast of Northern Zealand, Denmark. *Geografiska Annaler. Series A, Physical Geography*, 70(1/2):59–67.
- Allan, J. C., Stephenson, W. J., Kirk, R. M., and Taylor, A. (2002). Lacustrine shore platforms at Lake Waikaremoana, North Island, New Zealand. *Earth Surface Processes and Landforms*, 27(2):207–220.
- Blanchard, B. S. and Fabrycky, W. J. (2014). *Systems Engineering and Analysis: Pearson New International Edition*. Pearson.
- Booij, N. and Holthuijsen, L. H. (1987). Propagation of Ocean Waves in Discrete Spectral Wave Models. *Journal of Computational Physics*, 68(2):307–326.
- Borger, G. J. and Ligtendag, W. A. (1998). The role of water in the development of the Netherlands - a historical perspective. *Journal of Coastal Conservation*, 4(2):109–114.
- Bosboom, J. and Stive, M. (2015). *Coastal Dynamics I, lecture note CIE4305*. Delft Academic Press.
- Boskalis Nederland (2015). EMVI 2 - Landschappelijke Kwaliteit Vogelparadijs. Technical report, Boskalis Nederland. Beoordelingsdocument voor de aanbesteding van de opdracht met zaaknummer: 31091560 voor het project eerste fase Marker Wadden.
- Boskalis Nederland (2021). Drone challenge. <https://werkenbij.boskalis.com/drone-challenge/>. Accessed on March 24, 2021.
- Cooper, J. A. G., Lewis, D. A., and Pilkey, O. H. (2007). Fetch-limited barrier islands: Overlooked coastal landforms. *GSA Today*, 17(3):4–9.
- De Rijk, S., Noordhuis, R., Van Kessel, T., and Ellen, G. J. (2018). Monitoring and evaluatie programma marker wadden. Technical report, Deltares. Preliminary report.
- De Schipper, M. (2020). University lecture slides CIE4039 coastal dynamics ii; waves and currents in the nearshore. May 2020.
- Deltares (2021a). Delft3D-FLOW, simulation of multi-dimensional hydrodynamic flows and transport phenomena, including sediments, user manual. Technical report, Deltares.
- Deltares (2021b). Delft3D-WAVE, simulation of short-crested waves with swan, user manual. Technical report, Deltares.
- Deltares (2021c). Quickin: Generation and manipulation of grid-related parameters such as bathymetry, initial conditions and roughness, user manual. Technical report, Deltares.
- EcoShape (2021a). Multi-Stakeholder Approach. <https://www.ecoshape.org/en/enablers/stakeholder-model/>. Accessed on June 01, 2021.
- EcoShape (2021b). What is Building with Nature. <https://www.ecoshape.org/en/the-building-with-nature-philosophy/>. Accessed on June 01, 2021.
- Eurobarometer (2008). Attitudes of European citizens towards the environment. https://ec.europa.eu/commfrontoffice/publicopinion/archives/ebs/ebs_295_sheet_nl.pdf. Fieldwork, results for the Netherlands.
- Hegge, B., Eliot, I., and Hsu, J. (1996). Sheltered Sandy Beaches of Southwestern Australia Sheltered Sandy Beaches of Southwestern Australia. *Journal of Coastal Research*, 12(3):748–760.
- Holthuijsen, L. H. (2019). *Waves in Oceanic and Coastal Water*. Cambridge University Press.
- Hoogheemraadschap Hollands Noorderkwartier (2020). Prins hendrikzanddijk - texel. <https://www.hhnk.nl/prinshendrikzanddijk>. Accessed on January 5, 2021.

- Hulsbergen, R. and Kuijper, M. (2007). Modelling slibhuishouding markermeer. Technical report, WL Delft Hydraulics (Deltares).
- Hüsken, L. (2020). Marker wadden: van pilot naar opschaling. Technical report, Deltares. Working paper.
- Island Wards Natuurmonumenten (2021). Personal communication.
- Jackson, N. L., Nordstrom, K. F., Eliot, I., and Masselink, G. (2002). 'Low energy' sandy beaches in marine and estuarine environments a review. *Geomorphology*, 48(1-3):147–162.
- Jensen, J. H., Madsen, E., and Fredsøe, J. (1999). Oblique flow over dredged channels; i: Flow description. *Journal of Hydraulic Engineering*, 125(11):1181–1189.
- Johnson, H. K. (1998). On Modelling Wind-Waves in Shallow and Fetch Limited Areas Using the Method of Holthuijsen, Booij and Herbers. *Journal of Coastal Research*, 14(3):917–932.
- KIMA (2018). Intentieverklaring kima.
- Kirk, R. M., Komar, P. D., Allan, J. C., and Stephenson, W. J. (2000). Shoreline Erosion on Lake Hawea, New Zealand, Caused by High Lake Levels and Storm-Wave Runup. *Journal of Coastal Research*, 16:346–356.
- Lorang, M. S. and Stanford, J. A. (1993). Variability of shoreline erosion and accretion within a beach compartment of Flathead Lake, Montana. *Limnology and Oceanography*, 38(8):1783–1795.
- Musch, S. (2020). Code geel voor storm dennis, eerste lentedag van het jaar. *NRC*.
- Noordhuis, R. (2014). Water quality and ecological changes in lake markermeer-ijmeer. *Landschap*, 1:13 – 22.
- Nordstrom, K. F. and Jackson, N. L. (1992). Two-dimensional change on sandy beaches in meso-tidal estuaries. *Zeitschrift fur Geomorphologie*, 36(4):465–478.
- Nordstrom, K. F. and Jackson, N. L. (2012). Physical processes and landforms on beaches in short fetch environments in estuaries, small lakes and reservoirs: A review. *Earth-Science Reviews*, 111(1-2):232–247.
- Posthoorn, R., Vijverberg, T., De Visser, R., and Viveen, B. (2019). Restoration through reclamation. *Civil Engineering Magazine*, 89:64 – 71.
- Programmadirectie Natura 2000 (2009). Natura 2000-gebied Markermeer & IJmeer. PDN/2009-073.
- Rijksoverheid (2020). Klimaatverandering en gevolgen. <https://www.rijksoverheid.nl/onderwerpen/klimaatverandering/gevolgen-klimaatverandering>. Accessed on November 11, 2020.
- Rijkswaterstaat (2018). Peilbesluit ijsselmeergebied. Technical report, Ministerie van Infrastructuur en Waterstaat. RWS-2018/16279.
- Rijkswaterstaat (2021). Waterinfo. <https://waterinfo.rws.nl/#!/nav/index/>. Accessed on May 05, 2021.
- Royal Netherlands Meteorological Institute (KNMI) (2020). Uurgegevens van het weer in nederland. <https://www.knmi.nl/nederland-nu/klimatologie/uurgegevens>. Data downloaded from 2019, 2020 and 2021.
- Sallenger, A. H. J. (2000). Storm Impact Scale for Barrier Islands. *Journal of Coastal Research*, 16(3):890–895.
- Steetzel, C. (2017). The behaviour of the sandy shores of the Marker Wadden. Master's thesis, University of Twente, the Netherlands.
- Steetzel, H., van der Groot, F., Fiselier, J., de Lange, M., Penning, E., Van Santen, R., and Vuik, V. (2017). Building with nature pilot sandy foreshore Houtribdijk design and behaviour of a sandy dike defence in a lake system. *Coastal Dynamics*, (063):1–14.
- The SWAN team (2020a). SWAN, Scientific and Technical Documentation. Technical report, Delft University of Technology.
- The SWAN team (2020b). SWAN, User Manual. Technical report, Delft University of Technology.
- Ton, A. M. (2020). Personal communication.

- Ton, A. M., Vuik, V., and Aarninkhof, S. G. J. (2019). Formation of Sandy Foreshores in Low-Energy Microtidal Environments. pages 754–764.
- Ton, A. M., Vuik, V., and Aarninkhof, S. G. J. (2020). Sandy beaches in low-energy, non-tidal environments: Linking morphological development to hydrodynamic forcing. *Geomorphology*, page 107522.
- Van Riel, M. C., Vonk, J. A., Noordhuis, R., and Verdonschot, P. F. M. (2019). Novel ecosystems in urbanized areas under multiple stressors: Using ecological history to detect and understand ecological processes of an engineered ecosystem (lake markermeer). Technical report, Wageningen Environmental Research, Wageningen UR.
- Van Rijn, L. C. (1986). Sedimentation of dredged channels by currents and waves. *Journal of Waterway, Port, Coastal, and Ocean Engineering*, 112(5):541–559.
- Van Santen, R. (2016). Marker Wadden - ontwerp en verificatie zachte randen. Technical report, Arcadis Nederland B.V. MW-UO-WP-OW04-v2.
- Verhagen, H. J. and Schiereck, G. J. (2019). *Introduction to bed, bank and shore protection*. Delft Academic Press.
- Vijverberg, T. (2008). Mud dynamics in the Markermeer, Silt traps as a mitigation measure for turbidity. Master's thesis, Delft University of Technology, the Netherlands.
- Vila-Concejo, A., Gallop, S. L., and Largier, J. L. (2020). *Sandy beaches in estuaries and bays*. Elsevier Ltd.
- Vuik, V., Thonus, B., and Kramer, M. (2019). Houtribdijk monitoring and research program. Technical report, HKV. PR3916.10; draft report.
- Young, I. R. and Verhagen, L. A. (1996). The growth of fetch limited waves in water of finite depth. part 1: Total energy and peak frequency. *Coastal Engineering*, 29:47–78.
- Zijlema, M. (2020). University lecture slides CIE5315 computational hydraulics. July 2020.

VI

Appendices



Measuring Instruments and Available Data

This appendix discusses the measuring instruments and the available data. First the instruments and obtained data at the offshore measuring location FL66 are discussed in section A.1. This includes a small section on the KNMI data concerning wind data. Next the instruments and data needed for the morphodynamic analysis are discussed in section A.2.

A.1 FL 66 - Measuring Instruments

FL66 is one of the multiple offshore measuring stations in the Markermeer (figure 2.4) located near the Noordstrand. FL66 has the following measuring instruments:

- Step gauge - STB (Dutch: *Stappenbaak*)
- Acoustic Doppler Current Profiler - ADCP

A.1.1 Step gauge - STB

The step gauge measures the water level using electrodes placed every 5 centimeters over a 3 meter long shaft (Vuik et al., 2019). The high sampling frequency of 4 Hz means wave height and period can be obtained during the post-processing of the data. Processed output is available every 15 minutes.

Obtained data from step gauge:

1. Gregorian time - time of measurement
2. Frequency in Hz
3. Water level relative to NAP in meter
4. Significant wave height in meter - H_{m0}
5. Peak period in Hz - T_p
6. Wave period from m0 to m1 - T_{m01}
7. Wave period from m0 to m2 - T_{m02}
8. Wave period from m-1 to m0 - T_{mm10}

Errors and limitations

The main limitation of the step gauge data is the spacing between the electrodes. It only measures a change in water level if a next electrode is submerged or has fallen dry. This introduces a main error of 5 centimeter.

A.1.2 ADCP - Acoustic Doppler Current Profiler

An ADCP measures the flow at different locations over the vertical (Vuik et al., 2019). It can measure 24 vertical layers, positioned 0.25 meter apart. Averaged output is available every 10 minutes, using burst measurements (500 pings per ensemble).

Obtained data from ADCP:

- | | |
|---|--|
| 1. Gregorian time - time of measurement | 5. Velocity current in northern direction in m/s |
| 2. Layer levels | 6. Velocity current in eastern direction in m/s |
| 3. Elevation bottom lake (GPS during maintenance) | 7. Velocity current in upward direction in m/s |
| 4. Flow direction in degrees | 8. Water temperature in °C |

Errors and limitations

The ADCP has two main limitations. The instrument itself is placed on the bottom of the lake and the first 0.25 meter above the instrument cannot be measured. Second the instrument cannot measure velocities completely up to the water surface as this water level fluctuates under the influence of wind, set-up and waves. This can lead to a blank distance of almost a meter near the surface. Thus the ADCP provides data on the current in the middle of the water column, but lacks information at the bottom and top of the water column.

A.1.3 KNMI data - Houtribdijk

Wind data is collected by the KNMI (Royal Netherlands Meteorological Institute (KNMI), 2020). We are interested in station number 258, situated at the Houtribdijk and station Berkhout (station number 274). Output is available every hour.

The following data is available

- | | |
|---|---|
| 1. Mean wind direction (in degrees from North) - DD | 3. Mean wind speed (in 0.1 m/s) during previous 10 minutes - FF |
| 2. Hourly mean wind speed (in 0.1 m/s) - FH | 4. Maximum wind gust (in 0.1 m/s) during the hourly division - FX |

A.2 GPS - Measuring Instruments

Elevation measurements used for the morphodynamic analysis are obtained in three different ways. The availability of this data differs and is summarised in table A.1.

- Meteor boat - bathymetry
- Sirius drone - topography
- Transects at beach - GPS using Leica GNS 14 all-in-one

A.2.1 Bathymetry and topography

Bathymetry and topography data are provided every three months by Boskalis. Topography data obtained by an unmanned aerial vehicle (Sirius drone) includes measurements of the higher part of the beach: upper beach face and dunes (Boskalis Nederland, 2021). Bathymetry measurements up to a water depth of approximately 1 meter are obtained by a smaller boat. Data around the waterline is obtained by additional measurements (see next paragraph).

A.2.2 Leica GNS 14 All-in-one

Additional measurements around the waterline are obtained by surveyors either from Boskalis or researchers from Delft University. Field campaigns have used the Leica GS 14 all-in-one or an equivalent GNSS device, providing elevation data with an accuracy of at least 0.10 meter. These datasets include information on the error. This information is used during raw data processing.

KIMA section

The middle of the Noordstrand, from 600 to 800 horizontal meters from the reference point, right is front of FL66 is part of the KIMA sections. This means this part of the beach is observed in more detail, at this location 20 meter transect are measured every 3 months.

Table A.1: Overview when data concerning elevation was obtained; split into bathymetry, topography and GPS measurements.

Period	Bathymetry (Multibeam)	Topography (Drone)	GPS transects	Notes
2018 Q3	July 2018	July 2018	July 2018	Transects GPS; 17 in middle: 10m
2018 Q4	January 2019	January 2019	January 2019	Transects GPS; 17 in middle: 10m
2019 Q1	April 2019	May 2019	June 2019	Transects GPS; 7 in middle 20 m; 2 transects more to left
2019 Q2	August 2019	July 2019	-	
2019 Q3	October 2019	October 2019	Sep 2019	Transects GPS; 13 over total beach: 100m; 9 in middle: 20m
2019 Q4	January 2020	January 2020	January 2020	Transects GPS; 9 in middle: 20m
2020 Q1	April 2020	April 2020	April 2020	Transects GPS; 13 over total beach: 100m; 9 in middle: 20m
2020 Q2	July 2020	July 2020	July 2020	Transects GPS; 9 in middle: 20m
2020 Q3	November 2020	November 2020	-	(GPS available of Zuidstrand)
2020 Q4	-	-	December 2020	Own GPS measurements: 25 over total beach: 50m
2021 Jan	-	-	January 2020	Own GPS measurements: 25 over total beach: 50m
2021 Mrt	-	-	March 2020	Own GPS measurements: 25 over total beach: 50m

B

Data Analysis: Hydrodynamics

This appendix provides additional information on the data analysis discussed in chapter 6. It is similarly split into a data-processing part, section B.1, showing additional graphs for chapter 5. Then a general part, section B.2, showing two overviews of the used rose and derived directions in the vicinity of the entire Marker Wadden and Markermeer. Third, additional wind and current roses around and at peak events are introduced in section B.2. Fourth, the results of all individually analysed high-energy events and calm periods are shown in section B.4. Two alternative methods to find peak events, based on water level fluctuations at FL66 and the comparison between water levels at FL66 and FL67, are discussed in the last section, section B.5.

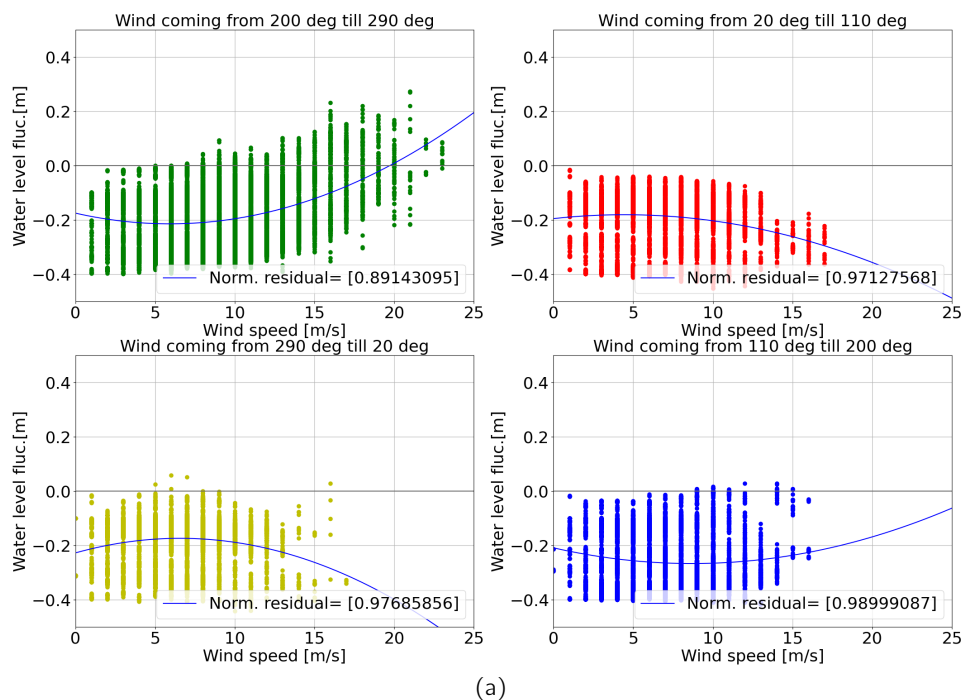
B.1 Data-processing

This section shows the two additional plots in which water level data is fitted to a second order polynomial. Figure B.1a shows the fit using water level relative to NAP. For the fit in figure B.1b the difference in water level at FL66 and FL67 is computed, this results in information on set-up/down levels relative to the Houtribdijk (located in north-eastern direction of the Noordstrand).

B.2 General

Two additional plots showing the rose with directions in the context of the Marker Wadden and Markermeer. Figure B.2a shows the hard edge in the bottom left corner and the sandy edge in the top right. When looking at figure B.2b one can see the same direction plot, but now with respect to the Houtribdijk. FL67, used to investigate the amount of set-up/down over the Markermeer is located in front of the yellow pin 'Houtribdijk'.

Comparing wind conditions and water level relative to NAP



Comparing wind conditions and Set-up or set-down compared with HRD (FL67)

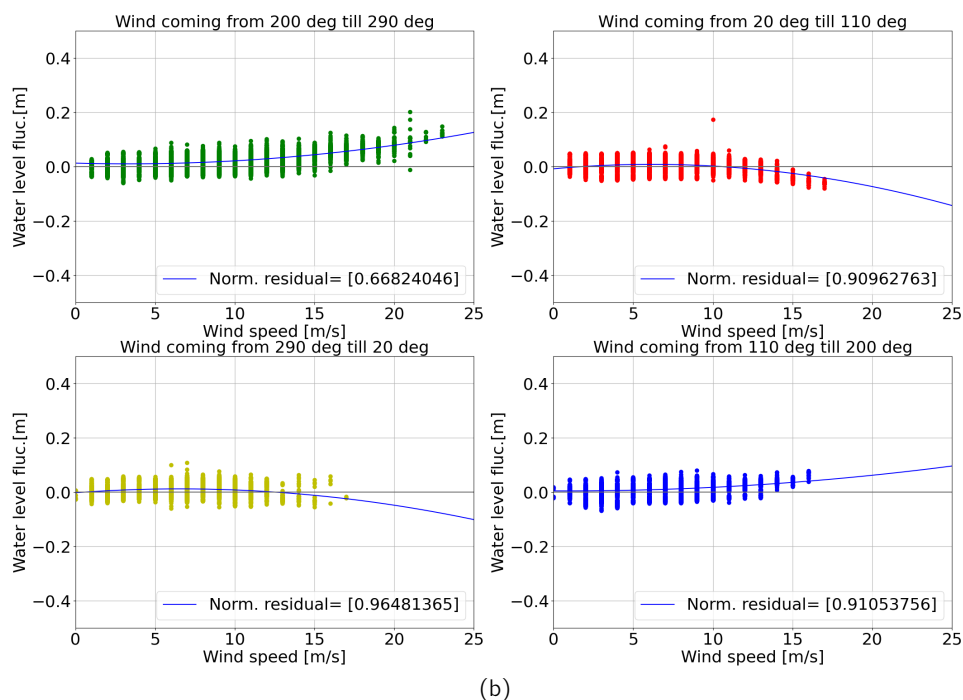
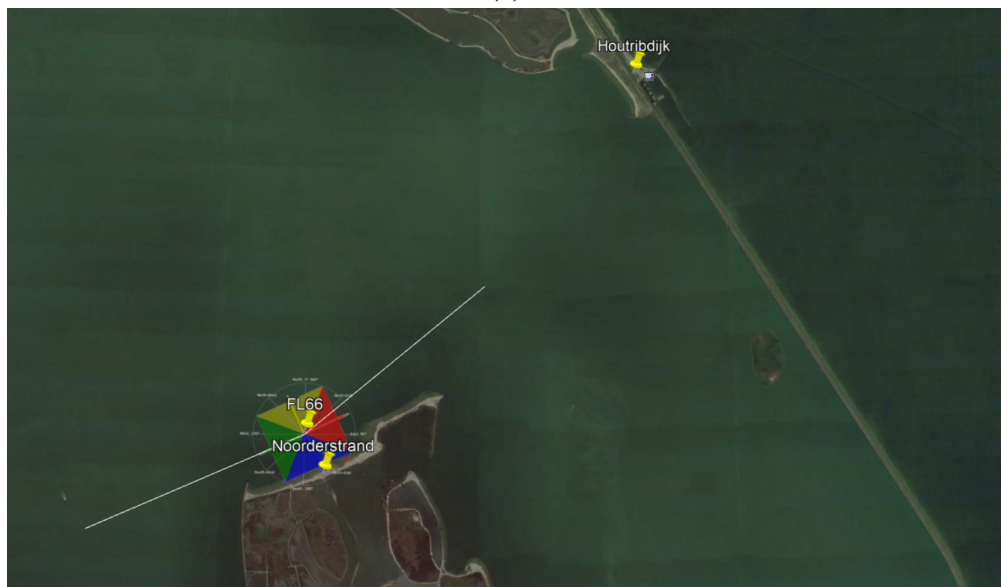


Figure B.1: Two figures showing: (a) Hourly averaged wind speed versus water level relative to NAP; (b) Hourly averaged wind speed versus water level difference between FL66 and FL67. Each figure showing four different plots, each representing a different segment based on wind direction (see figure 6.1). A second order polynomial (blue line) is plot through the datapoints and the normalised residual of the least squares method is shown in the lower right. The closer to zero, the better the fit of the polynomial to the data.



(a)



(b)

Figure B.2: General direction roses: (a) Rose with direction classification used in the hydrodynamic analysis of wind and current, shown on top of a Google Earth image of the Noordstrand; (b) Same rose now shown on top of a Google Earth image of the Markermeer. In the top right corner the Houtribdijk is visible. The two prolonged white lines show the main direction of wind and current as found in the hydrodynamic analysis (section 6.1.4, namely 50 and 245 degrees).

B.3 High-Energy Events - General

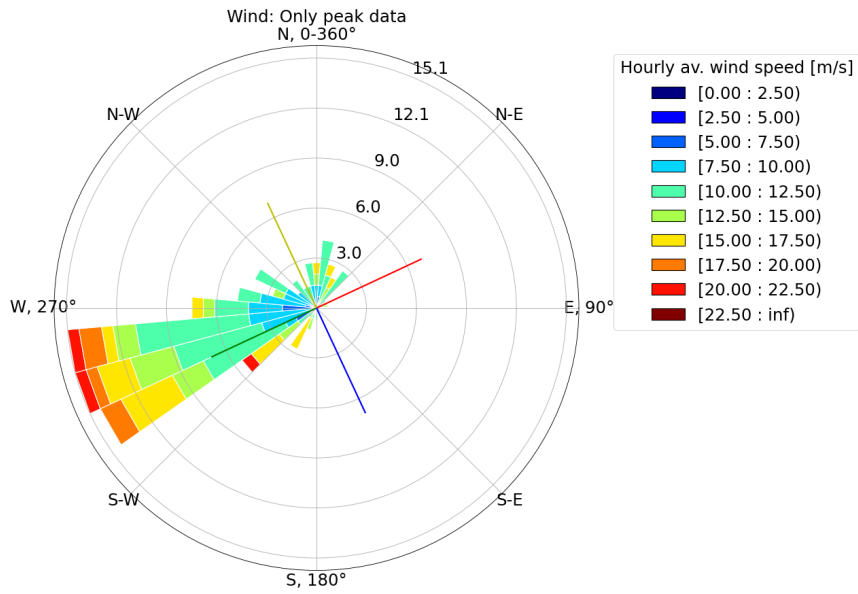
This section includes the additional graphs concerning high-energy events in general, closer investigation of individual events are discussed later.

B.3.1 *Wind roses*

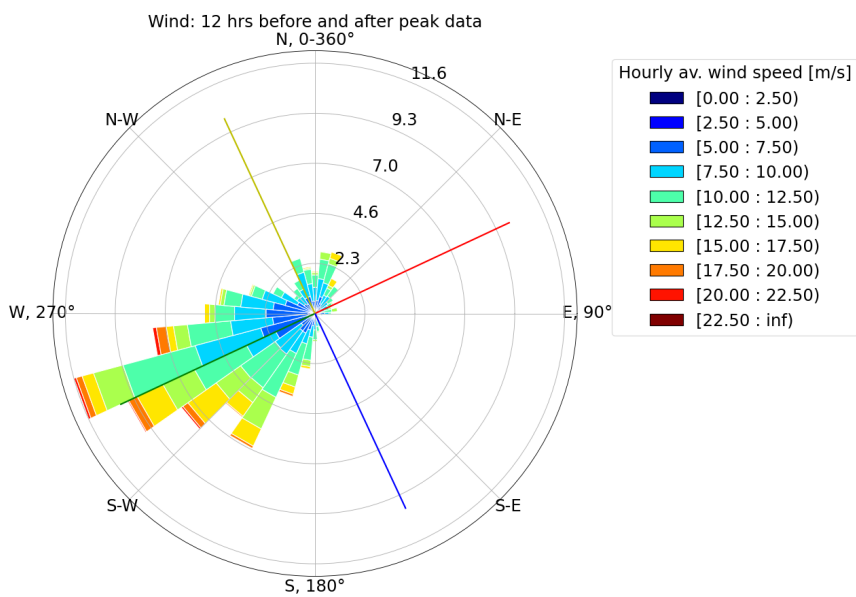
Plot B.3a and plot B.3b shows the computed wind roses for the peak data and 12 hours before and after these peaks respectively. The peaks are identified using the peak-over-threshold method as described in section 5.2.2, based on significant wave height.

B.3.2 *Current roses*

Plot B.4a and plot B.4b shows the computed current roses for the peak data and 12 hours before and after these peaks respectively. The peaks are identified using the peak-over-threshold method as described in section 5.2.2, based on significant wave height.

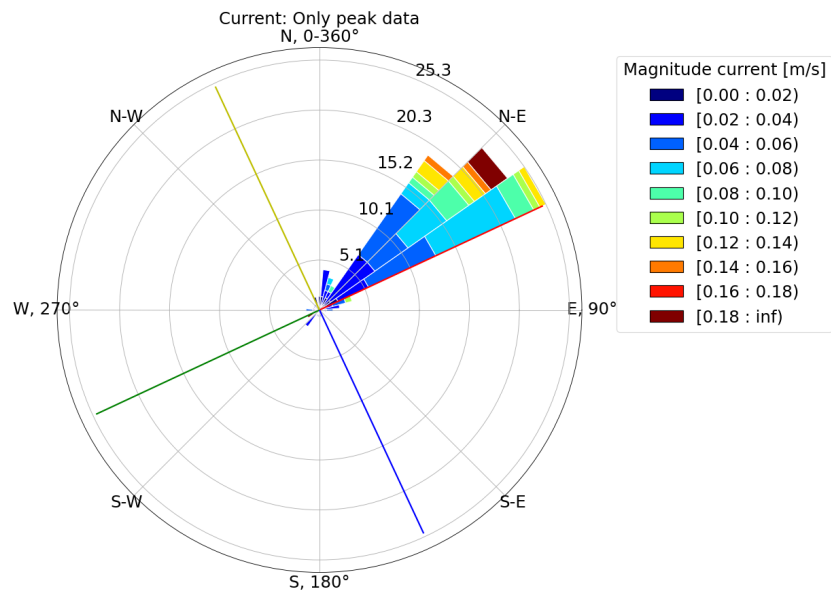


(a)

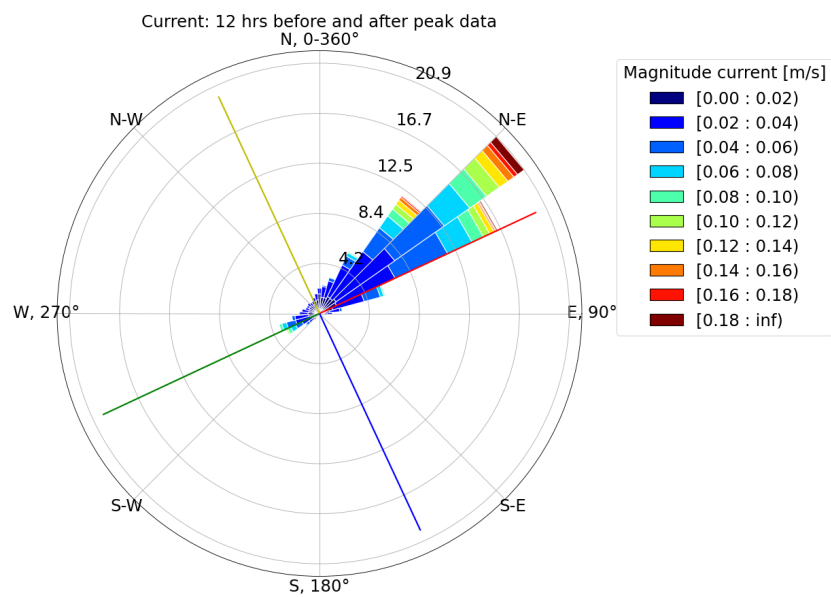


(b)

Figure B.3: Wind roses: (a) At high-energy (peak) even; (b) At 12 hours before and after high-energy (peak) event. The colours of the bars indicate the hourly average wind speed in m/s. The bars are normalised, meaning the length of the bar corresponds to the relative frequency of occurrence. The angle is the direction the wind is coming from.



(a)



(b)

Figure B.4: Current roses: (a) At high-energy (peak) even; (b) At 12 hours before and after high-energy (peak) event. The four coloured lines correspond to the different directions (figure 6.1). The colours of the bars indicate the depth-averaged current magnitude in m/s. The bars are normalised, meaning the length of the bar corresponds to the relative frequency of occurrence. The angle is the direction the current is *coming from*.

B.4 High-Energy Events - Individual Events

This section includes additional information on the individually analysed high-energy events. A summary of the considered events is presented in table 5.2.

B.4.1 *High-energy event: 7 - 19 February 2020*

This high-energy event includes the storms Ciara and Dennis and is used as a representation of what happens during high-energy events at the Noordstrand (section 6.2.2 of the main document). The general overview plot is shown in figure 6.11.

FL66: Events from 2020-02-07 00:00:00 till 2020-02-19 00:00:00

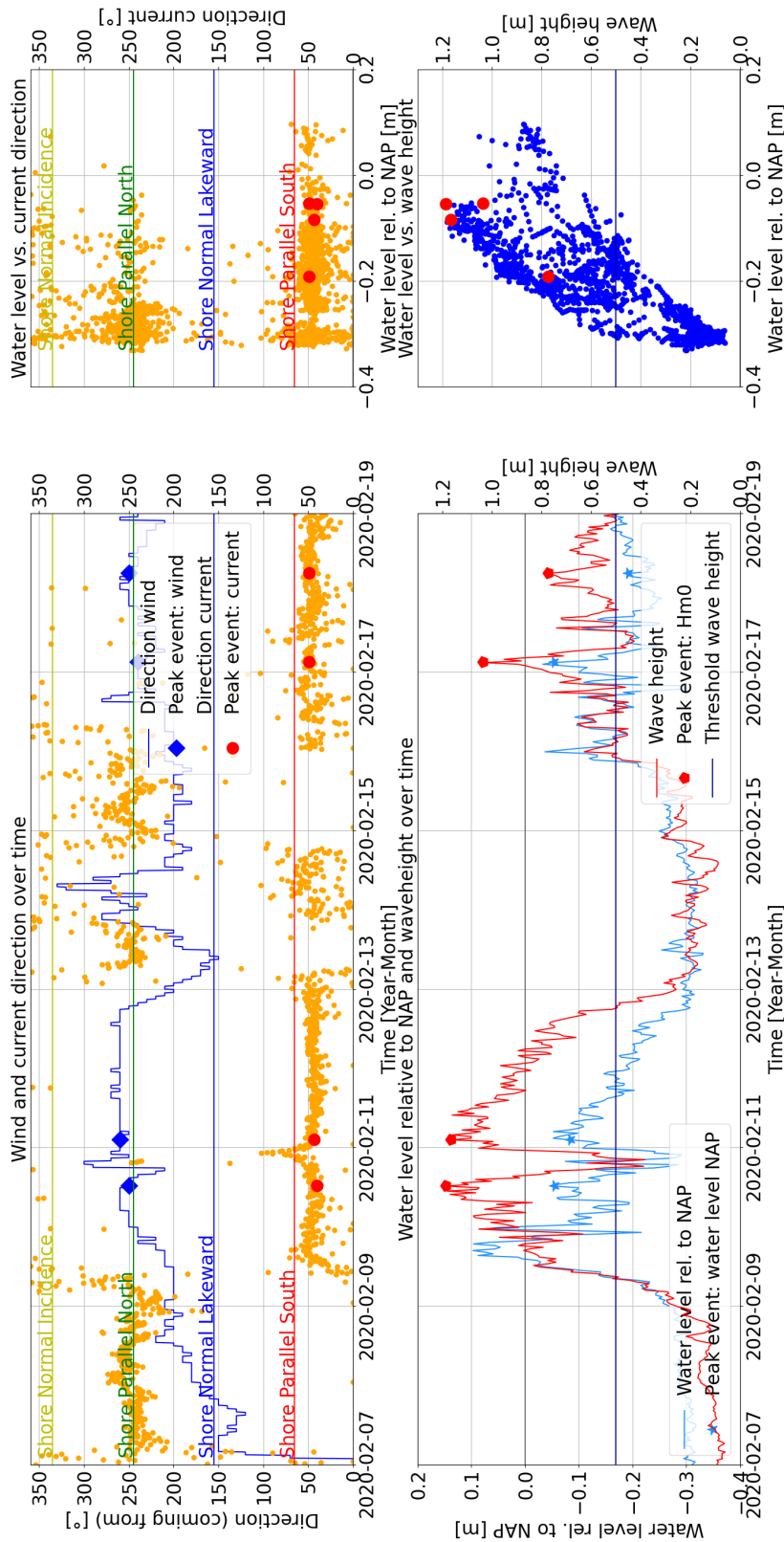


Figure B.5: **7 - 19 February 2020**; Left side: time series of wind, current, wave and water level relative to NAP versus direction current (coming from). Bottom right: water level relative to NAP versus wave height. Peak events are the categorised high-energy events. Top two figures include four coloured horizontal lines linked to the categorisation of four directions relative to the Noordstrand shoreline orientation (figure 6.1).

FL66: Events from 2020-02-07 00:00:00 till 2020-02-19 00:00:00

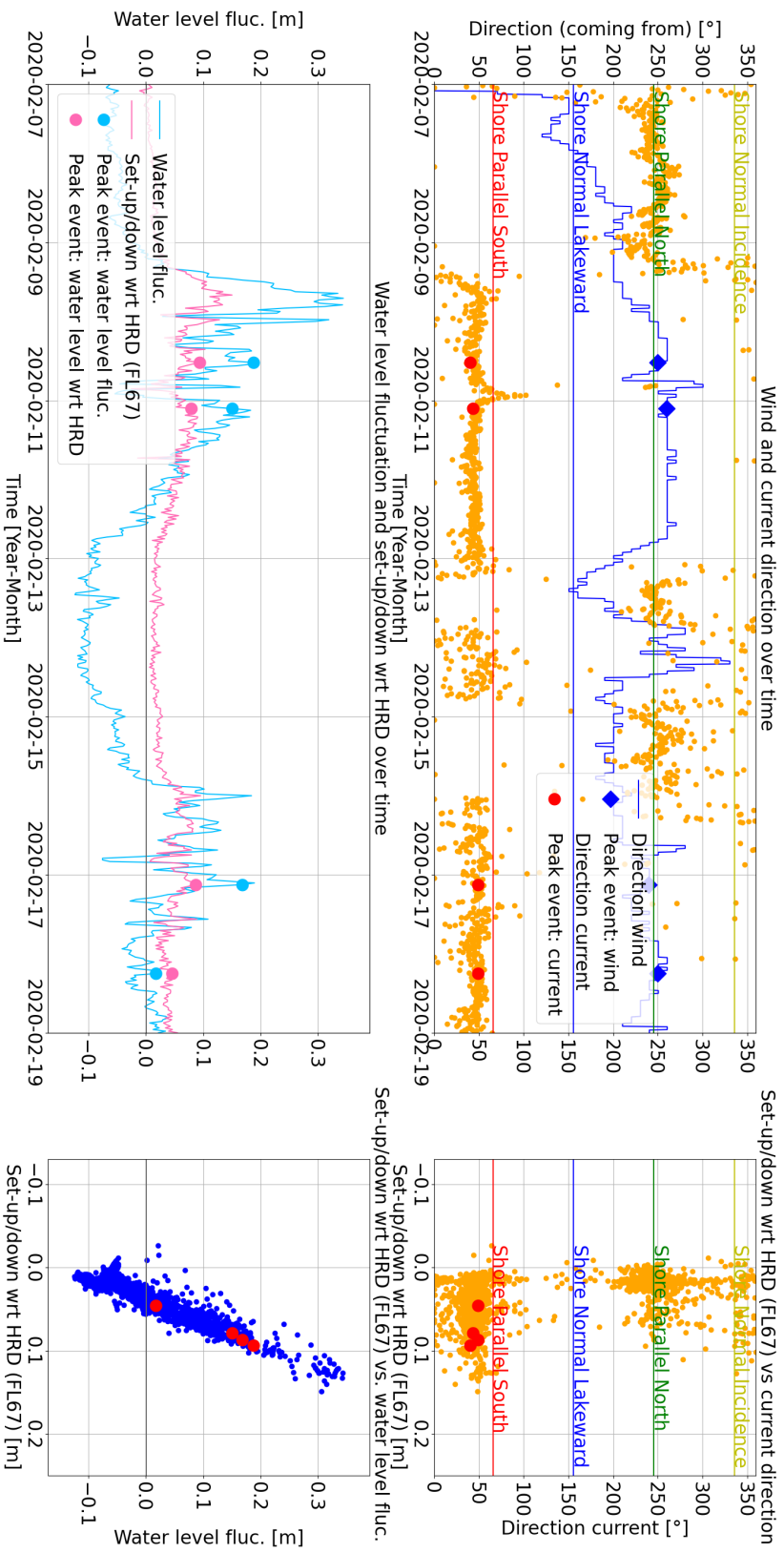


Figure B.6: **7 - 19 February 2020**. Left side: time series of wind, current, water level fluctuations at FL 66 and set-up/down with respect to FL67 (Houtribdijk). Top right: set-up/down with respect to FL67 versus direction current (coming from). Bottom right: set-up/down with respect to FL67 versus water level fluctuation at FL66. Peak events are the categorised high-energy events. Top two figures include four coloured horizontal lines linked to the categorisation of four directions relative to the Noordstrand shoreline orientation (figure 6.1).

FL66: Events (linking wind and current) from 2020-02-07 00:00:00 till 2020-02-19 00:00:00

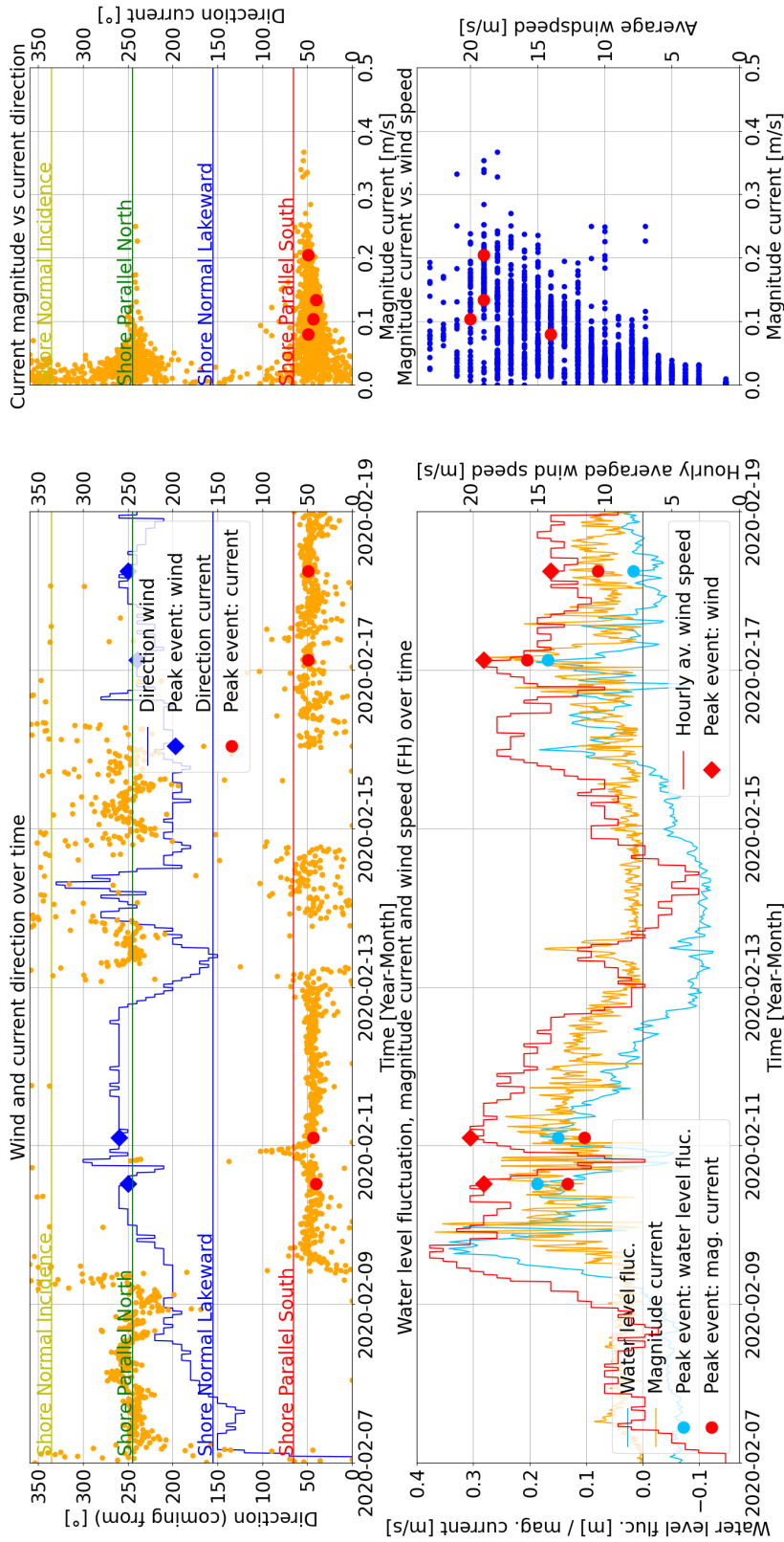


Figure B.7: **7 - 19 February 2020**; Top left: time series of wind and current direction (coming from). Bottom left: time series of water level fluctuation, magnitude current and the hourly averaged wind speed. Top right: magnitude current versus direction current (coming from). Bottom right: magnitude current versus average wind speed. Peak events are the categorised high-energy events. Top two figures include four coloured horizontal lines linked to the categorisation of four directions relative to the Noordstrand shoreline orientation (figure 6.1).

B.4.2 High-energy event: 6 - 13 June 2019

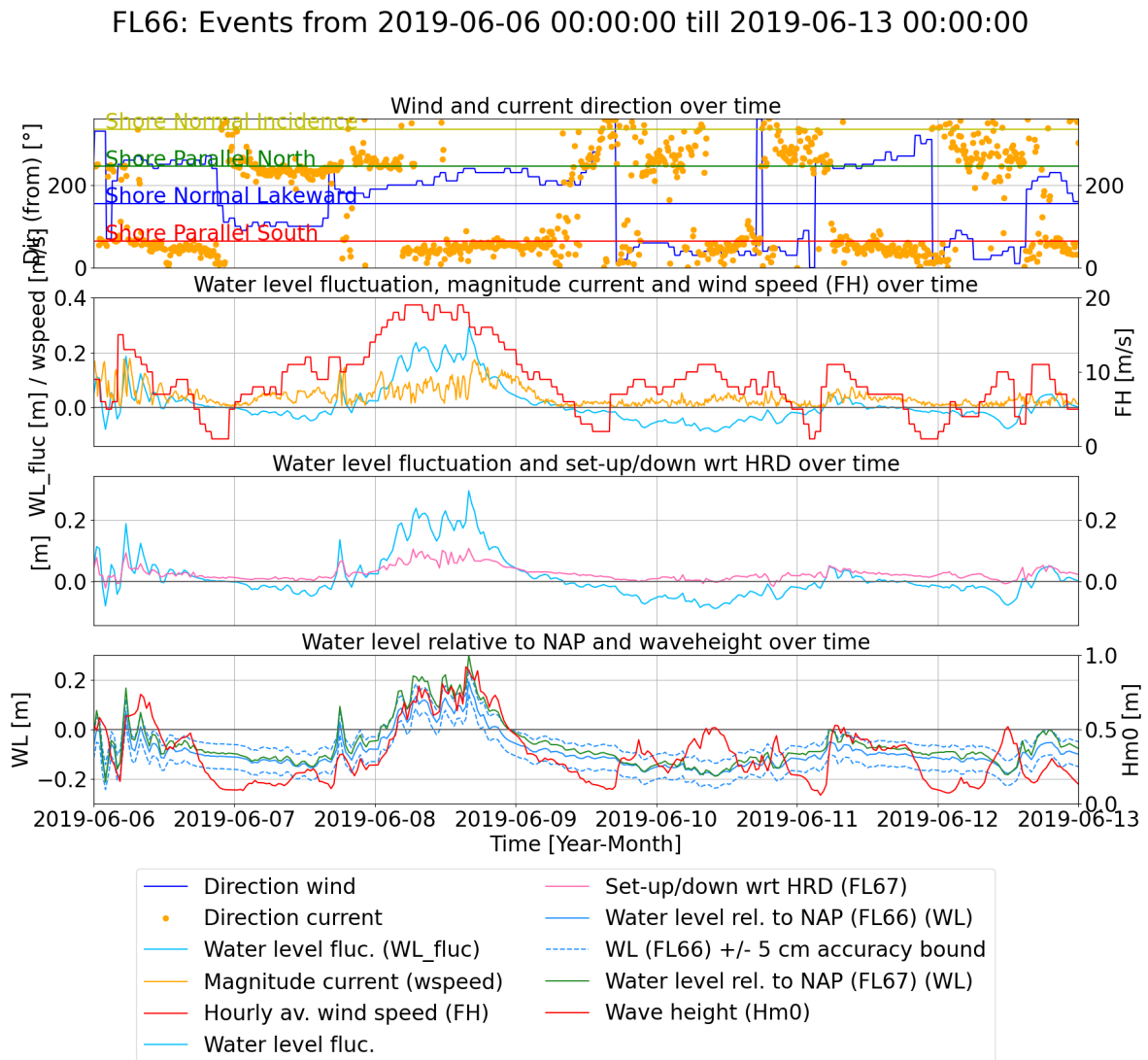


Figure B.8: **6 - 13 June 2019**; overview plot of all conditions. From top to bottom: 1) Wind and current direction (coming from), coloured vertical lines link to directions as specified in figure 6.1. 2) Water level fluctuations at FL66, magnitude current and hourly averaged wind speed. 3) Water level fluctuations at FL66 (obtained by removing 10-day average water level) and set-up/down compared with FL67 (Houtribdijk). 4) Water level relative to NAP at FL66 and its 5 cm accuracy bounds, water level relative to NAP at FL67 and wave height.

FL66: Events from 2019-06-06 00:00:00 till 2019-06-13 00:00:00

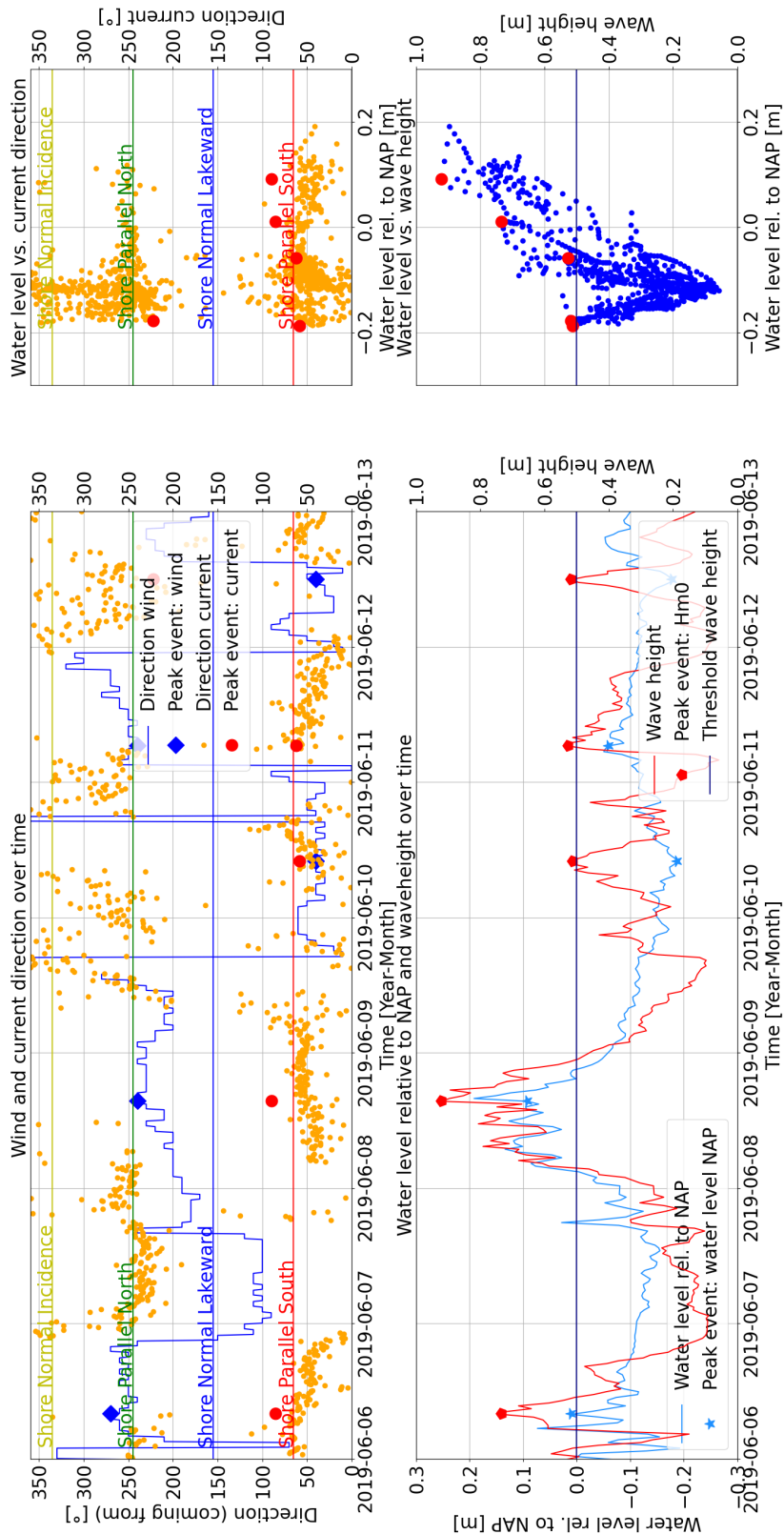


Figure B.9: **6 - 13 June 2019**, Left side: time series of wind, current, wave and water level conditions. Top right: water level relative to NAP versus direction current (coming from). Bottom right: water level relative to NAP versus wave height. Peak events are the categorised high-energy events. Top two figures include four coloured horizontal lines linked to the categorisation of four directions relative to the Noordstrand shoreline orientation (figure 6.1).

FL66: Events from 2019-06-06 00:00:00 till 2019-06-13 00:00:00

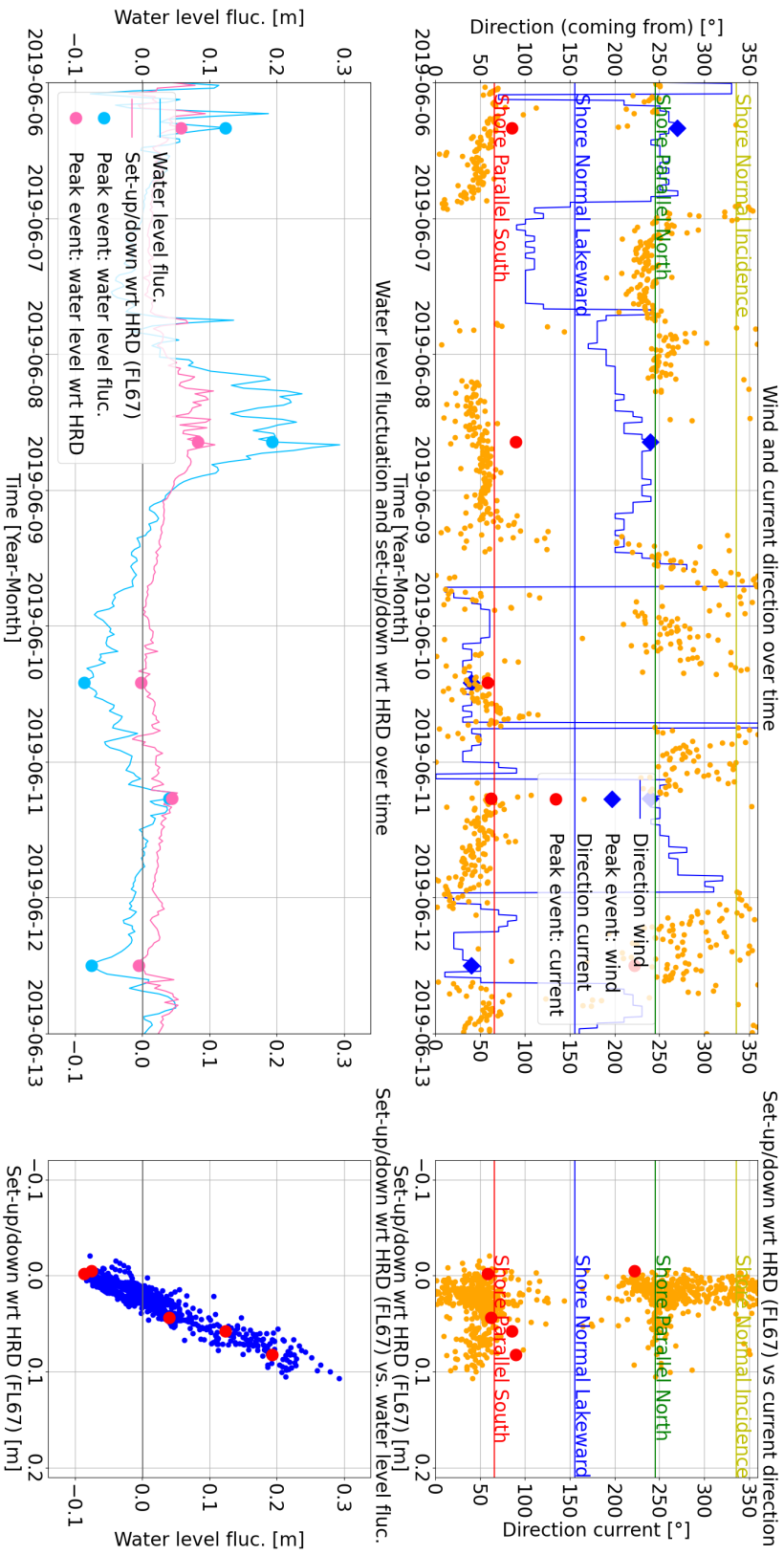


Figure B.10: **6 - 13 June 2019**. Left side: time series of wind, current, water level fluctuations at FL 66 and set-up/down compared with FL67 (Houtribdijk). Top right: set-up/down with respect to FL67 versus direction current (coming from). Bottom right: set-up/down with respect to FL67 versus water level fluctuation at FL66. Peak events are the categorised high-energy events. Top two figures include four coloured horizontal lines linked to the categorisation of four directions relative to the Noordstrand shoreline orientation (figure 6.1).

FL66: Events (linking wind and current) from 2019-06-06 00:00:00 till 2019-06-13 00:00:00

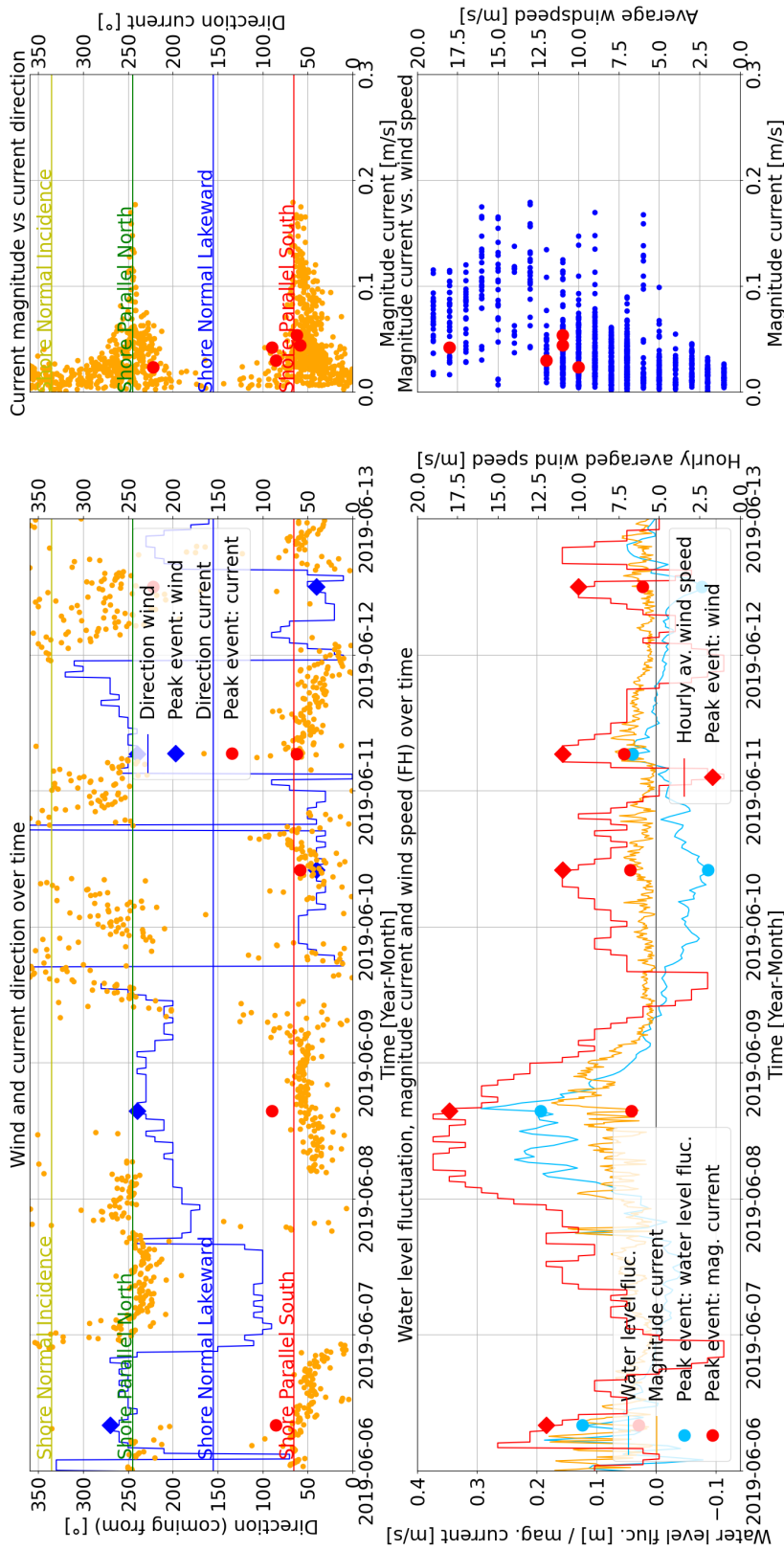


Figure B.11: **6 - 13 June 2019**; Top left: time series of wind and current direction (coming from). Bottom left: time series of water level fluctuation, magnitude current and the hourly averaged wind speed. Top right: magnitude current versus direction current (coming from). Bottom right: magnitude current versus average wind speed. Peak events are the categorised high-energy events. Top two figures include four coloured horizontal lines linked to the categorisation of four directions relative to the Noordstrand shoreline orientation (figure 6.1).

B.4.3 High-energy event: 24 - 30 August 2020

FL66: Events from 2020-08-24 00:00:00 till 2020-08-30 00:00:00

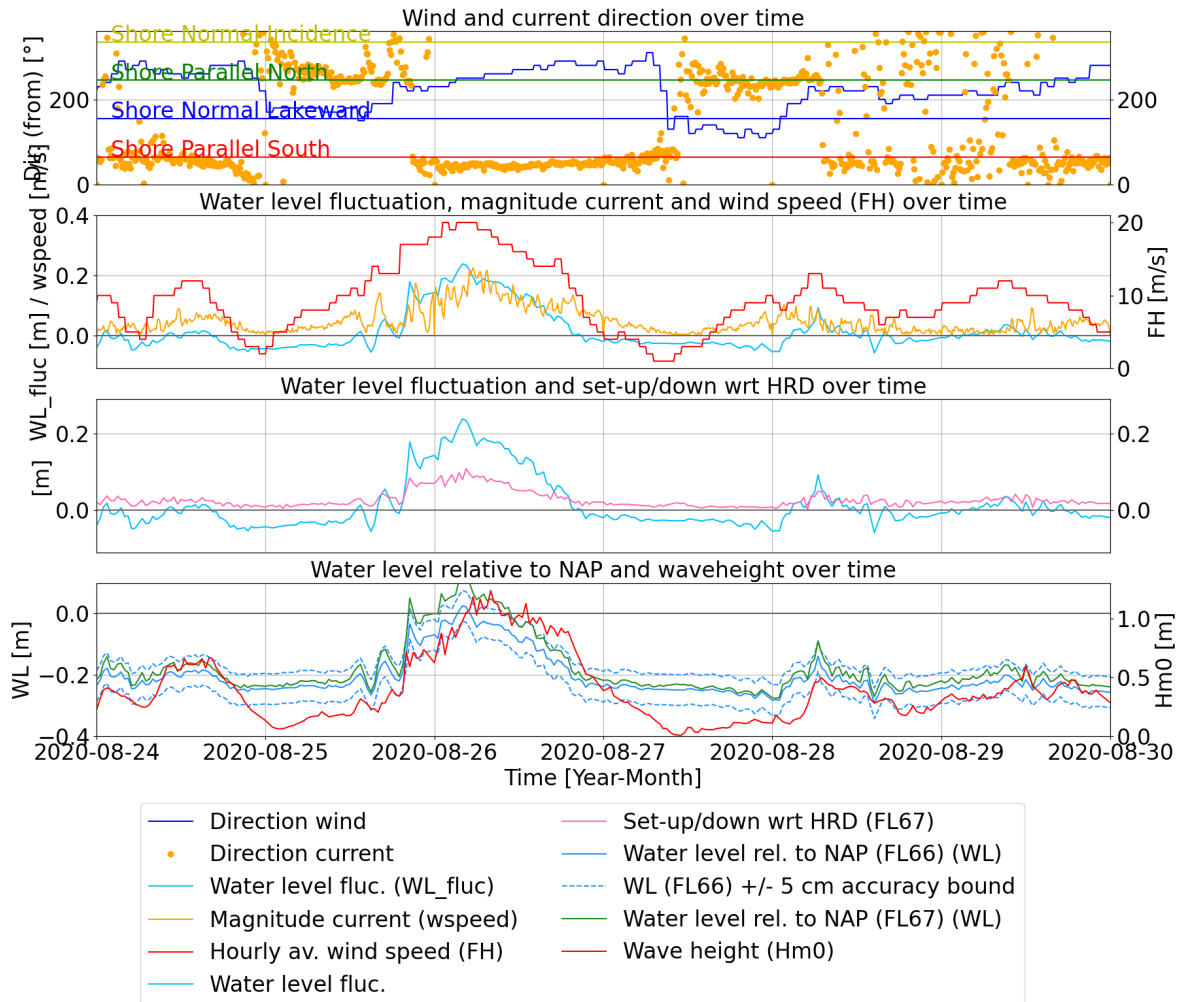


Figure B.12: **24 - 30 August 2020**; overview plot of all conditions. From top to bottom: 1) Wind and current direction (coming from), coloured vertical lines link to directions as specified in figure 6.1. 2) Water level fluctuations at FL66, magnitude current and hourly averaged wind speed. 3) Water level fluctuations at FL66 (obtained by removing 10-day average water level) and set-up/down compared with FL67 (Houtribdijk). 4) Water level relative to NAP at FL66 and its 5 cm accuracy bounds, water level relative to NAP at FL67 and wave height.

FL66: Events from 2020-08-24 00:00:00 till 2020-08-30 00:00:00

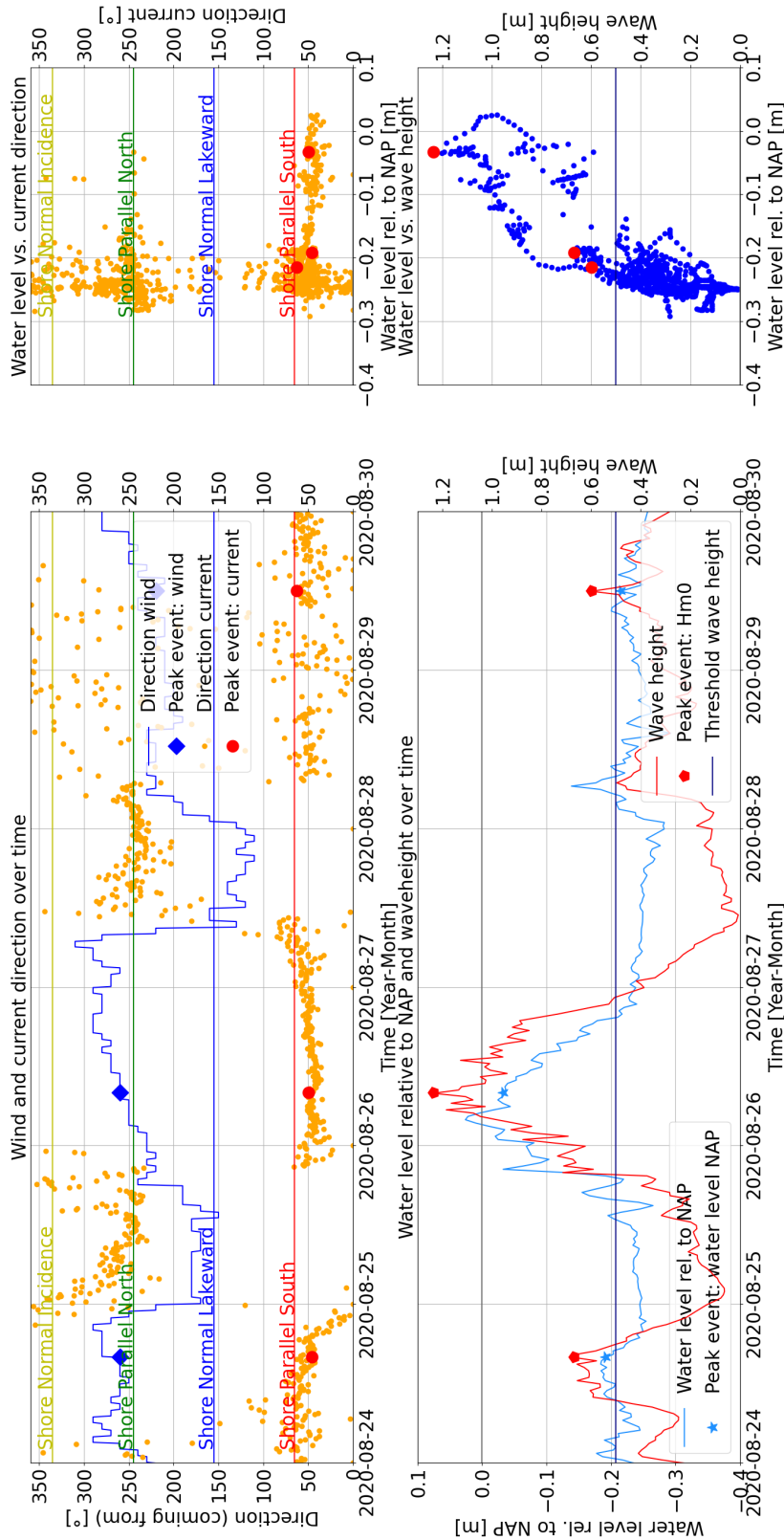


Figure B.13: **24 - 30 August 2020**; Left side: time series of wind, current, wave and water level conditions. Top right: water level relative to NAP versus direction current (coming from). Bottom right: water level relative to NAP versus wave height. Peak events are the categorised high-energy events. Top two figures include four coloured horizontal lines linked to the categorisation of four directions relative to the Noordstrand shoreline orientation (figure 6.1).

FL66: Events from 2020-08-24 00:00:00 till 2020-08-30 00:00:00

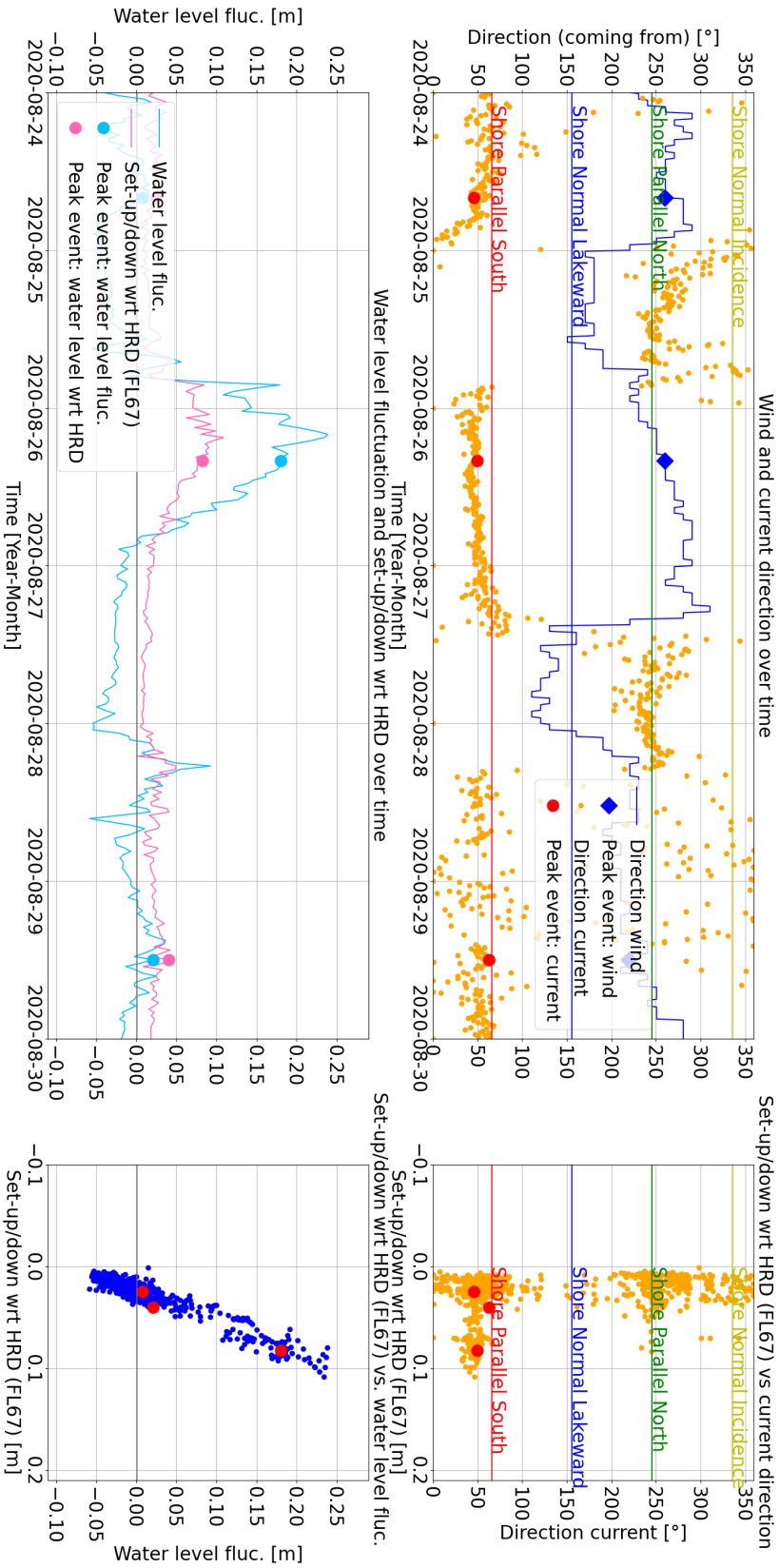


Figure B.14: **24 - 30 August 2020**: Left side: time series of wind, current, water level fluctuations at FL 66 and set-up/down compared with FL67 (Houtribdijk). Top right: set-up/down with respect to FL67 versus direction current (coming from). Bottom right: set-up/down with respect to FL67 versus water level fluctuation at FL66. Peak events are the categorised high-energy events. Top two figures include four coloured horizontal lines linked to the categorisation of four directions relative to the Noordstrand shoreline orientation (figure 6.1).

FL66: Events (linking wind and current) from 2020-08-24 00:00:00 till 2020-08-30 00:00:00

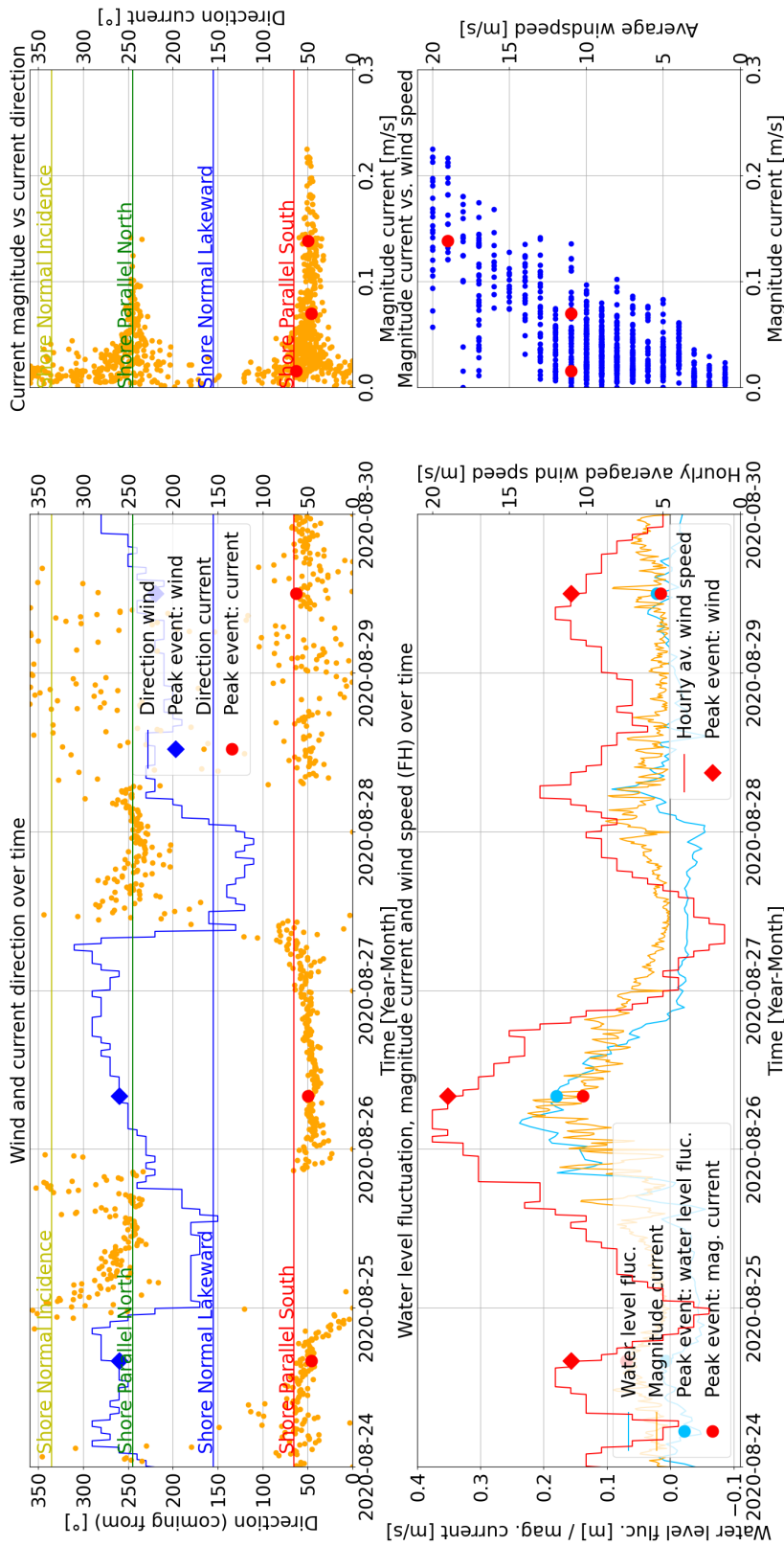


Figure B.15: **24 - 30 August 2020**; Top left: time series of wind and current direction (coming from). Bottom left: time series of water level fluctuation, magnitude current and the hourly averaged wind speed. Top right: magnitude current versus direction current (coming from). Bottom right: magnitude current versus average wind speed. Peak events are the categorised high-energy events. Top two figures include four coloured horizontal lines linked to the categorisation of four directions relative to the Noordstrand shoreline orientation (figure 6.1).

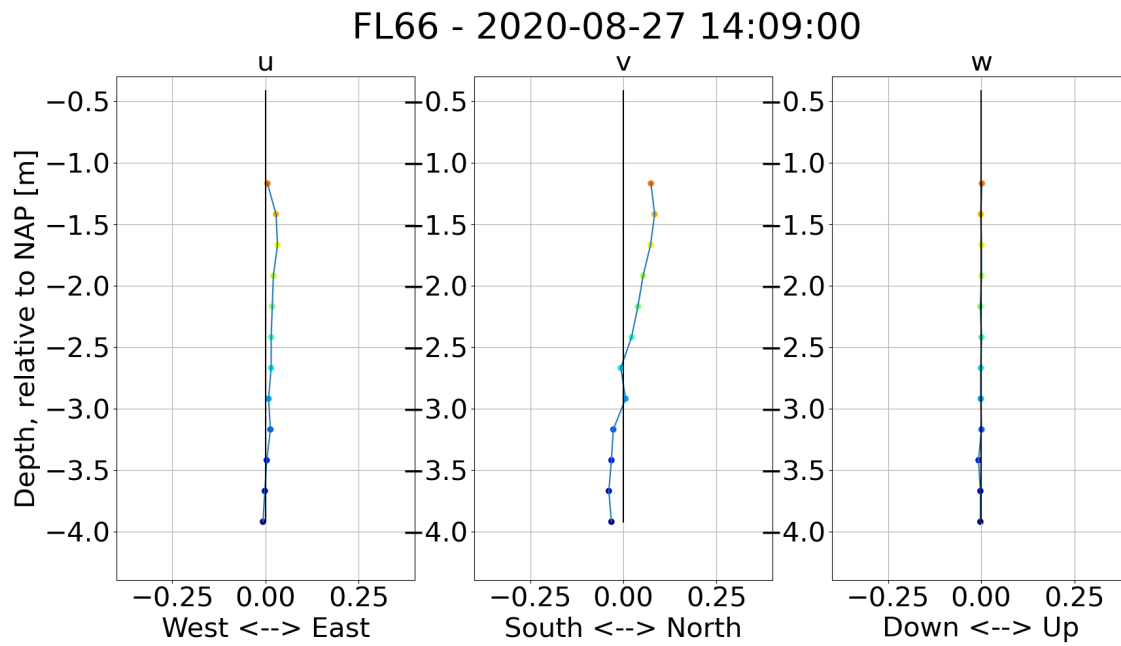


Figure B.16: Current profile over depth, showing current magnitude in the three main directions in three different plots. The coloured dots indicate the layer levels as measured by the ADCP. The bottom of the graphs indicate the bottom level of the lake. The top of the graphs indicate the elevation of the water level. Shortcomings of the ADCP measurements near the bottom and surface are discussed in more detail in section A.1.2. *Data-processing script courtesy of Anne Ton*

B.4.4 Calm period: 5 - 12 April 2020

FL66: Events from 2020-04-05 00:00:00 till 2020-04-12 00:00:00

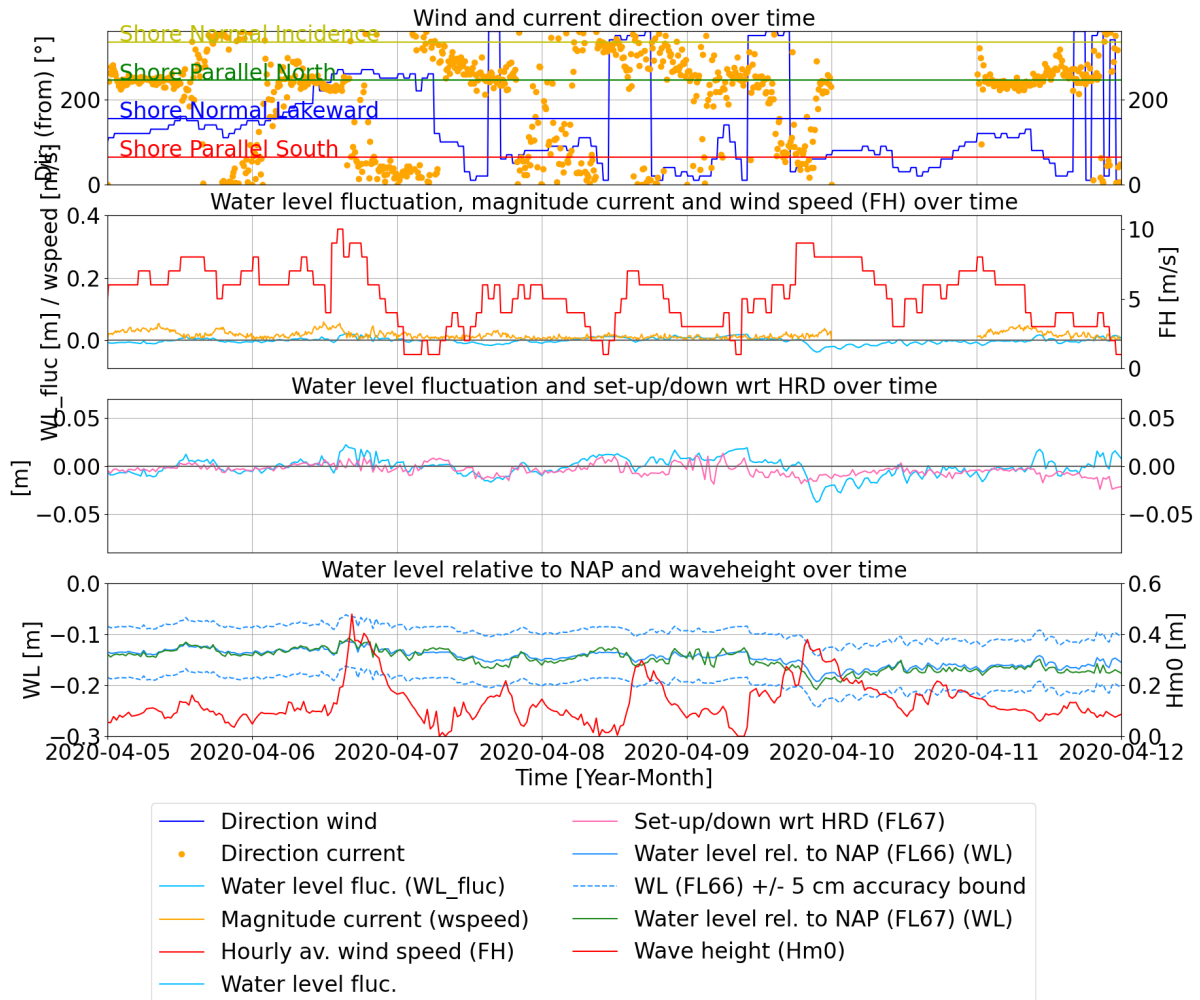


Figure B.17: **5 - 12 April 2020**; overview plot of all conditions. From top to bottom: 1) Wind and current direction (coming from), coloured vertical lines link to directions as specified in figure 6.1. 2) Water level fluctuations at FL66, magnitude current and hourly averaged wind speed. 3) Water level fluctuations at FL66 (obtained by removing 10-day average water level) and set-up/down compared with FL67 (Houtribdijk). 4) Water level relative to NAP at FL66 and its 5 cm accuracy bounds, water level relative to NAP at FL67 and wave height.

FL66: Events from 2020-04-05 00:00:00 till 2020-04-12 00:00:00

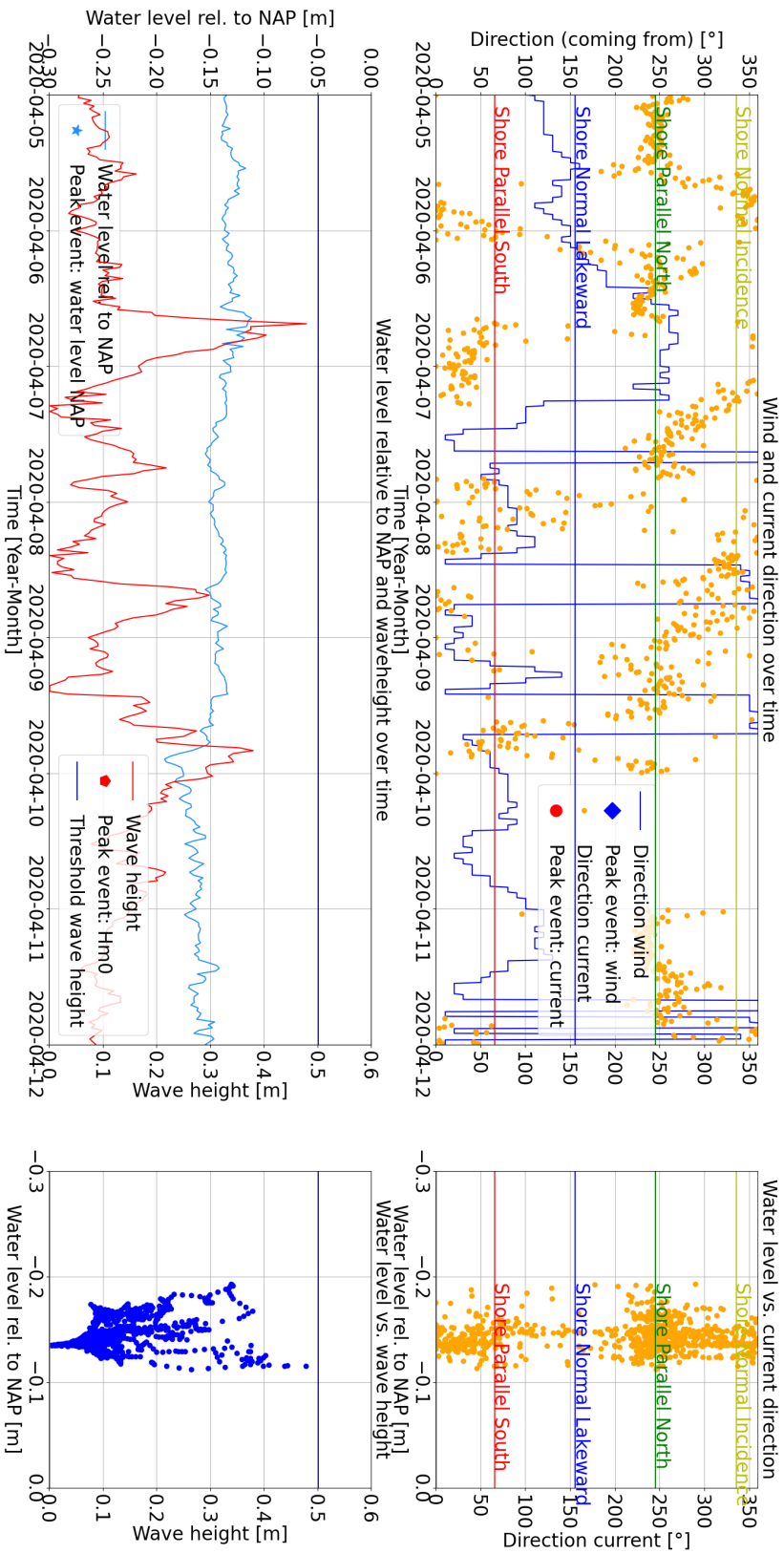


Figure B.18: **5 - 12 April 2020**: Left side: time series of wind, current, wave and water level conditions. Top right: water level relative to NAP versus direction current (coming from). Bottom right: water level relative to NAP versus wave height. Top two figures include four coloured horizontal lines linked to the categorisation of four directions relative to the Noordstrand shoreline orientation (figure 6.1).

FL66: Events from 2020-04-05 00:00:00 till 2020-04-12 00:00:00

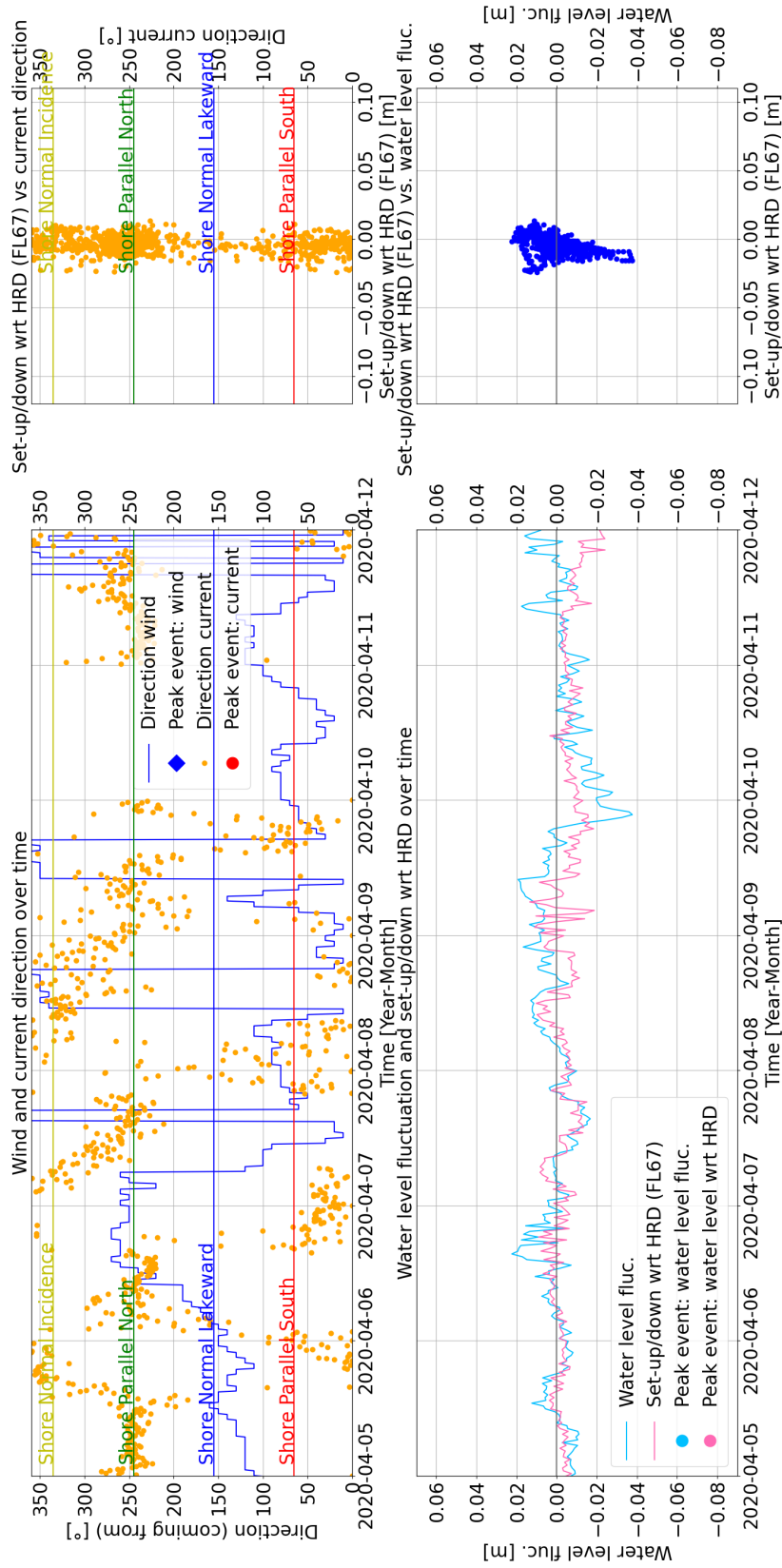


Figure B.19: **5 - 12 April 2020**: Left side: time series of wind, current, water level fluctuations at FL 66 and set-up/down compared with FL67 (Houtribdijk). Top right: set-up/down with respect to FL67 versus direction current (coming from). Bottom right: set-up/down with respect to FL67 versus water level fluctuation at FL66. Top two figures include four coloured horizontal lines linked to the categorisation of four directions relative to the Noordstrand shoreline orientation (figure 6.1).

FL66: Events (linking wind and current) from 2020-04-05 00:00:00 till 2020-04-12 00:00:00

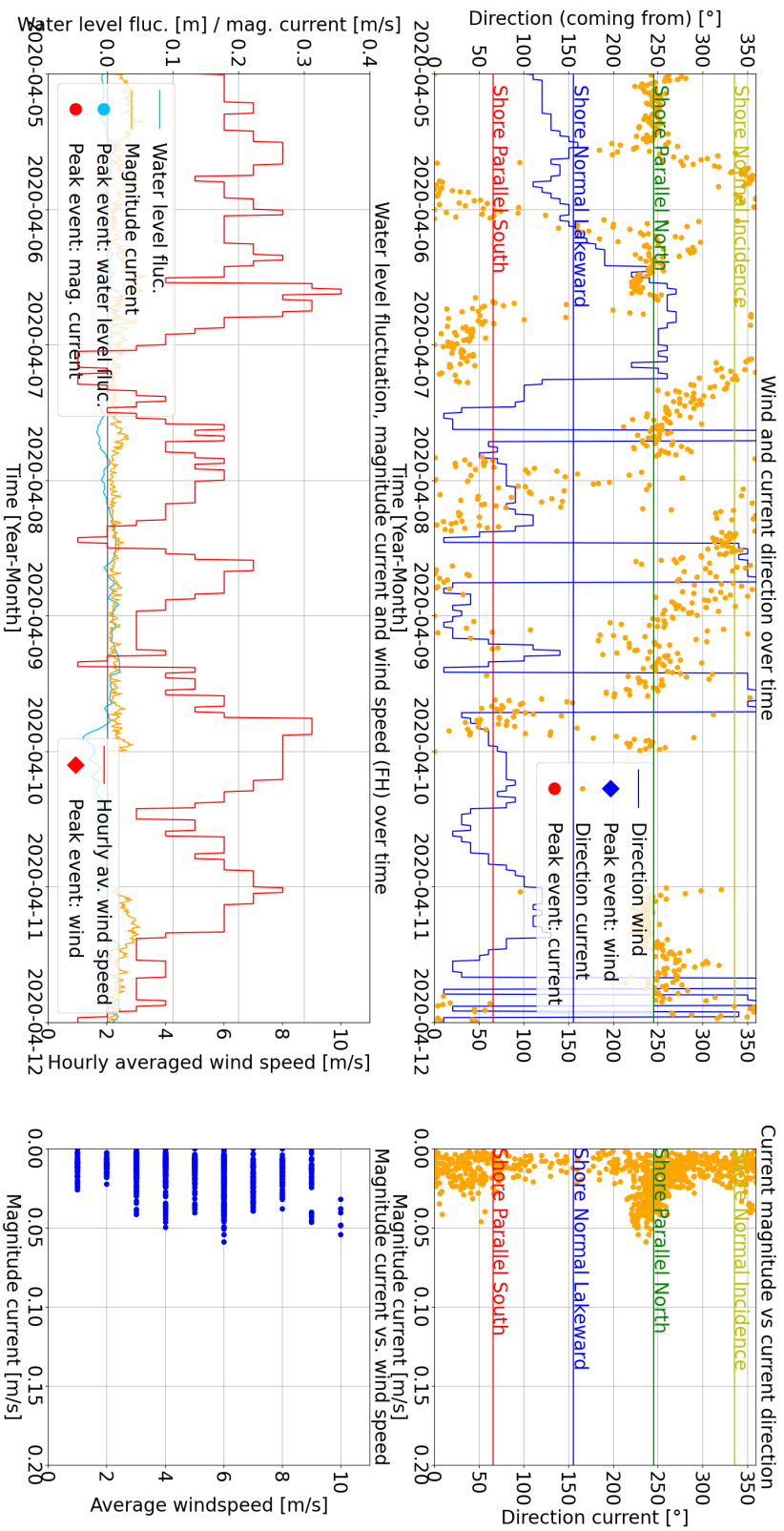


Figure B.20: **5 - 12 April 2020.** Top left: time series of wind and current direction (coming from). Bottom left: time series of water level fluctuation, magnitude current and the hourly averaged wind speed. Top right: magnitude current versus direction current (coming from). Bottom right: magnitude current versus average wind speed. Top two figures include four coloured horizontal lines linked to the categorisation of four directions relative to the Noordstrand shoreline orientation (figure 6.1).

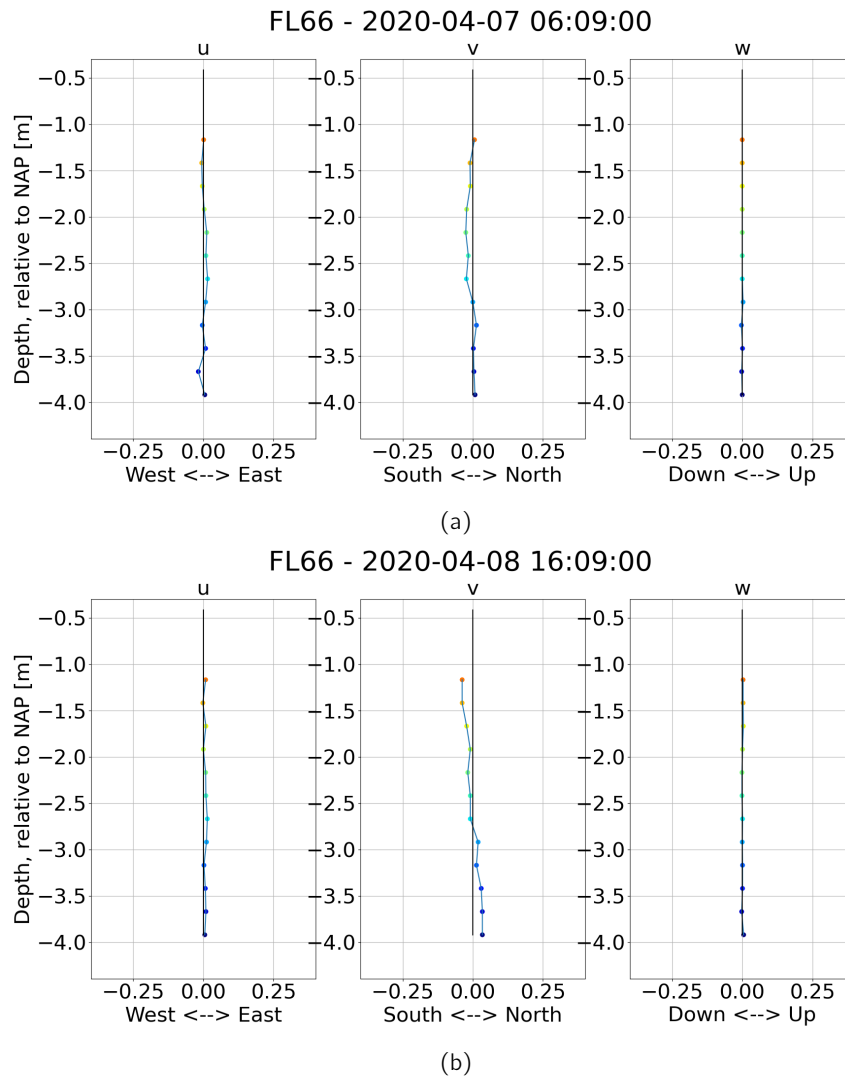


Figure B.21: Current profile over depth, showing current magnitude in the three main directions in three different plots. The coloured dots indicate the layer levels as measured by the ADCP. The bottom of the graphs indicate the bottom level of the lake. The top of the graphs indicate the elevation of the water level. Shortcomings of the ADCP measurements near the bottom and surface are discussed in more detail in section A.1.2. (a) Current profile over depth at 7 April 2020, 06:09:00; Current is uniform over depth. (b) Current profile over depth at 8 April 2020, 06:09:00; the second plot shows a small linear gradient in magnitude over depth. *Data-processing script courtesy of Anne Ton*

B.4.5 Calm period: 11 - 18 July 2020

FL66: Events from 2020-07-11 00:00:00 till 2020-07-18 00:00:00

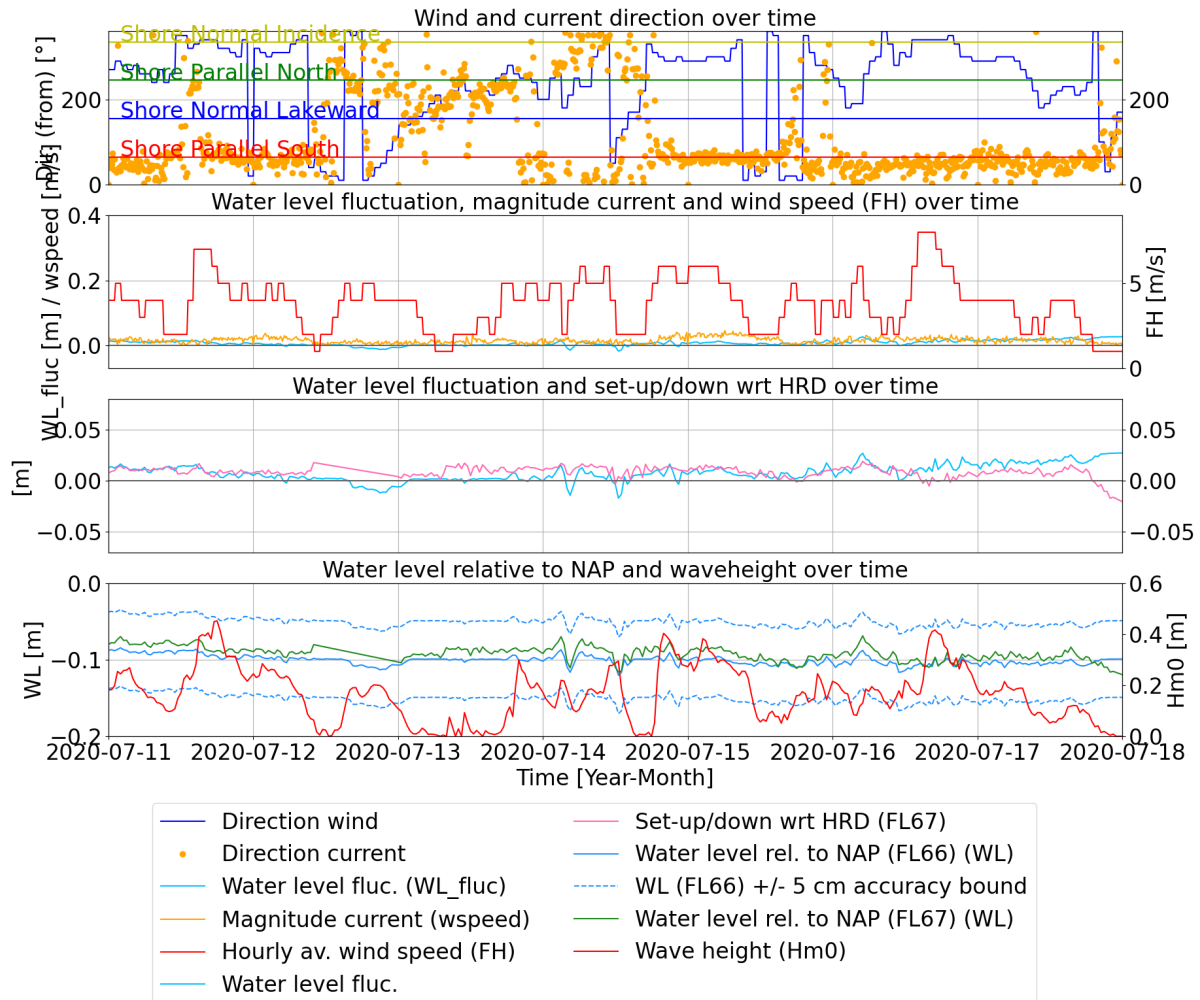


Figure B.22: **11 - 18 July 2020**; overview plot of all conditions. From top to bottom: 1) Wind and current direction (coming from), coloured vertical lines link to directions as specified in figure 6.1. 2) Water level fluctuations at FL66, magnitude current and hourly averaged wind speed. 3) Water level fluctuations at FL66 (obtained by removing 10-day average water level) and set-up/down compared with FL67 (Houtribdijk). 4) Water level relative to NAP at FL66 and its 5 cm accuracy bounds, water level relative to NAP at FL67 and wave height.

FL66: Events from 2020-07-11 00:00:00 till 2020-07-18 00:00:00

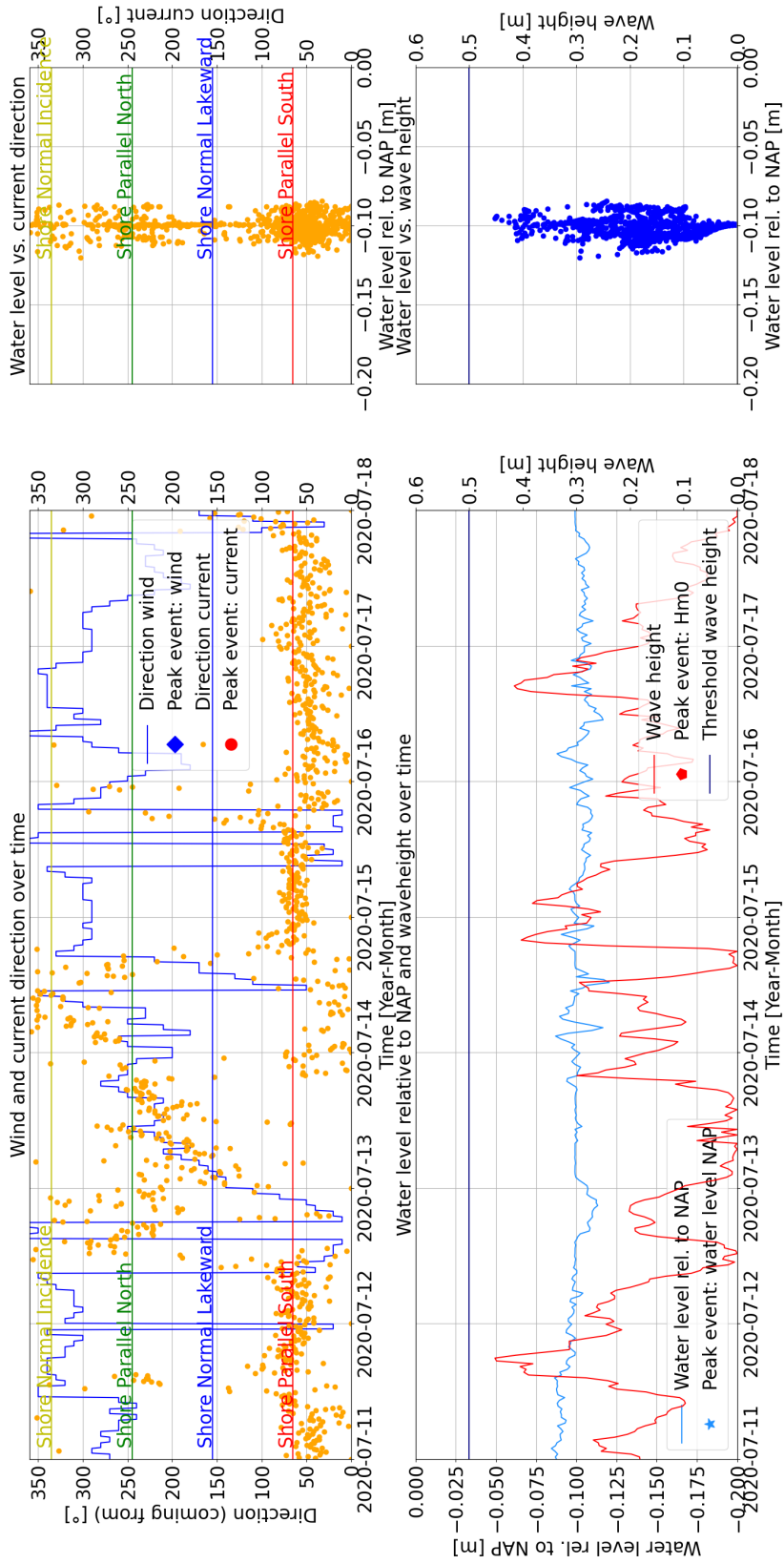


Figure B.23: **11 - 18 July 2020**, Left side: time series of wind, current, wave and water level conditions. Top right: water level relative to NAP versus direction current (coming from). Bottom right: water level relative to NAP versus wave height. Top two figures include four coloured horizontal lines linked to the categorisation of four directions relative to the Noordstrand shoreline orientation (figure 6.1).

FL66: Events from 2020-07-11 00:00:00 till 2020-07-18 00:00:00

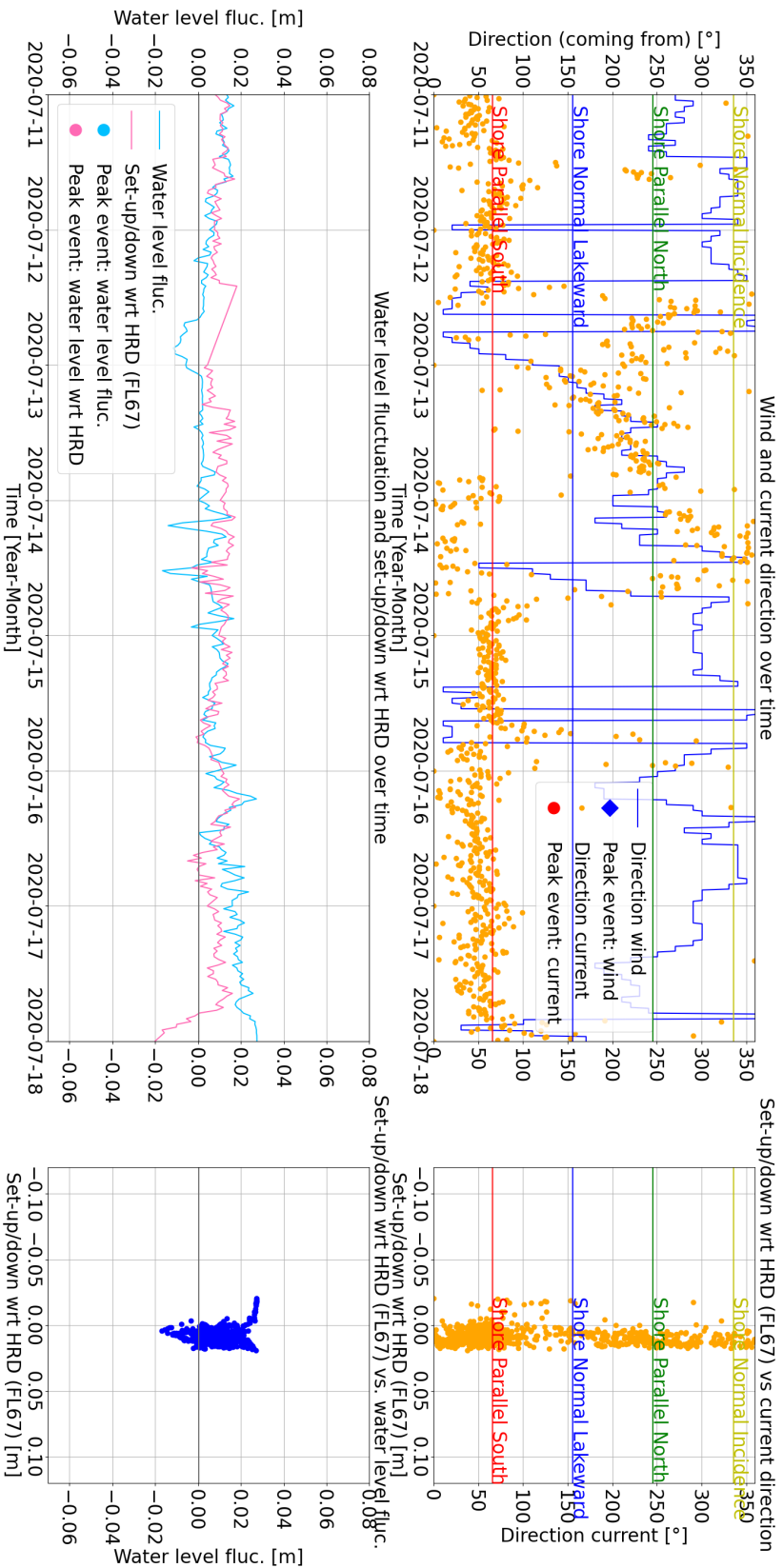


Figure B.24: **11 - 18 July 2020**. Left side: time series of wind, current, water level fluctuations at FL 66 and set-up/down compared with FL67 (Houtribdijk). Top right: set-up/down with respect to FL67 versus direction current (coming from). Bottom right: set-up/down with respect to FL67 versus water level fluctuation at FL66. Top two figures include four coloured horizontal lines linked to the categorisation of four directions relative to the Noordstrand shoreline orientation (figure 6.1).

FL66: Events (linking wind and current) from 2020-07-11 00:00:00 till 2020-07-18 00:00:00

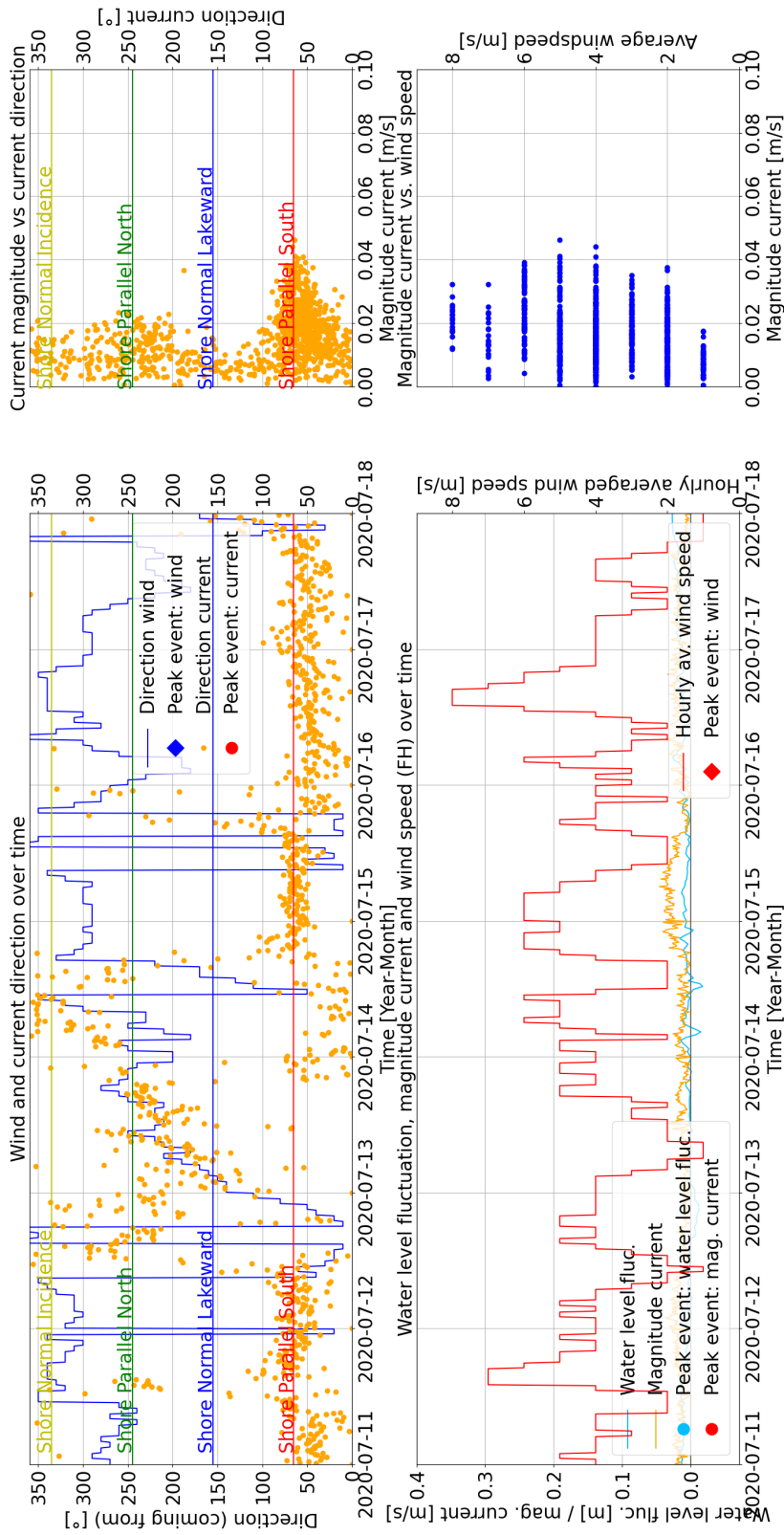


Figure B.25: **11 - 18 July 2020**; Top left: time series of wind and current direction (coming from). Bottom left: time series of water level fluctuation, magnitude current and the hourly averaged wind speed. Top right: magnitude current versus direction current (coming from). Bottom right: magnitude current versus average wind speed. Top two figures include four coloured horizontal lines linked to the categorisation of four directions relative to the Noordstrand shoreline orientation (figure 6.1).

B.5 Additional Peak-over-Threshold Methods

This additional section includes the peak-over-threshold method for water level and for set-up/down compared to the Houtribdijk (by computing the water level difference between FL66 and FL67). Both methods were investigated and its results are shown here for completeness.

B.5.1 *Water level fluctuations at FL66*

The amount of events (peaks) during which water level fluctuations exceeds 0.1 meter is 51. The input for this analysis can be found in table B.26 and the results are shown in figure B.26.

Table B.1: Input for peak-over -threshold method to identify high-energy (peak) events, based on water level fluctuations at FL66.

Peak-over-threshold parameter	Setting	Unit	Source (if relevant)
Threshold	0.1	meter	-
Minimum distance between peaks	12	hours	-
Prominence	0.05	meter	-

B.5.2 *Water level difference FL66 and FL67*

Input (see B.1) is the same as used for water level fluctuations at FL66 (10-day average removed), but now the water level difference between FL66 and FL67 is used to compare the threshold value of 0.1 meter to. The amount of events (peaks) during which set-up of water level compared with the Houtribdijk exceeds 0.1 meter is 12 (figure B.27).

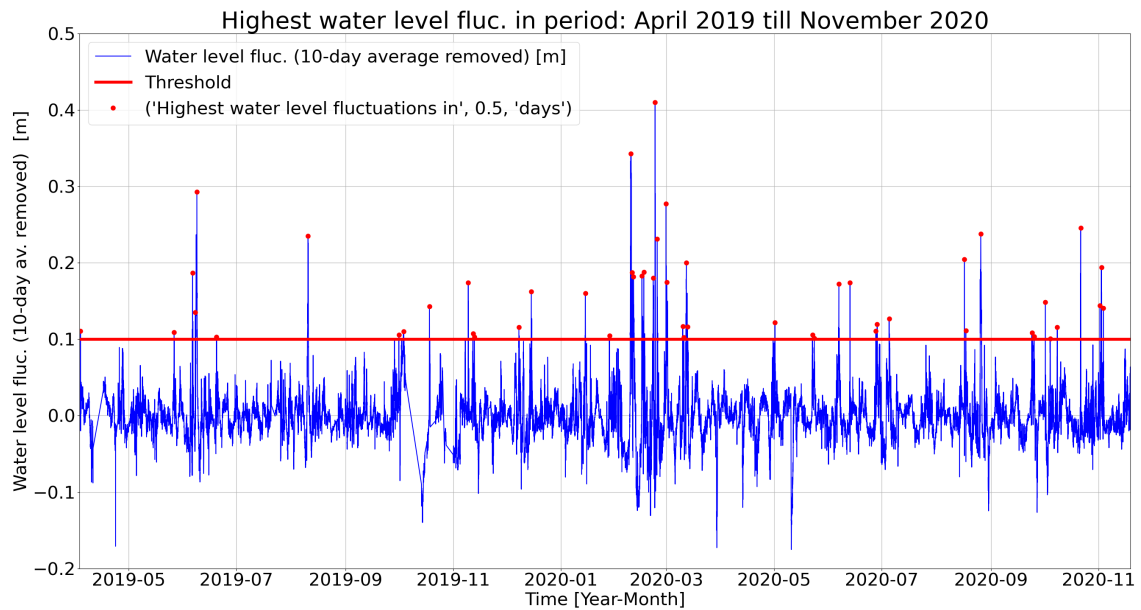


Figure B.26: Time series of water level points relative to NAP at FL66, used to identify peak-over-threshold events (or high-energy events). In red the threshold value set to 0.1 meter. The red dots indicate individual peak events, in total 51 events are found in the period from April 2019 till November 2020.

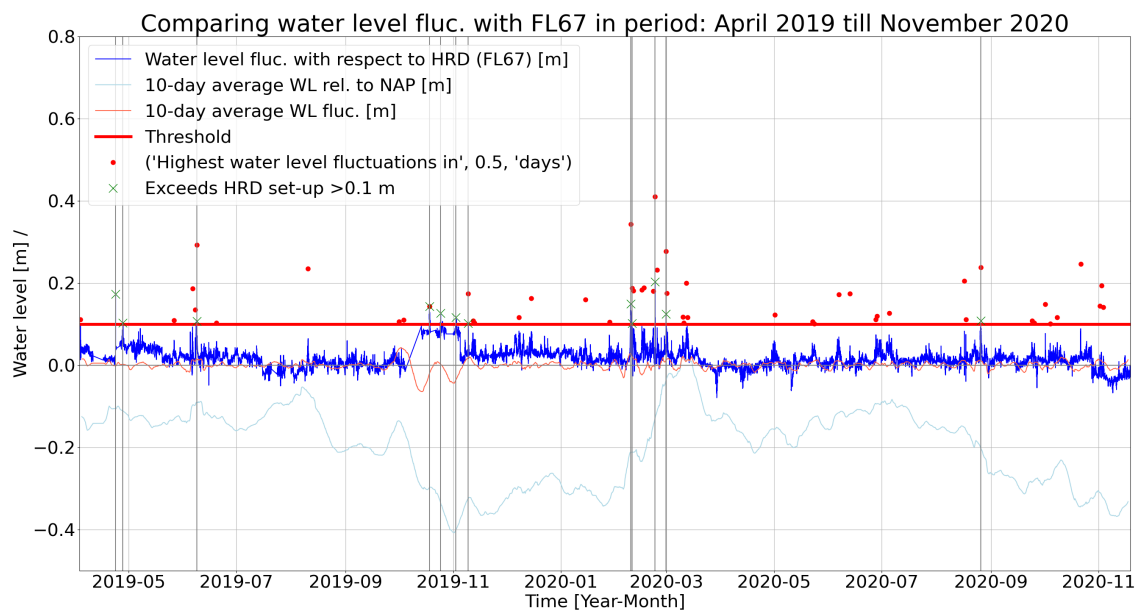


Figure B.27: Time series of water level differences between FL66 and FL67, used to identify peak-over-threshold events (or high-energy events). In red the threshold value set to 0.1 meter. The red dots indicate individual peak events, in total 12 events are found in the period from April 2019 till November 2020.



Data Analysis: Morphodynamics

This appendix provides additional information on the data analysis discussed in chapter 7. It is similarly split into a data-processing part, section C.1, showing additional graphs for chapter 5. Next a general part, section C.2, showing the general overview using a different scale. Last the analysis of the morphodynamic change for all transects in the period of 2019 Q3 till 2020 Q1 is presented in section C.3.

C.1 Data-processing

The important features for projection and interpolation of the data on a grid are shown in figure C.1. The polygon is larger than the considered grid as in the future the upper new part (an extension of the sandy edge) might also be considered and can be readily be included.

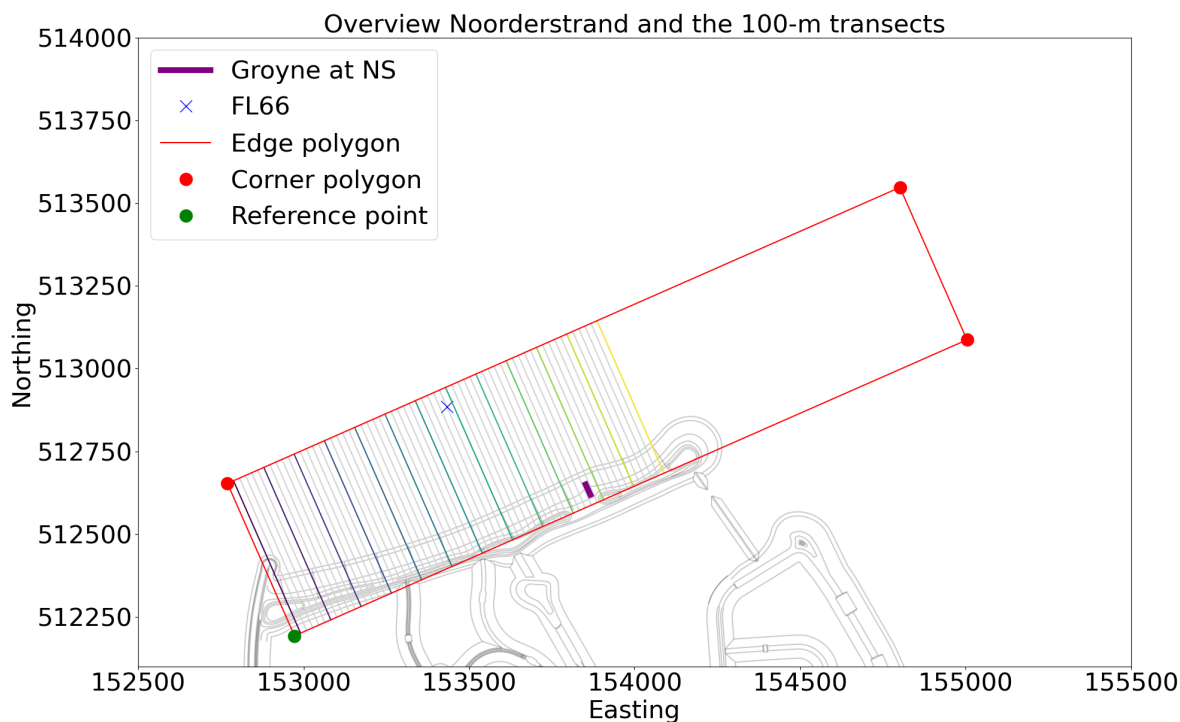


Figure C.1: An overview of the Noordstrand. The used grid to project the data on is shown as grey vertical lines. The data is interpolated in the polygon shown by the red rectangle, points outside this polygon are no longer considered. The different 100 meter transects are coloured lines within the grid. The reference point of the grid, shown as a green dot, is used to translate and rotate the data.

C.2 General

Figure 7.2 is shown again in figure C.2 but now with a different scale bar to highlight the erosion and sedimentation hotspots more clearly.

Figure C.3 shows the general development of the Noordstrand in periods of 9 months, with the bottom plot showing the total rate of change.

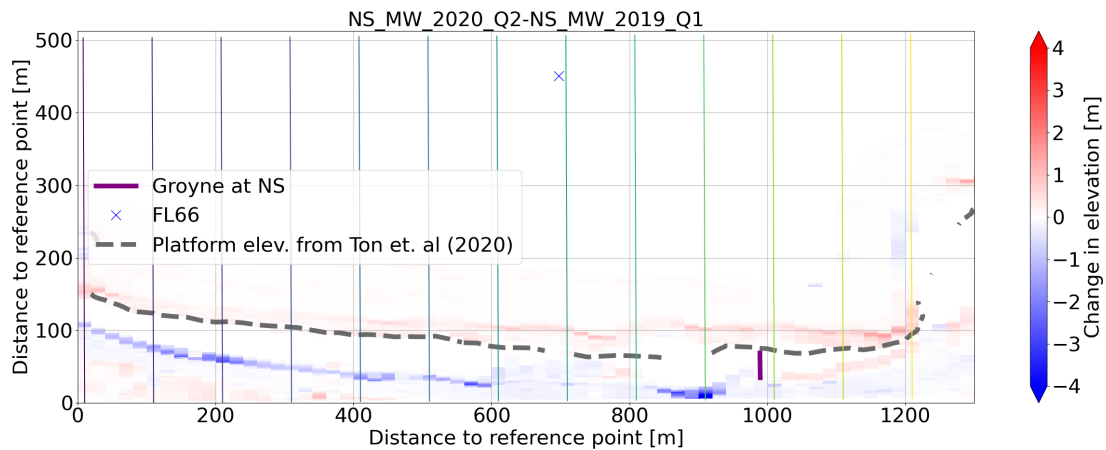


Figure C.2: Changes in elevation when comparing measurements at the start of the interesting period (2019 Q1) with the end (2020 Q2). Same as figure 7.2, but the colour scale is now changed to range from -4 meter NAP to +4 meter NAP, to highlight the location of erosion and sedimentation hot spots. Positive changes in elevation are shown in red and are associated with sedimentation. Negative changes in elevation are shown in blue and indicate erosion. Measurements around the waterline are missing as only topography and bathymetry data are available for this period of time. The dashed grey line indicates the location of the offshore platform using an elevation of -1.11 meter relative to NAP (from Ton et al. (2020)) using the data at the start of the mentioned period. This to show the development of the platform offshore.

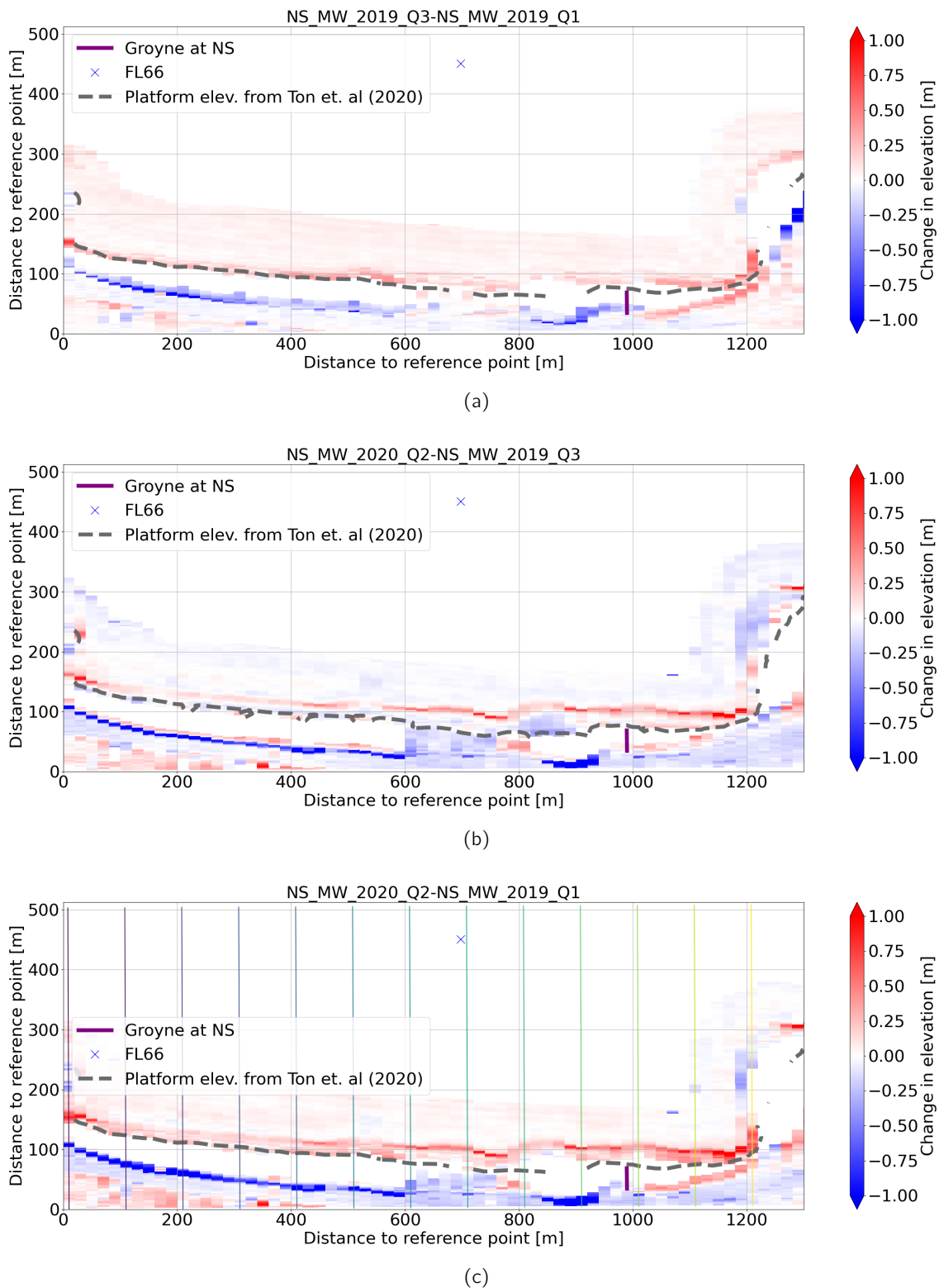


Figure C.3: Overview of changes in elevation when comparing measurements at the start of the interesting period (2019 Q1) with the end (2020 Q2). (a) shows the development of the elevation in the first months (2019 Q1 till 2019 Q3); (b) shows the development during the last months (2019 Q3 till 2020 Q2); (c) is the same as figure 7.2 and shows the total rate of change. Positive changes in elevation are shown in red and are associated with sedimentation. Negative changes in elevation are shown in blue and indicate erosion. Measurements around the waterline are missing.

C.3 Transects 2019 Q3 - 2020 Q1

For the other periods of time the analysis of different transects is interesting as data round the waterline is missing. Periods 2019 Q3 and 2020 Q1 do have 100 meter transect measurements and are thus interesting to analyse in more detail.

C.3.1 Overview transects

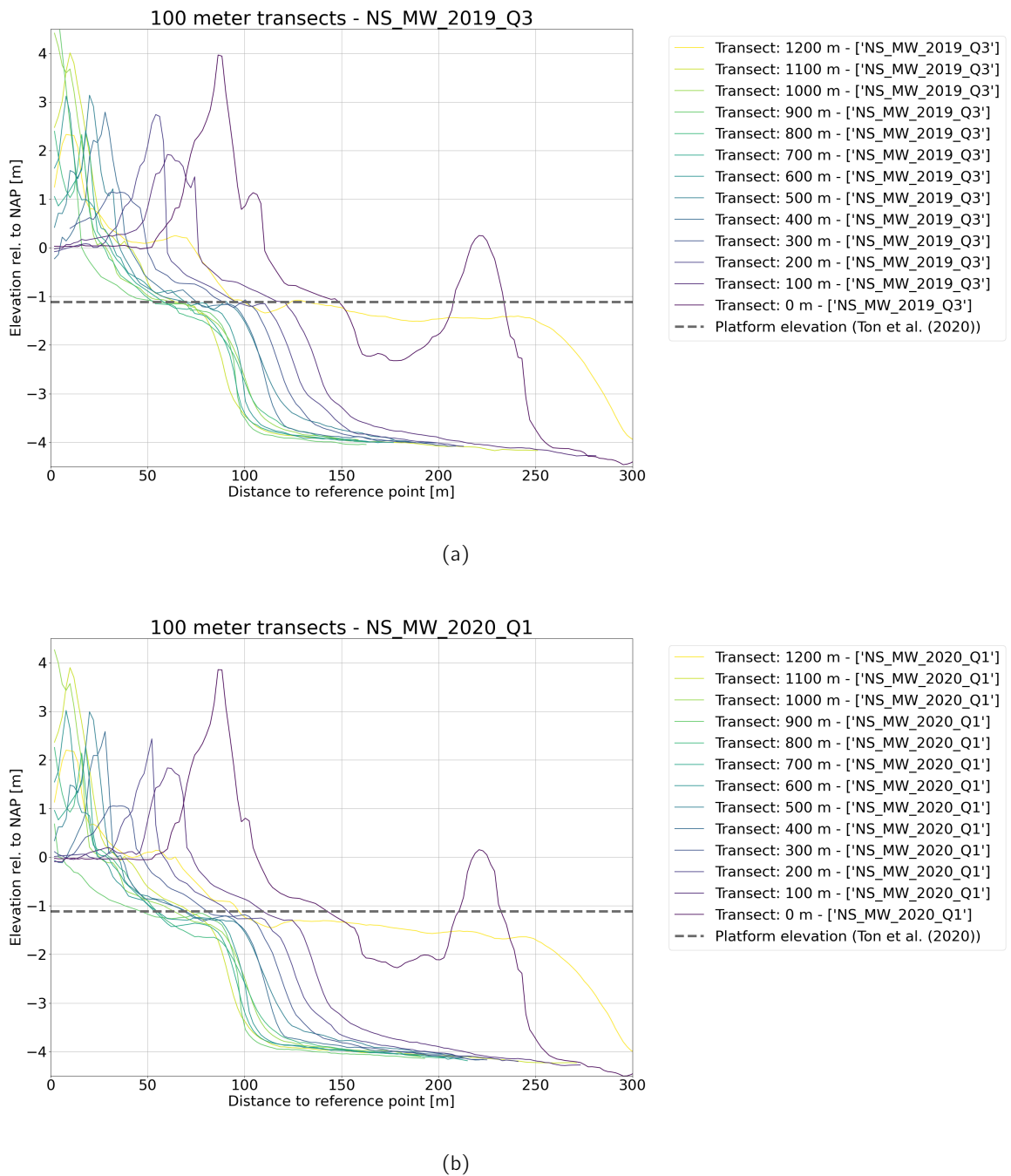


Figure C.4: Overview of the different transects in one plot. (a) 100 meter transects for the data of 2019 Q3; (b) 100 meter transects for the data of 2020 Q1. Colours correspond to the transects as shown in figures 5.2 and C.1.

C.3.2 Analysis of individual transects

Figure C.5 shows the 13 transects which are considered in more detail on the next pages. Transect 300, 700, 900 and 100 are also shown in the main document.

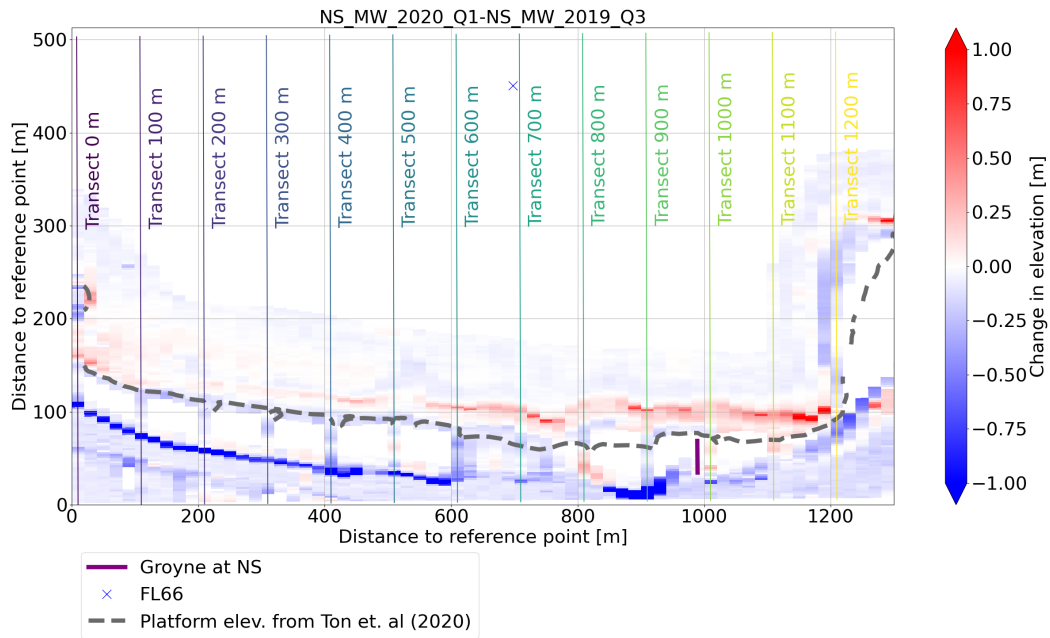
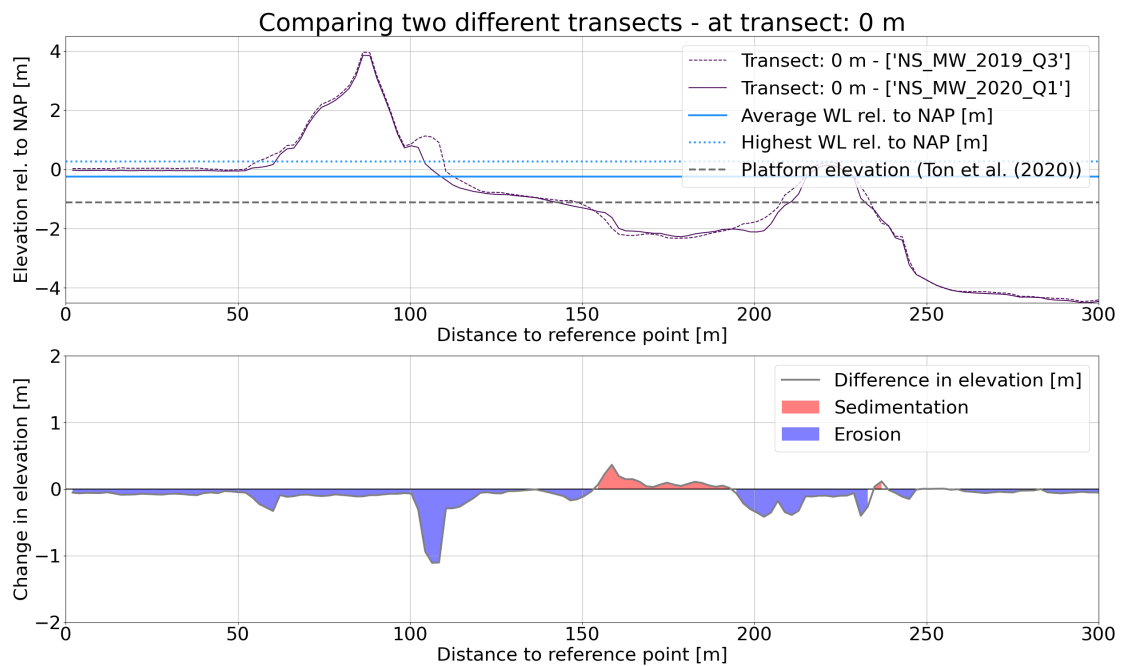
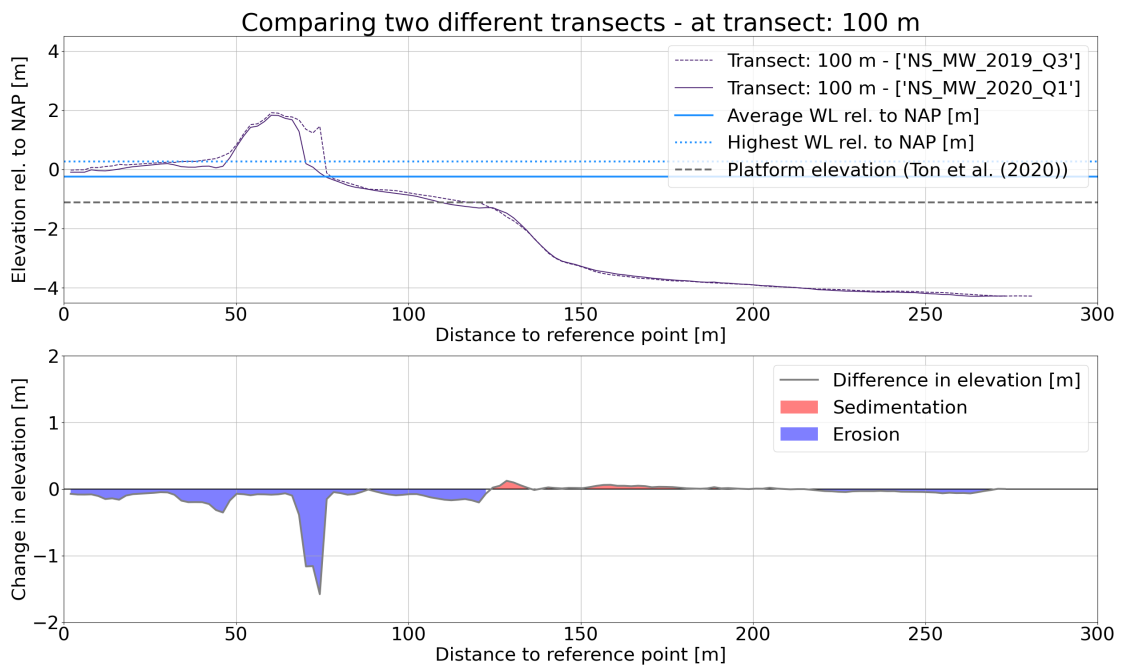


Figure C.5: Elevation change from 2019 Q3 till 2020 Q1, including the 100 meter transects along which water line measurements are available. Colours correspond to the transects as shown in figures 5.2 and C.1.

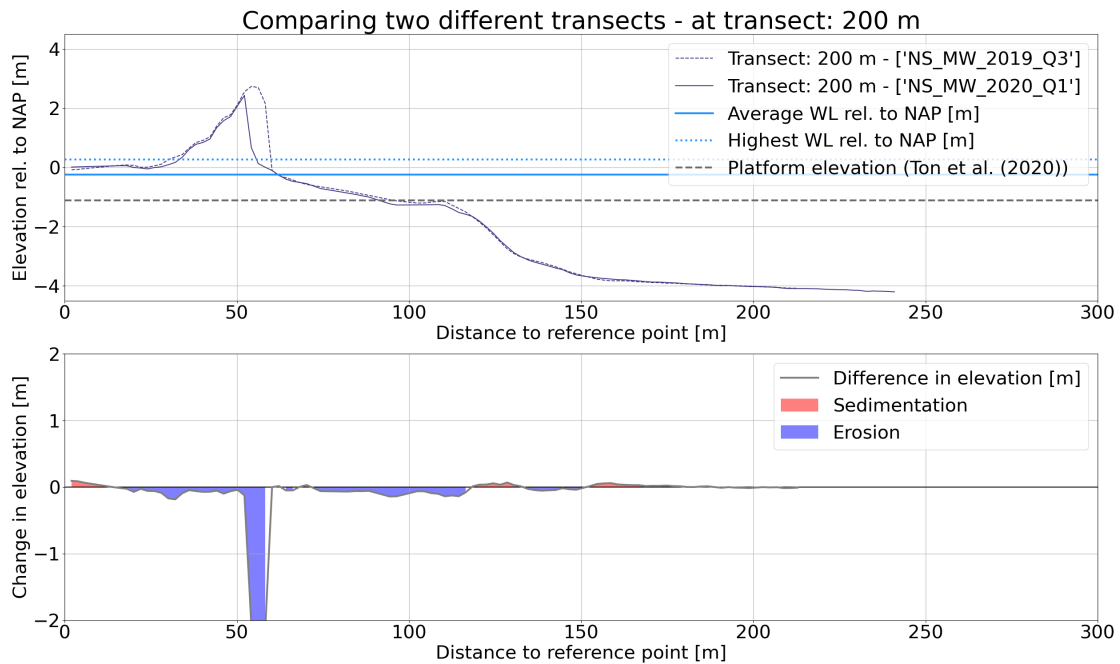


(a)

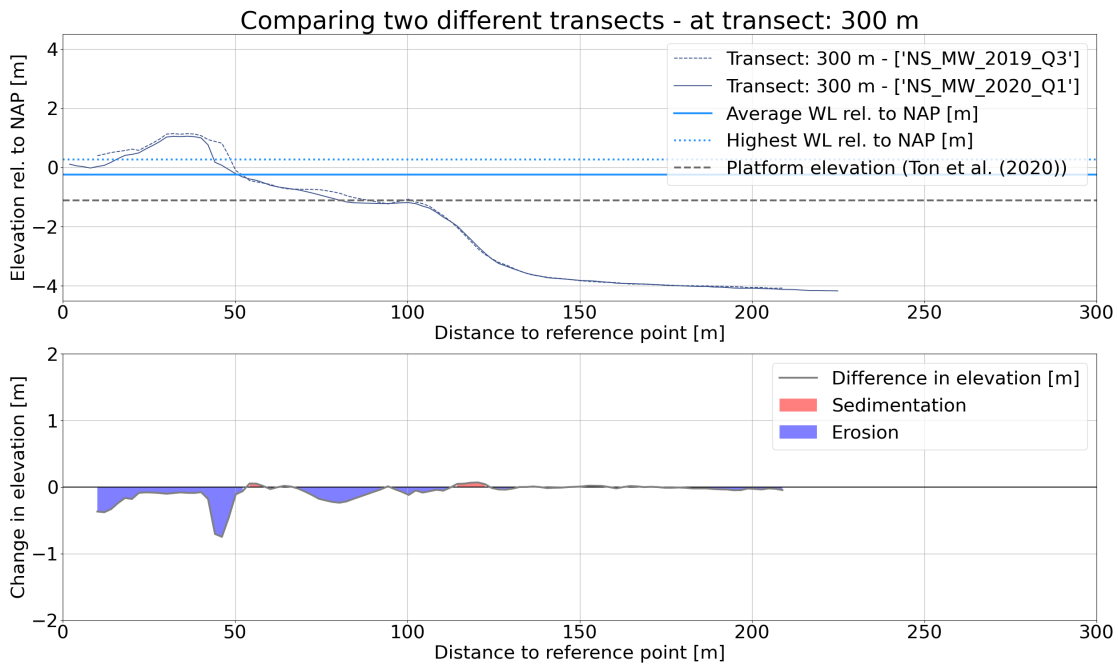


(b)

Figure C.6: (a) Transect 0 meter; (b) Transect 100 meter; Comparing two different transects, 2019 Q3 (dotted line) to 2020 Q1 (solid line). Top plot: The colour of the transect plot corresponds to the colour visible in figure 7.3. The solid blue horizontal line is the average water level relative to NAP in the considered period, with the dotted blue horizontal line being the maximum water level relative to NAP in the same period. The elevation of the platform is represented as a grey dashed line (elevation taken from Ton et al. (2020)). Bottom plot: difference in elevation (2020 Q1 - 2019 Q3), sedimentation given in red and erosion given in blue. The distances are vertical distances to the reference point.

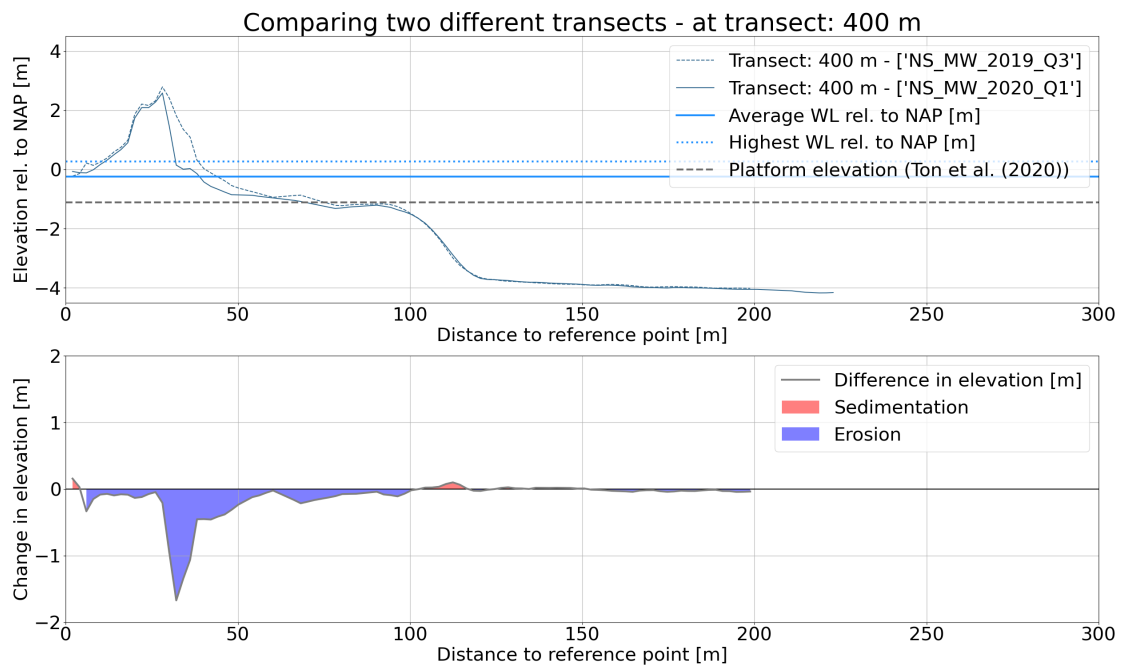


(a)

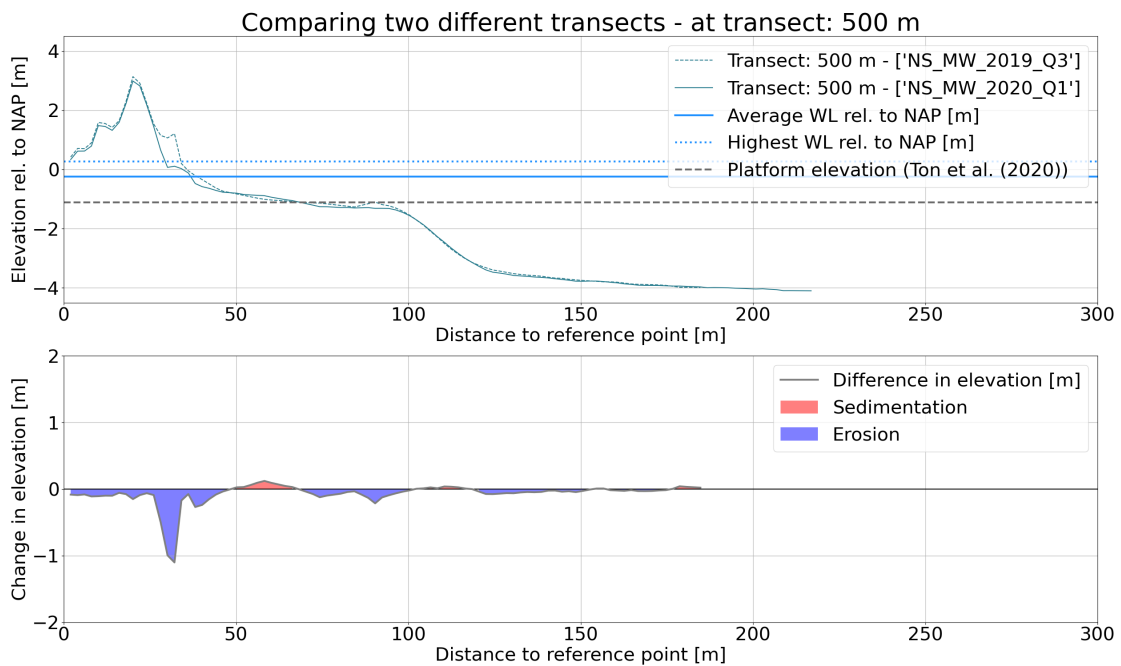


(b)

Figure C.7: (a) Transect 200 meter; (b) Transect 300 meter; Comparing two different transects, 2019 Q3 (dotted line) to 2020 Q1 (solid line). Top plot: The colour of the transect plot corresponds to the colour visible in figure 7.3. The solid blue horizontal line is the average water level relative to NAP in the considered period, with the dotted blue horizontal line being the maximum water level relative to NAP in the same period. The elevation of the platform is represented as a grey dashed line (elevation taken from Ton et al. (2020)). Bottom plot: difference in elevation (2020 Q1 - 2019 Q3), sedimentation given in red and erosion given in blue. The distances are vertical distances to the reference point.

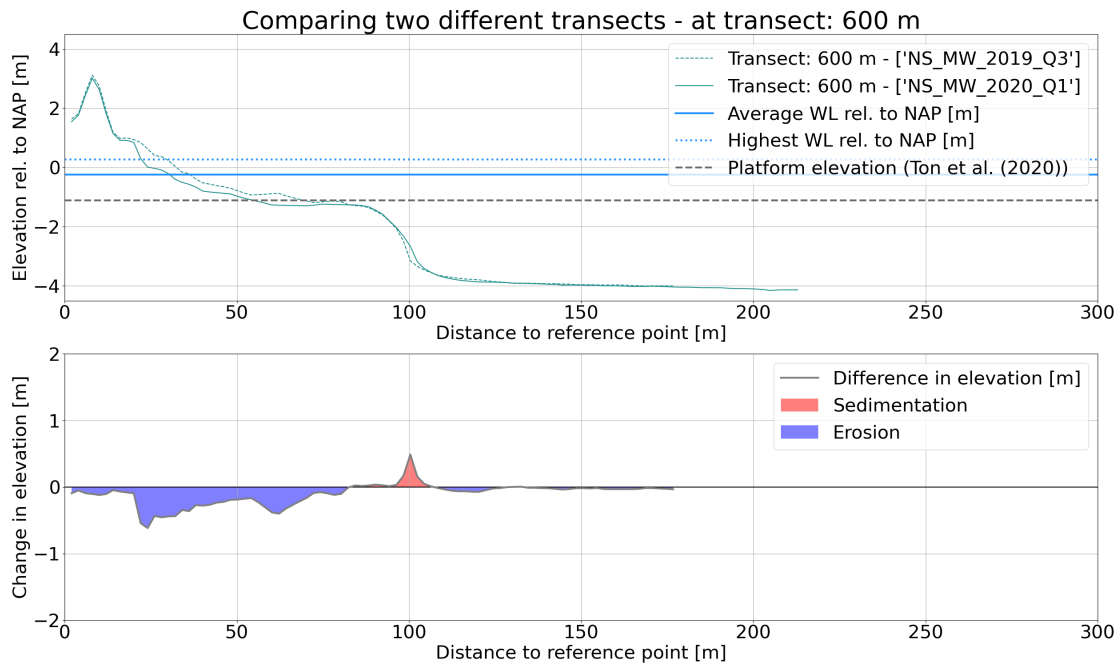


(a)

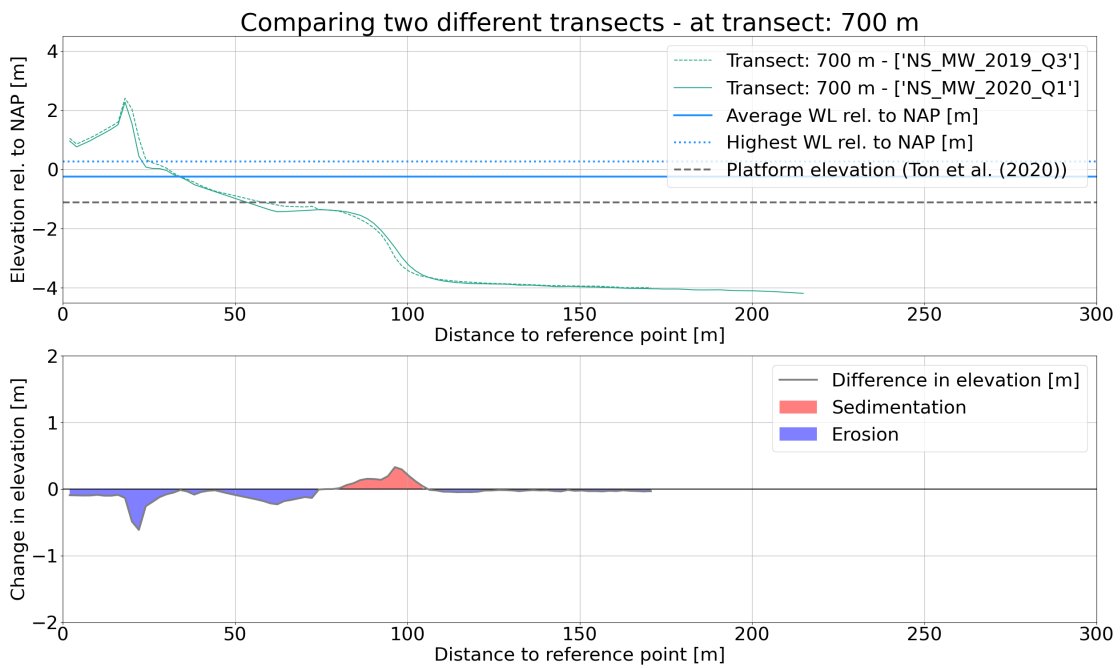


(b)

Figure C.8: (a) Transect 400 meter; (b) Transect 500 meter; Comparing two different transects, 2019 Q3 (dotted line) to 2020 Q1 (solid line). Top plot: The colour of the transect plot corresponds to the colour visible in figure 7.3. The solid blue horizontal line is the average water level relative to NAP in the considered period, with the dotted blue horizontal line being the maximum water level relative to NAP in the same period. The elevation of the platform is represented as a grey dashed line (elevation taken from Ton et al. (2020)). Bottom plot: difference in elevation (2020 Q1 - 2019 Q3), sedimentation given in red and erosion given in blue. The distances are vertical distances to the reference point.

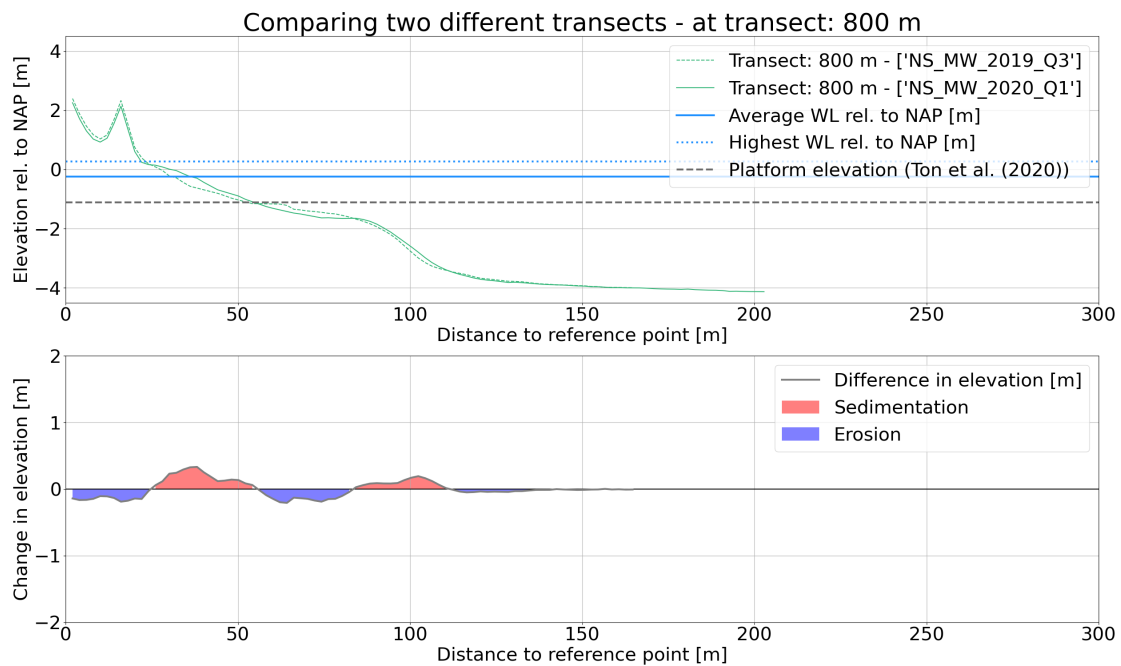


(a)

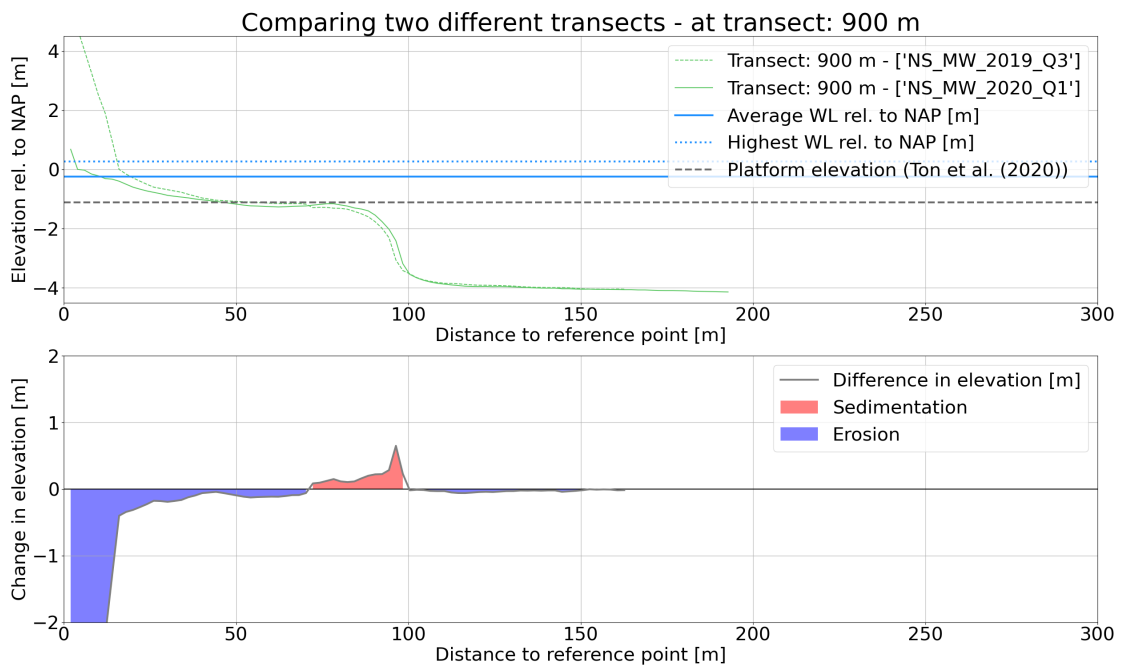


(b)

Figure C.9: (a) Transect 600 meter; (b) Transect 700 meter; Comparing two different transects, 2019 Q3 (dotted line) to 2020 Q1 (solid line). Top plot: The colour of the transect plot corresponds to the colour visible in figure 7.3. The solid blue horizontal line is the average water level relative to NAP in the considered period, with the dotted blue horizontal line being the maximum water level relative to NAP in the same period. The elevation of the platform is represented as a grey dashed line (elevation taken from Ton et al. (2020)). Bottom plot: difference in elevation (2020 Q1 - 2019 Q3), sedimentation given in red and erosion given in blue. The distances are vertical distances to the reference point.

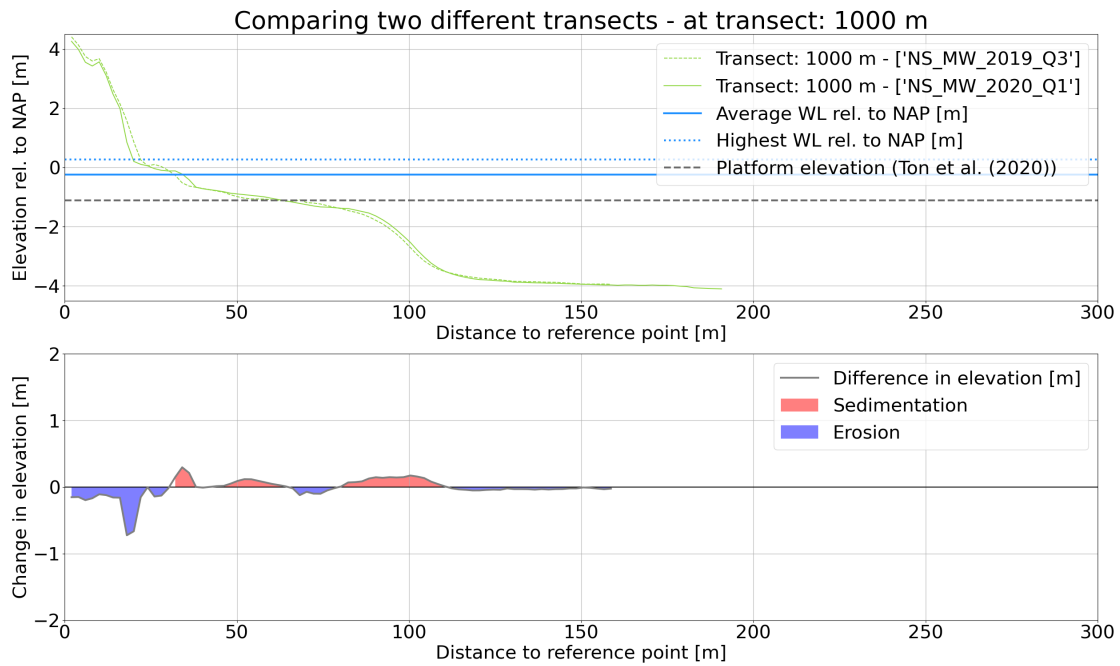


(a)

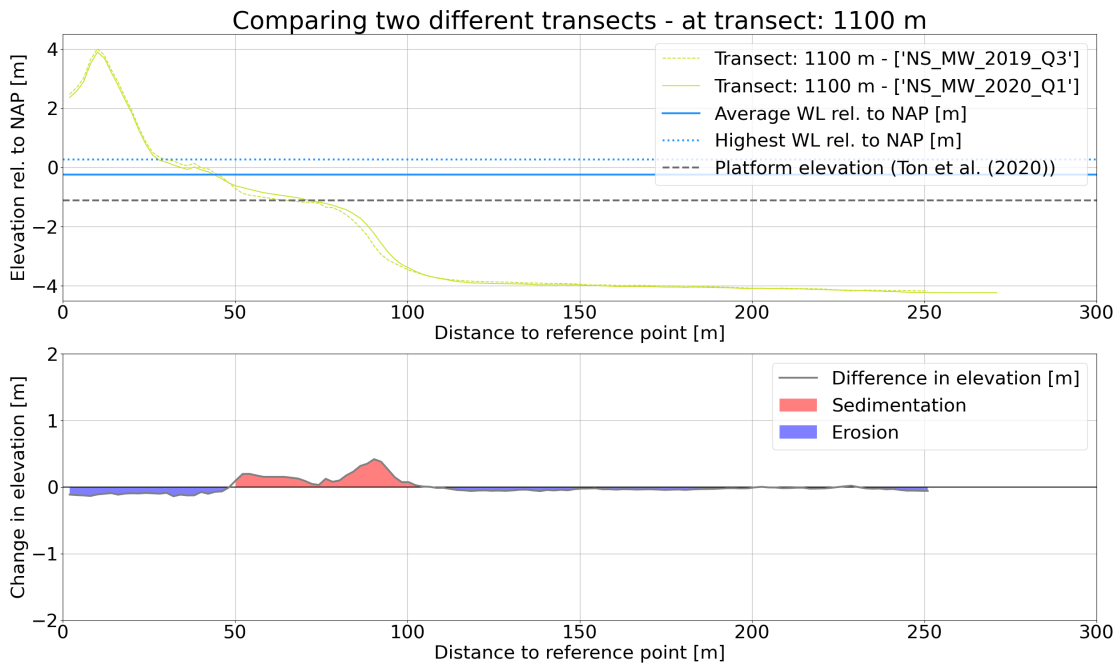


(b)

Figure C.10: (a) Transect 800 meter; (b) Transect 900 meter; Comparing two different transects, 2019 Q3 (dotted line) to 2020 Q1 (solid line). Top plot: The colour of the transect plot corresponds to the colour visible in figure 7.3. The solid blue horizontal line is the average water level relative to NAP in the considered period, with the dotted blue horizontal line being the maximum water level relative to NAP in the same period. The elevation of the platform is represented as a grey dashed line (elevation taken from Ton et al. (2020)). Bottom plot: difference in elevation (2020 Q1 - 2019 Q3), sedimentation given in red and erosion given in blue. The distances are vertical distances to the reference point.



(a)



(b)

Figure C.11: (a) Transect 1000 meter; (b) Transect 1100 meter; Comparing two different transects, 2019 Q3 (dotted line) to 2020 Q1 (solid line). Top plot: The colour of the transect plot corresponds to the colour visible in figure 7.3. The solid blue horizontal line is the average water level relative to NAP in the considered period, with the dotted blue horizontal line being the maximum water level relative to NAP in the same period. The elevation of the platform is represented as a grey dashed line (elevation taken from Ton et al. (2020)). Bottom plot: difference in elevation (2020 Q1 - 2019 Q3), sedimentation given in red and erosion given in blue. The distances are vertical distances to the reference point.

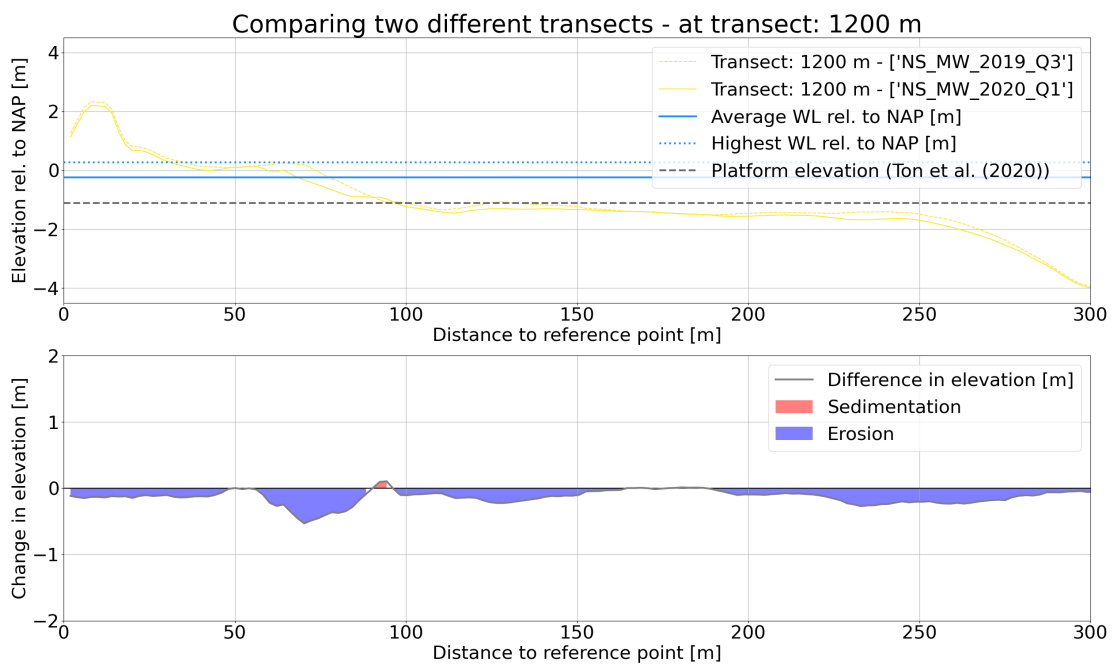
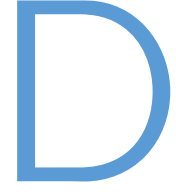


Figure C.12: Transect 1200 meter; Comparing two different transects, 2019 Q3 (dotted line) to 2020 Q1 (solid line). Top plot: The colour of the transect plot corresponds to the colour visible in figure 7.3. The solid blue horizontal line is the average water level relative to NAP in the considered period, with the dotted blue horizontal line being the maximum water level relative to NAP in the same period. The elevation of the platform is represented as a grey dashed line (elevation taken from Ton et al. (2020)). Bottom plot: difference in elevation (2020 Q1 - 2019 Q3), sedimentation given in red and erosion given in blue. The distances are vertical distances to the reference point.



D3D Model Set-up

This appendix contains additional information and figures concerning the set-up of the Marker Wadden model as explained in chapter 8. Section D.2 contains two additional plots considering the Markermeer bathymetry and and zoom in of the computational grid near the Noordstrand. Section D.3 shows the additional graphs used to verify the calibration of the D3D model.

D.1 Introduction Delft3D

This section gives a brief introduction into Delft3D, split into the subsections: flow, waves and numerical modelling.

D.1.1 Flow

Deltares (2021a): 'Delft3D-FLOW is a multi-dimensional (2D or 3D) hydrodynamic (and transport) simulation program which calculates non-steady flow and transport phenomena that result from tidal and meteorological forcing on a rectilinear or a curvilinear, boundary fitted grid. In 3D simulations, the vertical grid is defined following the σ co-ordinate approach.' Delft3D-FLOW solves the unsteady shallow water equations in two (when depth-averaged) or three dimensions. These shallow water equations are derived from the Navier-Stokes equations using the following assumptions (Zijlema, 2020):

- Incompressibility: density does not depend on pressure.
- Hydrostatic pressure assumption: vertical length scales are much smaller than horizontal length scales. Delft3D can only solve the long wave equation and is thus not capable of resolving short waves (Deltares, 2021a).
- Boussinesq approximation: density variations are really small and only impact the baroclinic forcing term of the momentum equations.

Delft3D-FLOW solves the depth-integrated shallow water equations (2DH SWE) as described by equations D.1 till D.5 if run in 2DH mode (which is primarily used in this research). The model and equations can be extended to represent 3D flow, in which the vertical velocities are computed from the continuity equation (Deltares, 2021a).

$$\frac{\partial \zeta}{\partial t} + \frac{\partial hu}{\partial x} + \frac{\partial hv}{\partial y} = 0 \quad (D.1)$$

$$\frac{\partial u}{\partial t} + u \frac{\partial u}{\partial x} + v \frac{\partial u}{\partial y} - \nu_h \left(\frac{\partial^2 u}{\partial x^2} + \frac{\partial^2 u}{\partial y^2} \right) = -g \frac{\partial \zeta}{\partial x} - \frac{\tau_{b,x}}{\rho_0 h} + f v + \frac{\tau_{w,x}}{\rho_0 h} - \frac{1}{\rho_0} \frac{\partial p_{atm}}{\partial x} \quad (D.2)$$

$$\frac{\partial v}{\partial t} + u \frac{\partial v}{\partial x} + v \frac{\partial v}{\partial y} - \nu_h \left(\frac{\partial^2 v}{\partial x^2} + \frac{\partial^2 v}{\partial y^2} \right) = -g \frac{\partial \zeta}{\partial y} - \frac{\tau_{b,y}}{\rho_0 h} - f u + \frac{\tau_{w,y}}{\rho_0 h} - \frac{1}{\rho_0} \frac{\partial p_{atm}}{\partial y} \quad (D.3)$$

$$\vec{\tau}_w = \rho_{air} c_d \vec{U}_{10} |\vec{U}_{10}| \quad (D.4)$$

$$\vec{\tau}_b = \rho_0 c_f \vec{u} |\vec{u}| \quad (D.5)$$

Equations D.4 and D.5 are directly linked to the boundary conditions of the computational domain. $\vec{\tau}_w$ relates to the wind shear stress acting on the water surface. The wind being an energy source. Wind input is required in Delft3D-FLOW and is the forcing of our Marker Wadden model. $\vec{\tau}_b$ acts on the bottom of the water column and is the bottom shear stress generated by bottom friction, causing energy dissipation.

D.1.2 Waves

The Delft3D-WAVE module uses the third-generation SWAN model to simulate the evolution of random, short-crested wind-generated waves (Deltares, 2021b). SWAN is able to describe wave propagation, generation and dissipation processes (The SWAN team, 2020a). Waves influence the flow pattern of the mean flow, due to wave set-up and wave-induced currents in the breaker zone.

Delft3D-WAVE is not a wave resolving model, meaning not every single wave is simulated. It is a wave averaging model, we observe the mean wave shoaling and breaking (De Schipper, 2020). The continuity and momentum equations are averaged over the wave period (Deltares, 2021a), as a result the non-linear advection terms give rise to momentum fluxes: radiation stresses (Zijlema, 2020). The spectral wave model, SWAN in this case, determines the radiation stresses which are added to the shallow water equations (equations D.1, D.2 and D.3) in the form of driving forces to account for wave motions.

SWAN uses the spectral action balance to describe the evolution of the wave spectrum (equation D.6, from Deltares (2021b)). The different terms are described by Deltares (2021b): 'The first term in the left-hand side of this equation represents the local rate of change of action density in time, the second and third term represent propagation of action in geographical space (with propagation velocities c_x and c_y in x - and y -space, respectively). The fourth term represents shifting of the relative frequency due to variations in depths and currents (with propagation velocity c_σ in σ -space). The fifth term represents depth-induced and current induced refraction (with propagation velocity c_θ in θ -space). The expressions for these propagation speeds are taken from linear wave theory. The term S ($= (\sigma, \theta)$) at the right-hand side of the action balance equation is the source term in terms of energy density representing the effects of generation, dissipation and non-linear wave-wave interactions.'

$$\frac{\partial}{\partial t} N + \frac{\partial}{\partial x} c_x N + \frac{\partial}{\partial y} c_y N + \frac{\partial}{\partial \sigma} c_\sigma N + \frac{\partial}{\partial \theta} c_\theta N = \frac{S}{\sigma} \quad (\text{D.6})$$

D.1.3 Numerical modelling

The numerical method of Delft3D is based on finite differences and uses a staggered grid. In whole indices of the grid the water level is considered and at half the indices the velocity (figure D.1).

The time integration in Delft3D-FLOW is fully implicit, using the ADI method to solve the penta-diagonal matrix which results from integrating the shallow water equations. This ADI (Alternating Direction Implicit) method splits the time step into two stages: an *implicit* and *explicit* stage, creating tri-diagonal matrices which are less computationally demanding to solve (Zijlema, 2020). The ADI method is unconditionally stable and at least second order accurate in space (Deltares, 2021a).

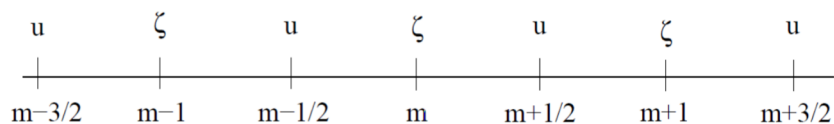


Figure D.1: Visualisation staggered grid taken from Zijlema (2020)

D.2 Domain, Grid and Bathymetry

The important D3D settings considering the *total* and *nested* model are discussed in the main document. This section adds two figures of the *nested mode* bathymetry and computational grid. One can observe how the structured grid will create a step-wise, opposed to smooth, representation of the waterline (figure D.3). This could be improved by adjusting the resolution of the grid or by using another type of grid: D3D Flexible Mesh.

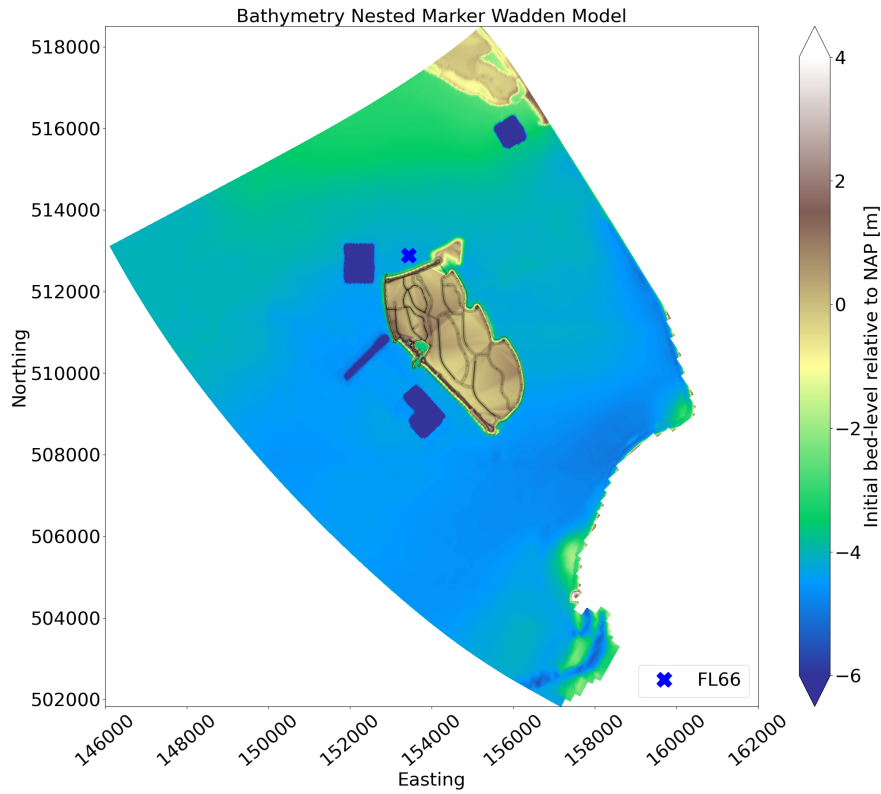


Figure D.2: Bathymetry of the nested model.

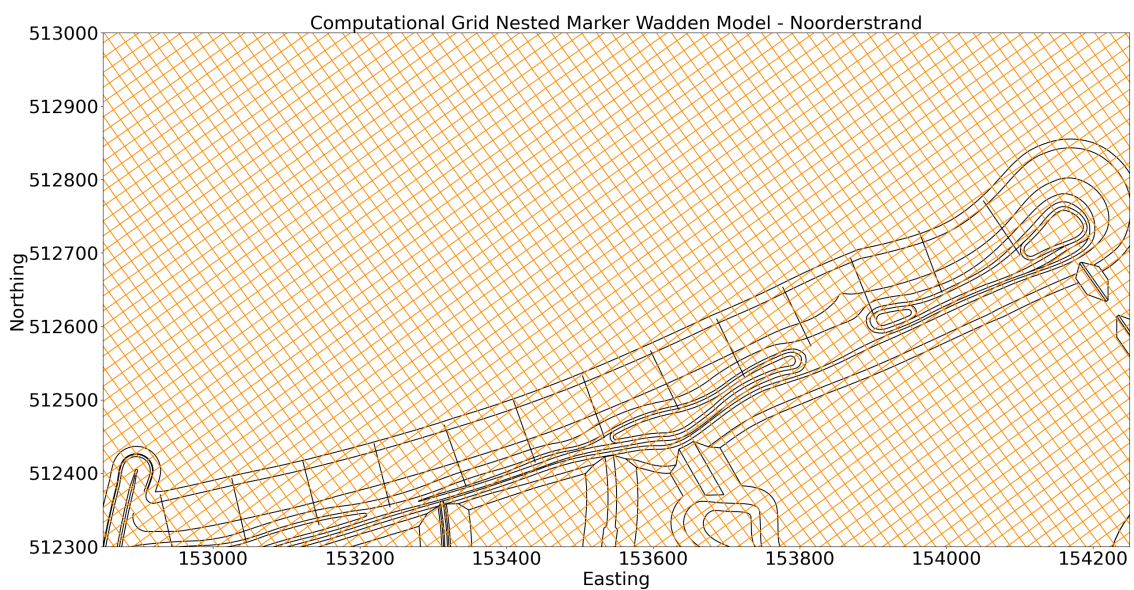


Figure D.3: Visualisation of the nested model's computational grid near the Noorderstrand.

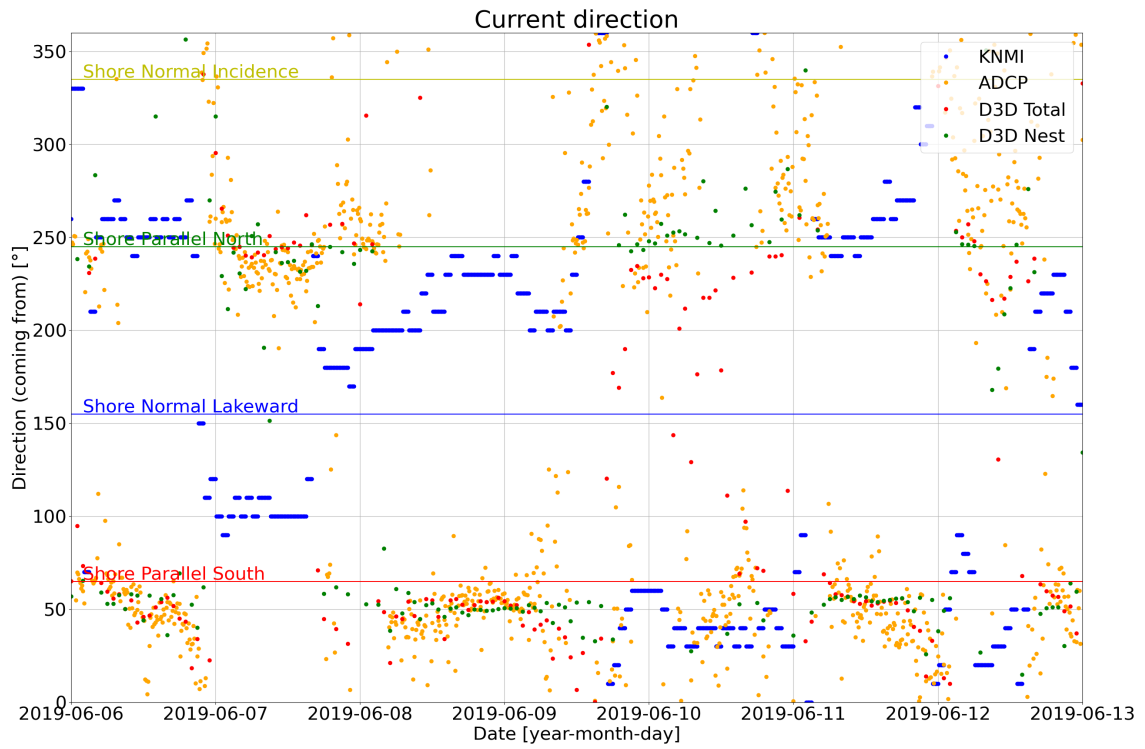
D.3 Calibration

Three periods, two high-energy and one calm, are used to validate the model outcomes. The model output is compared to the STB and ADCP measurements of FL66. The following three periods are considered:

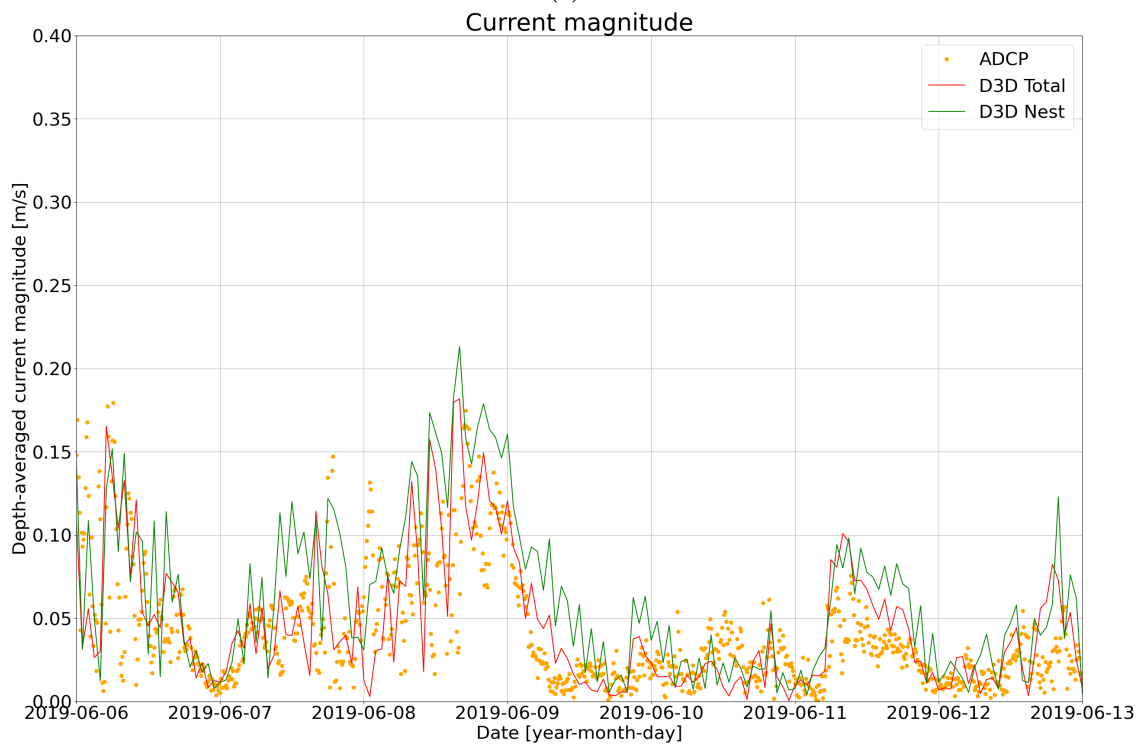
- High-energy period: 6 - 13 June 2019 (analysis in section B.4.2)
- High-energy period: 7 - 15 February 2020 (analysis in section 6.2.2)
- Calm period: 5 - 12 April (analysis in section B.4.4)

One should note that for these runs the initial water level was changed from -0.34 meter to the water level as measured by the STB at the start of to-be simulated period. Subsequent runs have shown that using an initial water level of -0.34 meter instead of the real measured water level at the start of the period does not change the results considerably. For the calibration run of February 2020 a water level of -0.34 meter was used and not the water level measured by the STB.

D.3.1 High-energy event: 6 - 13 June 2019

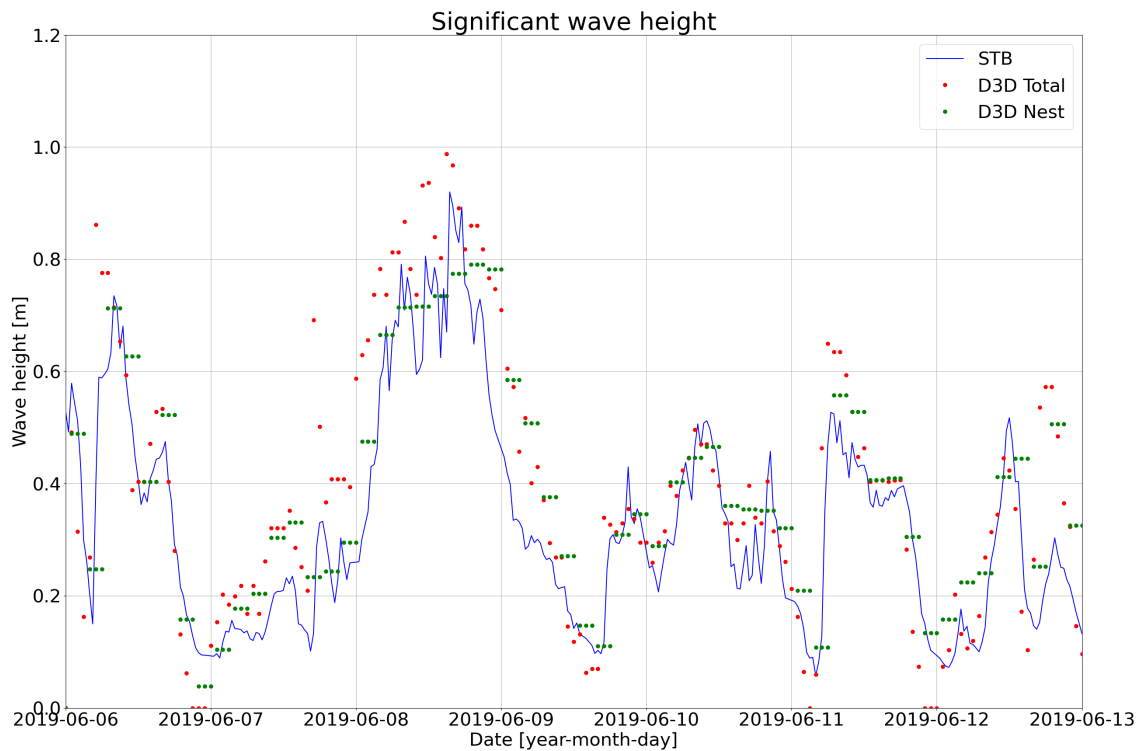


(a)

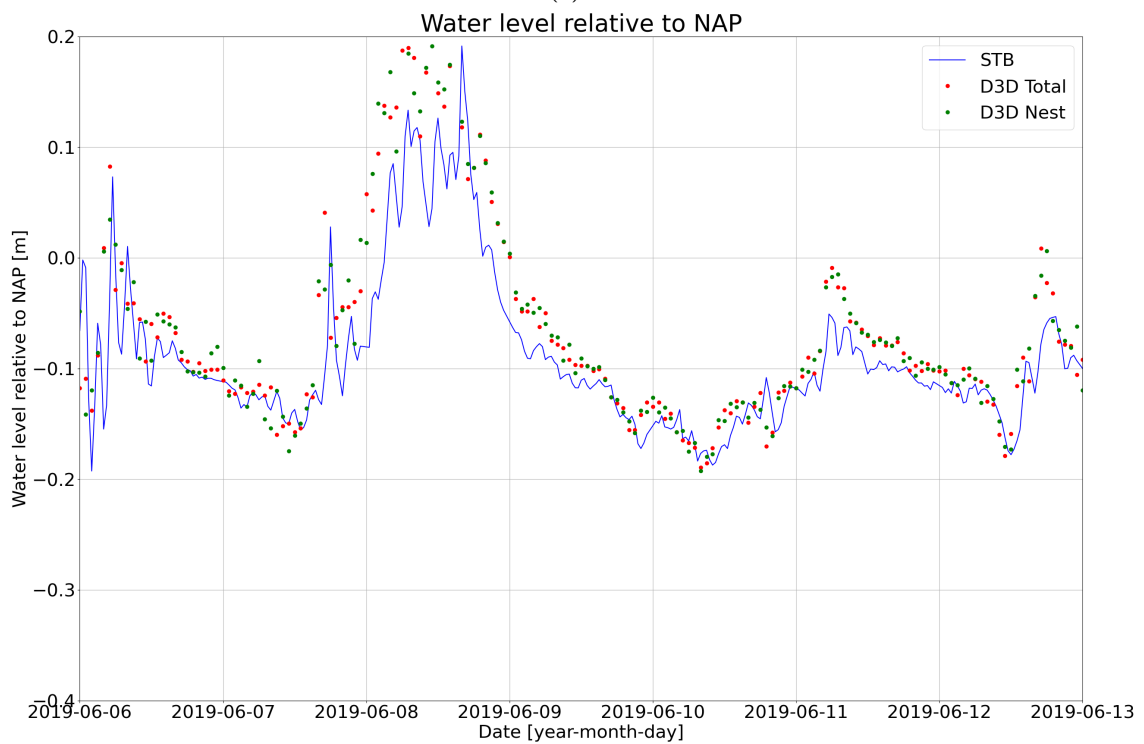


(b)

Figure D.4: Two figures showing: (a) Current direction comparing ADCP measurements obtained at FL66 (orange dots) and model output at observation point FL66 (total model results are the red dots and nested model results are shown in green); (b) Current magnitude comparing ADCP measurements obtained at FL66 (orange dots) with model results (red dots represent total model results and green dots are nested model results).



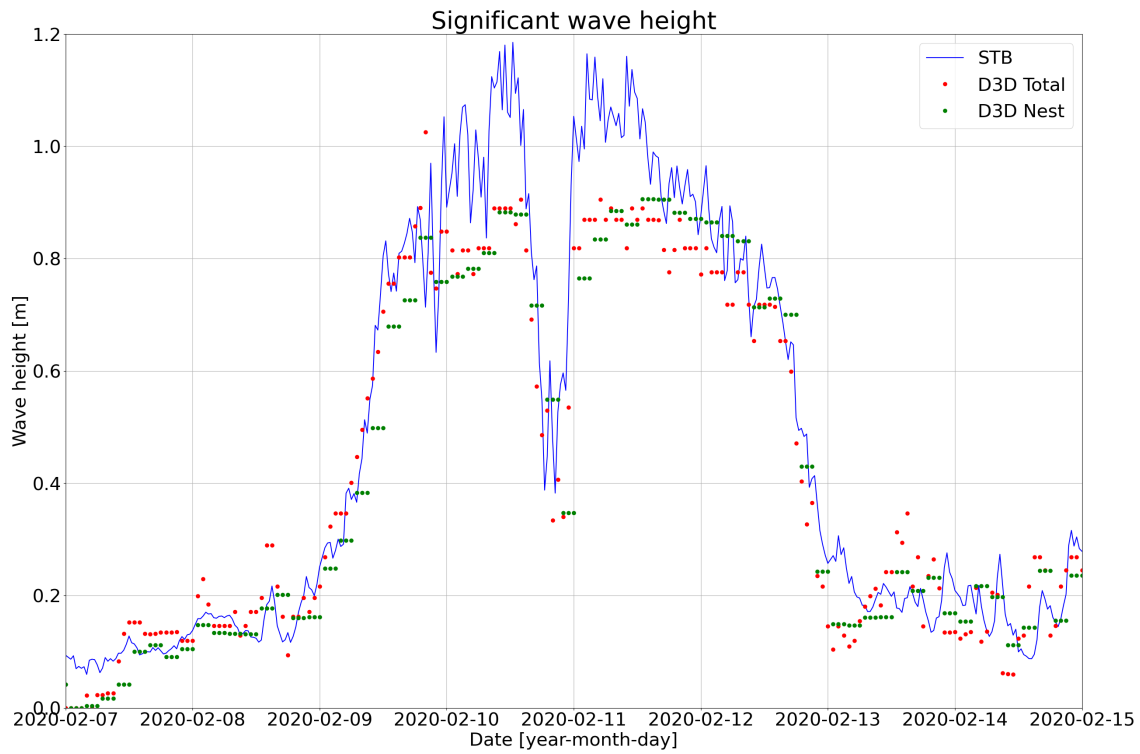
(a)



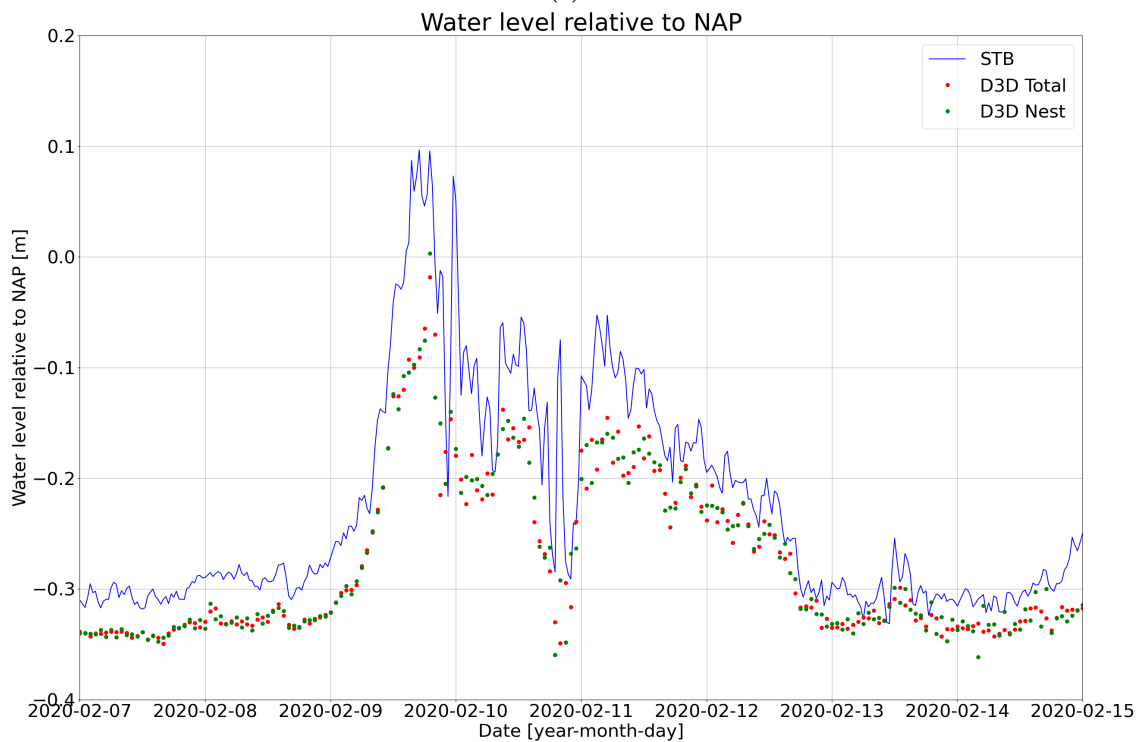
(b)

Figure D.5: Two figures showing: (a) Significant wave-height obtained by the STB at FL66 (blue line) compared to computed significant wave-height at the FL66 observation point in D3D (total model are the red dots, nested model are the green dots); (b) Water level relative to NAP as obtained by the STB at FL66 (blue line) and by the model (total model are the red dots, nested model are the green dots).

D.3.2 High-energy event: 7 - 15 February 2020



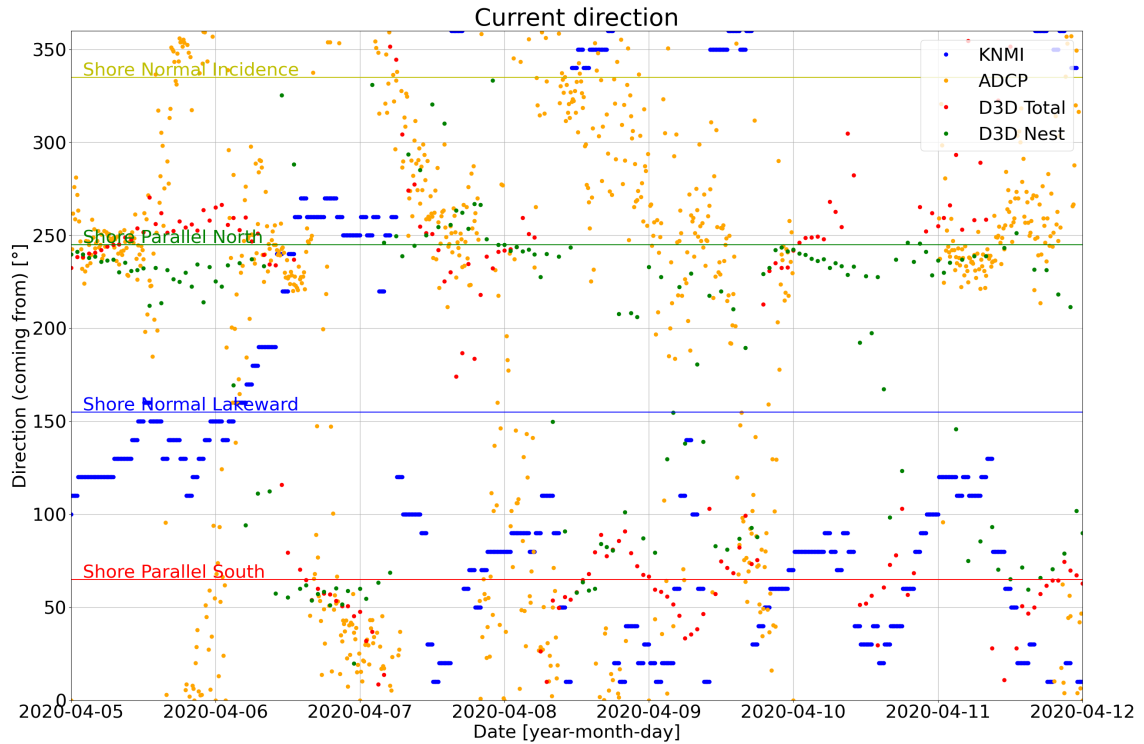
(a)



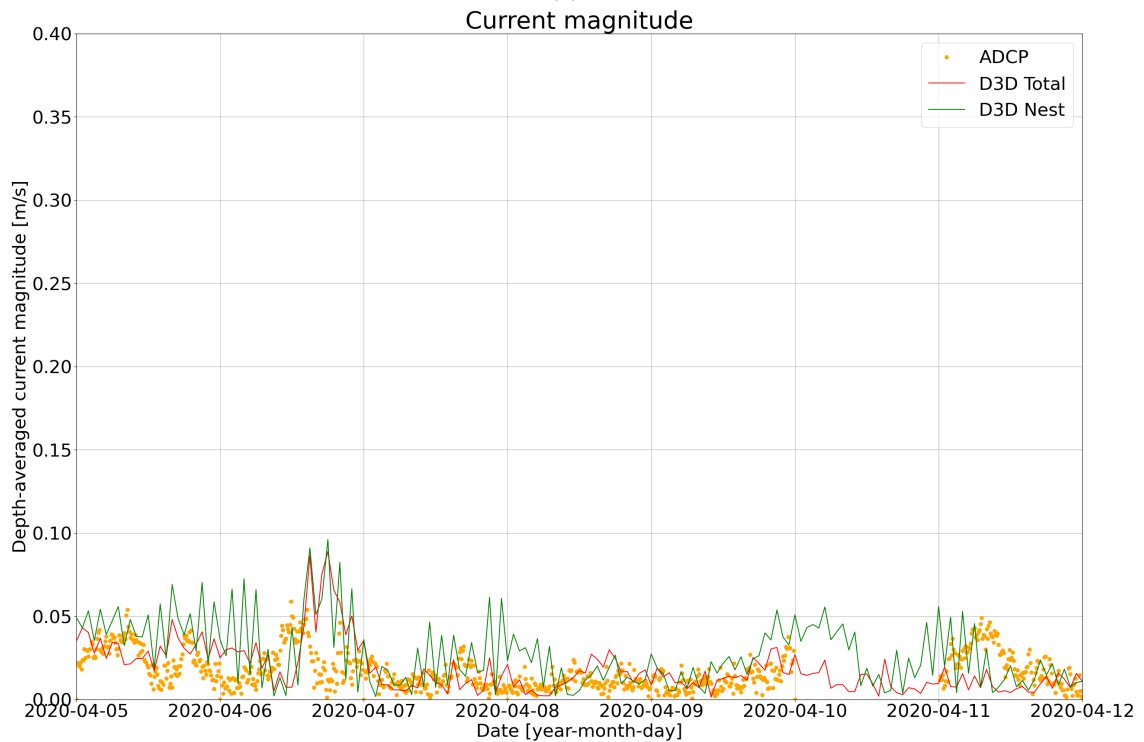
(b)

Figure D.6: Two figures showing: (a) Significant wave-height obtained by the STB at FL66 (blue line) compared to computed significant wave-height at the FL66 observation point in D3D (total model are the red dots, nested model are the green dots); (b) Water level relative to NAP as obtained by the STB at FL66 (blue line) and by the model (total model results are the red dots, nested model results are the green dots).

D.3.3 Calm period: 5 - 12 April 2020

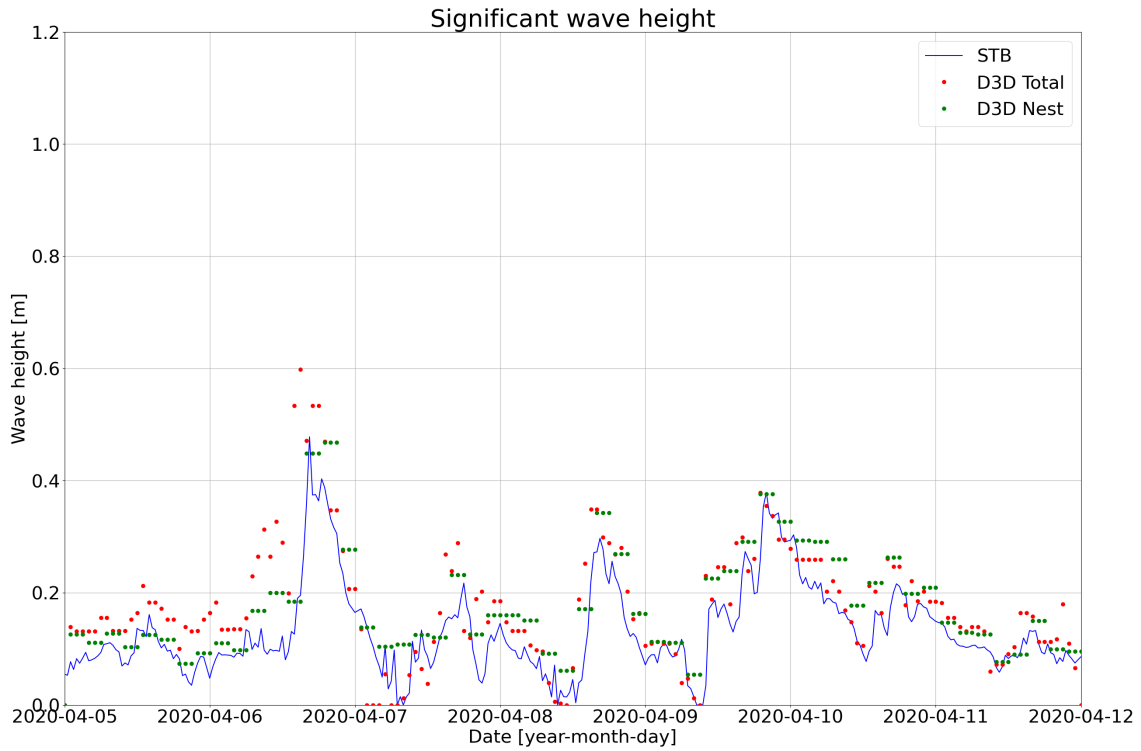


(a)

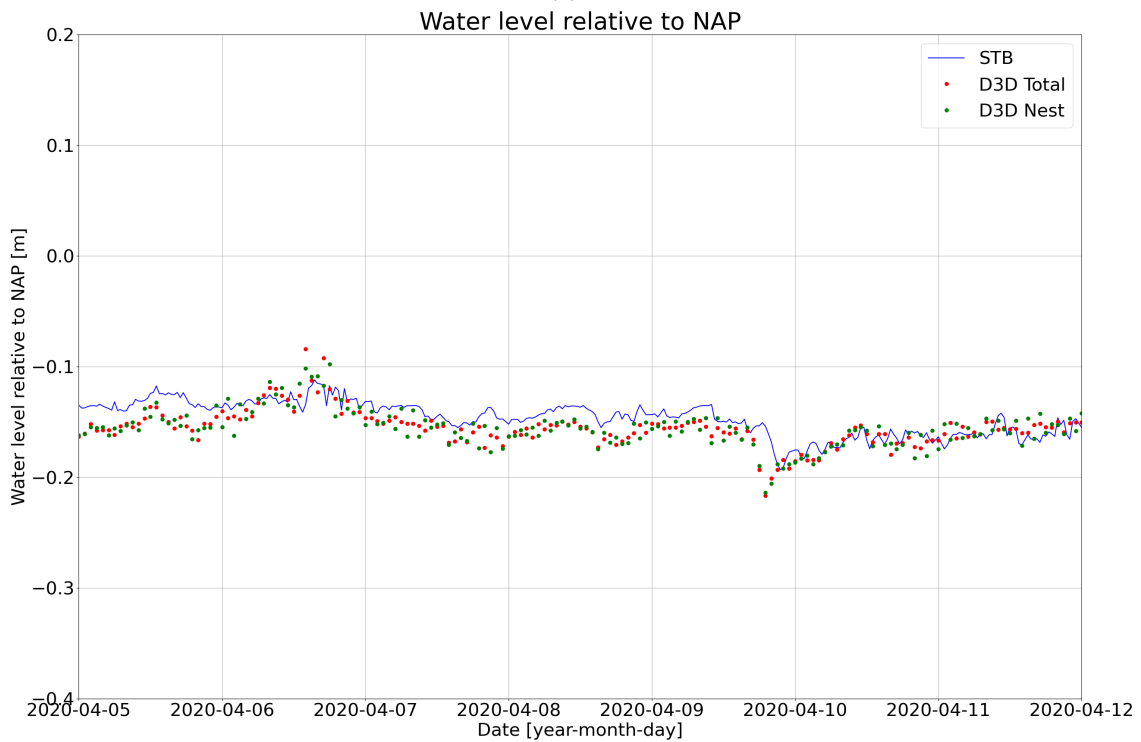


(b)

Figure D.7: Two figures showing: (a) Current direction comparing ADCP measurements obtained at FL66 (orange dots) and model output at observation point FL66 (total model results are the red dots and nested model results are shown in green); (b) Current magnitude comparing ADCP measurements obtained at FL66 (orange dots) with model results (red dots represent total model results and green dots are nested model results).



(a)



(b)

Figure D.8: Two figures showing: (a) Significant wave-height obtained by the STB at FL66 (blue line) compared to computed significant wave-height at the FL66 observation point in D3D (total model are the red dots, nested model are the green dots); (b) Water level relative to NAP as obtained by the STB at FL66 (blue line) and by the model (total model results are the red dots, nested model results are the green dots).

D3D Model Results

This appendix contains supplementary results of the Marker Wadden model. The main important results are presented in chapter 9.

E.1 Idealised Wind Schematization Runs

For the seven identified wind directions the model outcomes of the *nested model* are shown in this section. Presenting an overview of the entire *nested model*, a close-up of the northern part of the Marker Wadden and a zoom-in of the Noordstrand.

E.1.1 Wind coming from 20°

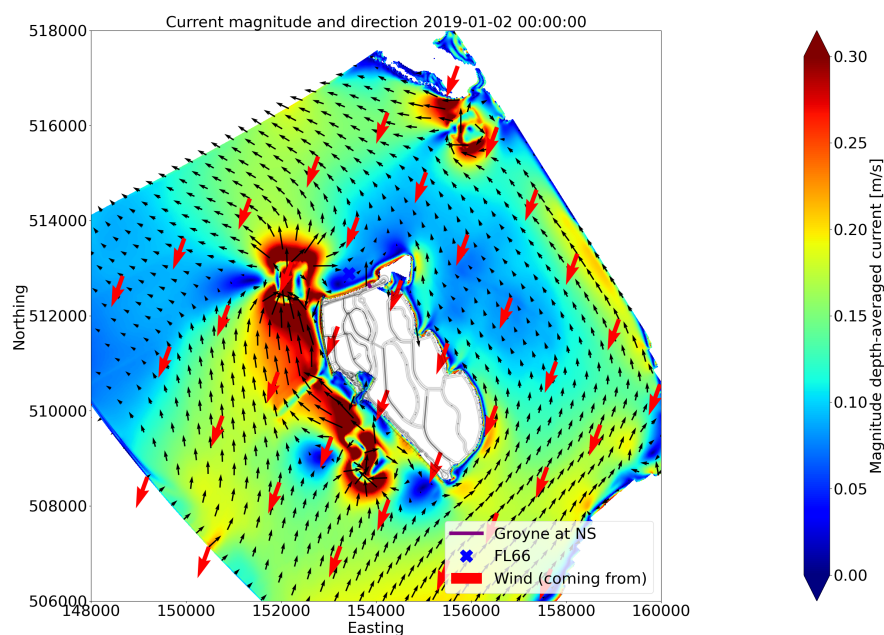
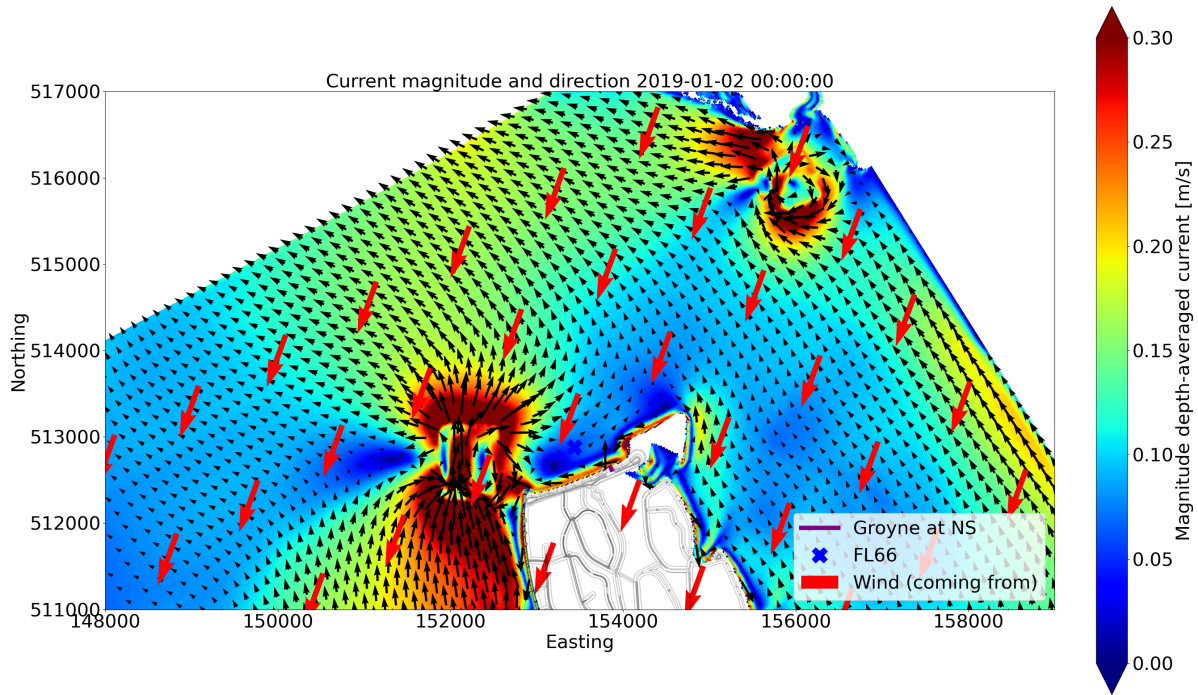
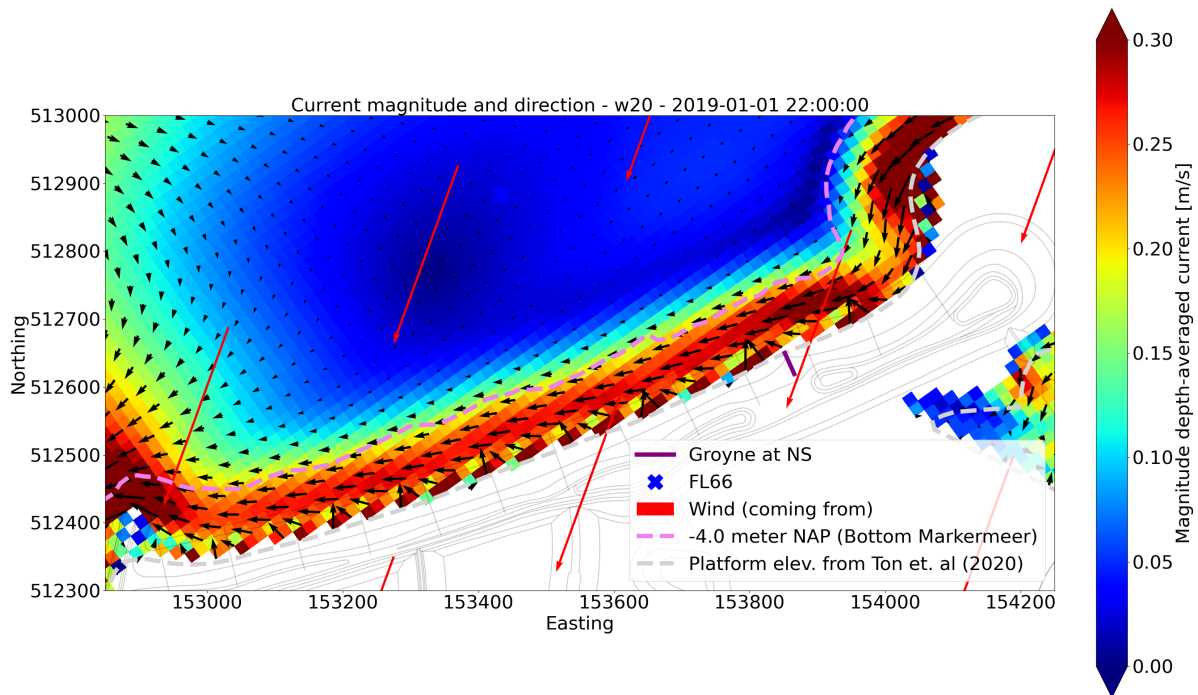


Figure E.1: Current magnitude and direction for **wind coming from 20°** at the moment of maximum wind speed, showing the entire *nested model* and thus the flow circulation around the Marker Wadden. The boundaries on the top and bottom left are connected to the *total model* (not visible in this plot). The boundaries in the top (Houtribdijk) and bottom right are land boundaries and thus closed.



(a)



(b)

Figure E.2: Two figures showing: (a) Current magnitude and direction for **wind coming from 20°** at the moment of maximum wind speed, showing the northern part of the *nested model*, the boundary on the top left is connected to the *total model* (not visible), the boundary on the top right is a land boundary, representing the Houtribdijk; (b) Current magnitude and direction for **wind coming from 20°** at the moment of maximum wind speed zooming in to the Noordstrand. For both figures: The dashed lines indicate depth contours: bottom lake (pink) and offshore platform (grey). The red arrows indicates direction the wind is blowing to and the length of the arrow indicates the wind speed. FL66 is visible in the top middle of the figure (blue cross).

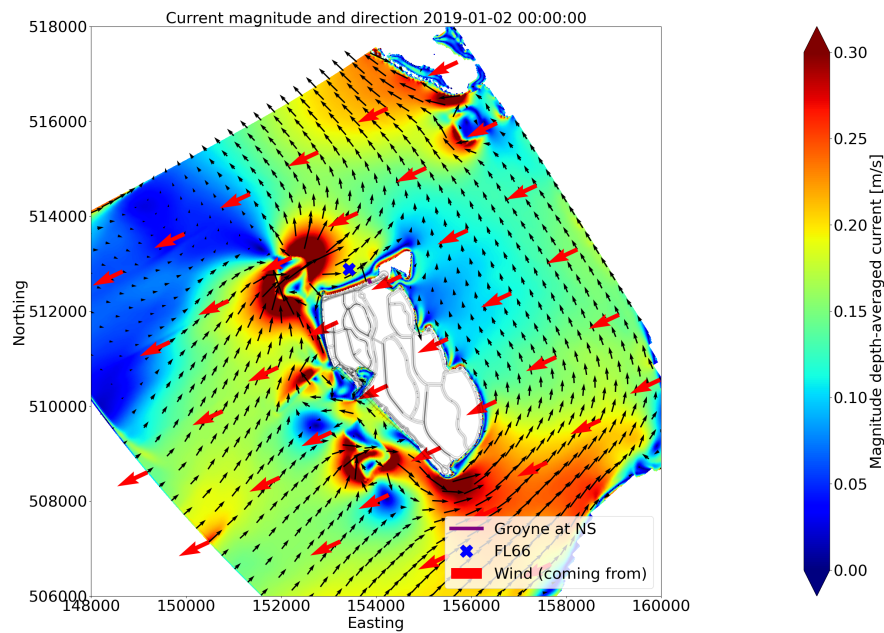
E.1.2 *Wind coming from 65°*

Figure E.3: Current magnitude and direction for **wind coming from 65°** at the moment of maximum wind speed, showing the entire *nested model* and thus the flow circulation around the Marker Wadden. The boundaries on the top and bottom left are connected to the *total model* (not visible in this plot). The boundaries in the top (Houtribdijk) and bottom right are land boundaries and thus closed.

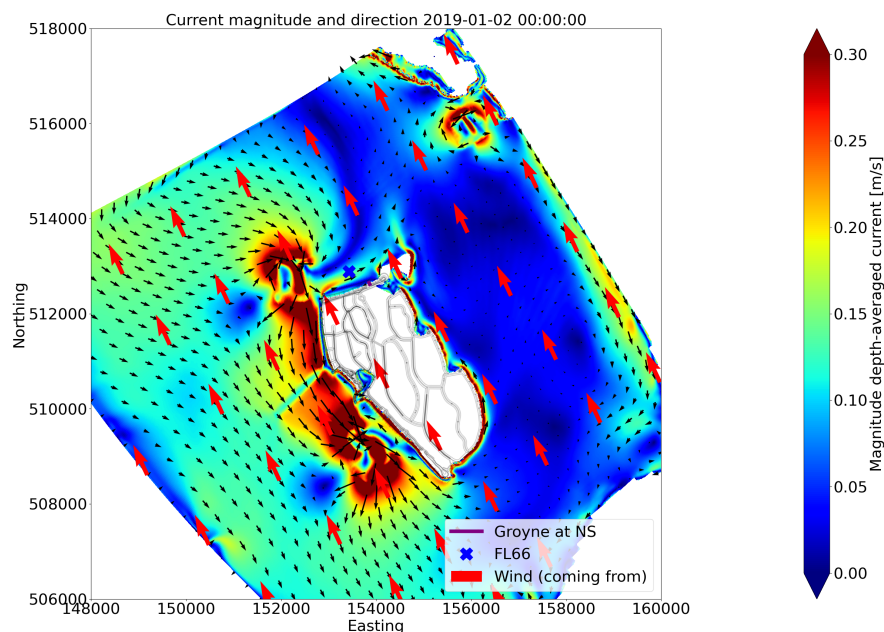
E.1.3 *Wind coming from 155°*

Figure E.4: Current magnitude and direction for **wind coming from 155°** at the moment of maximum wind speed, showing the entire *nested model* and thus the flow circulation around the Marker Wadden. The boundaries on the top and bottom left are connected to the *total model* (not visible in this plot). The boundaries in the top (Houtribdijk) and bottom right are land boundaries and thus closed.

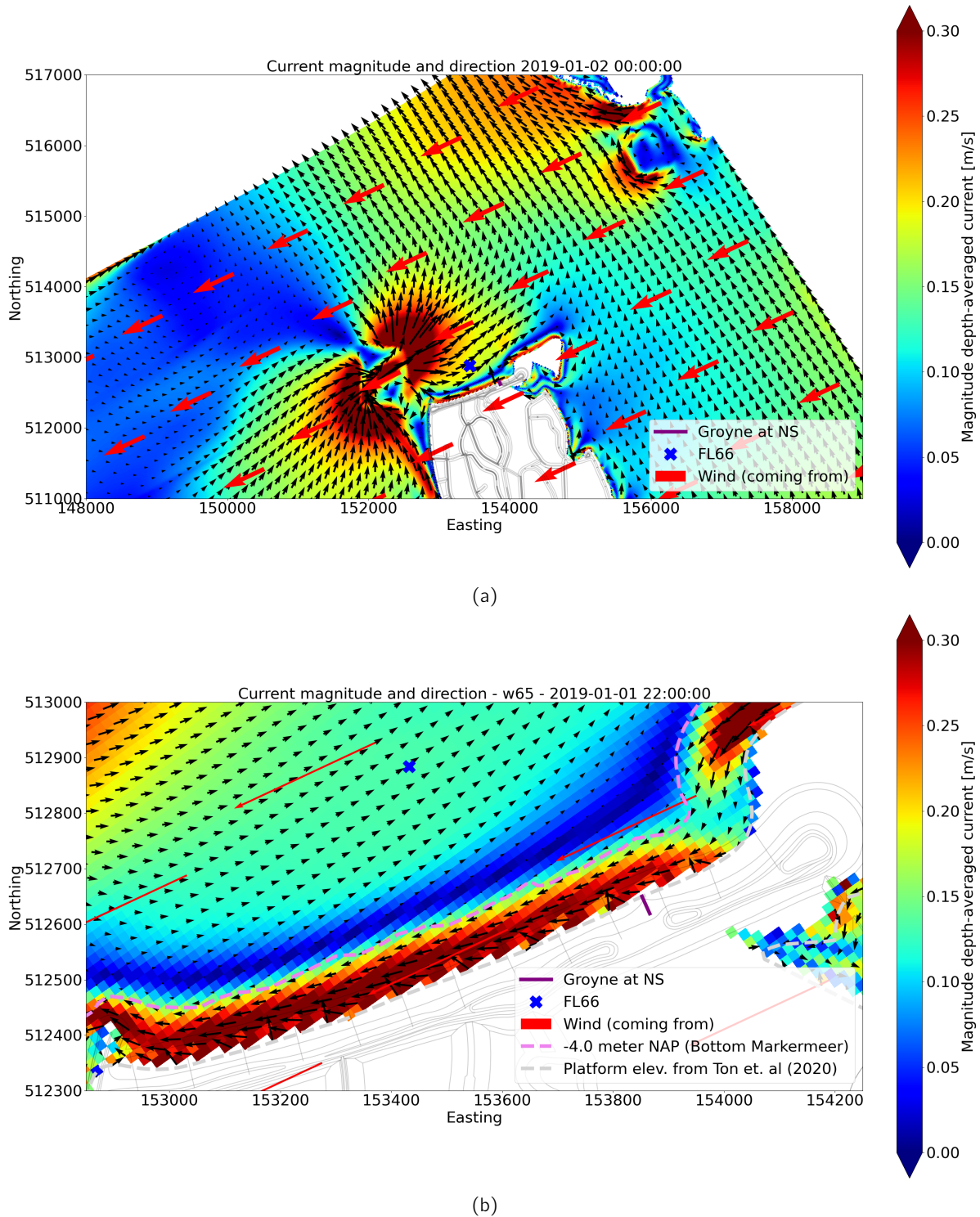


Figure E.5: Two figures showing: (a) Current magnitude and direction for **wind coming from 65°** at the moment of maximum wind speed, showing the northern part of the *nested model*, the boundary on the top left is connected to the *total model* (not visible), the boundary on the top right is a land boundary, representing the Houtribdijk; (b) Current magnitude and direction for **wind coming from 65°** at the moment of maximum wind speed zooming in to the Noordstrand. For both figures: The dashed lines indicate depth contours: bottom lake (pink) and offshore platform (grey). The red arrows indicates direction the wind is blowing to and the length of the arrow indicates the wind speed. FL66 is visible in the top middle of the figure (blue cross).

Wind coming from 155°

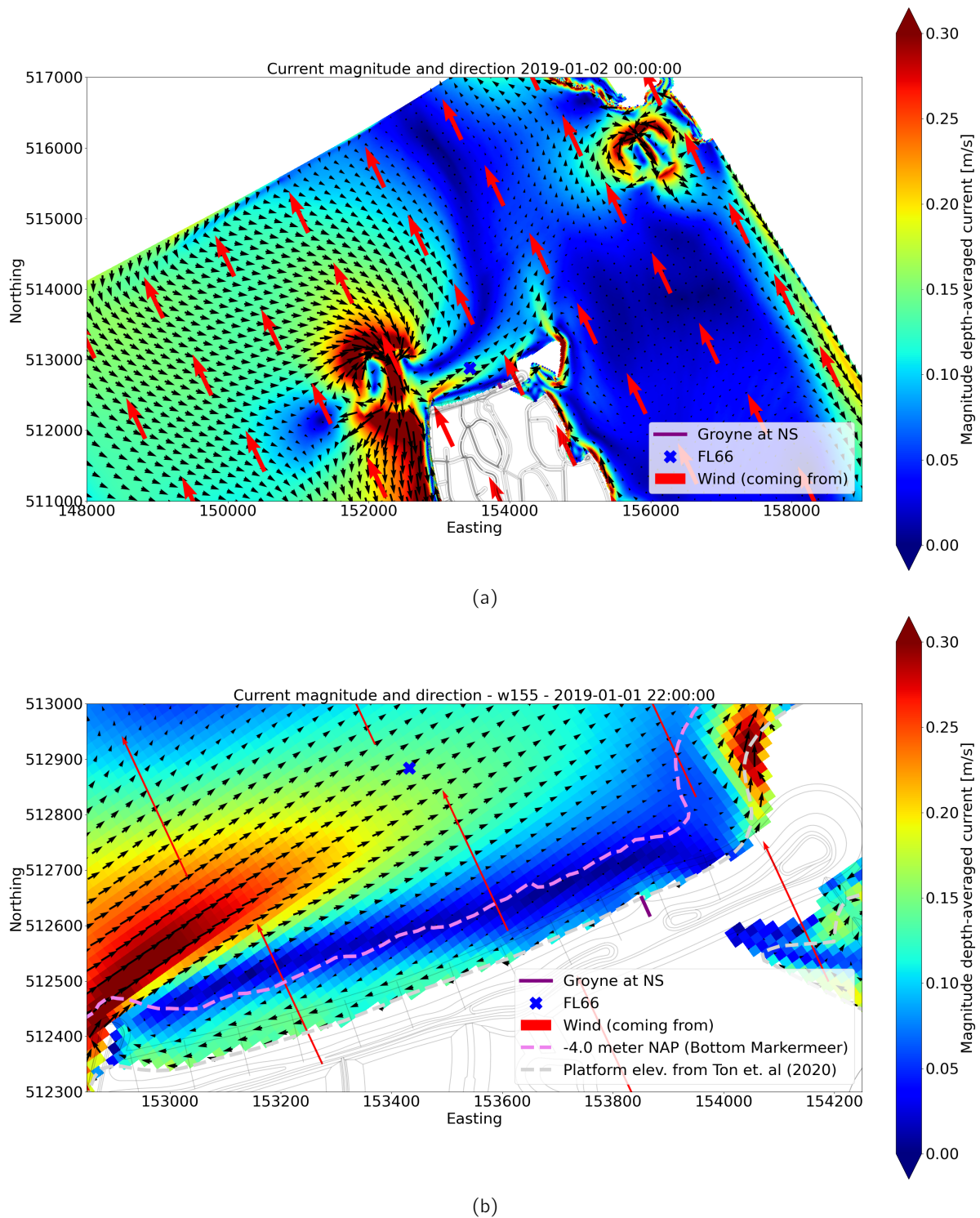


Figure E.6: Two figures showing: (a) Current magnitude and direction for **wind coming from 155°** at the moment of maximum wind speed, showing the northern part of the *nested model*, the boundary on the top left is connected to the *total model* (not visible), the boundary on the top right is a land boundary, representing the Houtribdijk; (b) Current magnitude and direction for **wind coming from 155°** at the moment of maximum wind speed zooming in to the Noordstrand. For both figures: The dashed lines indicate depth contours: bottom lake (pink) and offshore platform (grey). The red arrows indicates direction the wind is blowing to and the length of the arrow indicates the wind speed. FL66 is visible in the top middle of the figure (blue cross).

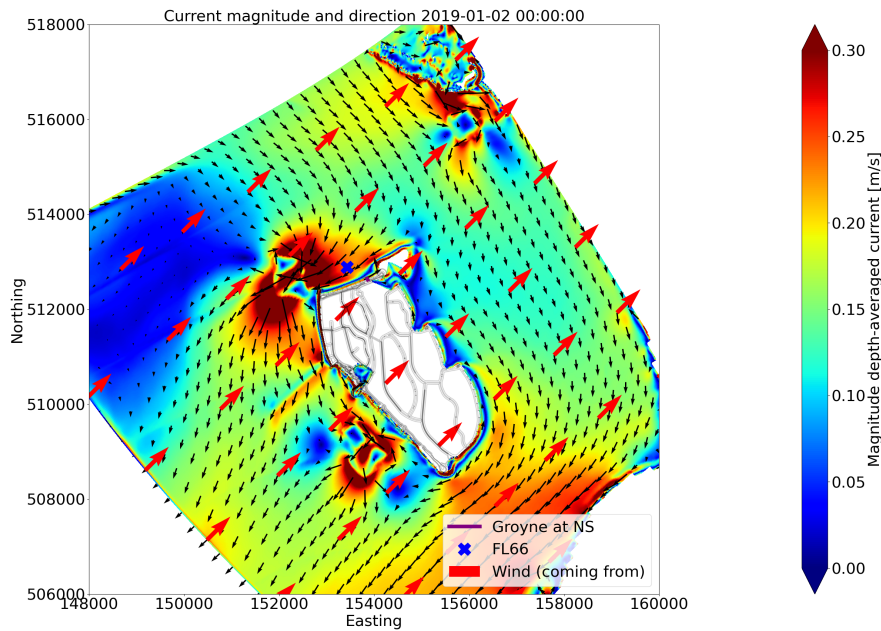
E.1.4 *Wind coming from 225°*

Figure E.7: Current magnitude and direction for **wind coming from 225°** at the moment of maximum wind speed, showing the entire *nested model* and thus the flow circulation around the Marker Wadden. The boundaries on the top and bottom left are connected to the *total model* (not visible in this plot). The boundaries in the top (Houtribdijk) and bottom right are land boundaries and thus closed.

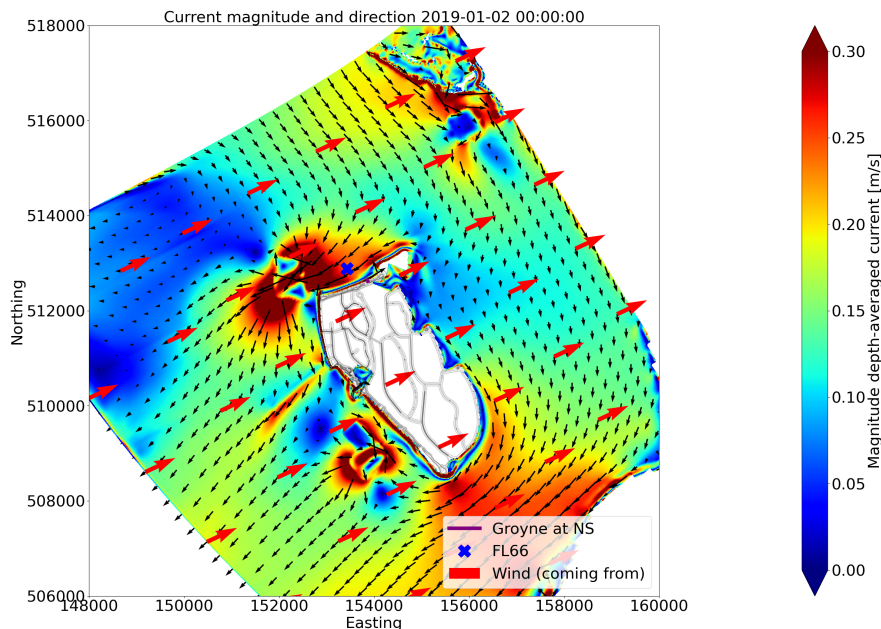
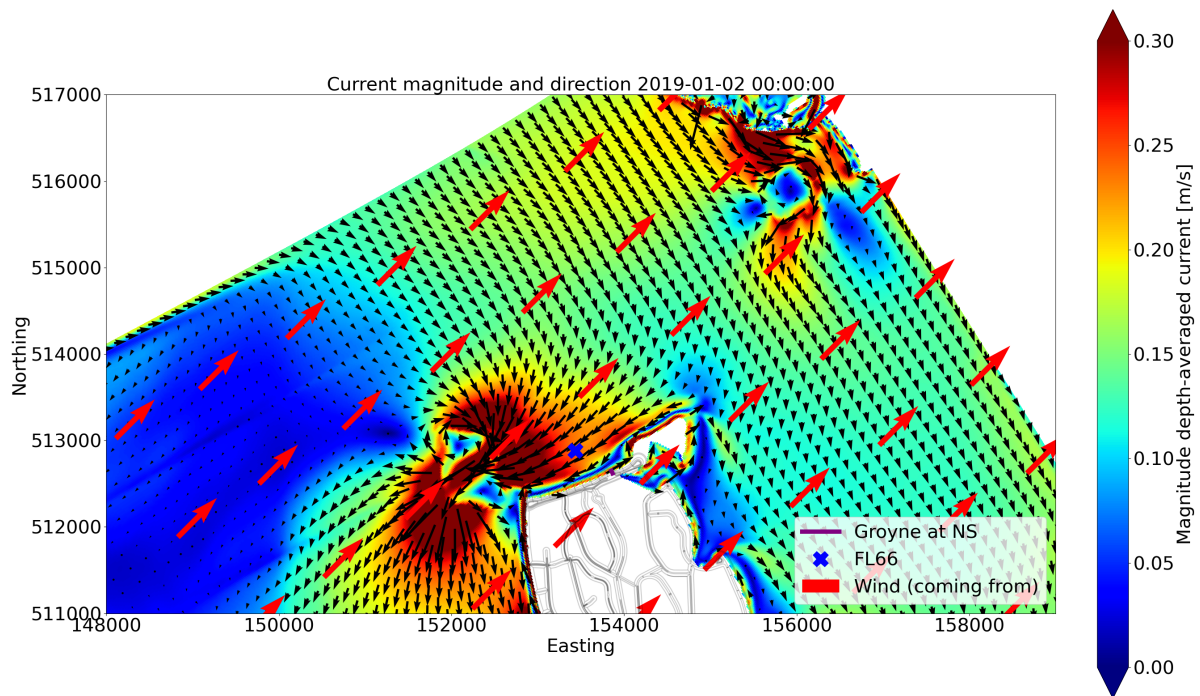
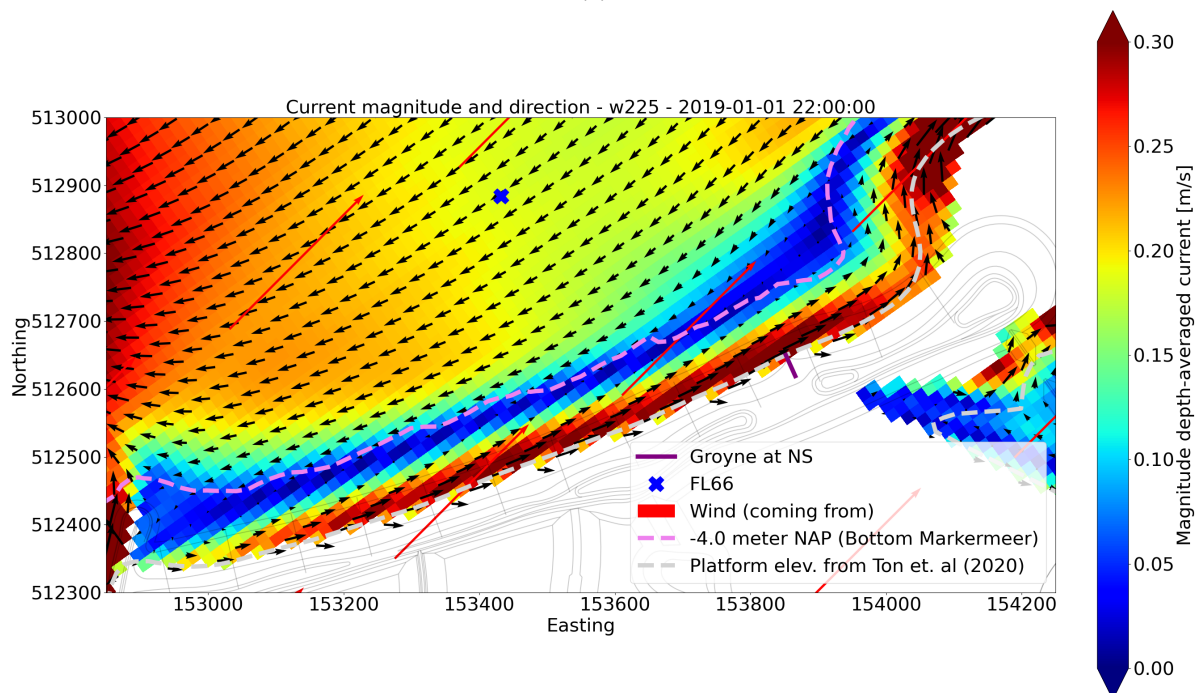
E.1.5 *Wind coming from 245°*

Figure E.8: Current magnitude and direction for **wind coming from 245°** at the moment of maximum wind speed, showing the entire *nested model* and thus the flow circulation around the Marker Wadden. The boundaries on the top and bottom left are connected to the *total model* (not visible in this plot). The boundaries in the top (Houtribdijk) and bottom right are land boundaries and thus closed.

Wind coming from 225°



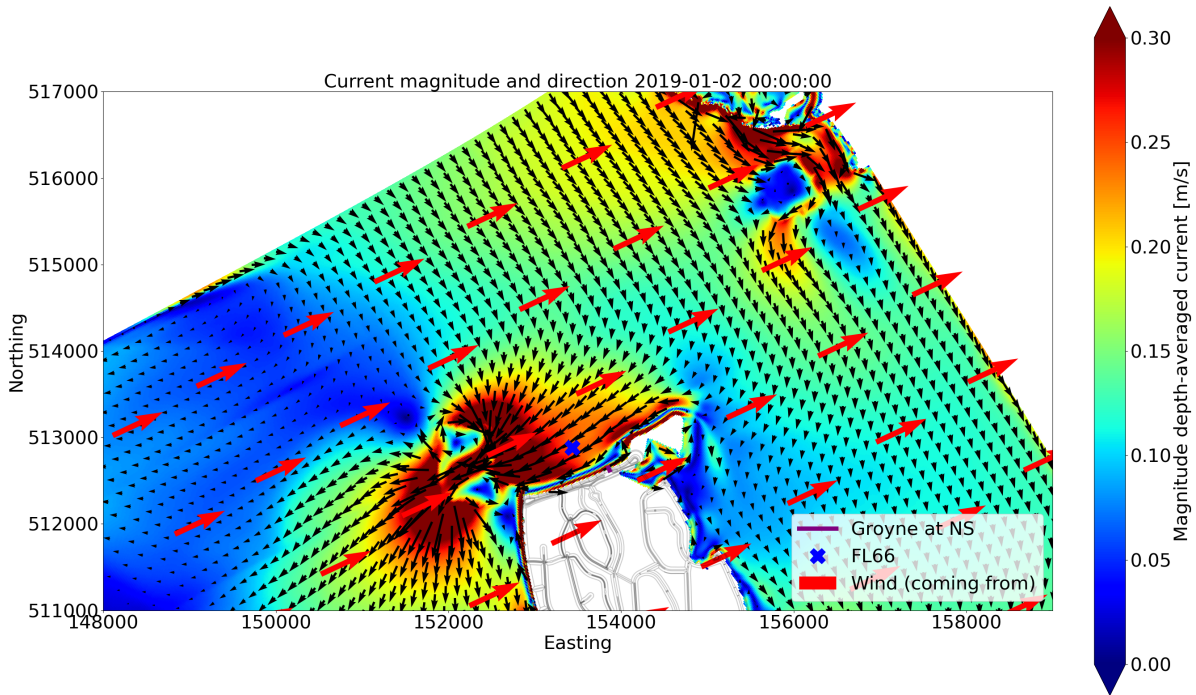
(a)



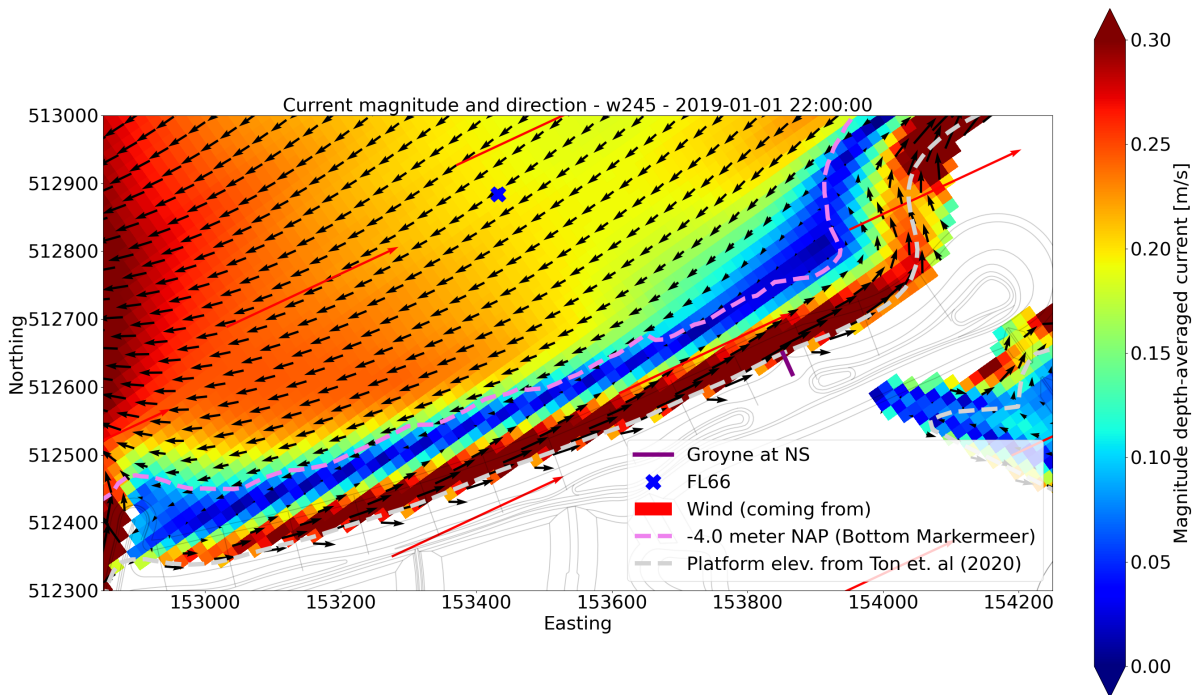
(b)

Figure E.9: Two figures showing: (a) Current magnitude and direction for **wind coming from 225°** at the moment of maximum wind speed, showing the northern part of the *nested model*, the boundary on the top left is connected to the *total model* (not visible), the boundary on the top right is a land boundary, representing the Houtribdijk; (b) Current magnitude and direction for **wind coming from 225°** at the moment of maximum wind speed zooming in to the Noordstrand. For both figures: The dashed lines indicate depth contours: bottom lake (pink) and offshore platform (grey). The red arrows indicates direction the wind is blowing to and the length of the arrow indicates the wind speed. FL66 is visible in the top middle of the figure (blue cross).

Wind coming from 245°



(a)



(b)

Figure E.10: Two figures showing: (a) Current magnitude and direction for **wind coming from 245°** at the moment of maximum wind speed, showing the northern part of the *nested model*, the boundary on the top left is connected to the *total model* (not visible), the boundary on the top right is a land boundary, representing the Houtribdijk; (b) Current magnitude and direction for **wind coming from 245°** at the moment of maximum wind speed zooming in to the Noordstrand. For both figures: The dashed lines indicate depth contours: bottom lake (pink) and offshore platform (grey). The red arrows indicates direction the wind is blowing to and the length of the arrow indicates the wind speed. FL66 is visible in the top middle of the figure (blue cross).

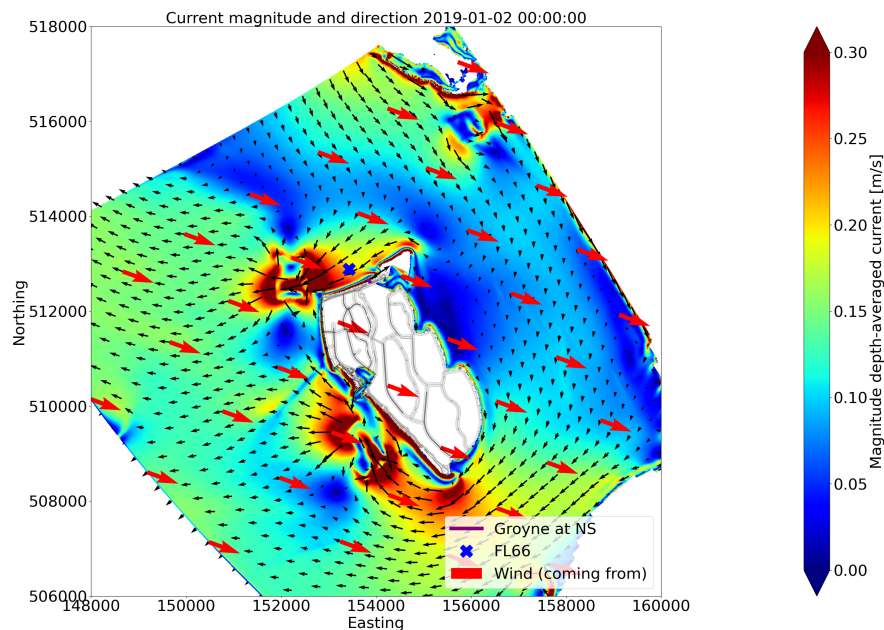
E.1.6 *Wind coming from 290°*

Figure E.11: Current magnitude and direction for **wind coming from 290°** at the moment of maximum wind speed, showing the entire *nested model* and thus the flow circulation around the Marker Wadden. The boundaries on the top and bottom left are connected to the *total model* (not visible in this plot). The boundaries in the top (Houtribdijk) and bottom right are land boundaries and thus closed.

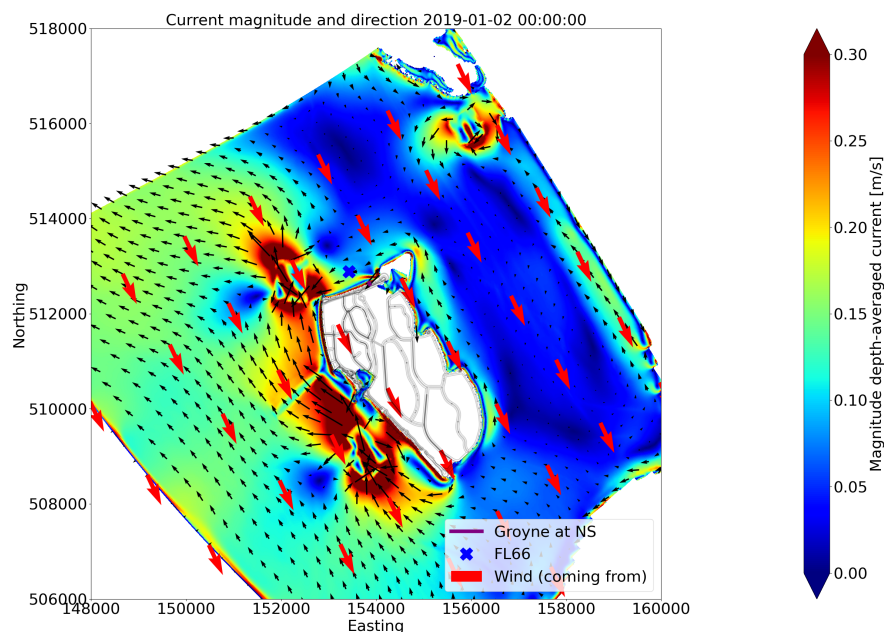
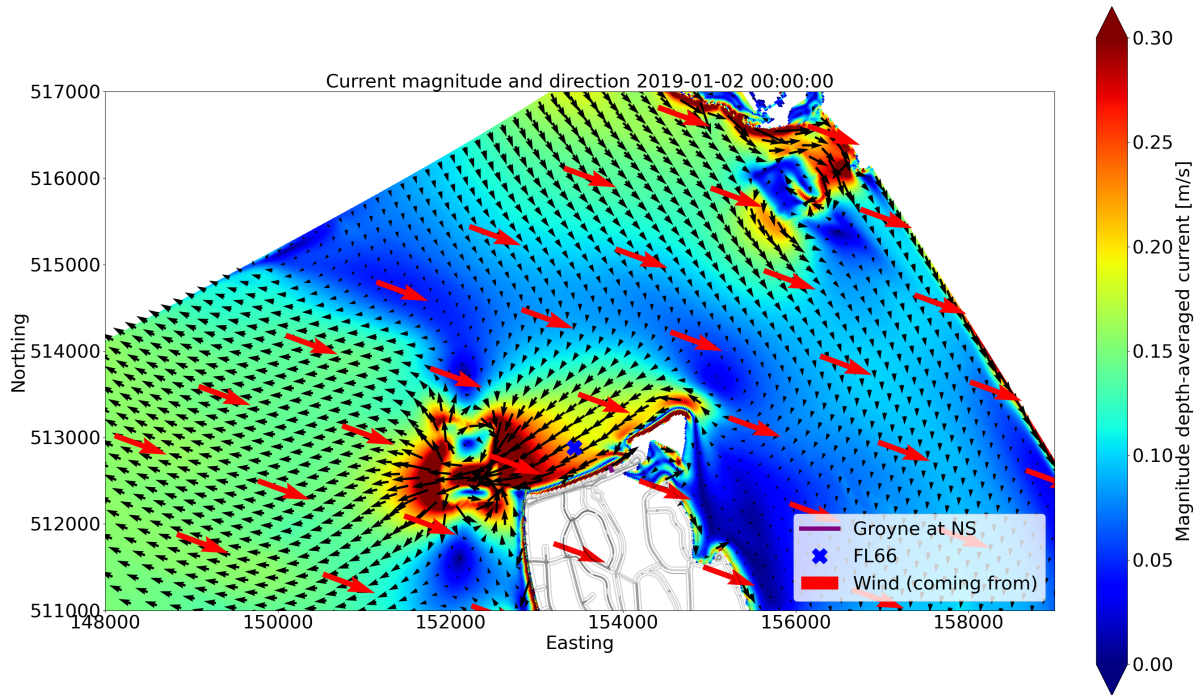
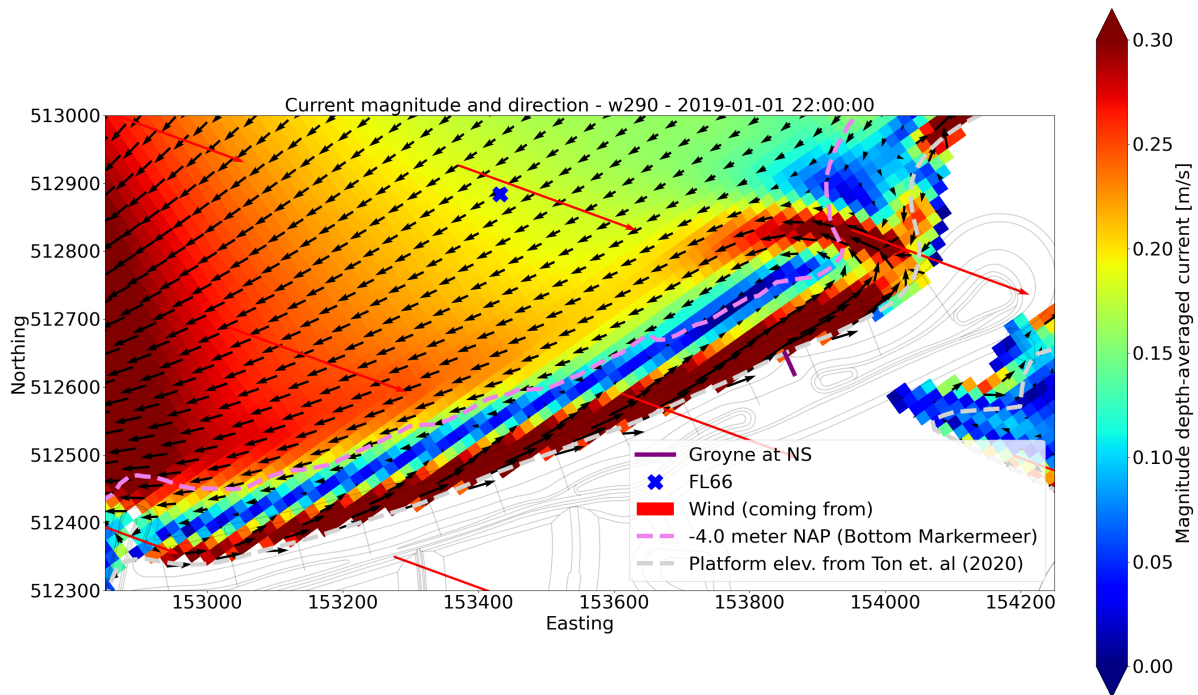
E.1.7 *Wind coming from 335°*

Figure E.12: Current magnitude and direction for **wind coming from 335°** at the moment of maximum wind speed, showing the entire *nested model* and thus the flow circulation around the Marker Wadden. The boundaries on the top and bottom left are connected to the *total model* (not visible in this plot). The boundaries in the top (Houtribdijk) and bottom right are land boundaries and thus closed.

Wind coming from 290°



(a)



(b)

Figure E.13: Two figures showing: (a) Current magnitude and direction for **wind coming from 290°** at the moment of maximum wind speed, showing the northern part of the *nested model*, the boundary on the top left is connected to the *total model* (not visible), the boundary on the top right is a land boundary, representing the Houtribdijk; (b) Current magnitude and direction for **wind coming from 290°** at the moment of maximum wind speed zooming in to the Noordstrand. For both figures: The dashed lines indicate depth contours: bottom lake (pink) and offshore platform (grey). The red arrows indicates direction the wind is blowing to and the length of the arrow indicates the wind speed. FL66 is visible in the top middle of the figure (blue cross).

Wind coming from 335°

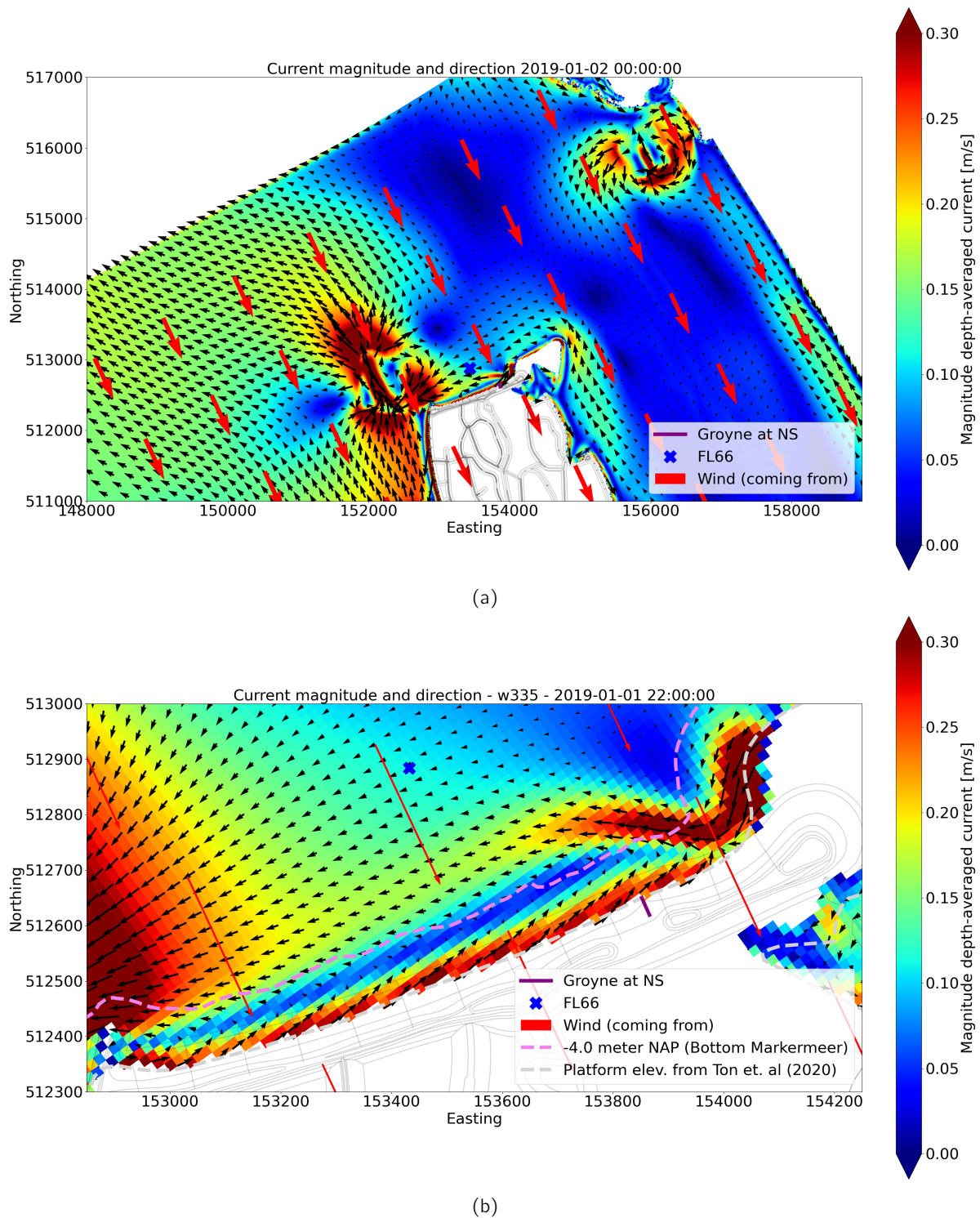


Figure E.14: Two figures showing: (a) Current magnitude and direction for **wind coming from 335°** at the moment of maximum wind speed, showing the northern part of the *nested model*, the boundary on the top left is connected to the *total model* (not visible), the boundary on the top right is a land boundary, representing the Houtribdijk; (b) Current magnitude and direction for **wind coming from 335°** at the moment of maximum wind speed zooming in to the Noordstrand. For both figures: The dashed lines indicate depth contours: bottom lake (pink) and offshore platform (grey). The red arrows indicates direction the wind is blowing to and the length of the arrow indicates the wind speed. FL66 is visible in the top middle of the figure (blue cross).

E.2 Comparing Flow & Waves to Only Flow

The previous section has shown results considering the flow and waves computations (the idealized wind schematization runs). In this section the flow & waves computations are compared to the flow only computations. Considering a wind direction of 245° and 335°.

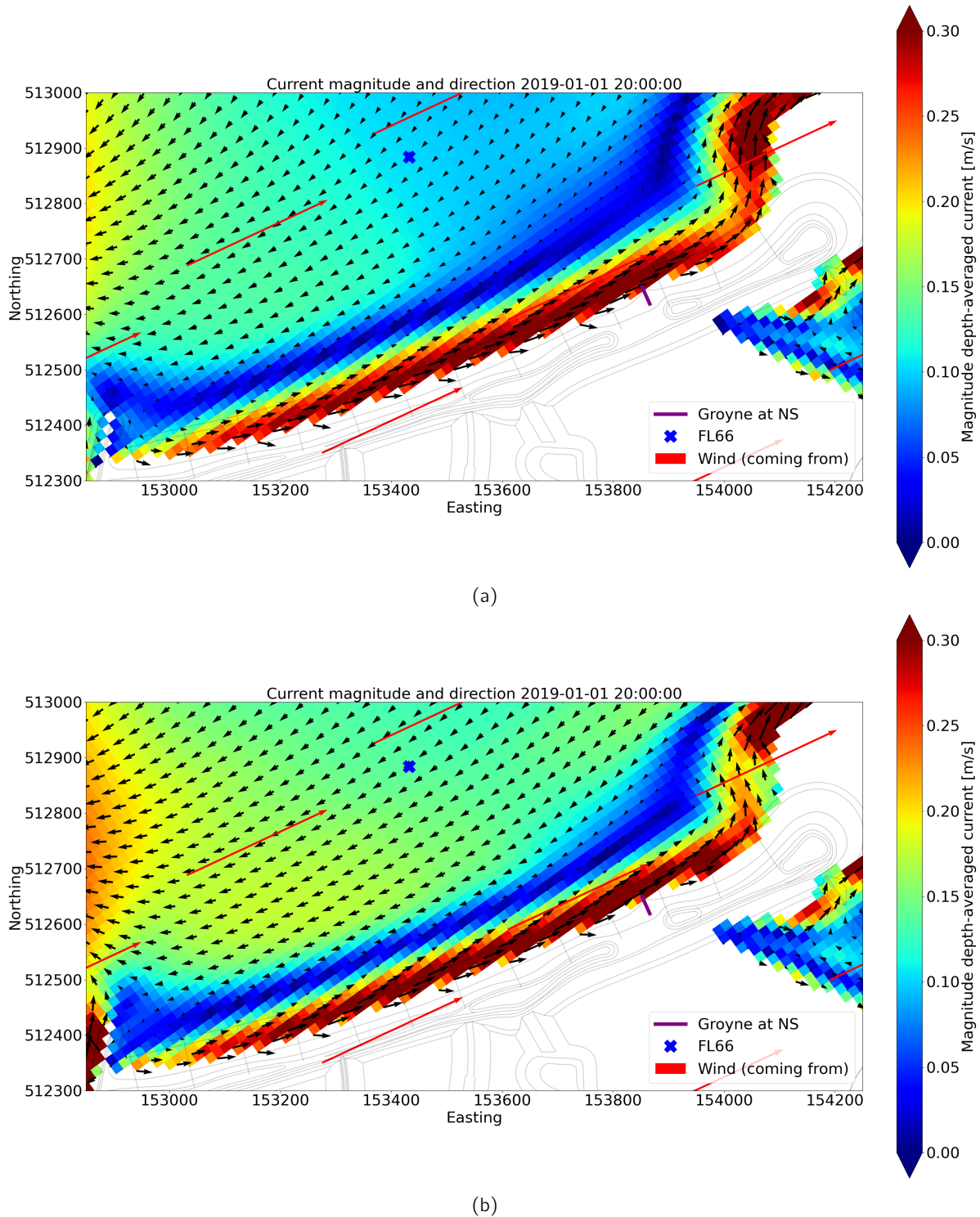


Figure E.15: Comparing flow and waves to only flow for **wind coming from 245°**, just now wind speed is maximum: (a) **FLOW** computation only: current magnitude and direction; (b) **FLOW & WAVES** computation: current magnitude and direction

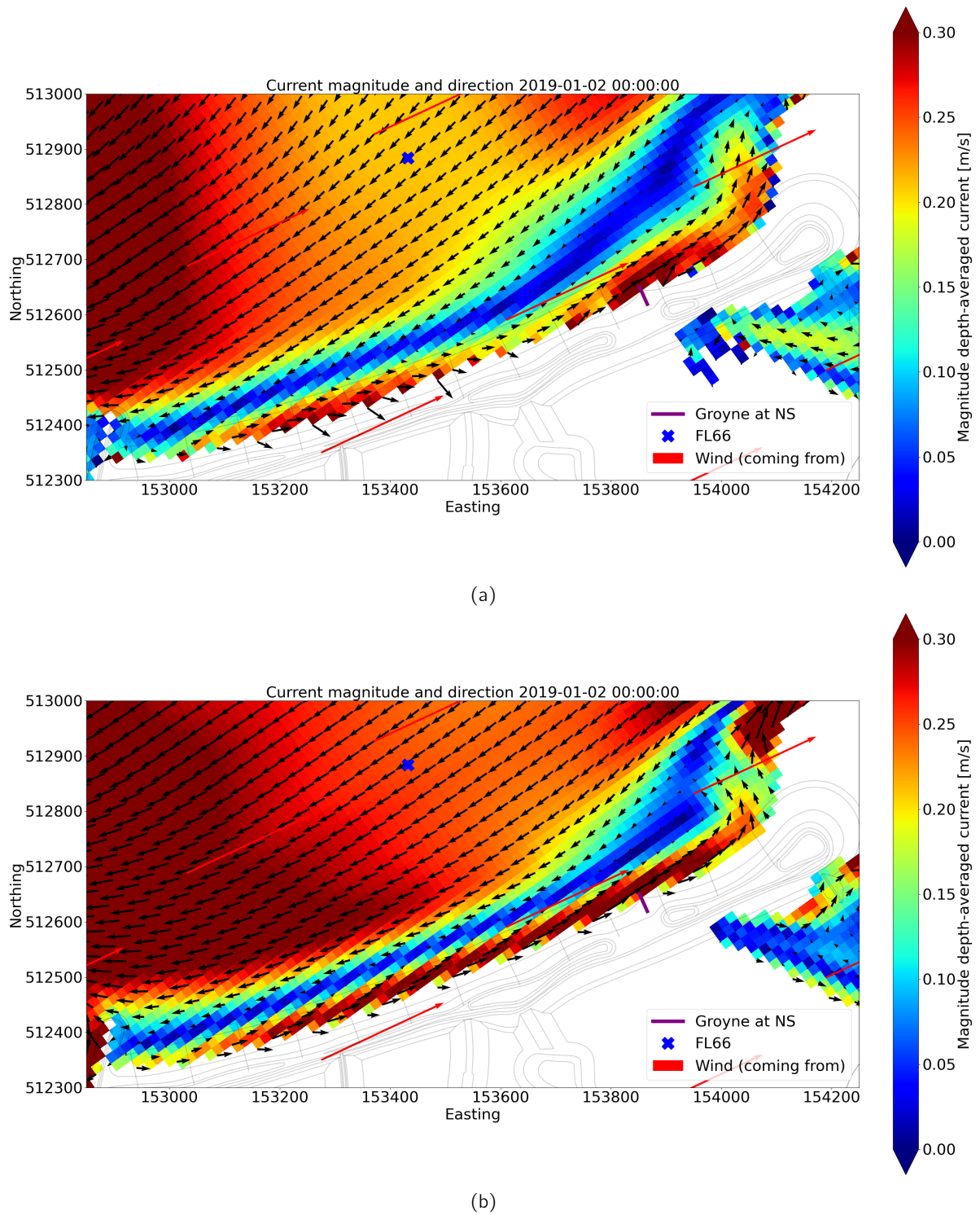
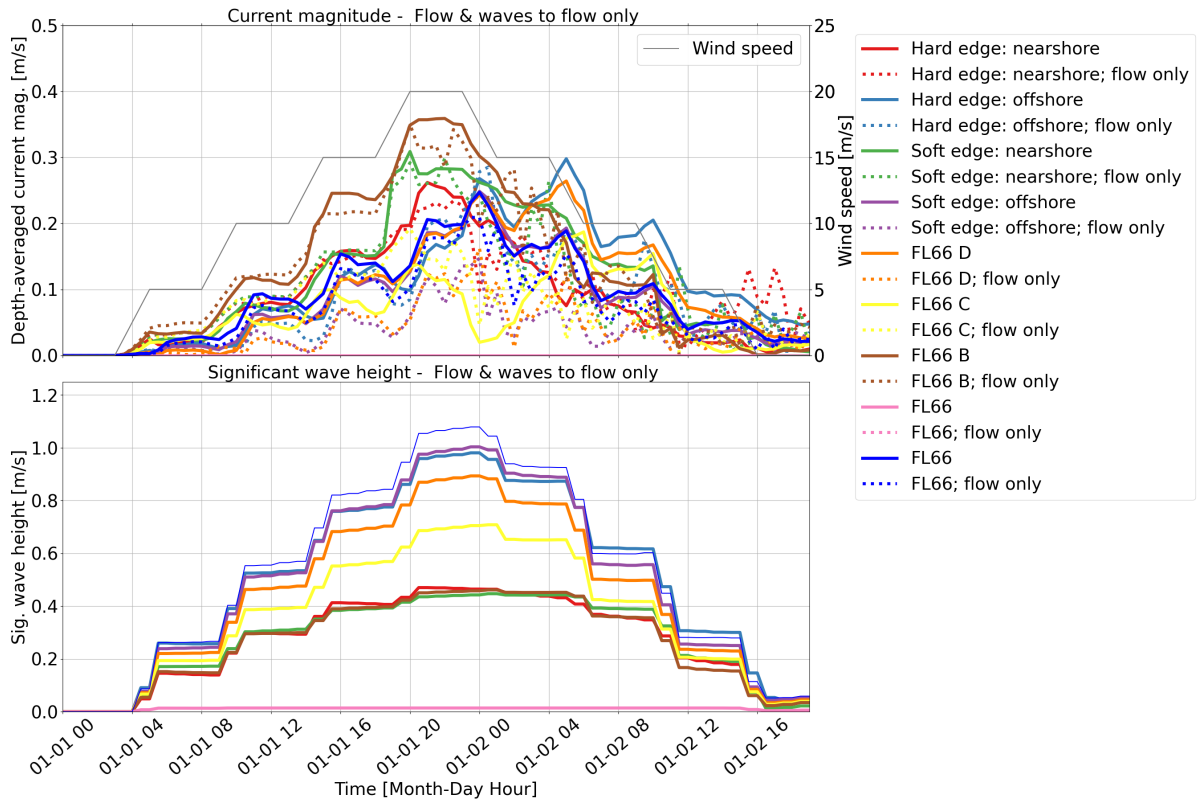
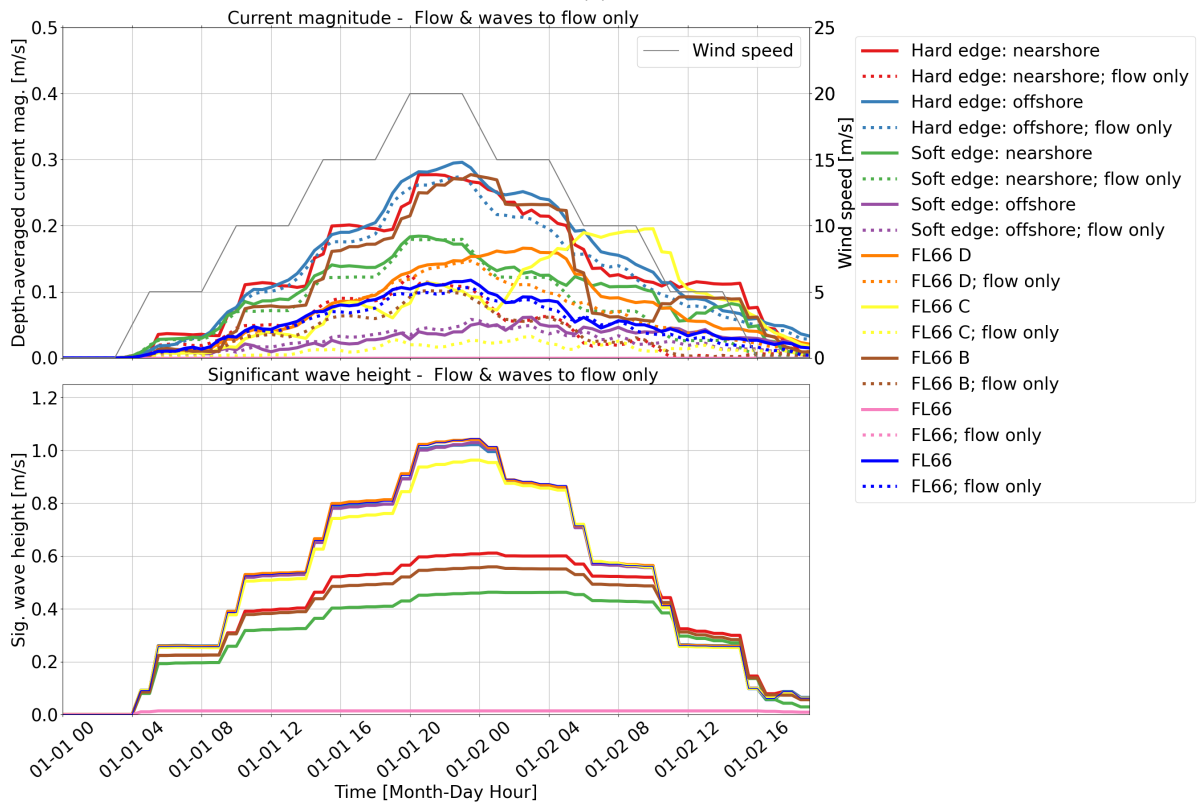


Figure E.16: Comparing flow and waves to only flow for **wind coming from 245°**, 1 hours after wind speed was maximum: (a) **FLOW** computation only: current magnitude and direction; (b) **FLOW & WAVES** computation: current magnitude and direction



(a)



(b)

Figure E.17: Current magnitude (top) and significant wave height (bottom) in the observation points. The development of the wind speed is shown in grey in the top figure. Colours of the lines correspond to the locations as shown in figure 8.10. Solid lines indicate *flow & waves*, dashed lines *only flow*. As a result the bottom plot only shows wave heights for the *flow & wave* computation. (a) **wind coming from 245°**; (b) **wind coming from 290°**

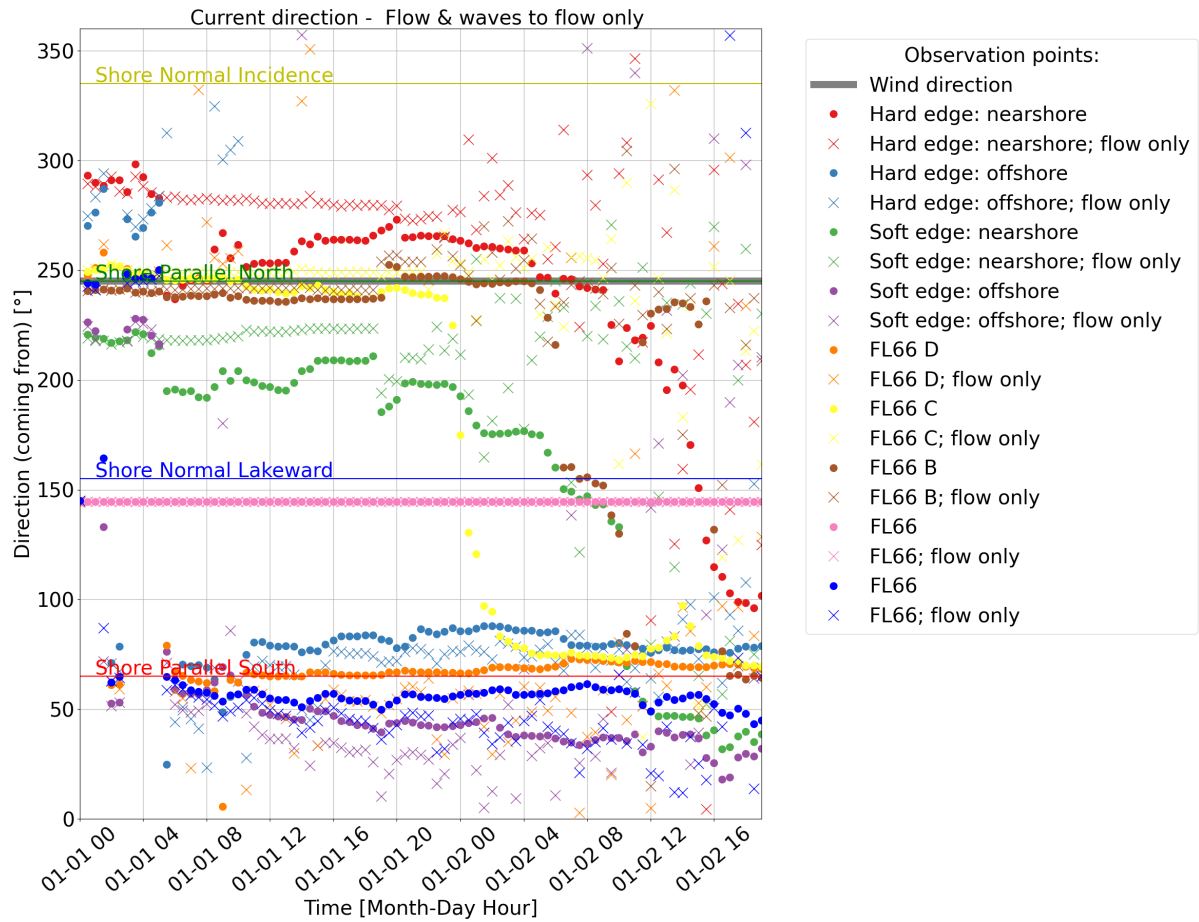


Figure E.18: Current direction (coming from) in the observation points for wind coming from 245° . The direction of the wind is shown in grey. Colours of the lines correspond to the locations as shown in figure 8.10. Solid dots indicate flow & waves, x's only flow.

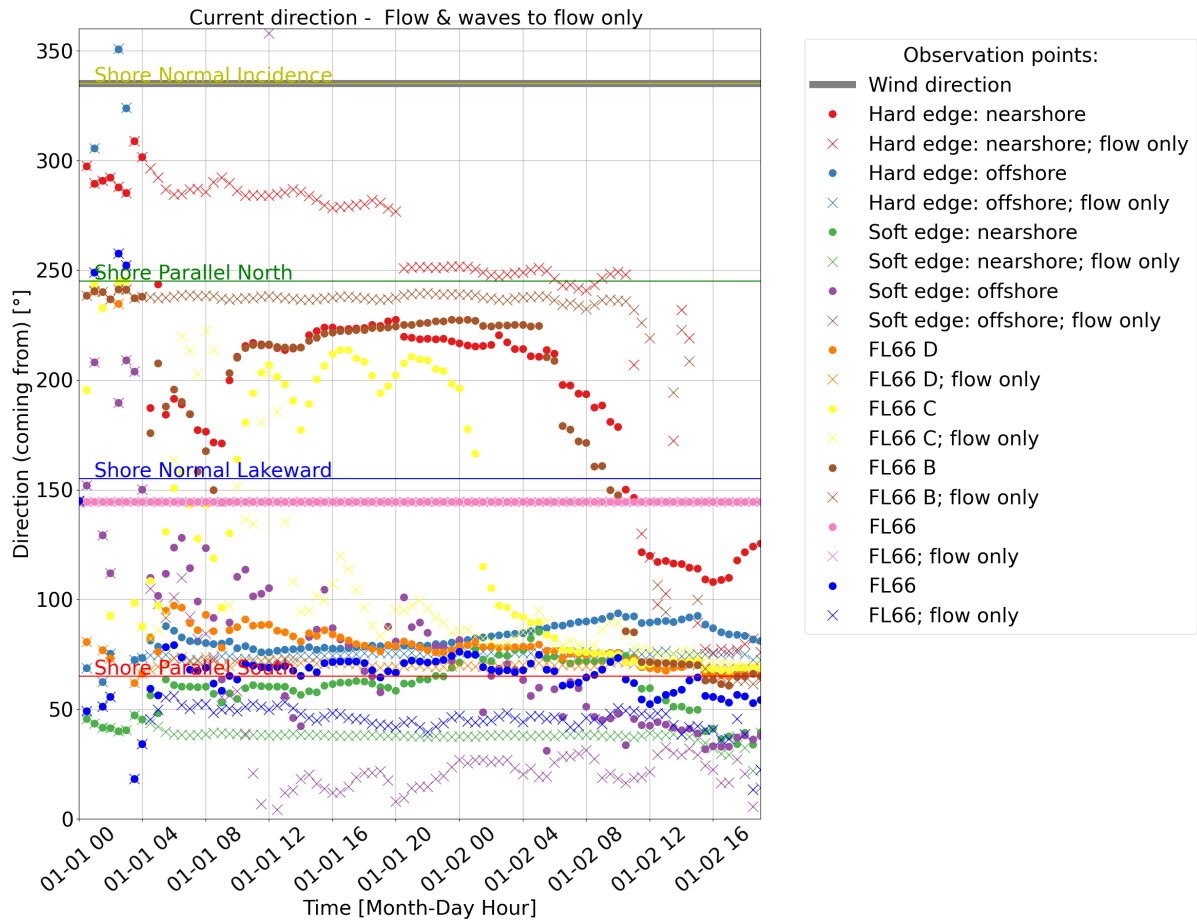


Figure E.19: Current direction (coming from) in the observation points for wind coming from 335°. The direction of the wind is shown in grey. Colours of the lines correspond to the locations as shown in figure 8.10. Solid dots indicate flow & waves, x's only flow.

E.3 Sensitivity and Exploratory Runs

Additional model plots for each of the sensitivity or exploratory runs are shown in this section. General results and conclusions are drawn in the main document. The following runs are added to the analysis:

E.3.1 3D Model

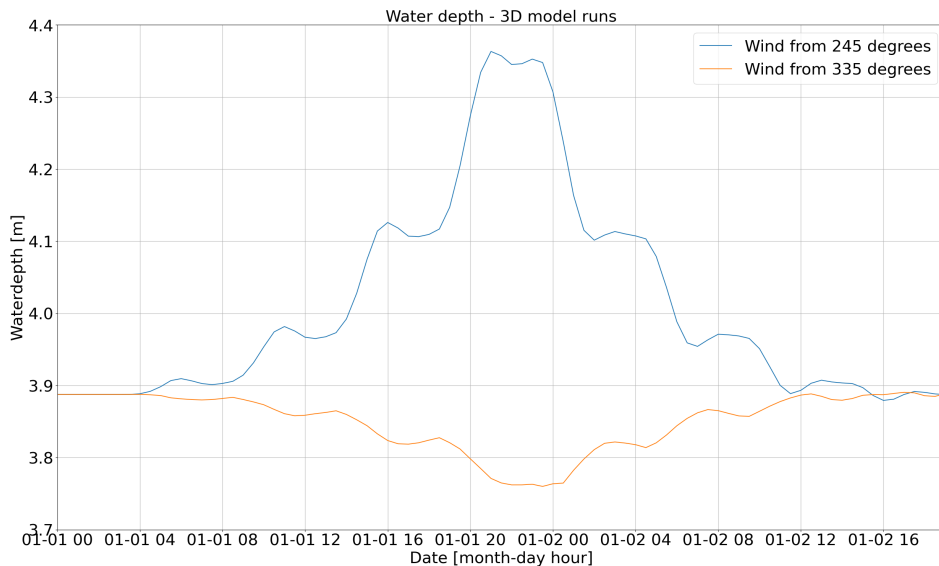


Figure E.20: Water depth at FL66 for 3D model runs of the Marker Wadden model (*total model*). For wind from 245° (blue line), resulting in enlarged water depth at FL66 (set-up) and wind from 335° (orange line) with a decreasing water depth for increasing wind speed (set-down).

E.3.2 Influence hard edge

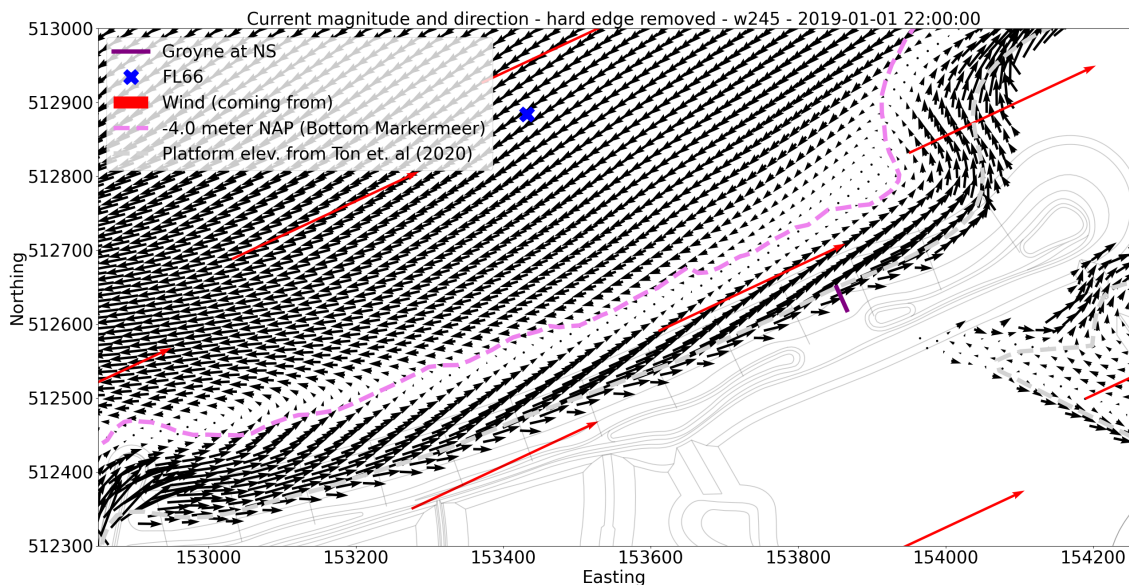


Figure E.21: Hard edge is removed from the Marker Wadden model, meaning flow is possible where first the breakwater was located. Overview of the entire Noordstrand. Black arrows indicate current magnitude and direction. Wind is coming from 245°.

E.3.3 Wind and Current: Use and Extent

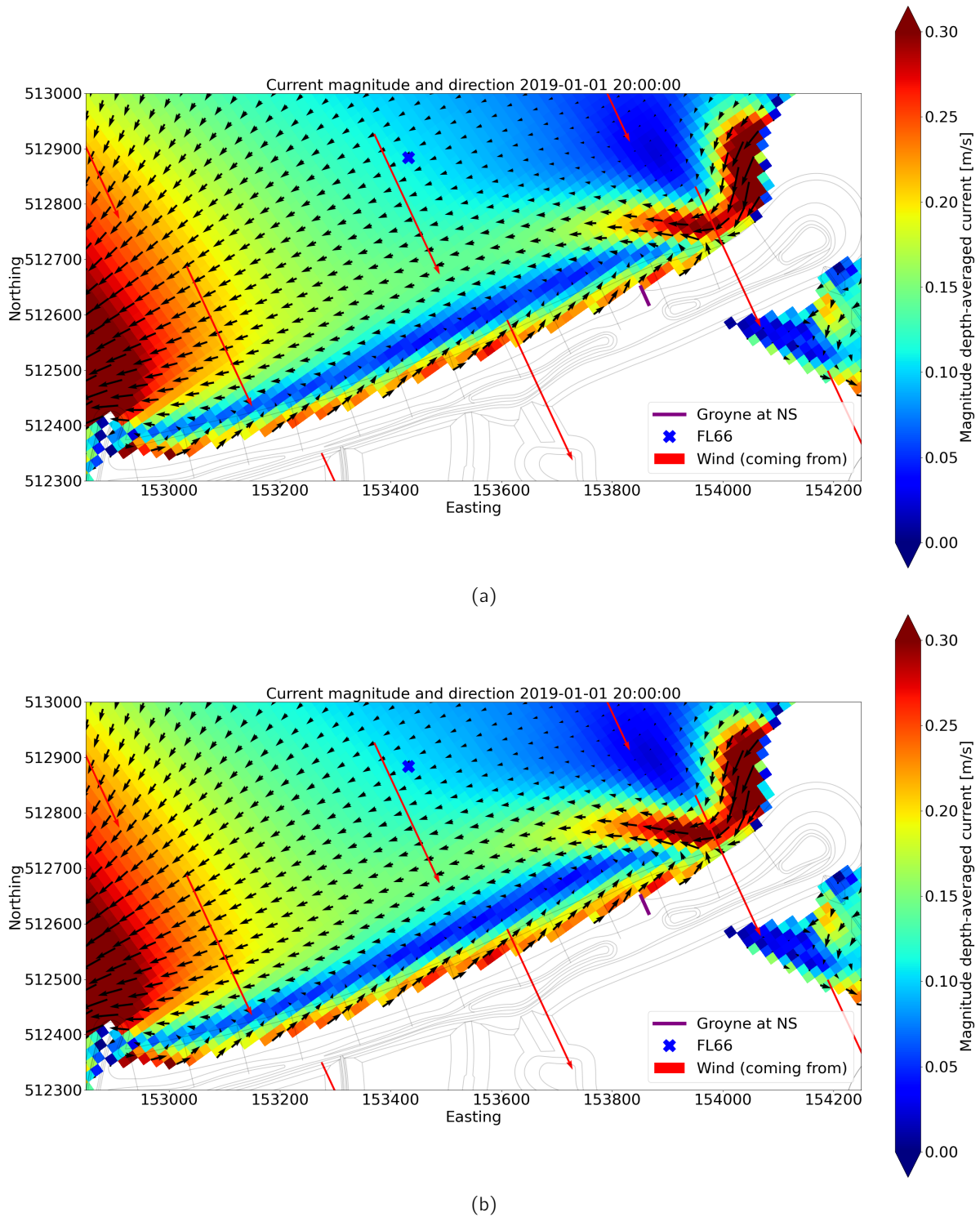


Figure E.22: Coupling Delft3D-FLOW and Delft3D-WAVE, comparing extend wind and current to only extend wind, for wind coming from 335° (a) **Extending wind and current**; (b) **Extending wind only**

E.3.4 Influence submerged platform

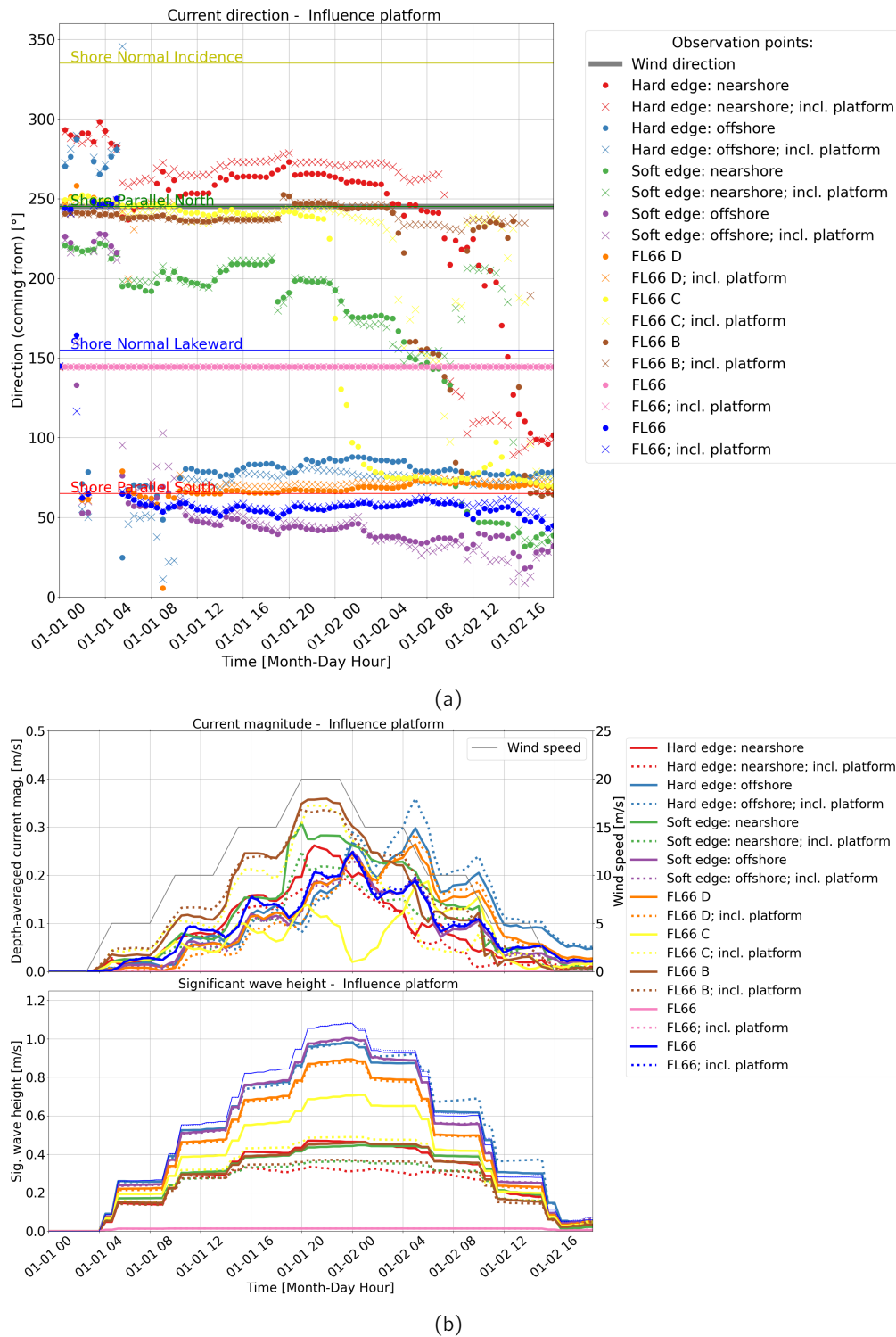


Figure E.23: Comparing the model runs with and without the submerged platform to investigate its influence; (a) Current direction showing the observation points for the runs without the platform (circles) and with the platform (crosses). The grey line indicates the wind direction (245°); (b) Current magnitude (top) and significant wave height (bottom) in the observation points for wind coming from 245°, excluding (solid lines) and including the platform (dotted lines). Colours of the lines correspond to the locations as shown in figure 8.10.

E.3.5 Influence sand extraction pit

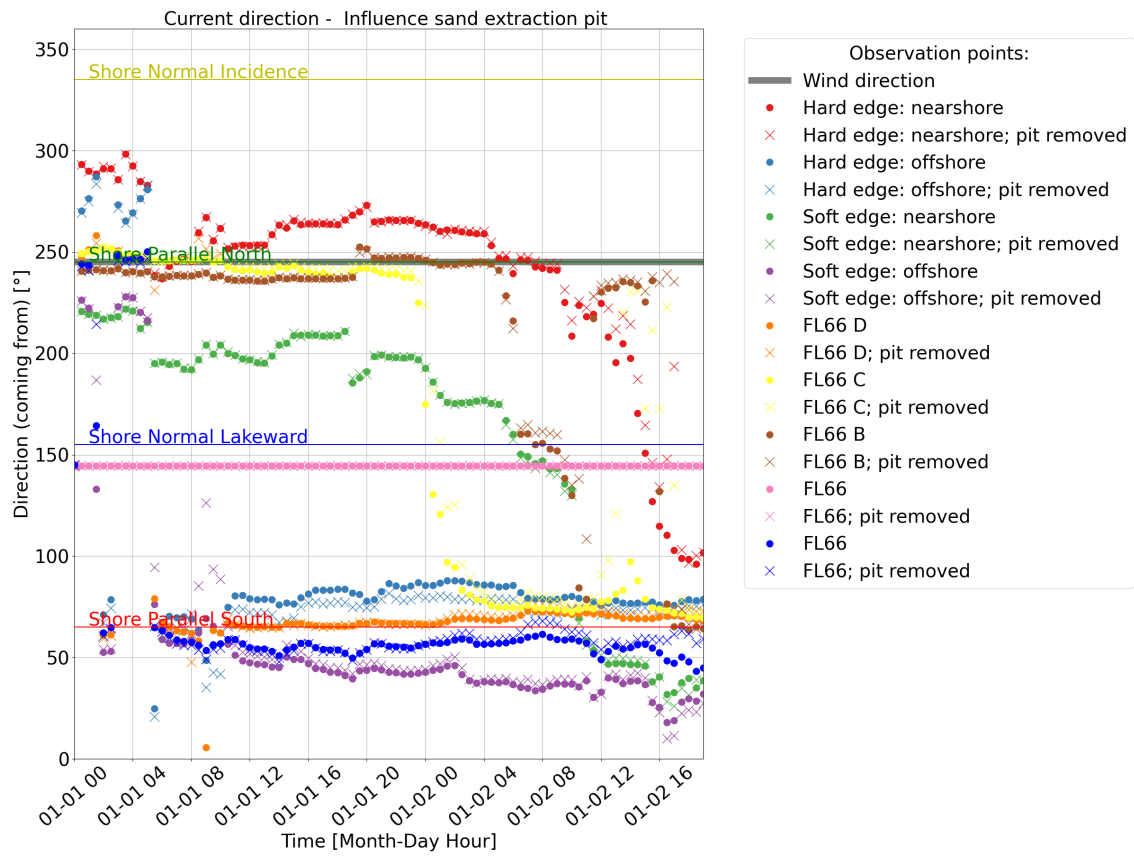


Figure E.24: Comparing the model runs with and without the sand extraction pit near the Noordstrand to investigate its influence; Current direction showing the observation points for the runs including the extraction pit (circles) and without the pit (crosses). The grey line indicates the wind direction (245°).



Exploratory Research - D3D Morphology

In addition to the main research and modelling a first attempt is made at the morphological modelling in Delft3D of the Noordstrand. First the morphological modelling in Delft3D in general is briefly discussed. This is followed by a short summary of the set-up of the Marker Wadden morphological model and ends with the results in the last section.

F.1 Set-up Marker Wadden Morphological Model

In the GUI of Delft3D-FLOW one activates the morphological modelling by activating the *Sediments* in *Processes*. For the relations of both current- and wave-related transport Delft3D uses equations F.1 and F.2 (Deltares, 2021a):

$$S_{total} = BED \cdot S_{bedloadcurrent} + BEDW \cdot S_{bedloadwaves} + SUSW \cdot S_{suspendedwaves} \quad (F.1)$$

$$\frac{dDPS}{dt} = S_{totalout} - S_{totalin} + SUS \cdot (Entrainment - Deposition) \quad (F.2)$$

With the tuning parameters BED , $BEDW$, $SUSW$ and SUS one can change the influence of the current- and wave-related forcing on the bedload and suspended load respectively.

F.1.1 Input

For the Marker Wadden model we use most default settings. As we are only looking at the transport rates we *do not update bathymetry during FLOW simulation*. This means sediment transport is not used to update the bed level. This saves considerable computation time, making the runs almost as fast as the flow & wave computations. The median sediment diameter (D50) is set to 350 μm according table 1.1. Using QUICKIN we create a sediment availability (.sdb file) around the Marker Wadden beaches but not too far offshore. This to limit the influence of offshore transport on the nearshore process, however initial model runs have shown the transport offshore is negligible. The spin-up interval is set to 60 minutes, meaning after an hour of simulated time the transport will be taken into account, giving the hydrodynamics in the system the chance to start up.

Anne Ton has been working on a morphological model for a longer period of time, mainly focusing on other beaches in the Marker Wadden. We have adopted her assumptions for the wave- and current-related transport factors. We set the wave-related transport factors ($BEDW$ and $SUSW$) to 0.1 and the current-related transport factors (BED and SUS) to 1.0. By changing these parameters we enhance the influence of the current-related parameters. Preliminary runs have shown that if the wave-related transport factors are similar to the current-related factors (say also 1.0) we will mostly observe cross-shore transports and cross-shore profile development. From our morphodynamic data analysis and on site observations we know this is not the case, and as a result we believe longshore transport must play a more important role in our system.

F.2 Results

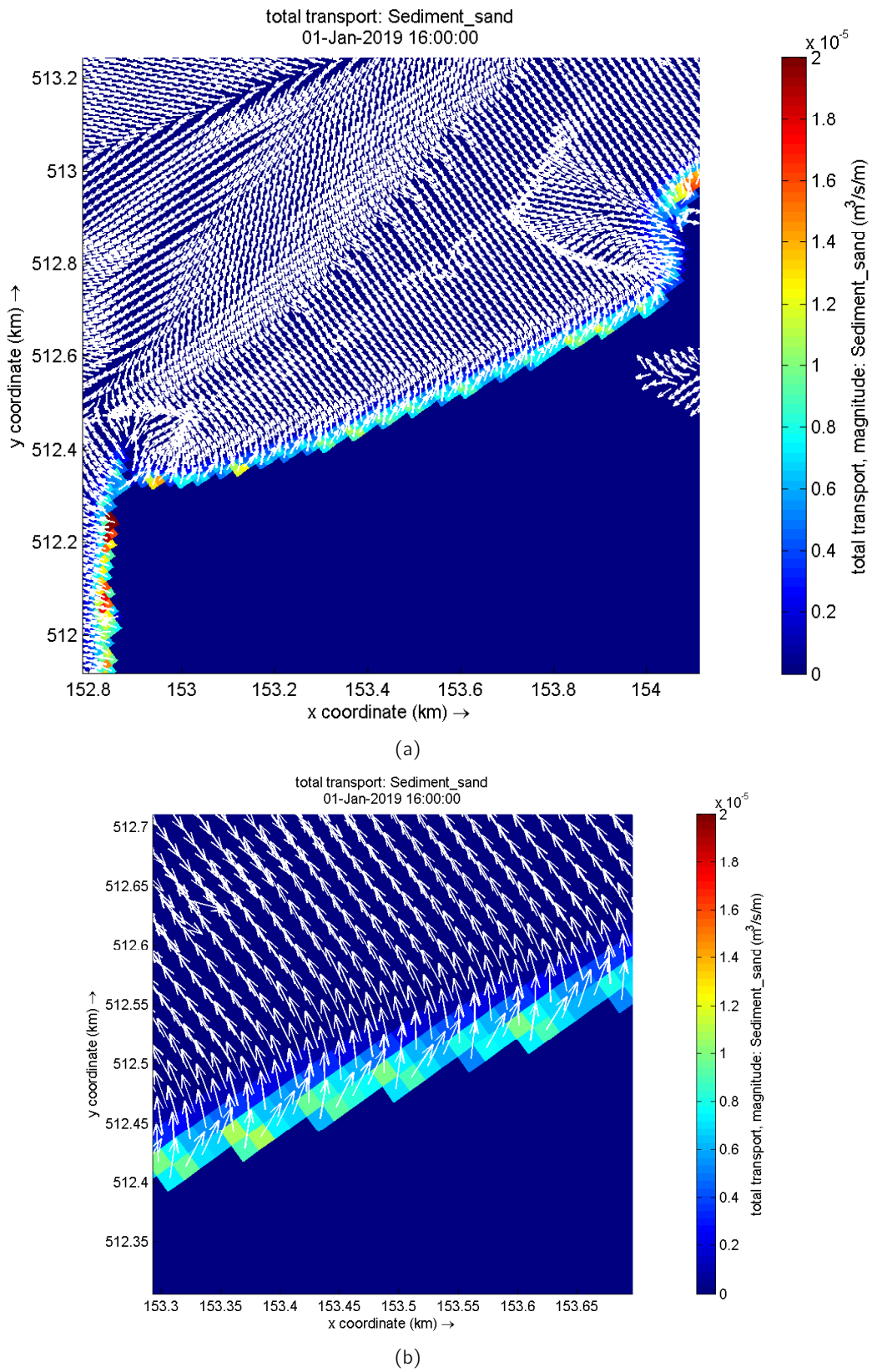


Figure F.1: Total transport magnitude (colourbar) and direction (white arrows) for wind coming from **245°**; (a) Total beach; (b) Zoom-in of middle Noordstrand

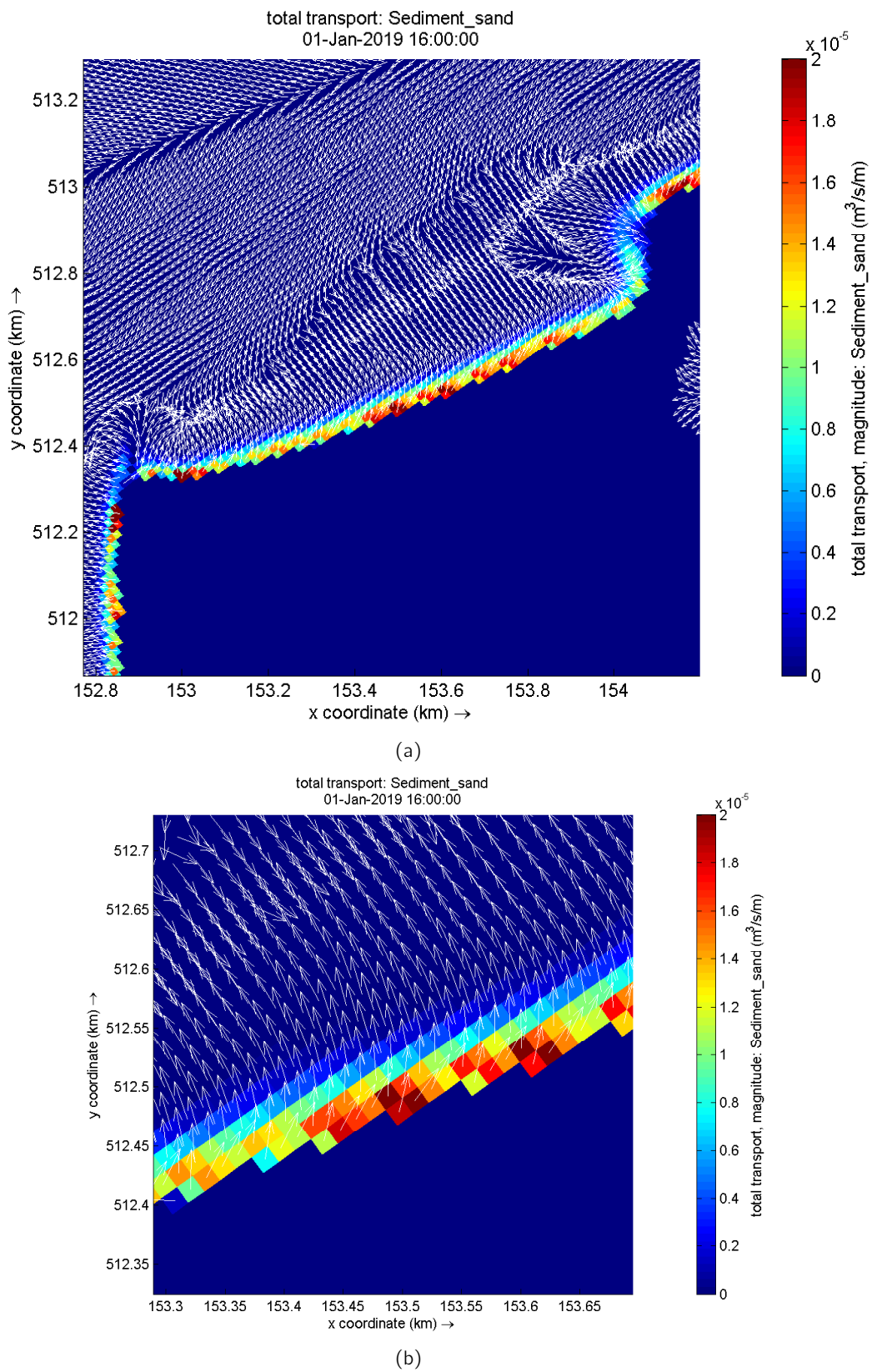
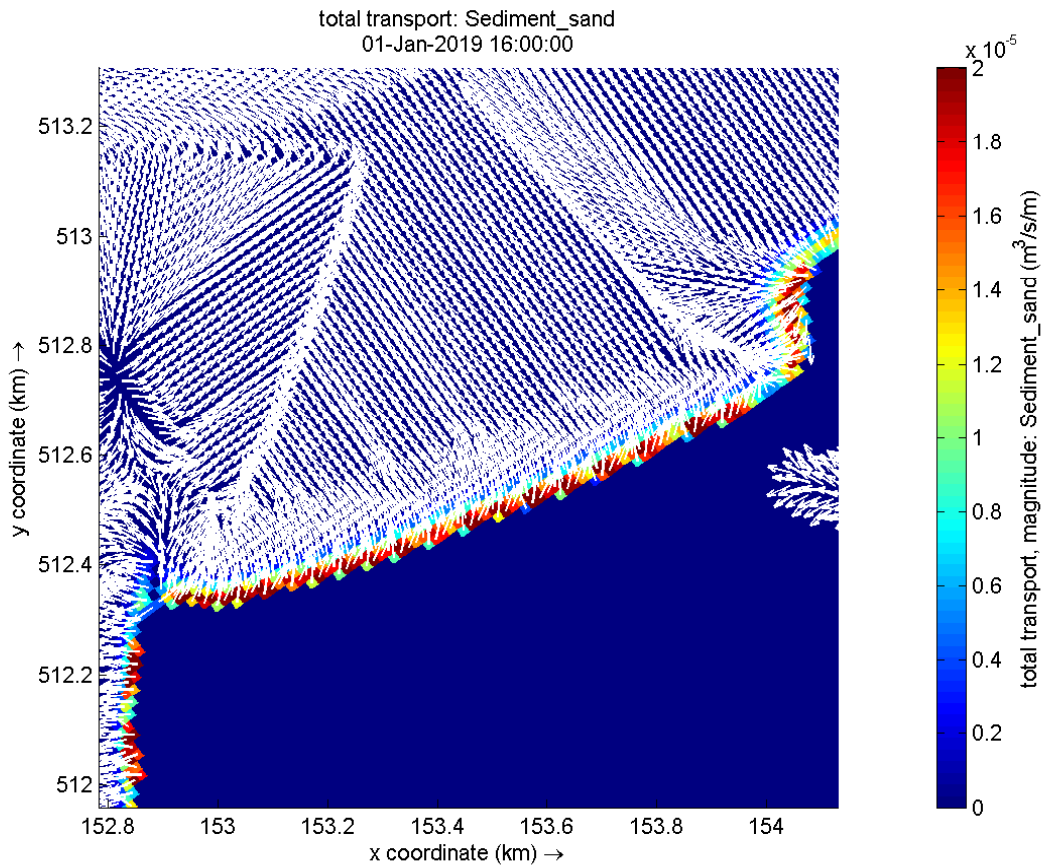
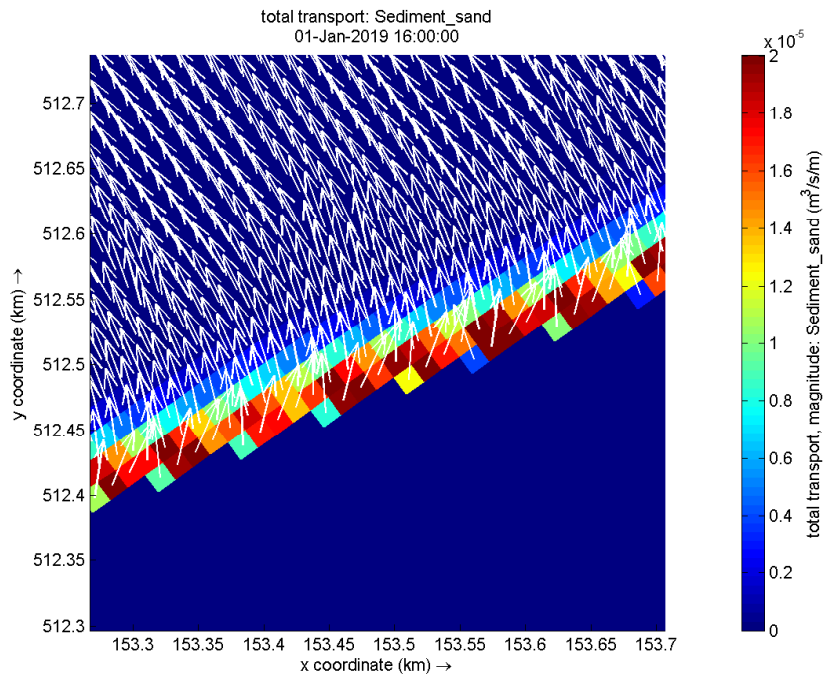


Figure F.2: Total transport magnitude (colourbar) and direction (white arrows) for wind coming from **290°**; (a) Total beach; (b) Zoom-in of middle Noordstrand



(a)



(b)

Figure F.3: Total transport magnitude (colourbar) and direction (white arrows) for wind coming from **335°**; (a) Total beach; (b) Zoom-in of middle Noordstrand

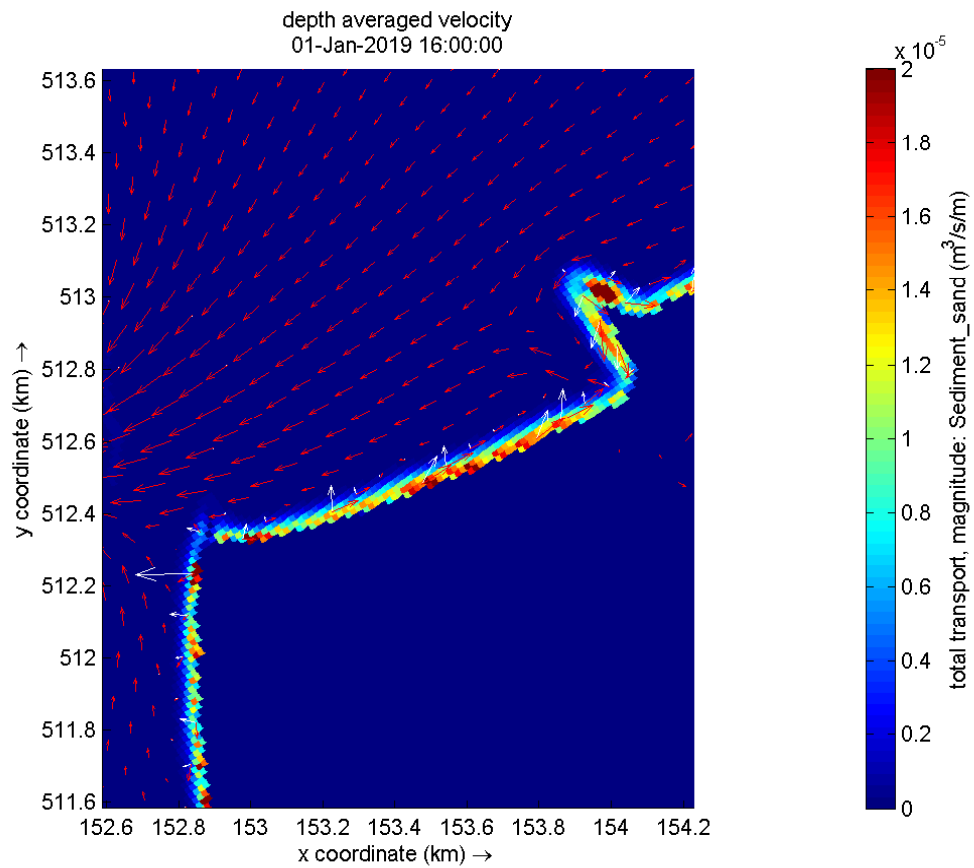
F.2.1 *Transport in case of extension soft edge*

Figure F.4: Total transport magnitude (colourbar) and direction (white arrows) for wind coming from **290°** shown together with the flow pattern (red arrows). In this scenario the soft edge (northeast of Noordstrand) is extended 200 meters to the northwest as to see the effect on beach development.

F.2.2 Transport in case of presence of submerged platform

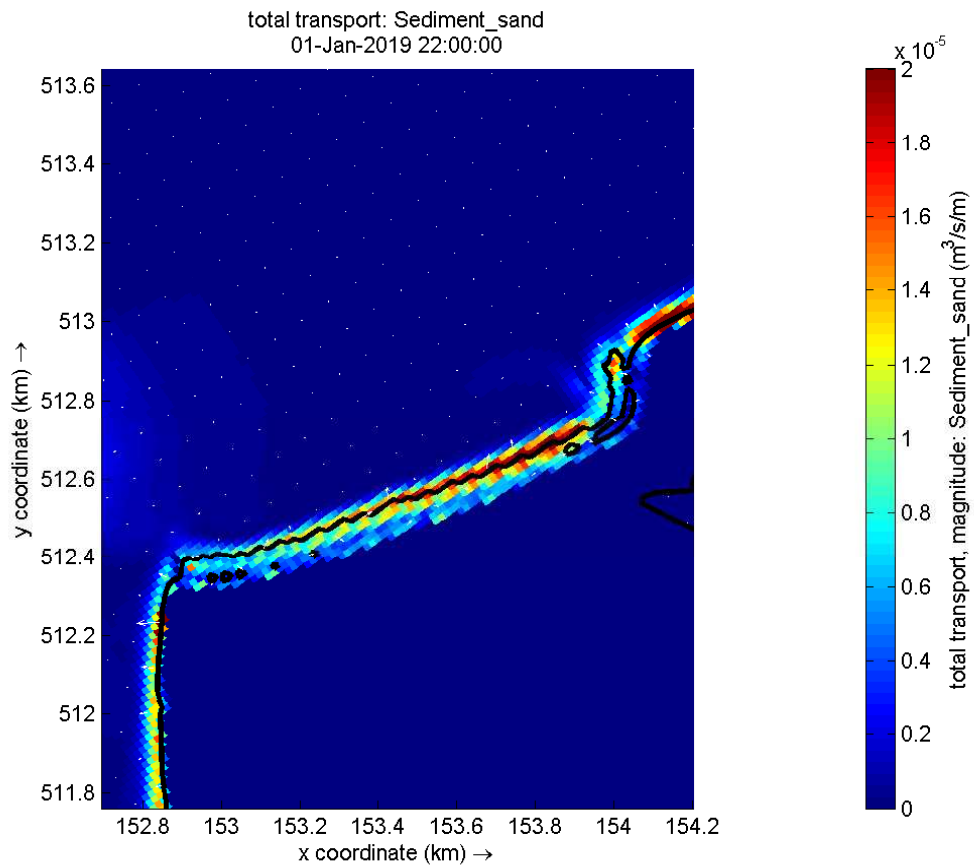


Figure F.5: Total transport magnitude (colourbar) and direction (white arrows) for wind coming from **290°** in case an extended submerged platform is present, platform is shown as the -1.11 meter NAP depth contour (black). The shown transport is due to a maximum wind speed of 20 m/s (8 Bft).



GPS Plan

This GPS plan explains which measurements will be executed at the Noordstrand after the nourishment of winter 2020 is finished. The expected end time of this nourishment is: Thursday 3th of December 2020.

The goal of this GPS measurement campaign is to: *Monitor the development of the North beach after additional nourishments of fall/winter 2020 are finished.* The preliminary results can be of added value for this thesis, but also provide topographic data for future research projects.

The GPS plan includes GPS measurements of different cross-sections of the Noordstrand. One walks several lines perpendicular to the orientation of the beach shoreline: transects. Along this line the x, y and z-coordinates relative to NAP are measured and saved. These kind of measurements of the Noordstrand are available from earlier measurement campaigns. This is combined with topographic data obtained by a drone and bathymetry measurement obtained by marine measurements.

G.1 Measurements

The considered section of the Noordstrand is approximately 1.5 km long and a trade-off between the amount of cross-sections/transects and the to be covered area of the beach is necessary. To be able to investigate both cross-shore and long-shore processes we propose the following:

- Measure transects from the SW edge to approximately 1.3 kilometres up to the NE edge, meaning the entire beach between the hard edge in the SW and the soft edge in the NE is covered.
- The transects are approximately 50 meters apart, incorporating the transects obtained by Boskalis every three months which are 100 meters apart. The Boskalis .dxf file with the Marker Wadden and to-be-measured transects is obtained and used as a reference for the additional 50 meter apart transects (longer red lines, figure G.1).
- If the time in the field allows the resolution is further enhanced by measuring additional transects which are 25 meters apart (shorter red lines, figure G.1).
- The GPS measurements of the transects are repeated once a month, starting in December, continuing in at least January, February and March.

The GPS equipment is reserved from the laboratory of Hydraulic Engineering, TU Delft. This includes:

- Leica GNSS-GPS GS14 All-in-One Antenna (Preferable option, others are also available)
- Carbon GPS pole
- Drysuits/wetsuits (depends on the water temperature)

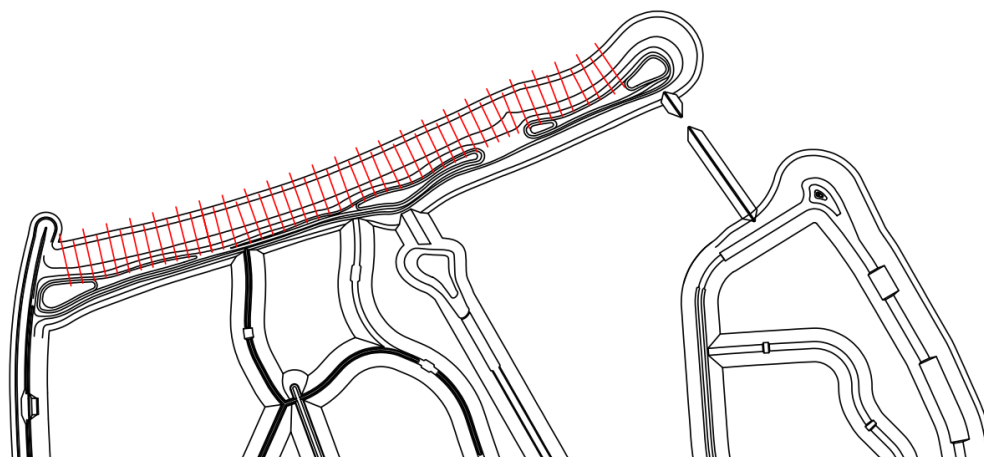


Figure G.1: Proposed transects for the GPS measurement campaign at the Noordstrand. The longer red lines indicate transects 50 meters apart, of set of these longer lines corresponds to the Boskalis transect (100 meters apart). The shorter red lines indicate the transects 25 meters apart. (Adjusted from .dxf file of Boskalis)

G.2 Planning

The nourishment of the Noordstrand was finished on December the 3th 2020. The first GPS measurements are planned in week 50. This results in the following rough planning:

- Thursday 10 December 2020
- January 2021 (Week 4, week of 25th of January)
- February 2021 (postponed to March)
- March 2021
- April 2021

The exact planning for the campaigns in 2021 depends on the availability of the GPS equipment, the availability of the Natuurmonumenten or Boskalis ferry to bring us to the Marker Wadden and the weather conditions. A wind force of maximum three Bft and a direction other than SW or NW is preferable. One should also consider the restrictions due to the **Corona Pandemic**, that is why the second fieldtrip is postponed from the beginning to the end of January.

G.3 Data Management

Data is stored on the GPS device and is exported to a .txt file using an USB stick. At home a back-up of the data has to be made. A small checklist is filled in and saved as a .docx (Word) file, describing:

- Name data file (.txt file)
- Date + time measurements
- Rough location of measurements on the beach (orientation from visual observations)
- Weather conditions
- Important visual observation of the beach + link to pictures
- Other important notes



Overview Fieldwork

This appendix provides an overview of the performed fieldwork measurements during the execution of this thesis. The plan for the GPS measurements is described in appendix G, this appendix is solely a summary of the different field campaigns.

H.1 Fieldwork December 2020

Table H.1: Overview of fieldwork trip of 10 December 2020

Date	10 December 2020	Thursday
Time	09:30-14:00	This only includes the time needed for measurements on site
Type of measurements	GPS	Leica GNSS-GPS GS14 All-in-One Antenne, 2m pole
Transport	Boskalis	Crew ferry and 4WD at our disposal at the Marker Wadden
Weather	Calm, sunny	
Wind	3 bft, NW	
Amount of transects	25	50 meters apart, 1200 meters of beach measured
Observations	Just after nourishment	Sand liquefied easily, possible to measure to a water depth of approx. 0.8 m
Comments	No time for 25m transects	Only main 50m transects were measured
Overview	Figure H.1	

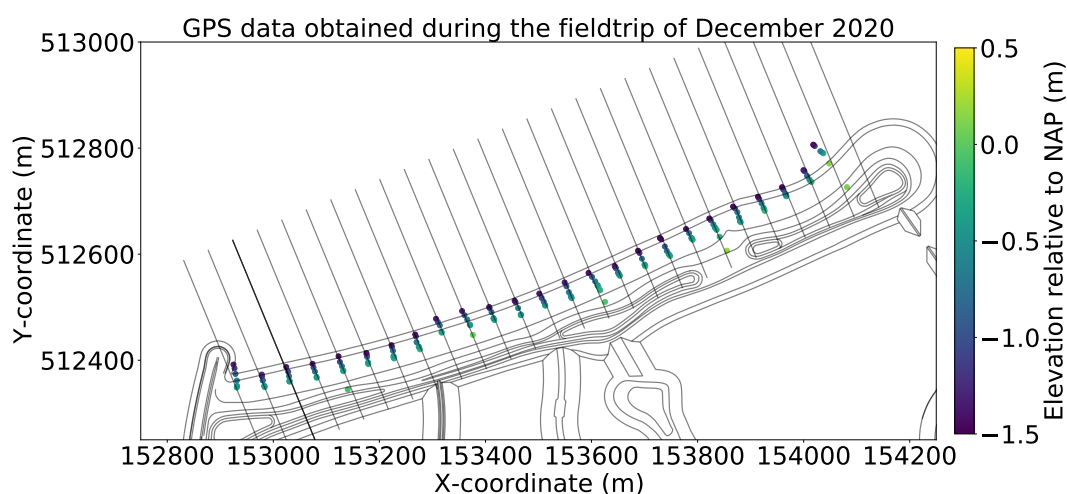


Figure H.1: Overview of the GPS points measured during the Fieldtrip of 10-12-2020. The figure shows the main part of the Noordstrand and the coloured points show the taken GPS measurements. The colour indicates the elevation relative to NAP in meter.

H.2 Fieldwork January 2021

Table H.2: Overview of fieldwork trip of 25 January 2021

Date	25 January 2021	Monday
Time	08:15-16:00	Time spent on Marker Wadden to measure Noordstrand and Zuidstrand
Type of measurements	GPS	Leica GNSS-GPS GS14 All-in-One Antenne, 2.8m pole
Transport	Natuurmonumenten	Electric 4WD at our disposal at the Marker Wadden
Weather	Calm, sunny	
Wind	3 bft, SW	Increased during the day
Amount of transects	25	50 meters apart, 1200 meters of beach measured
Observations	1 month after nourishment	Beach looked smaller, possible to measure to a water depth of approx. 0.8 m
Comments	No time for 25m transects	Due to measurements Zuidstrand less time overall
Overview	Figure H.2	

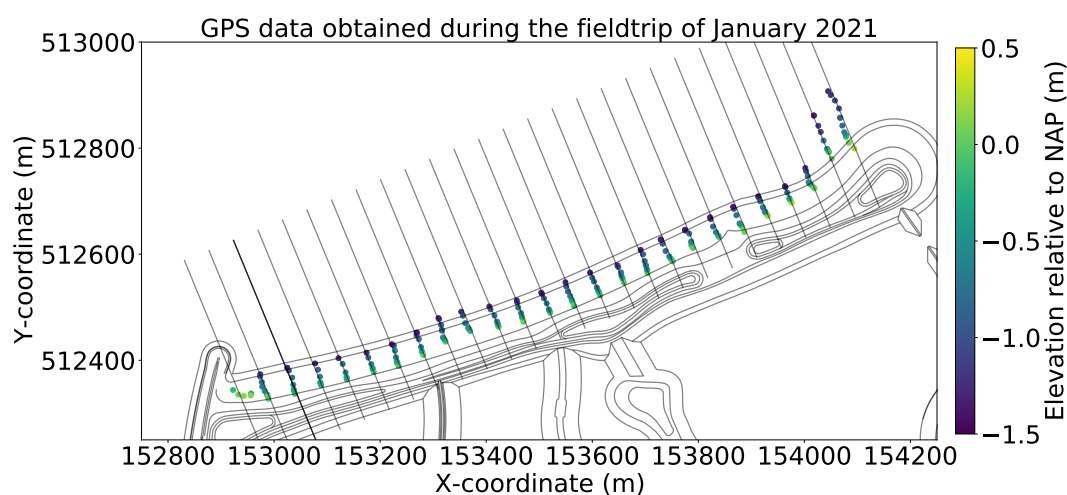


Figure H.2: Overview of the GPS points measured during the Fieldtrip of 25-01-2021. The figure shows the main part of the Noordstrand and the coloured points show the taken GPS measurements. The colour indicates the elevation relative to NAP in meter.

H.3 Fieldwork March 2021

Table H.3: Overview of fieldwork trip of 8 March 2021

Date	8 March January 2021	Monday
Time	11:00-16:00	Time spent on Marker Wadden to measure Noordstrand
Type of measurements	GPS	Leica GNSS-GPS GS14 All-in-One Antenne, 1.8m pole
Transport	Natuurmonumenten	Electric golf cart at our disposal at the Marker Wadden
Weather	Calm, cloudy/foggy	
Wind	3 bft, SW	Increased during the day
Amount of transects	25	50 meters apart, 1200 meters of beach measured
Observations	2 months after nourishment	Beach looked smaller, possible to measure to a water depth of approx. 1.0 m
Comments	No time for 25m transects	
Overview	Figure H.3	

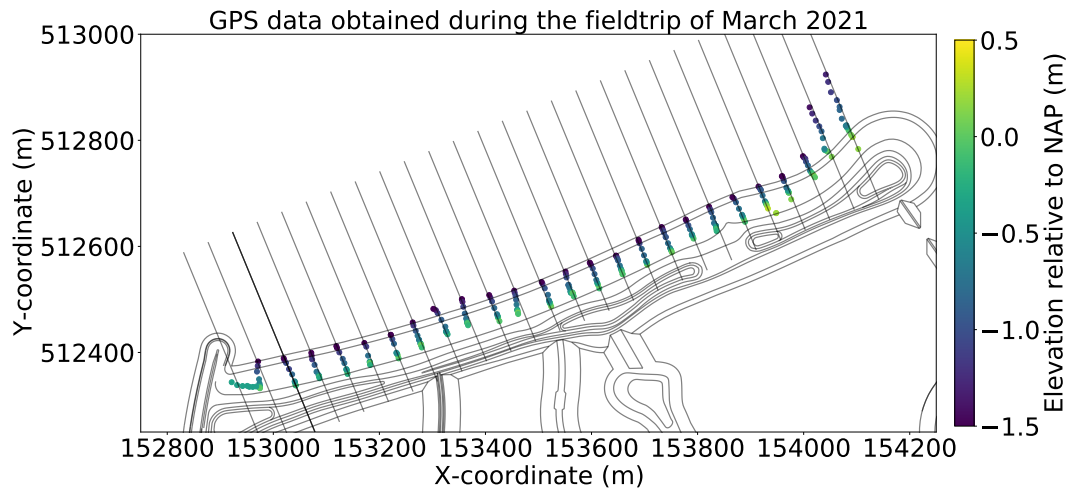


Figure H.3: Overview of the GPS points measured during the Fieldtrip of 08-03-2021. The figure shows the main part of the Noordstrand and the coloured points show the taken GPS measurements. The colour indicates the elevation relative to NAP in meter.

H.4 Fieldwork April 2021

Table H.4: Overview of fieldwork trip of 19 April 2021

Date	19 April January 2021	Monday
Time	11:00-16:00	Time spent on Marker Wadden to measure Noordstrand
Type of measurements	GPS	Leica GNSS-GPS GS14 All-in-One Antenne, 1.8m pole
Transport	Natuurmonumenten	Transportation by Natuurmonumenten officials
Weather	Calm, sunny/cloudy	
Wind	2 bft, N/NE	Increased a little during the day
Amount of transects	14	50/100 meters apart, 1200 meters of beach measured
Observations	3 months after nourishment Near soft edge	Possible to measure to a water depth of approx. 1.0 m Strong current present on platform towards soft edge
Comments	No time for all 50m transects	
Overview	Figure H.4	

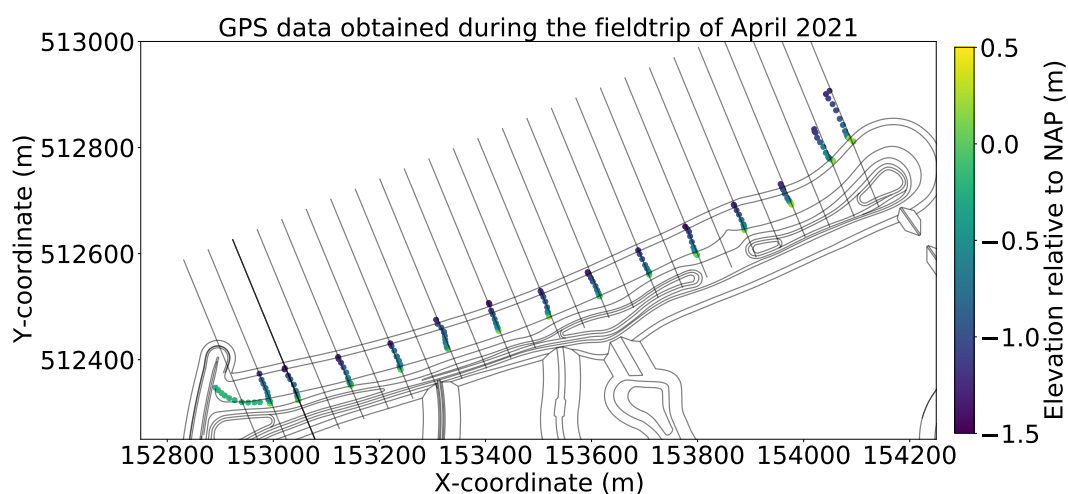


Figure H.4: Overview of the GPS points measured during the Fieldtrip of 19-04-2021. The figure shows the main part of the Noordstrand and the coloured points show the taken GPS measurements. The colour indicates the elevation relative to NAP in meter.



Integral Design and Management

In addition to the engineering project this thesis links the last phase to the learnt skills of the Integral Design and Management annotation. This annotation combines technical knowledge with other skills such as project- and asset management. This is particularly valuable for multi-disciplinary projects. The Marker Wadden project is an excellent example of such a project: different stakeholders and their wishes, different project aspects and innovative developments come together. This project concerning the Noordstrand and the realisation of the Marker Wadden are part of a bigger engineering development: using Building with Nature solutions to protect coastal systems. We have regarded the system engineering aspect in the general picture by looking at: Building with Nature: A System Engineering Approach.

I.1 Analysing Key Points

We discussed the concept of Building with Nature with two experts from the field, a designer and a contractor, both linked to the Marker Wadden project. During these interviews we identified three critical points of the Building with Nature approach: taking into consideration the development of the system after the final commissioning, uncertainties of innovative solutions and the understanding of an unknown system. We want to use the System Engineering approach to shine some light upon these points and use this approach to highlight pitfalls and opportunities.

To summarise the above, this has led to the following key points:

- Consider the project over a period of time rather than only the initial realisation of the project
- Consider the uncertainties and unknowns
- Consider the understanding of an unknown system

Ultimately these considerations can be translated to recommendations for the future: *Is Building with Nature a resilient and adaptive strategy for climate change and/or coastal protection in a low-energy environment?. We will analyse the identified key points using a system engineering approach.*

I.1.1 System life cycle

Building with Nature (BwN) projects are often dynamic, interacting with nature instead of working against nature. This means it is not a solution for a moment in time but rather a dynamic and adaptive solution for a longer period. From a system engineering perspective this means considering the system (or project) life cycle already in the initial phases. This means that next to the initial design, evolution of the system, of the monitoring and maintenance phases and of the costs need to be taken into account.

For BwN project it is often difficult to predict the behaviour of the system due to uncertainties. Not only uncertainties from the system (see next section: *system uncertainty*) but also external factors for which the system has been designed can change unexpectedly (due to for instance climate change). From a system engineering view it would be beneficial for the system life cycle to identify specific system design considerations from the designing for TY's perspective (figure I.3). Some TY's are already naturally part of a BwN project such as *Environmental sustainability* and *Technological feasibility*. We would like to add to the system design

considerations of a BwN project the *Reliability* and *Maintainability* of a system. By explicitly naming these design considerations during the design phase additional attention is given to the system life cycle. Different designs and scenarios can be checked for these specific TY's and we can evaluate how they add value to a BwN project. For correct implementation of these TY's limiting system uncertainties and encouraging system understanding is crucial, see the next paragraphs.

I.1.2 System uncertainty

As a BwN project is unique and site-specific, there are a lot of system uncertainties. Our Noordstrand is a good example, the design and construction of a beach with a non-equilibrium shoreline position in a low-energy environment has no antecedent. Uncertainties can be found in our understanding of the natural system, but also the reaction of the system to the BwN project can remain partly unknown. We can identify the following general uncertainties in Building with Nature projects:

- How adaptive is the considered solution?
- How to deal with uncertainties?
- What is the development of the BwN solution over time?
- How and when to intervene?

Some support in handling system uncertainty can be found when regarding the project from a system engineering perspective. An important consideration is the *solution space* of a project or system. Take the example of the Noordstrand: the need (and if yes, the amount and timing) of a nourishment is uncertain. In the current situation different physical measurements, such as volume of the beach, dune height and beach width, determine if a nourishment is necessary. The threshold values are determined by taking into account both the safety and recreational function of the beach. But if we extend our solution space there are more ways to deal with this uncertainty. One could for instance decide that the recreational function is of secondary importance. Therefore if the beach width is not sufficient, but the beach still fulfils its safety function, a nourishment is not (immediately) necessary. This flexible approach, depending on how the system develops during its life cycle, could result in less frequent and thus less costly maintenance. This *flexibility* towards requirements and risk management nicely fits with the dynamic character of BwN projects. For this flexibility close cooperation and communication between all stakeholders is necessary. All those involved should have a basic understanding of how the system works and how flexibility towards the system functionality can enhance risk management instead of the contrary.

Extensive risk management should be part of every BwN project, not only during the design and execution phase, but during the entire life cycle. The BwN philosophy includes several tools of which *visualising and managing uncertainties* is one. In addition we believe monitoring and research should be part of the risk mitigation measures as by updating our system understanding we limit the risks. Furthermore, the learnt-lessons and increased system understanding can be applied in the next BwN project.

I.1.3 System understanding

When designing a system from a system engineering point of view we often use a process model. This means we decompose the system into smaller subsystems and their components; by integrating and verifying these subsystems we arrive back at our general system (as the Process 'Vee' Model shows, figure I.1). Using this point of view on the system of the Marker Wadden, we observe how the Noordstrand system is only one component. On the other hand, its aspects influence the global aspects of the system and vice versa.

The Vee Process Model shows us how details on the smallest scale have to be understood before the entire system can be understood. Also different details and components need to be correctly linked for a correct functioning of the system. If we consider the system of the Noordstrand in this process model, we see how some *integration and verification* processes were only considered briefly. The effects of the bigger Markermeer system on the nearshore components of the Noordstrand were neglected and therefore the system was only partly understood. On the other hand there was no precedent with which the design of the Noordstrand could be verified, especially taking into consideration its non-equilibrium shoreline position. The uncertainties in the design were acknowledged as extensive monitoring and additional research regarding the development of the system are included in the project scope. As only part of the system was understood and taken into consideration in the general design of the Marker Wadden the negative effects of the breakwater (the formation of a rotation cell and consequently

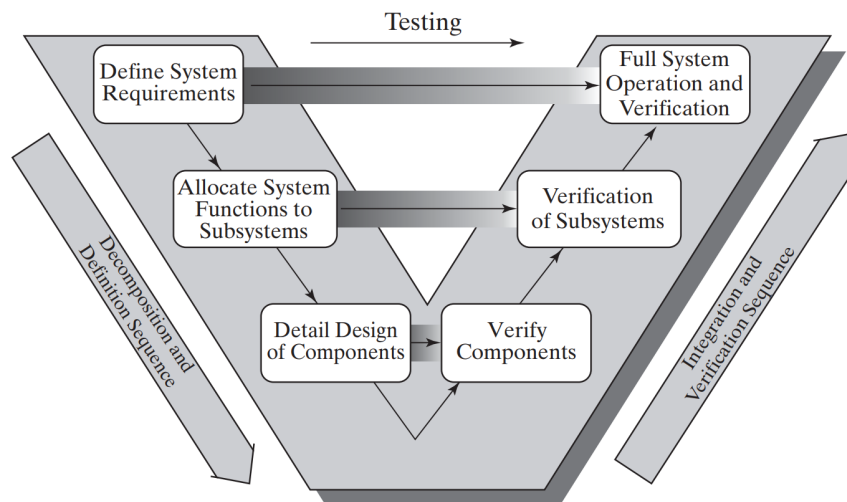


Figure I.1: 'Vee' Process Model taken from Blanchard and Fabrycky (2014)

enhanced erosion patterns) could not have been foreseen. System understanding can be enhanced by monitoring the different processes during the project life cycle, again highlighting the importance of considering the period of time after final commissioning until project closure.

The Marker Wadden project acknowledges its lack in system understanding and as a result the project objectives include: *learning, monitoring of effects and innovate* of three research topics: building with silt and sand, ecosystem with value and adaptive governance. Research regarding the Noordstrand system contributed to all three topics. The lessons learnt, the increased system understanding and its relation to the general Markermeer system adds value to future Building with Nature projects in the Markermeer or elsewhere. Also in light of System Engineering the evaluation of both the Building with Nature design and the process itself is important.

The functionality and performance of the Noordstrand system needs to be evaluated, taking into consideration the unforeseen circumstances and their influence on the beach development. In a more general sense the different stakeholders of the project have to review on their cooperation and their integral and multi-functional approach. This multi-stakeholder approach is one of the key aspects of a Building with Nature project (EcoShape, 2021a). Evaluation of the project is part of good system engineering, contributing to improved and optimised projects.

1.2 This Research - a System Engineering Approach

In addition we add an analyse on how a system engineering approach was used in this research. The used literature, Blanchard and Fabrycky (2014), focuses on system *design*, but we use their approach and tools in our search of system *understanding*.

1.2.1 Decomposition and Integration

To better understand the system's development one can use a process model. Blanchard and Fabrycky (2014) describes different process models such as the 'System Process Model', 'Waterfall Process Model' and 'Spiral Process Model'. The representation of this research can be found in the 'Vee Process Model' as we first use a top-down approach and continue with a bottom-up approach. Furthermore this model includes the link between technical aspects (Blanchard and Fabrycky, 2014), which are in our case the hydro- and morphodynamics near the Noordstrand. We have also seen in this research how the smaller details (local flow) is linked to larger components (nearshore flow around the Marker Wadden) and needs even to be linked to the full system (Markermeer system) for complete understanding of the different phenomena.

We use the Vee process model as a guidance through our research: we start with defining user needs. In our case this means defining the problem statement. From there we decompose (going down in the Vee model, figure I.2) to resolve the different aspects of the system and investigate details. For this initial decomposition

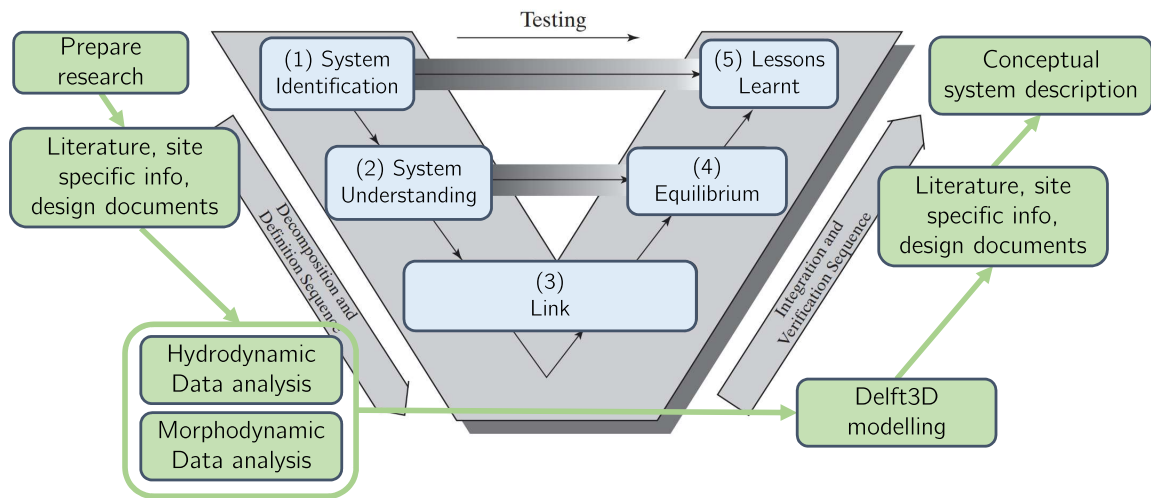


Figure 1.2: 'Vee' Process Model adapted from Blanchard and Fabrycky (2014) to include the different steps of this research as shown in the methodology, section 2.3 (figure 2.2)

we use site-specific information and design documents of the Markermeer and Marker Wadden. Additionally, we look into the technical aspects of similar low-energy systems by analysing available literature regarding this topic. This leads to increased system understanding and the possibility to identify the *gaps of knowledge* of our system. Next we dive further into the details of our system: the hydro- and morphodynamics near the Noordstrand. Using data available we are able to investigate the different components of each: for instance wave height and current magnitude direction. Essential is the link between different processes, which we need on the smallest system scale to be able to later link to the general beach development. For this we integrate the different components and verify their interaction with other components, we start to go up in the Vee model (figure 1.2). An example of this can be found in the influence of the local geometry on the bigger flow patterns. For some components the link cannot be made based on the field data only and we use a Delft3D model to be able to integrate the rest of the processes in our system. By combining all components and linking these to theoretical knowledge we are able to hypothesise the general system development, this results in the *conceptual system description*. This conceptual description enables us to investigate the possibility of equilibrium, monitoring and maintenance.

In short we have worked through the entire Vee process model, starting with the general lake system, breaking it down into smaller subsystems, components and details. From there we are able to link processes on the smallest scale, which we can combine and relate to the bigger picture. We are even able to *test* the conceptual system description, our 'product' so to say, with our own field measurements.

1.2.2 System Considerations

In the section considering system engineering and Building with Nature projects we already highlighted the possibilities of system design considerations: design for TY's. Essentially we have been focusing on some TY's in our own research (considerations defined with green box, figure 1.3).

Performance & Functionality

The main goal of this research is to find why the Noordstrand is not 'functioning' as expected. The observed erosion patterns were unforeseen and as a result the Noordstrand could no longer fulfil its recreational function. This meant the application of a costly nourishment for the contractor.

In order to prevent costly solutions to unforeseen circumstances we had to investigate the *performance* and

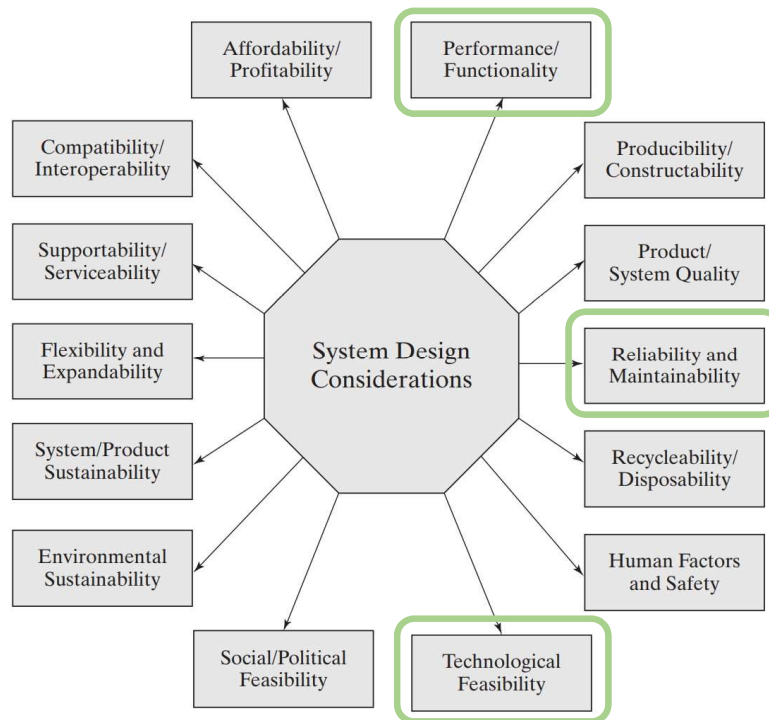


Figure I.3: System Design Considerations adapted from Blanchard and Fabrycky (2014) to include our focus on TY's in this research.

functionality of this beach in its low-energy environment. Our goal was to investigate the knowledge gaps and to expand our system understanding.

Reliability & Maintainability

Reliability and *maintainability* have been primary parts of this research as these system design considerations are directly linked to the research questions. An improved understanding of the Noordstrand system is ultimately needed for a higher reliability of the beach. According Blanchard and Fabrycky (2014): 'Reliability is that characteristic of design and installation concerned with the successful operation of the system throughout its planned mission and for the duration of its life cycle.' Reliability also highlights the importance of considering the system life cycle. An unreliably design or system can lead to an increase in 'downtime'. Using this term for a beach might seem inappropriate, but essentially 'downtime' is the period during which a system/project cannot fulfil its primary functions. This 'downtime' can be programmed (maintenance during nourishments) or unforeseen (for instance a breach in the dunes). Depending on the function the system can no longer fulfil, immediate action might be necessary. A more reliable design ultimately leads to less uncertainties in the system.

We have also investigated the 'maintainability' of the Noordstrand. Citing Blanchard and Fabrycky (2014) we can describe maintainability from a system engineering point of view: 'Maintainability is that characteristic of design and installation that reflects the ease, accuracy, safety, and economy of performing maintenance actions.' In this research we have been focusing on periodicity and thus indirectly the economy of maintenance actions. The idea of BwN projects is that these project adapt to their environment and minimal human interference is needed. In case of the Noordstrand this essentially comes to the question: *is an equilibrium position of the shoreline possible?* Using our conceptual system description we are able to answer this question: *no*. This means the beach needs to be maintained periodically with nourishments in regions of high erosion.

Technological Feasibility

We want to highlight the technological feasibility of this research as a state of the art computational modelling program, Delft3D, was used for linking different processes. Initially we could only work with offshore data gathered at one location of the Noordstrand system. The usage of the modelling software made it possible

to also investigate and link the different processes nearshore. The combination of data analyses and modelling made it possible to answer the stated research questions.

We can conclude the usage of Delft3D has been beneficial for this research, but on the other hand its application also result in new uncertainties. The model is only an approach of the real-life situation and has several limitations. As a result the model outcomes have to be regarded with care. This part is essentially linked to the topics discussed in the section on Critical Remarks (section 10.4). Truly this research is actually on the verge of whether it is technological feasible or not.

1.2.3 Evaluation & Recommendations

In essence this has been a master thesis with a technical focus, linking fluid mechanics to coastal engineering in a specific environment. To include system engineering aspects in the research approach appeared to be difficult at first, but when diving more into the applicability of system engineering assets we found these can actually help guide the technical aspects. Crucial in system engineering is to always consider the general system as a whole: how adaptations of details affect components of the system and the system in general. This way of looking at system design is very applicable and similar to understanding an existing system. Our Markermeer, Marker Wadden and Noordstrand systems are all connected and should be regarded in the general perspective, underlining the system engineering approach.

The entire life cycle of the Marker Wadden is a potential interesting case for a follow-up study entirely focusing on the System Engineering aspects. Numerous stakeholders and different aspects of the design make the entire life cycle an intricate multidisciplinary project. The design and construction of the archipelago is novel and innovative, creating possibilities for other Building with Nature projects just like the Marker Wadden. This novel and innovative project make this a particular interesting case as a complete analysis focusing on the System Engineering aspects can lead to improvements for new projects and their life cycles.